The Design of a Fracture Movement Transducer

Kathleen Elizabeth Tanner, B.A.

Lady Margaret Hall, University of Oxford

Submitted for the degree of Doctor of Philosophy

Trinity Term 1985

Abstract

The Design of a Fracture Movement Transducer

Kathleen Elizabeth Tanner, B.A., Lady Margaret Hall

Submitted for the degree of Doctor of Philosophy, Trinity 1985

The literature on bone growth, fracture healing, fracture treatment and the effects of forces and movements on these is reviewed. Some methods of assessing the progress of fracture union are considered. The conclusion from this is that a fracture movement transducer is needed for use on an external fracture fixator, and the design criteria are outlined.

The possible types of transducers are considered and a system of light falling on lateral effect photodetectors was used. The linearizing algorithms applicable to the employed detectors are discussed and tested. The electronic circuits were designed and revised, initially to produce a reasonable power consumption, and then to give a system with reduced noise levels and improved linearity. Isolation amplifiers were required to prevent leakage currents reaching the patient from the mains powered computer.

The algorithms relating the movements of the transducer to the movements at the fracture site were derived, including the use of elasticity theory to calculate the bending of the fixator pins. The engineering descriptions of the patient tests and the methods of calculating the fracture stiffness are considered. The transducer was calibrated, and consideration was given to the effect of the fixator pins loosening in the bone.

Seven patients, all with tibial fractures, six injured in road traffic accidents and one footballing injury, were tested and their clinical histories were reviewed. Comparison was made between the

results from the displacement transducer and a strain gauge transducer, related to the clinical history. It is concluded that this transducer, although useful, has more relevance as a research than as a clinical tool, but that further tests would lead to increased further understanding of fracture healing.

In memory of my Father,

who died while this work was in progress.

Acknowledgements

I would like to thank those who have helped me while I was doing the work that is reported in this thesis, and also all those who have bribed, cajoled, or bullied me into finally finishing writing up this work.

In particular my three supervisiors Dr M.W.Whittle, Dr J.J.O'Connor and Mr J.Kenwright for their assistance over the years. Dr Whittle for unmuddling both my computer programs and my convoluted grammar and spelling. Mr Kenwright for his clinical assistance and for permitting me access to his patients.

Mr J.D.Harris and past and present members of the Oxford Orthopaedic Engineering Centre, who have helped in various ways, throughout the time this work was progressing. Dr Alex Churches of the University of New South Wales for many helpful discussions while he was on sabbatical in Oxford.

Peter Brown and Wren Wooster of the Department of Engineering Science for their assistance with the final set of electronics used in the patient tests. Steven Blatchford for his help with three dimensional geometry calculations.

The patients for giving up their time to be subjects for this thesis, and not objecting to yet another person looking at their fractures.

Those responsible for funding this work: the Science and Engineering Research Council for a Research Studentship. Lady Margaret Hall for a Beatrice Warr-Goodman Research Studentship enabling me to finish this work. The Department of Engineering Science for funding to enable me to present this work at the 10th International Conference on Hoffmann External Fixation in Brussels.

My family for surviving this thesis.

And finally Sue Owen for typing this thesis, and succeeding in deciphering the squiggles which I presented her with, and also battling with my grammar and spelling.

CONTENTS

APPENDICES

List of Figures

Chapter 2

Chapter 3

List of Tables

CHAPTER 1

INTRODUCTION

INTRODUCTION

It is relatively simple to decide whether a bone is broken, and the Ancient Egyptians had methods of immobilizing fractures. However, it is more difficult to agree on the end of the healing process and even more difficult to ascertain whether, or not, healing is progressing. This work considers a method of following fracture healing by measuring the relative movements between two points on either side of a fracture and then mathematically relating these movements to the relative movement across the fracture site. Seven patients, all with tibial fractures, six caused by road traffic accidents, one a sporting injury and treated with the Oxford External Fixator, were studied as their fractures healed. The design criteria, and the resultant transducer are discussed, as is the calibration of the transducer. The results of the patient studies are compared with results obtained by another mechanical method of measuring fracture healing.

CHAPTER 2

HISTORICAL REVIEW

HISTORICAL REVIEW

2.1 Intact Bone

2.1(i) The Structure of Intact Bone

Pritchard (1972a) described bone as consisting of collagen fibres, crystals of a calcium phosphate, a type of "cement" binding them together, and a number of cells called osteocytes. The body of each osteocyte occupies a cavity or lacuna; they are spidery in shape, and have cellular extensions which extend throughout a bone volume of about 5×10^{-4} mm^3. Collagen comprises nearly one third of the dried weight of bone. It is in the form of fibers 4,000-12,000 nm in length, consisting of three left-handed helical chains twisted together into a right-handed helix, the collagen fibril (Fig. 2.1.1) (Piekarwski,1973). There are 5 types of collagen (Forster, 1984), although mainly type I is found in bone. The crystals are 300-500 nm in diameter by about 6,000 nm long, and produce an X-ray diffraction pattern similar to that of hydroxyapatite $3Ca_3(PO_4)_2 \cdot Ca(OH)_2$. They account for nearly two thirds of the dried weight of bone. The remainder is a cement which provides a continous phase through which the collagen and crystals are distributed, along with mucopolysaccharides, glycoproteins, lipids and other minor constituents of bone. These basic constituents are organised together in various ways, with different amounts of vascularity, to produce the different types of bone: fine cancellous, which is normally found in the foetus and in healing fractures, compact or cortical bone,which has a fine grained compact structure, and coarse cancellous bone. The basic unit of bone structure is the osteon, which is generally a cylindrical structure containing layers of bone around a central

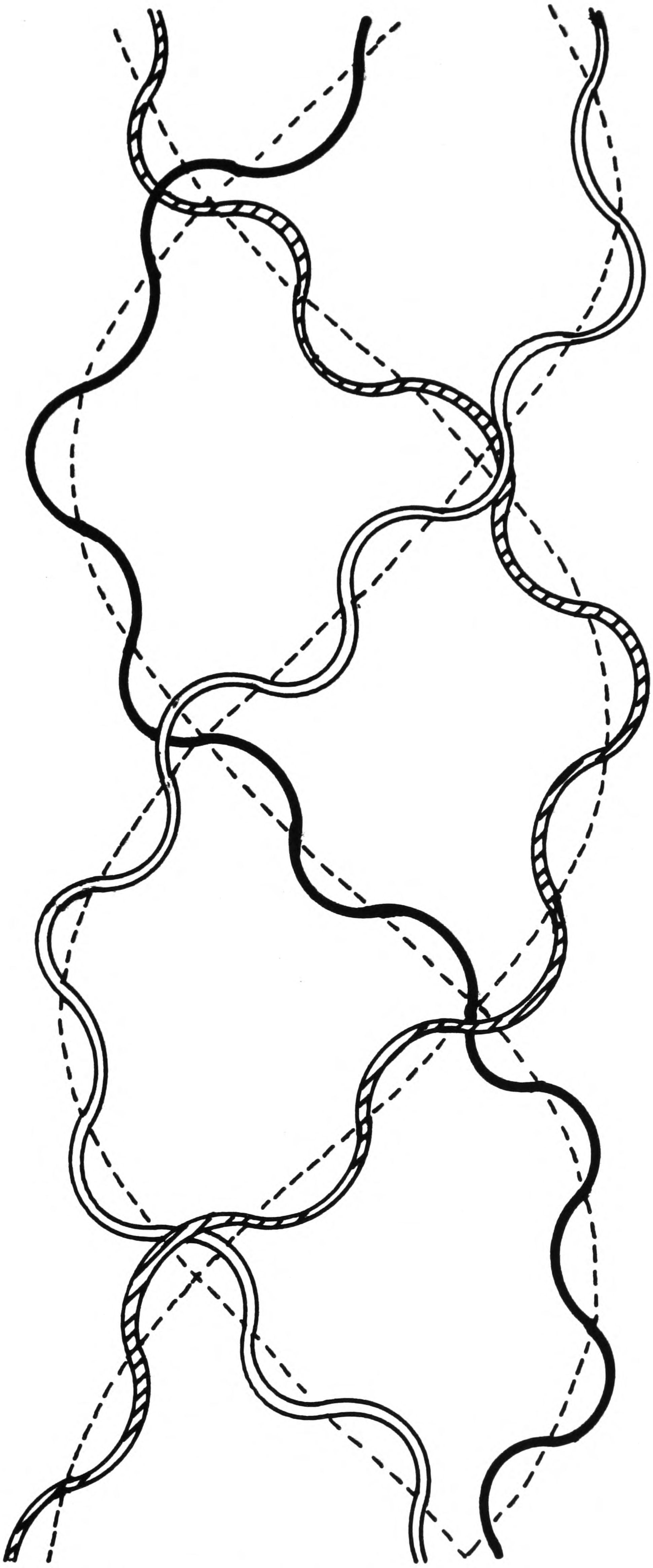

Collagen Fibril
From Bell et al (1976)

Fig 2.1.1

canal, containing blood vessels and nerve fibres. In young animals most growth occurs at the epiphyses, near the bone ends, and on the surface of the bone. In adult animals the growth is due to the production of secondary osteons leading to remodelling. Osteons are built around some, but not all, blood vessels in the bone, and the majority are orientated in the longitudinal direction of the bone. Those which are orientated in this direction are also known as Haversian systems, after Havers who first described them in 1691 (Bick, 1948). The osteocytes are arranged within the osteons, and are slightly more numerous at the ends than in the middle.

Pritchard (1972b) described bone being produced by osteoblasts, which are large cells 20 to 30 micrometers in length and of various shapes. They are found on the surface of new bone as they lay it down. They absorb amino acids, glucose and sulphate, and secrete collagen, mucopolysacchrides and glycoproteins, which become osteoid, the organic portion of bone. In adults the number of osteoblasts remains small until a fracture occurs. They are unable to divide, and are produced by the maturation of osteogenic cells, which have yet to be identified. Osteoblasts eventually mature into osteocytes.

Piekarwski (1973) analyzed bone as a composite engineering material using the Hirsch model (Hirsch, 1962), the compliance being given by:

$$\frac{1}{E_c} = x\,\frac{1}{V_1E_1 + V_2E_2} + (1-x)\,\frac{V_1}{E_1} + \frac{V_1}{E_2}$$

where E_c is the combined Young's Modulus, E_1 and E_2 are the Young's Moduli of the elements and V_1 and V_2 are the volume of the elements 1 and 2.

This is a combination of the Voigt model for uniform strain and the Reuss model for uniform stress; x is the proportion of the material obeying the Voigt model, and (1-x) is the proportion obeying the Reuss model as discussed by Hirsch. Bone approximates well to the Hirsch model with x=0.925, showing it mainly to be a uniform strain material.

2.1(ii) The Effect of Mechanical Forces on Intact Bone

Some of the early work on the effect of applied load on bone was done by Wolff (1892). Like Koch (1917) he postulated that bone remodels so that it can best resist the loads applied to it. Koch also showed that the pattern of the trabeculae follows the principal lines of stress in the bone. Bone adjusts its structure in response to the applied stress by laying down new bone in areas were the stresses are higher than optimal, and resorbing it where the stresses are lower than optimal (Goodship et al, 1979). Ascenzi and Bell (1972) quoted work by various authors, including Watt and Williams (1951), showing that rats fed a rougher diet have stronger jaw bones than those fed on a soft diet. Washburn (1947) severed muscle attachments to certain bones in growing animals; these bones were smaller than those of controls. In humans the ratio of total muscle weight to total bone weight is fairly constant at 2.4 : 1, despite varying amounts of bone (Doyle et al, 1970). The shape of the human tibia is a compromise between the circular cross-section required for optimal load bearing, and the effects of the muscles acting on it which force it into a triangular shape. The tibia of a foetus with paralysed legs was found to have a circular cross-section if the paralysis was of early onset, but the cross-section was triangular if the muscles had once functioned and subsequently become paralysed (Ralis,1980). Chamay and Tschantz (1972) showed that under tension mature bone atrophies, and under compression it hypertrophies. With static compression the growth only occured where there was plastic, rather than elastic, deformation of the bone, but with cyclic loading growth occured until the bone had adapted to the overload, whether it produced elastic or plastic deformation. Jankovich (1972) subjected rats to mechanical vibration; this did not affect body weight, bone weight, density or geometry, but it did increase the rigidity and the modulus of elasticity of the bones.

Schartzker et al (1978) tried to quantify the extent to which internal fixation of fractures protected the bones against applied stress. They strain-gauged bones in vitro, and then loaded them to determine the modulus of elasticity. The bone was then transected and repaired either by internal plates for transverse osteotomies either with or without compression, or by "lag" screws for oblique osteotomies. "Lag" screws are screws applied across an oblique fracture to stabilize the fracture. The modulus of elasticity was then determined again. The "lag" screws provided no stress protection but the plates did. The amount of stress protection did not depend on whether compression was applied to the bone, but it was affected by the stiffness of the plate. Internal fixation by plates has been used by various authors to decrease the stress applied to bone. Tonino et al (1976) used plates with different moduli of elasticity to produce different amounts of stress protection; the greater the stress protection the larger and more numerous they found were the cavities in the bone where resorption of the mineral had occurred. Woo et al (1976 and 1977) showed that stress protection reduced the ultimate yield strength of bone and the energy absorbed to failure. Paavolainen et al (1978) compared the strength loss of the tibiofibulae of rabbits when plated with and without compression, but they found no significant difference.

Goodship et al (1979) strain gauged pigs radii and removed a portion of their ulnae. This produced increased stress on the radii, but as the bone hypertrophied the strains gradually fell to those of the unoperated control limbs. Jaworski et al (1980) immobilised one hind leg in older dogs. There was a small but sharp drop in the strength of the bone compared to the contralateral control, followed by a more gradual drop which after a few months became irreversible. Hassler et al (1980) calculated, using finite element analysis, the stresses being applied to rabbit's skulls by cantilevers, and with dye techniques quantified the volume of new bone formed in the four weeks for which the loading was applied. Bone growth was accelerated with stresses up to 2 MPa; thereafter the growth rate was the same as that of the unstressed bone, until above 7 MPa bone destruction occured, due to avascular necrosis.

Thus it has been shown that intact bone reponds to the forces applied to it. If these forces are tensile then the bone atrophies, except in those regions, like the attachment points of muscles, which are adapted to tensile forces. If the applied forces are compressive then the effect depends on the level of stress which they produce. Every bone appears to have a region of optimal applied stress, although how this level is physiologically defined is not known. If the applied forces produce stresses below this level then bone absorption occurs until the stress levels are optimized. If the stress levels are excessively high, then avascular necrosis occurs. At stress levels below these, but still above the optimal region, then new bone formation occurs until the stresses fall within the optimal zone. Hassler et al (1980) appear to be the only workers to date who have quantified the region of optimal stress, and then only for rabbit skulls.

2.2 Fractures

2.2(i) The Fracturing of Bone

Bone is an anisotropic material which is weaker in tension than in compression. Long bones fracture more easily long itudinally than transversely (Evans, 1973; Pope and Outwater, 1972; Behiri and Bonfield, 1984). Adams (1978) described three basic causes of fractures: sudden injury, fatigue, and fracture due to pathological processes. Fatigue fractures are caused by repeated stresses below the ultimate yield stress, so that eventually the bone breaks before it has time to hypertrophy. An example of this is the "march" fracture, which is a fatigue fracture of the metatarsals, typically produced by marching. Pathological fractures are also produced by stresses below the ultimate yield stress for normal bone; they occur in a portion of bone weakened by disease. The cause may be a generalised bone disease such as osteoporosis, or a single area of weakened bone such as a bony metastasis from a primary tumour.

Adams (1978) also described the different types of fracture; transverse, oblique, spiral, compression, greenstick and comminuted. A transverse fracture (Fig. 2.2.1) occurs when the line of fracture is perpendicular to the long axis of the bone. An oblique fracture (Fig. 2.2.2) occurs when the fracture is on one plane, but this plane is at an angle to the long axis of the bone, generally of greater than 45^{o}. A spiral fracture (Fig. 2.2.3) occurs when the fracture spirals up the cortex, with a longitudinal fracture joining the two ends of the fracture (Bonfield and Grynpas , 1982). A compression fracture (Fig. 2.2.4) occurs typically in the vertebrae or os calcis, where the bone

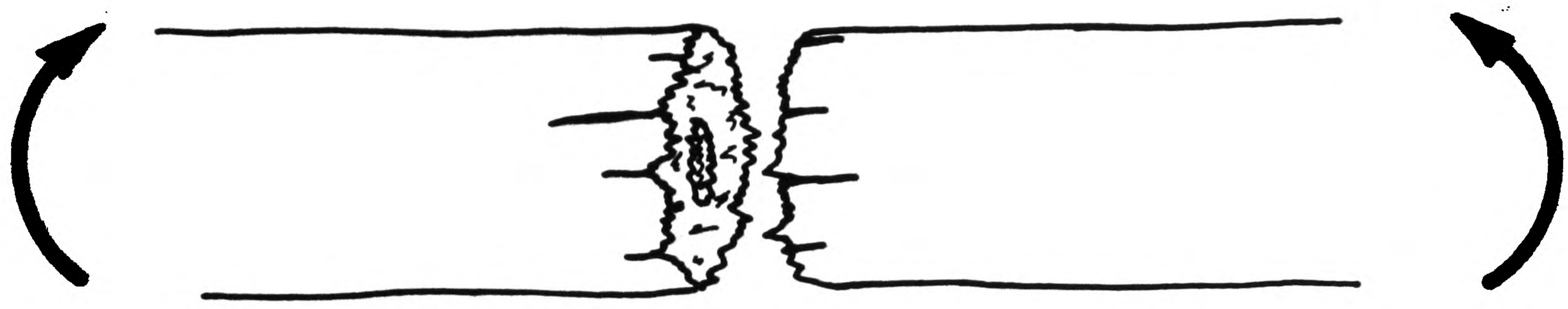

Transverse Fracture (Fig 2.2.1)

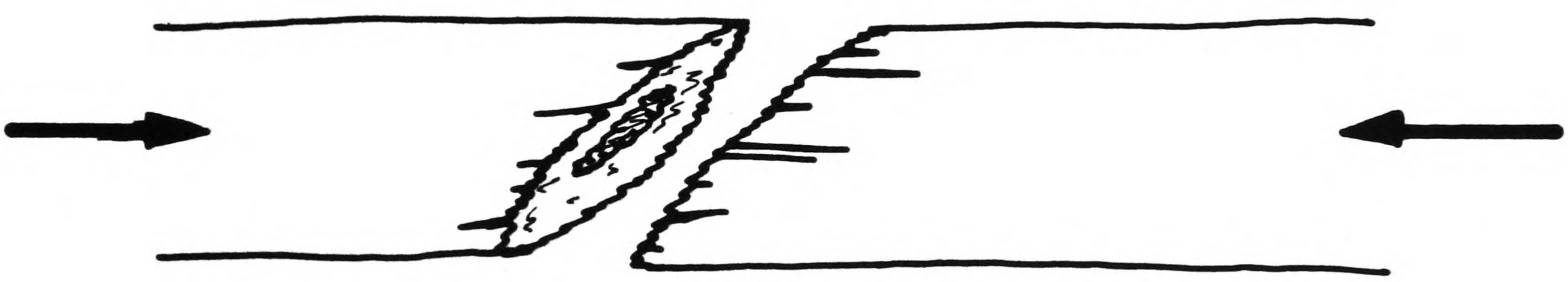

Oblique Fracture (Fig 2.2.2)

Spiral Fracture (Fig 2.2.3)

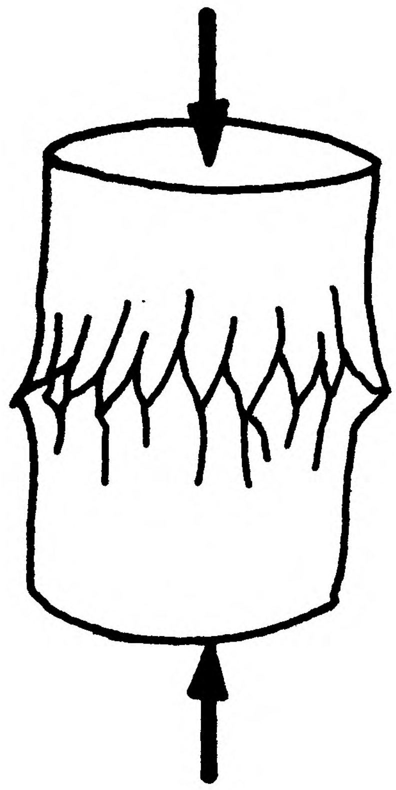

Compression Fracture (Fig 2.2.4)

Greenstick Fracture (Fig 2.2.5)

is crushed, rather than failing as a result of bending. Greenstick fractures (Fig. 2.2.5) generally only occur in young children. Their bones are more elastic and less brittle than those of adults, and when they fall, more energy is absorbed during the process of fracturing the bone, which does not fracture the whole way through. A comminuted fracture (Fig. 2.2.6) is one in which there are three or more fragments of bone: it frequently results from a high velocity injury in which a great deal of energy is dissipated. Fractures may be further divided into open or compound, where there is a wound leading to the fracture, and closed or simple, where there is no wound.

Alms (1961) described the possible mechanical causes of four different types of fracture: transverse, oblique, transverse-oblique and spiral. Simple traction is an uncommon cause of fracture, as muscular contraction generally produces compression of the bone. When traction does produce a fracture, it is generally of the transverse variety. Compression can either produce a crush fracture, as in the spine, or an oblique fracture at an angle greater than 45° to the transverse axis of the bone. Bending produces tension on one side of the bone and compression on the opposite side. The side under tension will fail, and the fracture will progress across the bone, generally producing a transverse fracture. However, if there is compression on the bone as well as bending, then as the fracture progresses across the bone, the area under compression will reach the compressive yield stress and will shear, resulting in either a transverse-oblique fracture, or a separate fragment being broken off, this being known as a butterfly fragment. Rotation produces a spiral fracture, which is a shear failure at an angle greater than 45° to the transverse axis of the bone, and progresses around the limb until the two ends are vertically one above the other, when a longitudinal fracture occurs between the two ends of the spiral.

The effect of the rate of strain on the formation of fractures has been investigated by McElhaney (1966). Under compressive loading at strain rates varying from 0.001 sec^{-1} to 1500 sec^{-1}, the ultimate compressive strength increases, the Young's modulus increases, the energy absorbed to failure increases and then decreases, and the strain at failure decreases. Panjabi et al (1973) tested bones to failure under torsion, at strain rates varying from 0.003sec^{-1} to 1.32sec^{-1}. As the strain rate increased up to 0.33sec^{-1}, they found an increase in the maximum torque, the strain at failure and the energy absorbed at failure. At higher strain rates they all fell. Saha (1977) found that increasing the linear strain rate in longitudinal shear, from 8.4 10^{-4} sec^{-1} to 8.4 10^{-3} sec^{-1} for embalmed bone led to a 16% reduction in in the strain at failure, but the energy absorbed to failure was not significantly changed. Bonfield et al (1978) investigated stably propagating cracks, with a factor of 13 between the fastest and slowest velocities of propagation. They found a tripling in the value of G_c, the critical strain energy release rate, and a doubling in the value of K_c, the critical stress intensity factor, as the crack velocity increased. Behiri and Bonfield (1980 and 1984) continued this work to include catastrophic fracture propagation. At catastrophic fracture K_c and G_c could not be measured, but the energy released at fracture fell from 2125Jm^{-2} to 125Jm^{-2} at the transition from controlled fracture to catastrophic failure. They found that controlled fracture propagation produced rough surfaces with the line of the fracture being diverted by the structures of the bone, whereas catastrophic failure produced smooth fracture surfaces. Most fractures occur at catastrophic rates rather than controlled rates.

2.2(ii) The Healing of Fractures.

According to Ham and Harris (1972) all free surfaces of bone are normally covered in either periosteum or endosteum. Endosteum is found on the surfaces of the Haversian canals, and periosteum is found on the outside of the bone. The periosteum consists of two layers, an outer fibrous layer and an inner layer of osteogenic cells. When a bone is fractured, the osteocytes near the fracture site die due to a lack of oxygen, through damage to the blood supply. A blood clot is formed between the bone ends.

There are two types of bone healing, primary and secondary. According to Danis (1949), primary bone healing occurs where there is rigid fixation and a very small gap between the bone ends, as may be seen with fractures treated by internal fixation. Under these conditions no external bridging callus is formed. The osteons whose Haversian canals cross the fracture die due to a lack of oxygen, but those which do not cross the fracture site are stimulated to proliferate, and burrow across the fracture. The continuum of osteons across the fracture site repairs the bone. The stimulus for this form of fracture repair is not known.

Where the fixation is less rigid, as in a plaster cast, secondary healing occurs (Danis, 1949). After the blood clot is formed, the cells of the osteogenic layer of the periosteum proliferate, lifting off the outer fibrous layer. This produces humps of periosteum either side of the fracture, which grow towards each other, and eventually fuse. The osteogenic cells secrete a tissue known as callus, made up of bone matrix, or osteoid, around the fracture. If there is plenty of oxygen the callus matures to form bone, but if the oxygen tension is lower then cartilage is formed. This is later replaced by bone when the oxygen supply improves, due to vascularisation of the fracture. Callus is also formed in the medullary cavity of long bones, but according to McKibbin (1978) the external callus is mechanically the most efficient, because of its distance from the neutral axis of the bone, and the amount formed is related to the amount of movement at the fracture site. The stimulus to fracture repair is unknown, and although some workers have postulated a "healing factor" which initiates healing, as yet this has not been identified.

Rhinelander (1968) investigated the blood supply in the long bones of dogs. In unfractured bones the inner 60 to 75% of the cortex is supplied by the medullary blood supply, and the rest by the periosteal blood supply. In undisplaced fractures the medullary supply is generally intact, and throughout the healing process the main supply is medullary. In displaced fractures the medullary supply is usually damaged, and the resulting haematoma prevents this from being immediately restored. Thus initially after fracture the blood supply is periosteal, the medullary supply becoming more important later in the fracture repair. In plated fractures there is little or no blood supply under the plate, despite the medullary blood supply. In nailed fractures, the medullary blood supply depends on the tightness of the nail; if it is tight then the medullary supply is obstructed and the blood supply is purely periosteal, but if the nail is loose then the medullary supply continues.

2.2(iii) Factors Affecting the Rate of Fracture Healing.

Nicholl (1964) performed a prospective study on 460 South African and 245 British patients who had sustained tibial fractures to ascertain what factors affect the rate of fracture healing. Mean time to fracture union was 15.9 weeks, with a 5% non-union rate, thus normal union was defined as 16 $\pm$ 4 weeks, i.e. between 12 and 20 weeks. They found that the factors having most effect on the union rate were initial displacement, comminution, soft tissue damage, infection and distraction. Delayed and non-union occurred in 36% of cases with moderate or severe displacement compared with 13% of cases with slight displacement. Thirty per cent of cases with moderate or severe comminution had delayed or non-union as opposed to 18% in patients with no or slight comminution. Moderate or severe non-infected wounds lead to delayed or non-union in 34% of cases, rather than 18% with nil or slight wound. Nicholl then divided the fractures into 8 grades, depending on whether displacement, comminution and wound were classed as nil/slight or moderate/severe. For each of these classes the delayed/non-union rate ranged from 9 to 55%, with an overall mean rate of 32%. The 9% rate was found in the group with no displacement, wound or comminution. Comminution alone increased the delayed and non-union rate to 15%: similarly a wound alone incresed the rate to 12% and displacement alone increased the rate to 27%. They also found that age between 16 and 60 made no difference to the healing rate.

Hoaglund and States (1976) considered some of the factors affecting the rate of healing of tibial fractures. They found that fractures healed faster in children. Open fractures took longer to heal than closed ones. High energy fractures, like those caused by car accidents, took longer to heal than low energy ones, such as were caused by a fall from a small height. High energy fractures were also more likely to be open. The position of the fracture in the bone, and its angle relative to the long axis of the bone, did not affect the healing rate, but a lack of bony opposition did increase the healing time, as did open reduction and internal fixation, although this observation may be misleading, since this type of treatment is commonly used for the worst fractures. Johnson and Pope (1977) found that amongst the skiers they studied, the fractures which did not require reduction healed faster than those which had to be reduced. Johnson and Pope were also unable to relate the healing time to the amount of comminution, the type of fracture (spiral or transverse), or the position of the fracture in the bone. Patients who were 16 or over took about 80% longer to heal than those under 16.

Allum and Mowbray (1980) reviewed 500 patients and they also found that with patients of 16 and under the rate of healing was faster than with adults. They also found there were no non-unions or delayed unions in the children. In these patients the cause of the fracture did not appear to influence the rate of repair. With patients over 16, fractures as a result of accidents to pedestrians or motorcyclists healed more slowly than those due to sport (mainly football or rugby) or caused to car occupants. The first two groups had higher rates of compound, comminuted and displaced fractures. The authors considered that pedestrians and motorcyclists, in general, suffered high energy or direct violence fractures, whereas car occupants and sportsmen generally suffered indirect or low velocity accidents. Surprisingly they found that an intact fibula decreased the time to healing, although this might indicate a low energy fracture.

Thus, in general, slow healing is expected with open, displaced, comminuted fractures with soft tissue damage and infection present. Other factors leading to delayed union, according to Adams (1978), are avascularity of a segment of the fracture, interposed soft tissue, and certain pathological conditions. Fractures through bone cysts and benign tumors heal slowly, but those through malignant tumors usually only heal after the treatment of the tumor. Corroding metal implants also delay healing.

2.2(iv) The Effect of Mechanical Forces on Fractures

Some of the early work on the healing of experimental fractures was done by Eggars et al (1949). They produced rectangular flaps in the skulls of rats, and applied a force at the free end of the flap, perpendicular to the two parallel sides, producing a gradually increasing stress across the osteotomy. They observed maximum healing at the area of medium compression. The area under maximal compression underwent avascular necrosis, and the area under minimum compression healed only slowly, showing that there is an optimum compressive stress. Freidenberg and French (1952) applied known compressive forces to the osteotomised ulnae of dogs; they found maximum healing with compressive forces of 0.6-0.8 N, and avascular necrosis with forces greater than 1.4N. However, they did not calculate the stresses produced by these forces. They believed that the enhanced healing was due to the more secure fixation and closer contact of the fragments. These two papers show the same pattern as the work of Hassler et al (1980) on intact bone (described in section 2.1(ii)).

Yamagishi and Yoshimura (1955) experimented with rabbits using external fixators to produce different types of loading conditions applied across experimental fractures. The loading conditions studied were, 1) firm fixation using a stiff fixator; 2) loosely controlled fixation where the pins were free to move along the bar; 3) compression of the fracture; 4) forced separation of the bone ends, and 5) alternating shearing forces. The latter were produced either by applying longitudinal varying compression to an oblique fracture, or by applying forces perpendicular to the long axis of the bone, the direction of force being altered every 24 hrs. Upon sacrifice the callus formed was inspected radiographically and histologically.

Different types of callus were formed depending on the type of force applied. Pseudoarthroses were produced by the shearing forces. The authors did not compare the healing rates for the different cases.

Lettin (1965) compared the healing of osteotomies in rabbits when treated by plating with compression, plating without compression and by plaster cast. It was found that plated fractures healed faster than those in plaster casts, but there was no significant difference between the two types of plating. The work of Schartzer et al (1978) showed that the amount of stress protection was unaffected by whether or not compression was applied by the plate (see section 2.1(ii)).

Hutzchenreuter et al (1969) altered the rigidity, and consequently the amount of stress protection, of internal fixation plates by altering their thickness. These plates were applied to osteotomised sheep's tibiae, after the removal of the periosteum. Weight-bearing was allowed after a few days. After 7 weeks, with the thinnest plates there was some bone resorption, but also some immature callus. However, after 4 months the callus had disappeared, and the osteotomy had widened. With the medium thickness plates there was less callus, but more osteoporosis, and with the thickest plates there was only a small amount of callus at 7 weeks, and after 4 months there was no visible sign of the osteotomy. However there were problems with the thickest plates, the bone tending to break at the end of the plate.

Hassler et al (1974) used finite element analysis to calculate the stresses which they applied to osteotomies in rabbits' skulls. These osteotomies were allowed to heal for two to four weeks, and 24 hours before sacrifice the rabbits were injected with 200 μCi of ^{45}Ca and 400 μCi of ^{3}H proline. After sacrifice, sections were examined for uptake of the radioactive isotopes, and also histologically for the "amount" of healing which has taken place. The maximum isotope uptake was for stresses in the range 0.07 to 0.2 MPa. Outside these ranges the healing rate was lower, but within this range the different measures of healing showed maxima at different stresses. The ^{45}Ca uptake was the highest for a stress of 0.11 MPa while ^{3}H proline uptake was maximum for 0.08 MPa. The maximum healing seen with histology was at 0.19 MPa. These are much lower than the stresses which they applied to the intact skulls of rabbits; accelerated bone growth was produced by stresses of 2 MPa and avascular necrosis was produced by stresses greater than 7 MPa. According to Laros (1974), after his experiments on rabbits with fixators with different amounts of rigidity and compression a small but unspecified amount of compression, increasing the rigidity, is optimal. Sarmiento et al (1977) showed in experiments on rats that a weight-bearing splint produced a callus which was initially quite plastic, but hardened quickly, whereas non-weight-bearing splintage produced less callus which hardened more slowly.

Panjabi et al (1977) and White et al (1977a and 1977b) osteomised the legs of rabbits and tried to compare the difference in healing between bones subjected to constant stress and those subjected to cyclic loading. The constant loading was 20 N, and the cyclic loading was from 0 to 40 N at a frequency of 55 cycles/min (0.92Hz) for 4 hours daily, and a constant load of 20 N for the rest of the time. There was no significant difference in the type or rate of healing between the two types of loading. The fractures were tested in torsion to failure, and showed four stages of healing. Stage I was a "rubbery" low stiffness failure with high angulation at failure; this lasted for 21 to 24 days. Stage II failure occured with a higher stiffness, but the failure occured entirely through the fracture site, and at failure the angulation was reduced and the torque had increased. Stage III failure was a high torque, high stiffness failure, with some of the new fracture line passing through previously intact bone. Stage IV failure occured entirely in the intact bone. This study agrees with the work of Kirillov et al (1978), also on rabbits, who also distinguished four distinct phases in fracture healing, which could be separated by the mechanical properties of the fracture callus. Kirillov et al also found a linear relationship between the Young's Modulus of the callus and its radiographic density.

Connolly et al (1978) tried to distinguish between the reactions of different bones to being fractured. They osteotomised one radius and several ribs of dogs, and allowed them to heal, splinted either by the ulna or by the other ribs as appropriate. The fracture testing was done mechanically, histologically and biochemically. The ribs quickly regained their strength, followed more slowly by their stiffness. However, the radii regained their stiffness before their strength, stiffness being considered by the authors to be the most important property of the bones in the forearm, the reverse of that for the ribs.

Bradley et al (1979) used plates of varying stiffness, with a factor of 12 between the minimum and maximum, to plate osteotomies of canine femurs. The bending strength at failure, and the bone structural stress at failure, were measured under the plate, and on the diametrically opposite side of the bone, after 16 weeks, and compared with the unplated contralateral control femur. The strength of the bone under the plate was almost unaffected by the rigidity of the plate, but that opposite the plate was significantly decreased with increasing rigidity of the plate. The movement opposite the plate is mainly due to the the bending of the plate whereas the movement under the plate is is mainly due to its compression, and as a result is much lower.

Sedel et al (1980) compared plating with nailing on the osteotomised metatarsals of sheep. The testing was done after 8 months, and for each sheep the osteotomised bone was compared with the contralateral limb. The normalised ultimate bending strength, stiffness, moment of inertia, energy absorbed to failure and maximum calculated stress at failure were all greater for the nailed than the plated bones. The main effect of an intramedullary nail is to prevent shearing and angulation, but compressive movements are free to occur. A plate prevents shearing and intermittent compression, but a static compressive force may be applied, and an externally applied compressive force may produce an angulation of the fracture. A nail takes only a small amount of any compressive force applied, whereas a plate takes most of it. A nail affects the medullary blood supply, while a plate effects the periosteal blood supply.

Henry et al (1968) compared the effects of the different fixation devices on the biological environment. Rabbit's radii were fractured, and then were either left alone to provide controls, or had two half nails or two half plates applied, so that none of these gave any mechanical fixation to the fracture. After healing, the bones were tested to failure under 4 point loading, and each leg was compared with its control. The stiffness and ultimate yield strength were compared for the three groups, and no significant difference was found, implying that the presence of the metal did not affect the healing, and that it is the different mechanical environments which produce the different rates of healing, not the changes in the blood supply.

Thus it seems clear that medium level compressive forces applied to a fracture appear to produce the maximum healing rate. If the forces applied are too great then avascular necrosis occurs, but if the compressive forces are low then healing occurs, but more slowly. If shearing forces are applied to the fracture then a pseudo-arthrosis may be produced. Different fixation devices produce different mechanical environments at the fracture site, and it is this factor, rather than the changes in blood supply, which appear to affect the rate of healing.

2.2(v) The Effect of Temperature

Eagleson et al (1967) tried to accelerate healing by warming the fracture. Electric coils were put in the plaster casts around osteomised canine tibiae, with a thermocouple in the leg, and the current was varied so that the internal temperature of the leg was increased by 1-2^{o}C over the contralateral control leg. More callus was seen radiographically, but there was no significant difference in the type of healing. Mostafa et al (1980) made use of the fact that the tail vertebrae of mice are at approximately room temperature. The rate of healing of fractured tail vertebrae was found to be greater in mice kept at higher ambient temperatures.

2.2(vi) Piezoelectricity and Electrical Stimulation

The piezoelectric effect in bone was discovered independently in the 1950s by Bassett and Becker in New York and by Fukada and Yasuda (Fukada, 1957) in Japan. According to Bassett (1968 and 1972) the electric potential is generated by the extra-cellular osseous matrix in both living and dead bone. When the bone is deformed, a voltage is produced due to the displacement of electrons, which gradually leak away until there is no net charge. When the load is removed, a reverse voltage is produced, which again leaks away. When a bone is loaded as a cantilever, the upper surface is in tension and produces a positive charge, and the lower surface is in compression and produces a negative charge. The voltage generated is affected by the strain rate; if the rate is low then the voltage leaks away as it is being generated. Above a certain strain rate the rate of production of the voltage is greater than the rate of leakage, and the effect of the leakage becomes less important. The voltage produced is linearly related to the load applied. Tendons are also piezoelectric, and it is not clear whether the effect in bone is produced by the collagen, or by the collagen-hydroxyapatite junction acting as a p-n piezoelectric junction (Williams and Breger, 1975).

Two techniques for the electrical stimulation of fractures have been described - electromagnetic and direct. Bassett et al (1977) used two Helmholtz coils, one on each side of a fractured limb, outside the plaster. The coils produced a magnetic field perpendicular to the limb, and thus induced a current through the limb and consequently through the fracture site. The current applied to the coils was pulsed, and either a single pulse or a train of pulses could be applied at a given frequency. Direct electrical stimulation was described by Romano et al (1976) and Watson (1979), who applied cathodes to the fracture site, with an anode at a remote site. Bone growth occured at the cathode, and bone destruction occurred at the at the anode, if it was in bone. This problem was solved by placing the anode on the skin, but it needed to be moved every few days to prevent skin irritation. Levy (1974) considered bone growth to be a feedback system, with stress producing a negative charge which stimulates bone growth. He produced a transfer function for the system, and calculated the frequency of oscillation of the system to be 0.7Hz. Using this system he altered the magnitude, direction and duration of the signal and found that pulsed stimulation was the most effective in vivo. Totally implanted direct stimulation of fractures is now commercially available.

2.3 Methods of Treatment of Fractures

2.3(i) The Treatment of Fractures in Ancient Times

Splints of various types have been used since at least the begining of recorded history (Epstein, 1937). Egyptian Mummies of the Fifth Dynasty (2750-2625 B.C.) have been found with broken bones which had been splinted (Smith, 1923). In India at an unknown date B.C. the Ajur-Veda of Susruta described the use of bamboo splints for the treatment of fractures (Bick, 1948). Hippocrates (c.420 B.C.) described the treatment of fractures using compression bandages for a week to ten days until the swelling went down, and thereafter bandaging splints on top of the compression bandage to immobolize the fracture. Traction was used to reduce the fracture and various types of traction device, both mechanical and manual, have been described. In Greece, Paul of Aegina (625-690 A.D.) discussed the problems of malunion and advised caution in the use of corrective osteotomies. In the 12th Century in Bologna improvements were made in the splints then in use (Bick, 1948). In the same century Guy de Chauliac (1300-1368) advocated the use of bandages steeped in egg whites and red oil for the treatment of fractures.

2.3(ii) Current Methods of Fracture Treatment

According to Adams (1978) the three basic methods of treating fractures are: external splintage, internal fixation, and external fixation.

The original method of splintage, by tying rigid supports around the broken limb, has now developed into the use of Plaster of Paris casts, and the more recent developements of heat-cured and ultra-violet light cured casts, as well as thermoplastic splints. Casts work by immobilizing the adjacent joints, thus reducing, but not totally eliminating, movement at the fracture site. The great advantage of this system is that it is non-invasive, but problems may arise from the limitation of movement at the adjacent joints, and also the plaster prevents access to the skin surface of the injured limb, which may be a problem if there is soft tissue damage which needs to be treated.

Internal fixation is a method of splinting the fracture directly. It is usually achieved either by a "plate" of a biocompatible material being screwed onto the bone, or an intramedullary nail passed along inside it. Surgical steel is usually the material employed, although titanium and cobalt-chromium alloys are also used. Plating (Fig. 2.3.1) has the advantage of rigidly fixing the fracture, while at the same time it permits movement of the adjacent joints, thus reducing the risk of osteoarthrosis which can occur following prolonged immobilisation of a joint. On the other hand, it has the disadvantages of being invasive, requiring a large incision to get the "plate" to the fracture site, and sometimes a futher operation later to remove it (London, 1980). This increases the chance of infection, and also requires the presence of viable skin over the fracture site. The problems commonly encountered are the screws loosening in the bone, thus losing the rigidity of the fixation, and fracture or bending of the "plate". Intramedullary nailing (Fig. 2.3.2) is achieved by a "nail" nearly as long as the bone, and approximately the same external diameter as the intramedullary cavity. The nail is introduced at one end of the bone and is driven into the cavity usually after reaming. It prevents shearing and angular displacements of the fracture, but

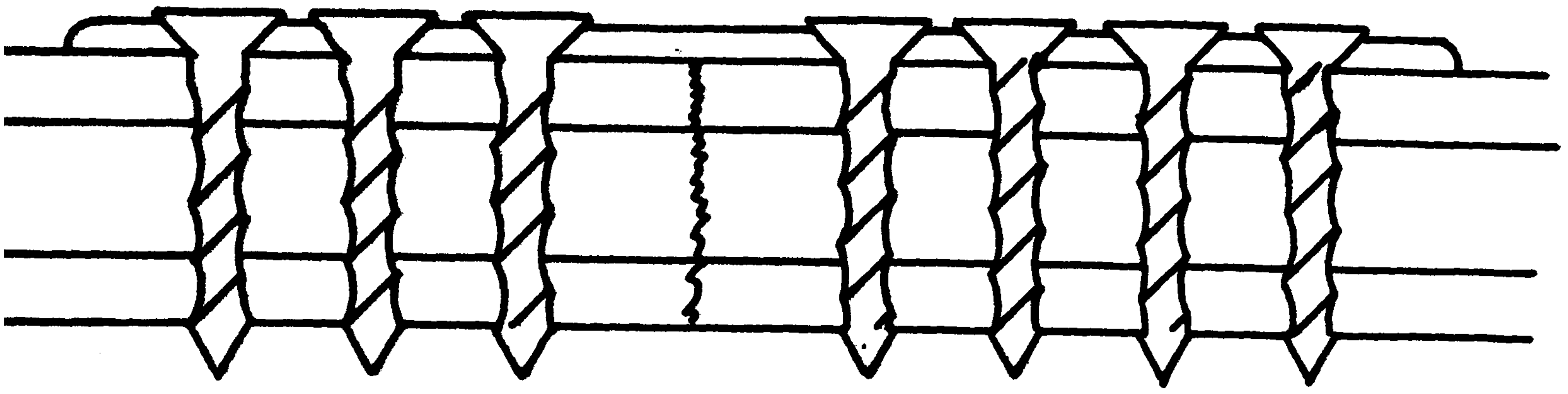

Bone Plate
(Fig 2.3.1)

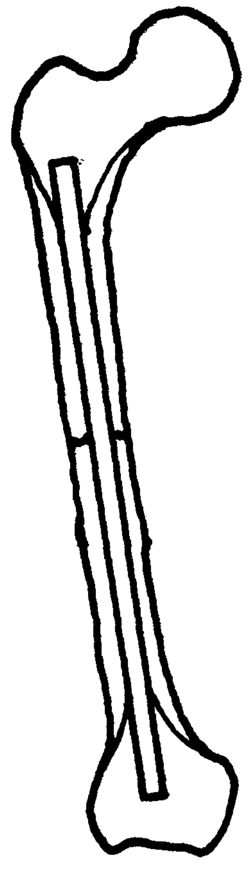

Intramedullary Nail
(Fig 2.3.2)

permits torsion and compression. It is not suitable for compound fractures. Other types of internal fixation which are used for simple oblique fractures consist of wires wrapped under tension around the bone to hold the two portions together (cerclage wires), and screws across the fracture site to join the two fragments together (lag screws).

External fixation is a method of "bridging" the fracture site, using transcutaneous "pins" and support bars. This method does not require the presence of viable skin over the fracture site, as the "pins" may be placed well away from the damaged area. This skin is then accessible for dressing and any other surgery necessary. The patient is able to move the adjacent joints and preserve muscle function. The main problems encountered are the loosening of the "pins", and infections of the pin tracks. The present study makes use of an external fixation device, which will be considered in more detail in the following sections.

2.3(iii) External Fracture Fixators

External Fracture Fixators can be divided into two basic types-single-sided (Fig. 2.3.3) and double-sided (Fig. 2.3.4). The single-sided consists of threaded pins screwed into the bone, above and below the fracture, connected together by a single support bar. The double-sided consists of pins passing through the bone, both above and below the fracture, with support bars at each end of the pins connecting the two sets, although the double-sided has various more complex variations.

Vidal (1983) divides external fracture fixators into six

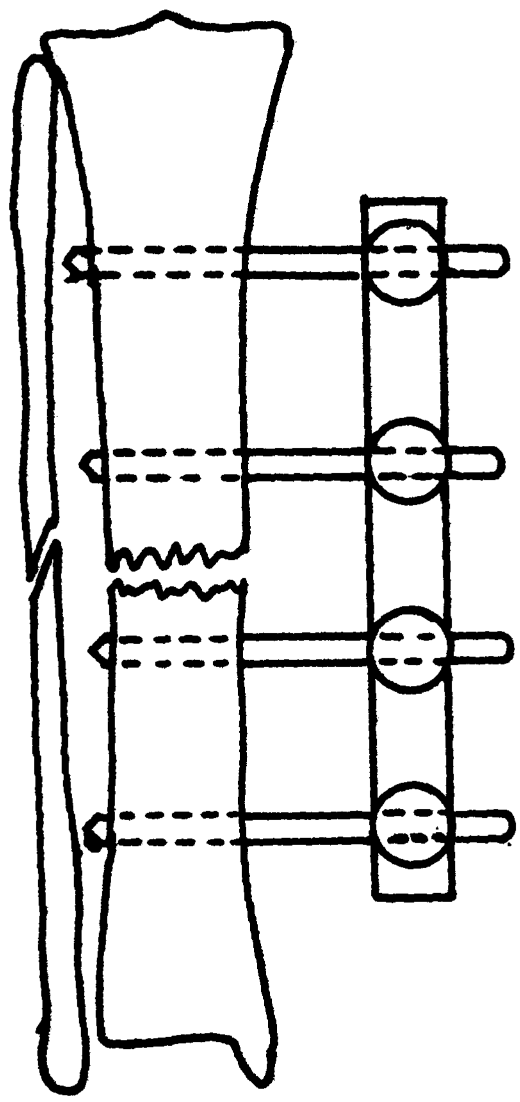

A Single-sided External Fixator

Fig 2.3.3

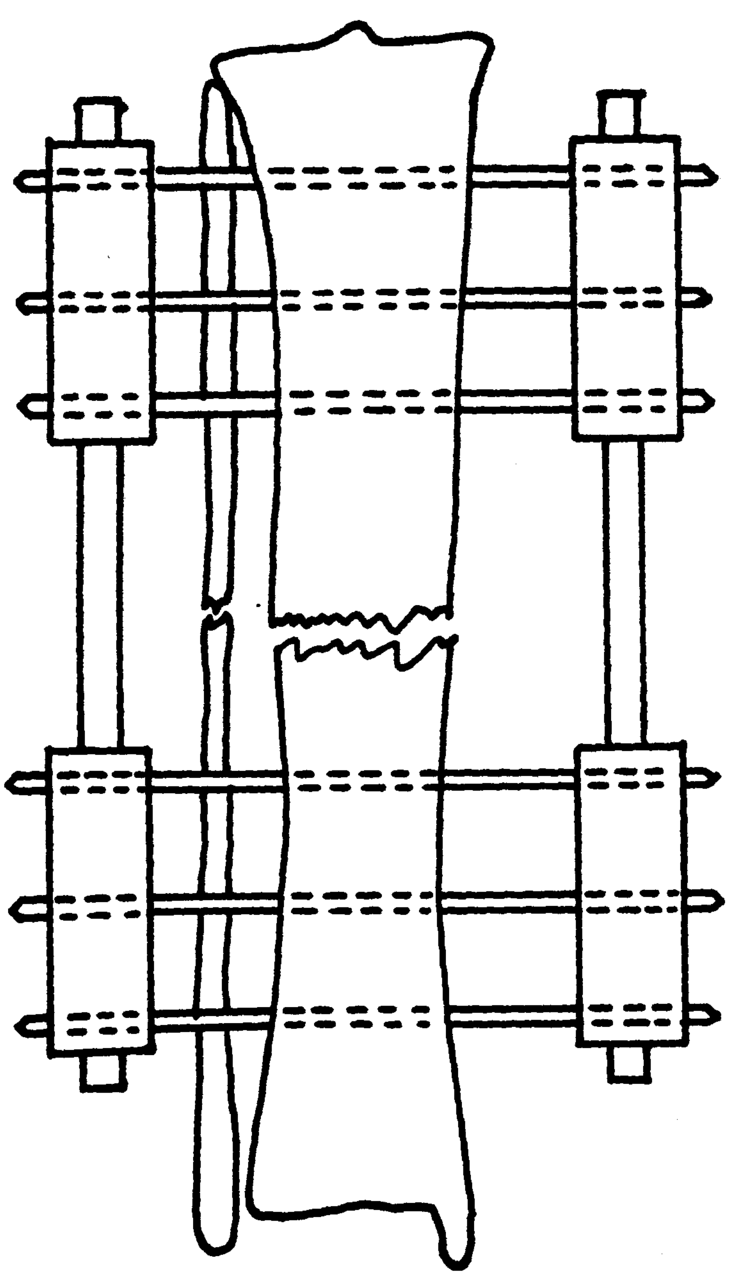

A Double-sided External Fixator

Fig 2.3.4

subgroups, unilateral or single-sided and then five groups of double-sided fixators. These groups are: a) bilateral, with a single support bar at each end of the pins (Fig. 2.3.4); b) quadrilateral (Fig. 2.3.5), with two support bars at each end of the pins, one on each side of the pin clamps; c) triangular (Fig. 2.3.6), a bilateral fixator with a single-sided fixator applied at an angle to the transfixing pins, with interconnecting rods connecting the single-sided fixator support bar, with each of the bilateral fixator support bars; d) semi-circular (Fig. 2.3.7), where the support bars hold semi-circular rings about the limb, and then pins pass into or through the base at various angles; e) circular (Fig. 2.3.8), where there are complete rings about the bone and various transfixing pins.

External Fracture Fixation was first used by Malgaigne in 1853, but the first published design was by Parkhill in 1897 and 1898 (Fig. 2.3.9). His fixator was made of silver plated steel. There were two pins above and two pins below the fracture, and two pairs of curved plates. Each pin was clamped to a plate, the outer pins being clamped to the longer plates. This was done by one nut above and one below the plate. The four plates were then clamped together by another two straight plates. This allowed for non-uniform distances between the pins, although the pins did have to be parallel. The limb was then encased in Plaster of Paris until the fracture had consolidated. He describes its use in 14 cases on the humerus, radius, ulna, femur, and tibia, for non-unions, malunions, and fractures with a tendency to displace, and claims (1897) 'no method has ever before given 100 percent of cures' although he only reports 9 cases in the 1897 paper and a further 5 in the 1898 paper.

Lambotte produced the next design in 1907 (Fig. 2.3.10). This was a single-sided fixator, with two pins above and two below the

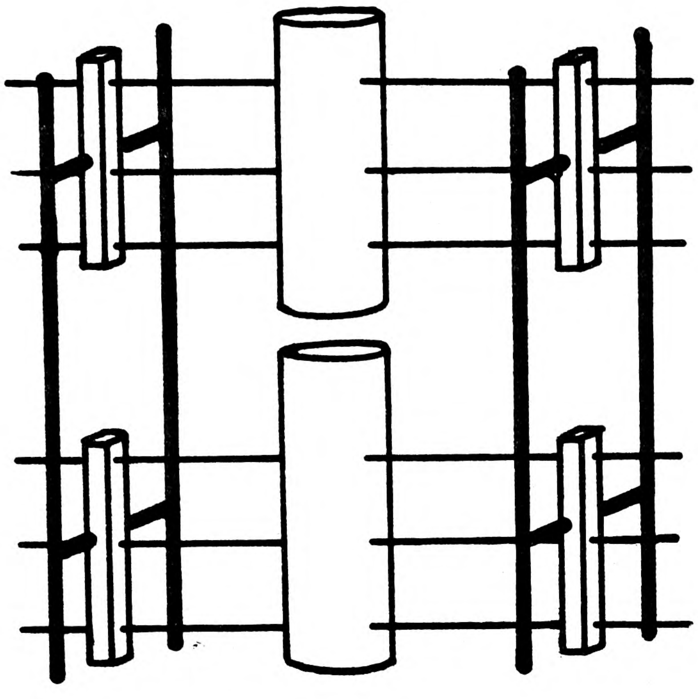

Quadrilateral

Fig 2.3.5

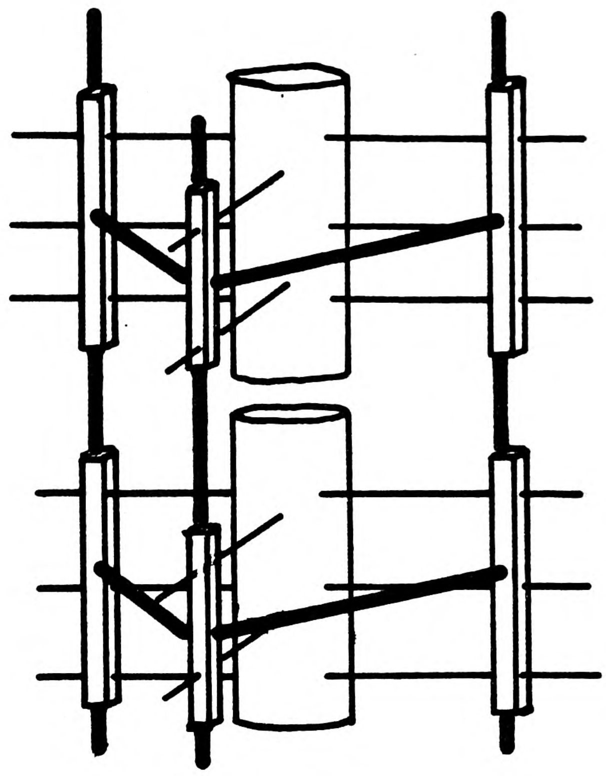

Triangular

Fig 2.3.6

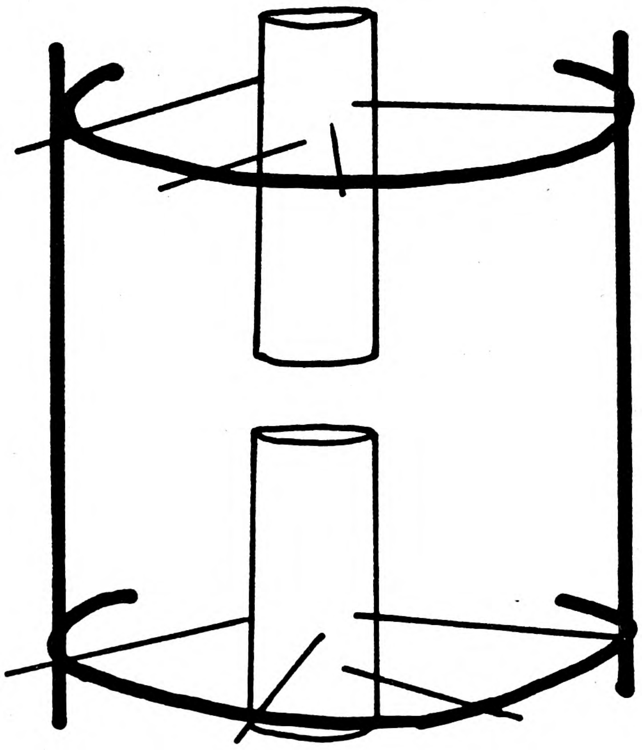

Semi-Circular

Fig 2.3.7

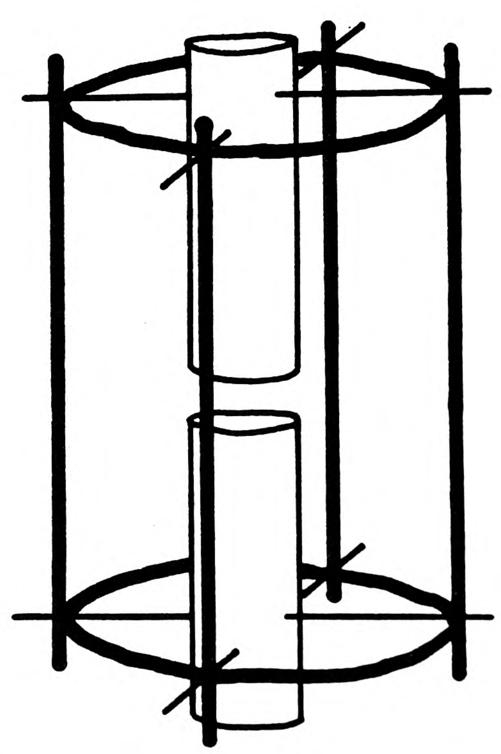

Circular

Fig 2.3.8

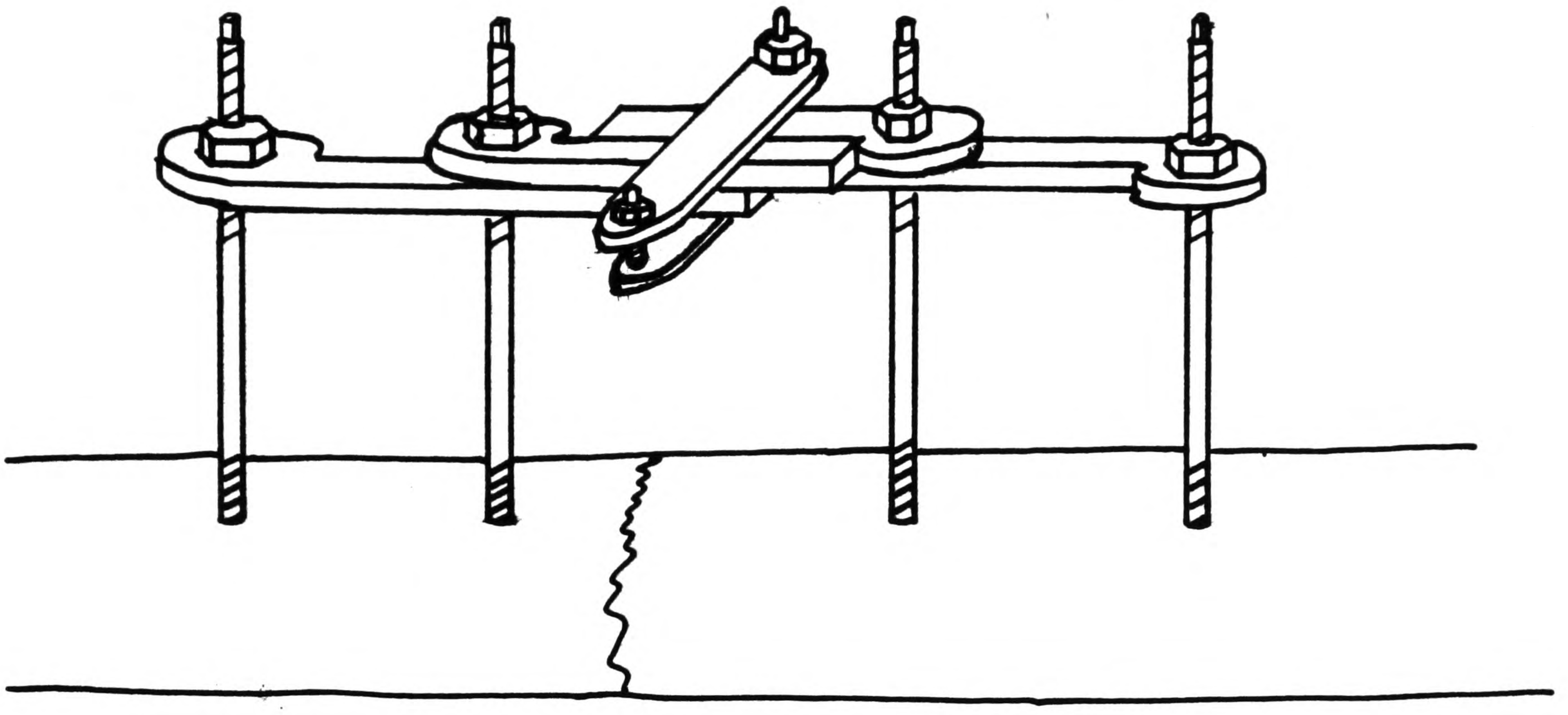

Parkhill (1897)

(Fig 2.3.9)

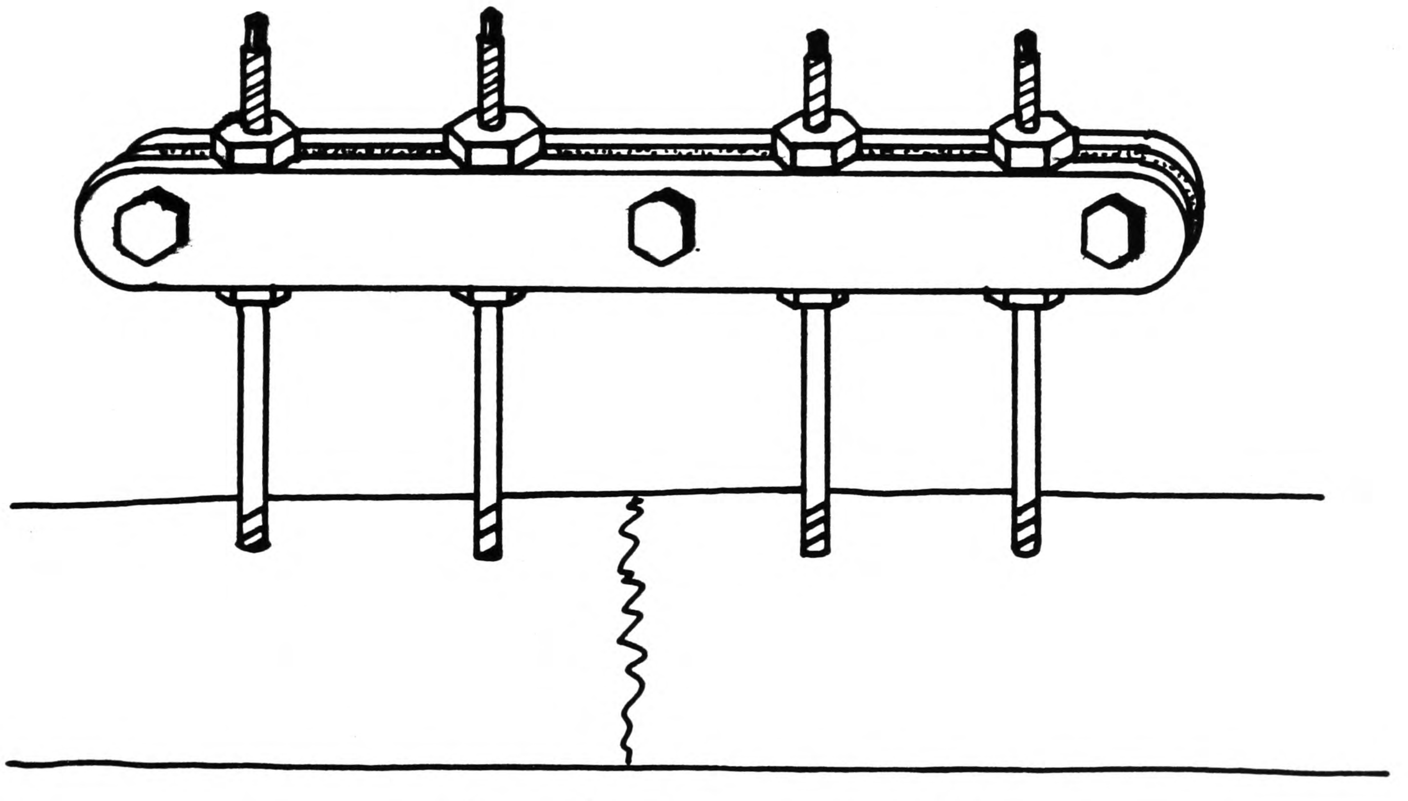

Lambotte (1902)

(Fig 2.3.10)

fracture site held between two pieces of metal clamped together. During the 1930s fixators were designed by Anderson (1934), Stader (1937 and 1939), Haynes (1939), Hoffmann (1938), and others. However, during the Second World War their use by American Army Surgeons was banned due to the high infection rate (Peterson, 1949 and Mears, 1979). Since then various types of fixators have been described. The double-sided include the "Audrey-Vidal" modification to the "Hoffmann" (Vidal et al, 1970), and others by Rezaian (1971) and Wynn-Jones (1978). Examples of the circular type are described by Dywer (1973), and Ilisarov (1976). Single-sided fixators have been described by, amongst others, Edge and Denham (1977), Banks and Dervin (1980) and Kenwright et al (1979).

More recently various authors have suggested that it would be advantageous to have variable stiffness fixators. Bucholz et al (1983) suggest that major injuries of the tibia should be initially treated with a triangular fixator, consisting of a doubled-sided fixator, connected by side members to a single-sided fixator. They then advised that as the fracture heals the side members should be removed, and then one of the fixators should be removed. A different philosophy has been adopted by Evans et al (1982) and De Bastiani et al (1984). Both these sets of authors have described single-sided external fracture fixators with a sliding mechanism in the support bar, thus permitting a controlled decrease in the axial stiffness while retaining high bending and torsional stiffness.

2.3(iv) Engineering Analyses of External Fixators

Various Authors have considered the mechanics of fracture fixators with the intention of increasing the stability of the fixator. Burny and Bourgois (1972) conducted experimental tests on the "Hoffmann" to determine the configuration which would have the greatest possible rigidity. They concluded that the rigidity was increased if more pins were used per clamp, if the distance between the clamps and the bone was reduced as far as possible, if one supporting bar was applied to each side of the pins, and if two fixators were used. They also felt that if the pins were smooth, rather than "notched", there would be less problems with fatigue fractures. The Stein mann pins they used were marked with a notch every centimetre, as a guide to the surgeon.

Hierholzer et al (1978) divided external fixators into three types; type I: a single-sided fixator, for example the single-sided A.O. or the Wagner; type II: double-sided like the A.O. or the Hoffmann, as shown in Figure 2.3.5; and type III: a double-sided fixator with a single-sided fixator applied perpendicular to it, either with or without the two sets of support bars connected to each other, as shown in Figure 2.3.6. They conducted mechanical tests of different arrangements of type III, with varying numbers of pins in each segment of bone. Using this type of fixator they found that it was possible to stabilize metaphyseal fractures where the size of the smaller segment was too small to permit either the 2 Stein mann pins necessary for a double-sided fixator, or the 2 Schanz pins reqired by a single-sided fixator. They used one Stein mann pin and one Schanz pin in the smaller segment, and achieved sufficient stability.

Chao et al (1979) analysed the "Hoffmann", varying the number of pins, the pin diameter and length, pin group separation, clamp separation, frame configuration, the number of supporting bars, the type of fracture, and the amount of compression applied to the fracture. They used an equivalent stiffness index to compare the different arrangments; this index combined the stiffnesses in different directions into a single figure. Behrens et al (1982) compared the A.O. (Arbeitsgemeinschaft fur Osteosynthesefragen, or The Association for the Study of Internal Fixation) and the Hoffmann fixators in both their single-sided and double-sided configurations, when applied in both anterior-posterior and lateral directions. They found that for the same distances between the pins, and between the bone and the support bar, the double-sided fixators were stiffer than the single-sided, and that the A.O. fixator was stiffer than the Hoffmann. Chao et al (1979) and Behrens et al (1982) found that increasing the inter-pin distances, decreasing the support bar to bone distance, and using stiffer pins produced stiffer fixation.

Evans et al (1979) calculated the conditions required for maximal stiffness of a single-sided fixator. The pins in each fragment should be separated as far as possible, the bar should be as close as possible to the bone, and the pin diameter should be optimised; the thicker the pin the lower the pin deformation and the shear stresses at the pin-bone and pin-clamp interfaces, but too large a pin would excessively weaken the bone. Pope et al (1983) analysed pin fixation and found that increasing the pin diameter from 3 mm to 5 mm decreased the deformation by between 197% and 228%, depending on the insertion technique. Boltze et al (1976) in an A.O. Bulletin, advised adding a set of Schanz pins to their double-sided fixator, with some extra supporting bars and clamps to produce a triangular structure about the limb. Boltze et al (1978), in a later A.O. Bulletin, also advised greater pin separation within the clamps, mutually tensioning the pins against themselves, putting the pins as close as possible to the fracture site and again using a set of Schanz pins to produce a triangular system about the limb.

Kempson and Campbell (1981) and Campbell and Kempson (1981) tested six different external fixation devices, both single and double-sided. The fixators tested were the Denham, the Day, the Vidal-Hoffmann, the A.O. tubular system, the Sukhtain-Hughes, and the Oxford. They found in general that the double sided were stiffer than the single sided. They found that an increase in the number and the diameter of the pins, and the number and the stiffness of the connecting bars, increased the stiffness of the fixator. Loosening of the pins in the bone, which was inclined to happen in weak or osteoporotic bone, led to reduced stiffness of the fixator bone system.

Karaharju and Aalto (1983) tested the A.O., the Day, the Hoffman and the Kalnberg external fixators, the first three of these both in single-sided and double-sided configurations. The Kalnberg, which consists of a circular frame with Kirschner wires, was only tested as a double-sided fixator. The pin separation in all cases was 5 cm in each bone segment, but the pin length was not stated. They were tested in torsion, bending both in the plane of the pins and perpendicular to it and in axial loading. They found double-sided fixators were stiffer than single-sided, that all the fixators were stiffer when the bone ends were in contact, but they decided that all were stiff enough even for severely comminuted fractures.

Churches et al (1985a and 1985e) in a mainly experimental study considered the stiffness of the "Oxford" fixator, both the Mark I and the Mark II sliding types. We found that stiffness was related to pin length to the power of -2.0 and pin separation had no significant effect in the axial direction but that in different directions different relationships applied. We also found that one loose pin decreased the axial stiffness by 23%, the torsional stiffness by 8% and the bending stiffness by 15% in one direction, and an amount dependent on the fixator geometry in the perpendicular direction.

2.4 The Stiffness of Healing Fractures

2.4(i) Mechanical Methods of Measurement

Various authors have considered the stability of tibial fractures while they are healing. Jernberger (1970) determined the stiffness of healing tibial fractures using a device which measured the deflection for a known load (Fig. 2.4.1). This instrument consisted of a steel beam attached to the bone by three pins inserted under local anaesthetic, with fracture between two of them. The two outside pins held the bar in place while a load was applied by the central pin. The deflection was read from a position transducer on the central pin; a similar measurement of the contralateral leg was used to give a measure of the deflection of the steel bar and the intact tibia. This device was used on 40 cases clinically, and in healing fractures the flexibility of the fracture decreased approximately exponentially, the time constant was not calculated. With delayed and non-unions no decrease was seen, and with premature weight-bearing an increase in the flexibility was seen.

Jørgensen (1972a,b,c and d) used a deflection measurement device (Fig. 2.4.2) on patients whose fractures were fixed with a single-sided "Hoffmann" fixator. The supporting side-bar was replaced by two bars connected by a dial micrometer. A known transverse load was applied in each direction to the distal part of the limb, and the deflection was recorded. The angulation of the fracture was calculated from the two deflections and the distance between the centre of the bone and the micrometer bars. Full weight bearing was allowed when the deflection was less than 0.5 degrees for a bending moment of 0.06 Nm (0.6 kgfm) at the fracture. After several weeks,

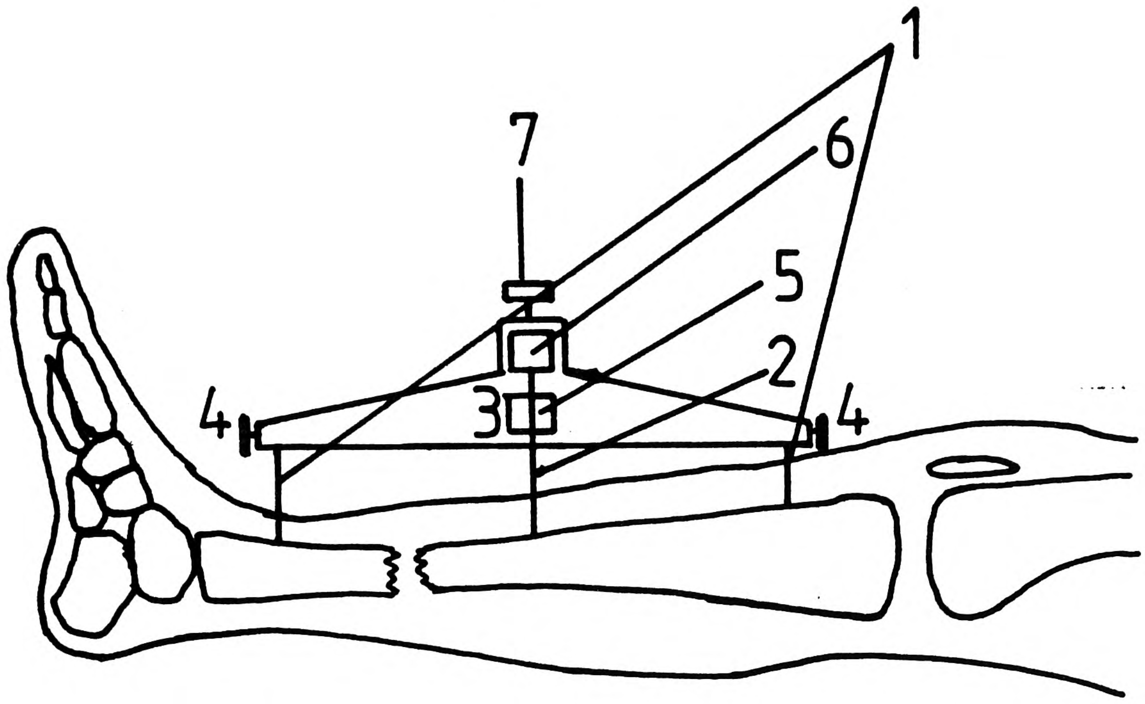

1 Outer Pins
2 Inner Pin
3 Measuring Bar
4 Outer Pin Clamps
5 Position Transducer
6 Force Transducer
7 Force Application Device

Jernberger's Measuring Device

A Typical Deflection Curve

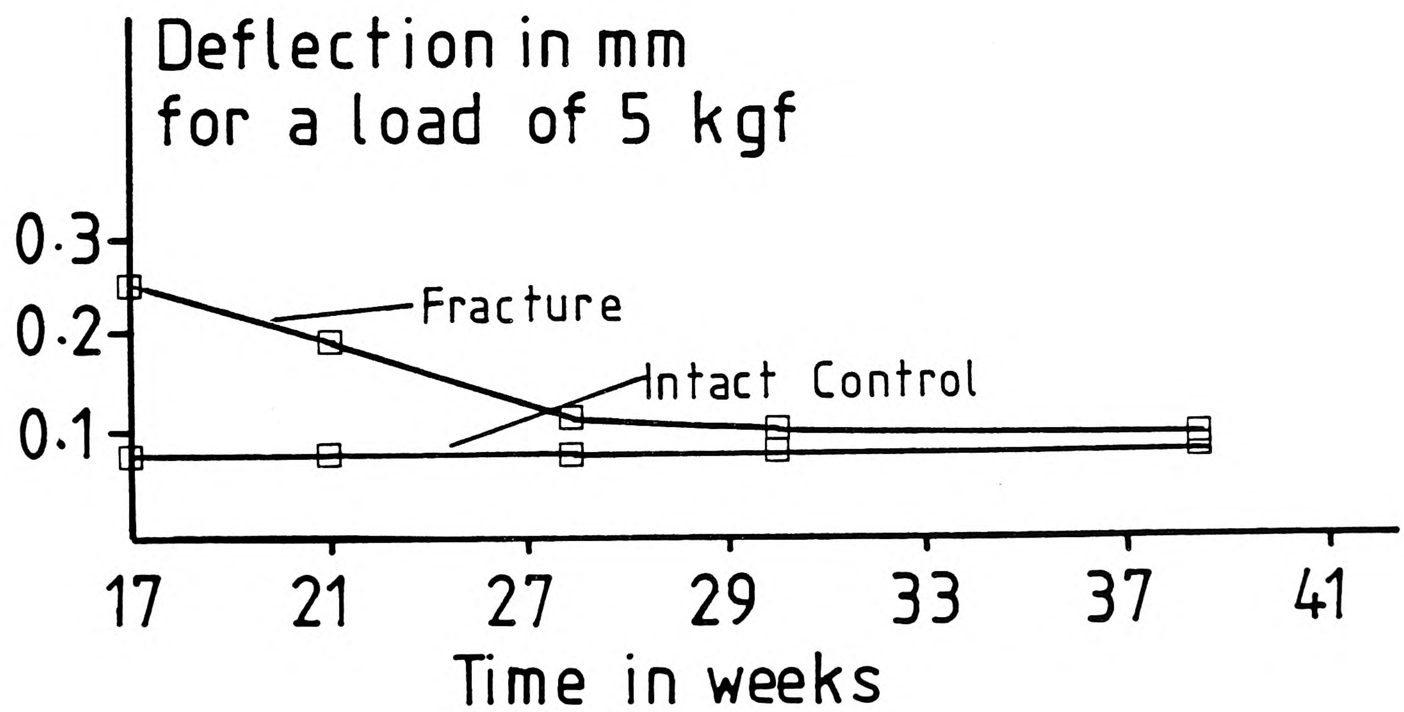

From Jernberger (1970)

Fig 2.4.1

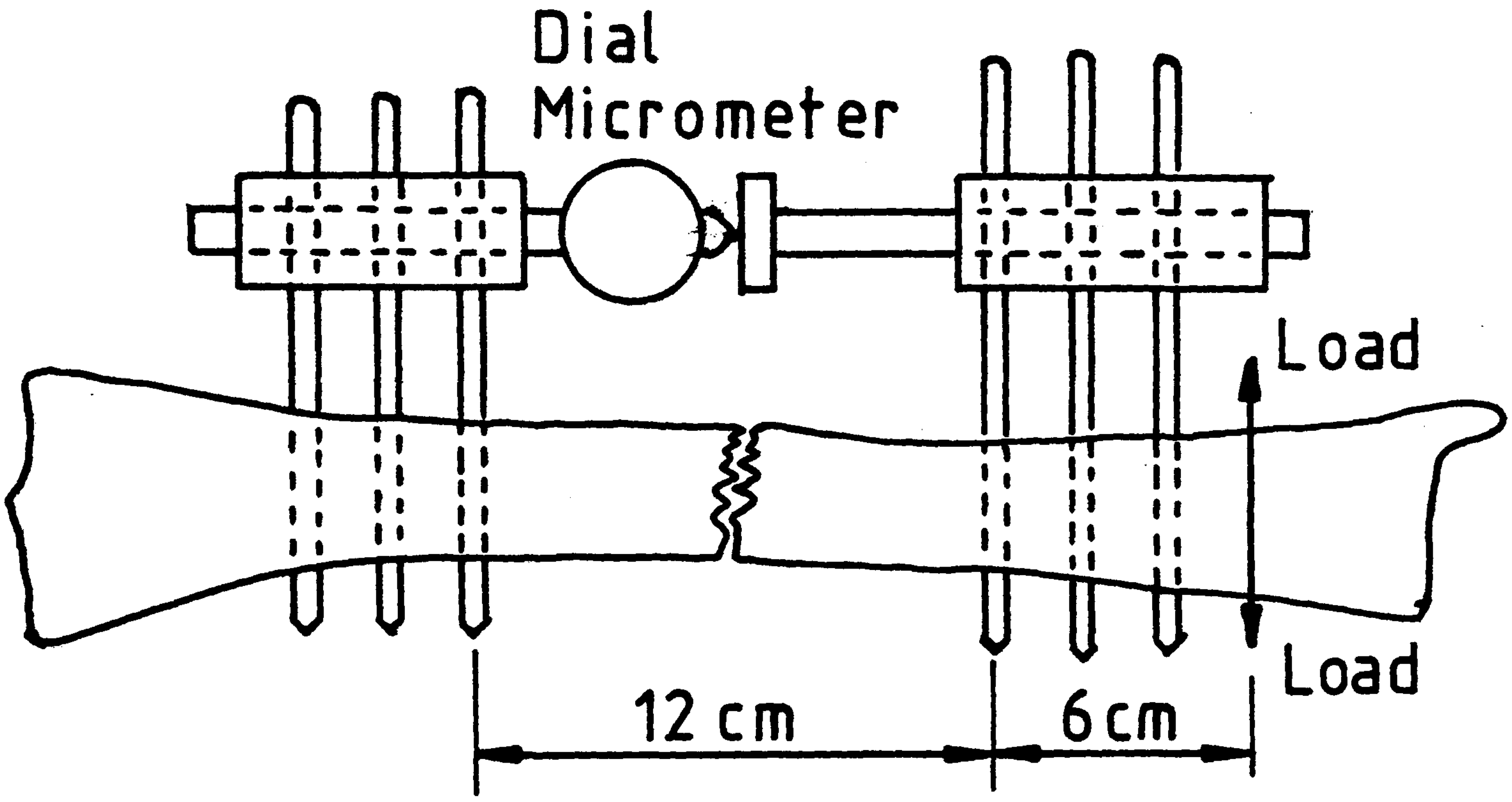

Jørgensen's Measuring Device

A Typical Deflection Curve

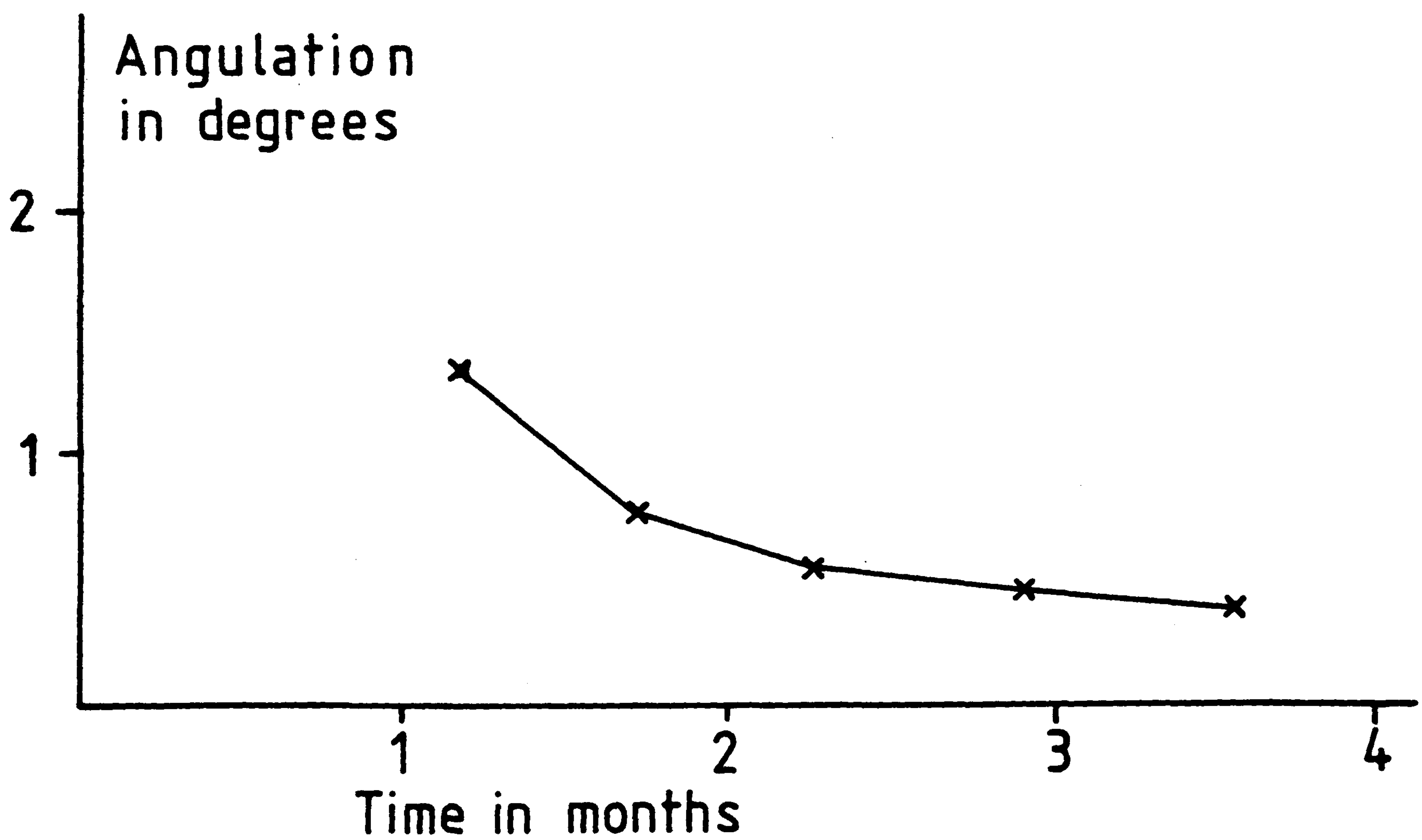

From Jørgensen (1972)

Fig 2.4.2

providing there was no pain or instability the fixator was removed.

Jofe et al (1982) measured the stiffness of healing osteotomies in sheep by applying a dial micrometer to the inner pins of an external fixator, and hanging weights from the distal pin. They monitored the sheep each week, and found a decrease in the deflection of the dial gauge. The increase in stiffness occurred in three stages: initially there was a slow increase in stiffness. Then there was an increase in rate, which coincided with the X-ray appearance of callus at the fracture site. Thereafter there was a slower stiffening of the fracture.

Bourgois and Burn y (1972) investigated the theoretical relationship between the percentage healing and the deformation at the fracture site. The percentage healing was considered to be the strength of the callus as a percentage of the strength of normal bone. They considered 5 different cases; (i) a long bone submitted to tension, (ii) a long bone submitted to bending, (iii) a fracture with an intramedullary nail, the deformation being measured by a strain gauge on the nail at the site of the fracture, (iv) a plated fracture with a strain gauge on the plate at the fracture site, and (v) an external fixator with a strain gauge on the bar of the fixator. All five cases produced hyperbolic relationships between the measured strain and the percentage healing. Subsequently, Burny et al (1978) used a strain gauged supporting bar on an external fixator to find the deformation of the bar, to measure the healing of fractures. For uncomplicated healing the graph was a decreasing exponential, but if healing was delayed then the slope of the curve was reduced. If there was no healing, then there was no drop in the curve of the percentage deformation, and if the healing was disrupted, for example by too early weight bearing, then there was a rise in the curve.

Lippert (1973) and Lippert and Hirsch (1974) used photogrammetry to calculate the movement at a fracture site. Two photogrammetric targets, consisting of V-shaped pieces of perspex, were fixed above above and one below the fracture site, each connected to the tibia by two Hoffmann pins applied to its antero-medial surface. The relative movement between the two "targets" was calculated using standard short range photogrammetry. They used this method to compare the effectiveness of various different types of plaster casts, which were applied with windows around the "targets". Six patients were studied, with fractures ranging from a day old fracture to a nine month old non-union, as well as a control with an intact tibia. In the control no movement was detected within the obtainable accuracy of 1.5 mm of translation and 1.5^{o} of rotation. In the patient with a non-union up to 10 mm of shear movement was found, whereas the other translations in this patient were less than 3 mm, and he showed less than 3^{o} of rotation. The amount of movement was greater in the more recent than in the less recent fractures, but in general the movements were up to 5 - 6 mm translation and about 5^{o} rotation. In some cases the movements were in different directions to the applied loads.

Stokes et al (1978) attempted to measure the movement on weight bearing of a fracture in a patient with an "Oxford" fixator, using biplanar radiography. The accuracy of the system was 1.5 mm and 1.5^{o}, and the movements which they measured were of the same order.

Beauprè et al (1983) applied a dial gauge between the inner pins of a 6 pin double-framed Hoffmann-Vidal External Fixator, to measure the displacement, in the axial direction, between two points on the pins. In this paper they backed this up with a finite element analysis of the fixator and an experimental study using various visco-elastic elements to model healing fractures. However, for routine clinical use they intended to use just the dial gauge.

Hammer et al (1984) used a method of superposition of X-rays, to measure the bending stiffness of the fracture. The fracture immobilization was released, the upper tibia was held still, and the heel was rested on a trolley, one X-ray was taken, a load of 2 to 8 kg was applied to the ankle, medio-lateral in the direction and a second X-ray was taken. The displacement angle was measured by superimposing the two X-rays, with an accuracy of 0.19^{o}. The deflection is divided by the bending moment and multiplied by the patient's weight, to give a deflection ratio. The deflection ratio versus time plotted on a log-log graph gave a linear relationship.

2.4(ii) Sonic and Ultrasonic Methods

If a bone is tapped at one end, a stethoscope at the other end will pick up a resonant ringing if the bone is solid, but if the bone is fractured then a dull thud is heard. This method of assessing bone union is known as osteophony, and according to Weiss et al (1977) it has been in use for about 200 years. They osteotomised rabbits' tibiae and allowed them to heal for varying lengths of time in plaster casts, either with or without intramedullary nails. The bones were X-rayed, and after sacrifice at different time intervals, the tibiae were dissected out and both ends were flattened off. A piezoelectric accelerometer was applied to one end and a pendulum was used to percuss the other end. Typically the output of the accelerometer was a decaying sinusoid. The damping ratio (the ratio of the magnitude of the first peak to that of the second peak) was measured. The bone was then loaded to failure under three point loading. There was a significant correlation between the fracture strength and the X-ray assessment, and between the fracture strength and the damping ratio. However, there was not a significant correlation between the X-ray assessment and the damping ratio. With increased healing time the damping ratio increased and a more reasonant sound was heard.

Seigal et al (1958) quantified the osteophonic assessment of a fracture, by measuring the velocity of sound across it. Soon after the fracture occurred, the haematoma transmitted sound at the same velocity as the bone. Once healing started the velocity dropped, and when cartilage was formed in the fracture site the velocity dropped again. However, once ossification started the velocity gradually rose to that of the contralateral limb. These measurements had to made at the same points on each limb, otherwise the differing amounts of soft tissue gave erroneous results. Abendschein and Hyatt (1970) measured Young's Modulus for bone specimens, mechanically and by using ultrasound. Young's Modulus for an elastic material is related to the velocity of sound in that material. It is given by the product of the density of the material and the square of the velocity of sound. Abendschein and Hyatt found significant correlations between Young's Modulus determined mechanically, and calculated using the velocity of sound. They also found significant correlations between Young's Modulus determined mechanically and both the velocity of sound and the bone density.

Lewis (1975), in vivo, projected a small air driven bullet at a metal plate at one end of a bone, and read the output from an accelerometer at the other end of the bone. He compared the injured and uninjured limbs to determine when healing had occurred. Sonstegard and Matthews (1976) inserted three hypodermic needles through the periosteum into bone. One, at an angle of 45 degrees was tapped to produce partially planar excitation. The other two needles had accelerometers at their ends, and were placed either side of the fracture, and again healing was determined by comparing the good and bad limbs. Saha and Lakes (1977) tried hitting one end of a bone with a hammer, and reading the output of an accelerometer at the other end, but they found that there was too much variability produced by the soft tissues, when they tried to compare the two legs, to assess the progress of healing.

Doemland et al (1982) developed a microprocessor-based "Long Bone Analytic Computer" which produced, in real time, the Fourier Transform analysis of the frequency response of the bone to percussion. The tibia was percussed at the medial malleolus, and monitored at the insertion of the semimembranosus muscle, and the fibula was percussed at the lateral malleolus, and monitored at its head. On control subjects the frequency response of one intact bone was generally very similar to that of the contralateral one. They monitored various fractures at different states of healing, and found differences between the two legs, and between fractures at different states of healing. However, they did not monitor any fracture serially as it healed, so it is difficult to know whether this method could be used to monitor fracture healing.

2.5 Scintigraphic Studies

O'Reilly et al (1981) attempted to differentiate between fractures which were healing normally, and those which were progressing to non-union. There was increased uptake of technetium^{99}-methylenediphosphonate at the fracture site compared to the contralateral limb, but there was no significant difference between those fractures progressing to union and those progressing to delayed or non-union.

2.6 Nuclear Magnetic Resonance Studies of Fractures

Nuclear Magnetic Resonance (N.M.R.) can be used in two modes. The first of these, imaging N.M.R., is used to look at sections through the human body, as described by various authors including Bottomley et al (1978). This uses ^{1}H, the common isotope of Hydrogen. The second mode of use, chemical shift spectroscopy, is used to look at the biochemical activity of a piece of tissue both *in vitro* and *in vivo* as described by Ackerman et al (1980). This looks at either ^{31}P or ^{13}C, the common isotopes of phosphorus and carbon. This method was used by Newman (1983) to study the healing of experimental fractures. In this study closed fractures were produced in rats' tibiae. These were then studied in a ^{31}P N.M.R., every day for 20 days when the fractures had healed; at the position of the inorganic phosphate relative to the phosphocreatine may be used to derive the intracellular pH of the fracture haematoma. The rats were X-rayed on the same days that they underwent N.M.R. to provide a correlation between the pH and the X-ray appearance. Two days post-injury when the first test was performed, the pH had risen to 7.2 from the normal range of 7.04 to 7.09. This rise continued until it reached 7.4 on day 20, with calcification of the callus seen on X-ray. When a second set of rats were given a steroid (prednisolone) to delay fracture healing, or in one rat whose fracture was open and became infected with staphylaccocucus aureus, the same rise in pH was seen but delayed the pH remaining at 7.2 until day 10 and as callus appeared on X-ray the pH increased although reaching 7.4 on day 25.

Although this gives an insight into the behaviour of the fracture, it cannot be used in any fracture treated by internal or external fixation with any, even slightly magnetic material, due to the high magnetic field (1.5 T)used in the technique.

CHAPTER 3

MECHANICAL AND ELECTRONIC DESIGN OF THE TRANSDUCER

MECHANICAL AND ELECTRICAL DESIGN OF THE TRANSDUCER

3.1 Aims of this Study

It was considered to be of interest to measure the movement at the fracture site. Various authors including Yamagishi and Yoshimura (1955) have suggested that shear displacements lead to the hypertropic or elephant-foot type of non-unions. Sarmiento (1970) and other authors have suggested that axial displacements lead to good fracture healing with abundant callus formation.

Lippert and Hirsch (1974) measured the movement at certain times in certain fractures, and they theorize the way the healing would proceed, but do not measure this progress in an individual fracture. The system used by Lippert and Hirsch would not be acceptable in this country for either individual or long-term studies. X-ray photogrammetry would probably also not be acceptable to perform long-term studies of fracture measurement due to the X-ray dose. If a suitable method of assessing fracture healing could be developed then the number of X-rays that would be taken could be reduced. Another advantage would be that mechanical testing shows up delayed or non-unions earlier than using X-rays to detect calcification of the fracture callus.

Strain gauge readings from internal fixation plates are possible but there are two major problems. One is transmission of the strain gauge signals from the plate; either a direct connection can be made through an incision in the skin as in animal studies, but this again would be unacceptable in clinical trials, or a radio signal can be used which can pass through the skin, but this has proved to be unreliable in previous trials. The second problem is that of attaching the strain gauges to the plate; in previous studies these have remained on a for a maximum of a few months (Burny et al, 1978), whereas it is said that an internal fixed tibial fracture can take up to 18 months to heal. Finally, internally fixed fractures heal by primary healing rather than secondary healing unlike most other fractures, so any results obtained would not be applicable to the most common types of fracture treatment.

It was considered that if the fractures studied were confined to tibial fractures which had been treated with the "Oxford" External Fracture Fixator, then a direct mechanical connection was available between the fractured bone and the outside world. Tibial fractures were chosen for study as they have a particularly high rate of non-union and delayed unions.

The "Oxford" External Fracture Fixator is a single-sided external fracture fixator; the pins used are 6 mm diameter stainless steel Schanz pins of various lengths. There is a threaded section 50 mm long at one end, with a self-tapping point, the core diameter is 4.0mm pitch is 2.75mm and the thread form has radiused bases, with square ends. These pins are inserted via an incision in the skin and a pre-drilled pilot hole. The pins are held in stainless steel clamps which permit up to 12° of angulation from the central position. The pin passes through a plastic sleeve in the clamp body which is filled with steel ball bearings, and these are compressed down with a grub screw in the cap of the clamp. These clamps are individually positioned on a 16 mm square stainless steel bar. Usually there are 2 pins above and 2 pins below the fracture site. The original fixator, the Mark I, has all four clamps rigidly clamped to the support bar, but the second fixator, the Mark II has two sliding clamps. These two clamps have a layer of low friction polytetrafluoroethylene on the surfaces with a coefficient friction of 0.09 (manufactured by Emralon 833 Acheson Colloids Co., Prince Rock, Plymouth, UK) in contact with the support bar, and the two clamps are connected together and then the interconnecting rod passes through a spring system which is clamped to the support bar. There were two different spring systems used in this study, the first, chronologically, was a pack of Bellville washers, the second was a pack consisting of a light spring (stiffness 5 - 10 Nmm^{-1}) held preloaded in a pack. Thus the fixator did not slide until the preload was overcome, once this had happened the fixator slid easily until the end stops were reached.

Thus what was required was a method of measuring the movements at the fracture site and thus deciding how the fracture was healing. It was decided to confine the study to patients treated with the "Oxford" fracture fixator. Allowance was needed to be made for the bending of the fixator pins and movements due to the sliding of the fracture fixator.

3.2 Mechanical Design of the Transducer

3.2(i) Design Criteria

The requirement was to measure the movement at the fracture site in terms of three linear translations and three angular rotations. As the fracture was inside the body direct mechanical measurement was impossible. The work of Stokes et al (1978) using biplanar radiography on external fixator patients found that they were measuring movements of the order of 1.5 mm and 1.5°, which was the same order as the accuracy of the system, so this method was discontinued. Lippert and Hirsch (1974) found in their patients treated in plaster casts the movements were much greater, up to 20 mm of translation and 8° of rotation for a grossly unstable fracture, and up to 8 mm of translation for other patients.

The movement at the fracture site can be related to the movement at the point where the pins enter the bone, provided the bone is considered a rigid member, and according to Evans (1973) its Young's modulus is or the order of 20 GPa, one tenth of that of steel. The movement between the pins and the bone depends on the forces being applied at the point where they meet. The deformation of the pins may be calculated by standard elasticity theory providing they are within their elastic range. The movement of the clamp-support bar system may also be calculated (Evans et al, 1979). If the relative movement between two points on pins on opposite sides of the fracture are known then the relative movement at the fracture site can be calculated; this is performed in Section 4.2.

From the work of Evans et al (1979) it was be estimated that the maximum movement at the fracture site would be $\pm$ 5 mm in any given direction and from this an estimate of $\pm$ 2.5 mm at the transducer was made. The transducer would also be required to fit in the space between the fixator support bar and the patient's leg, and between the two inner pins as shown in figure 3.2.1. The space available for the transducer was estimated to be 30 x 40 x 60 mm. The transducer would be required to be clamped to the pins and the clamps of the fixator permitted up to 12^{o} of angulation, so the transducer clamps should be able to accommodate this amount of angulation. The clamps should also not be so large as to affect the bending of the pins, and they should also be capable of being replaced in the same position on the pins each time they are used. The transducer should not take sufficient load appreciably to affect the stiffness of the fixator-bone system, and, finally, as much of the transducer as the patient was to be asked to carry should be sufficiently light so as to be conveniently portable by a patient with a fractured leg.

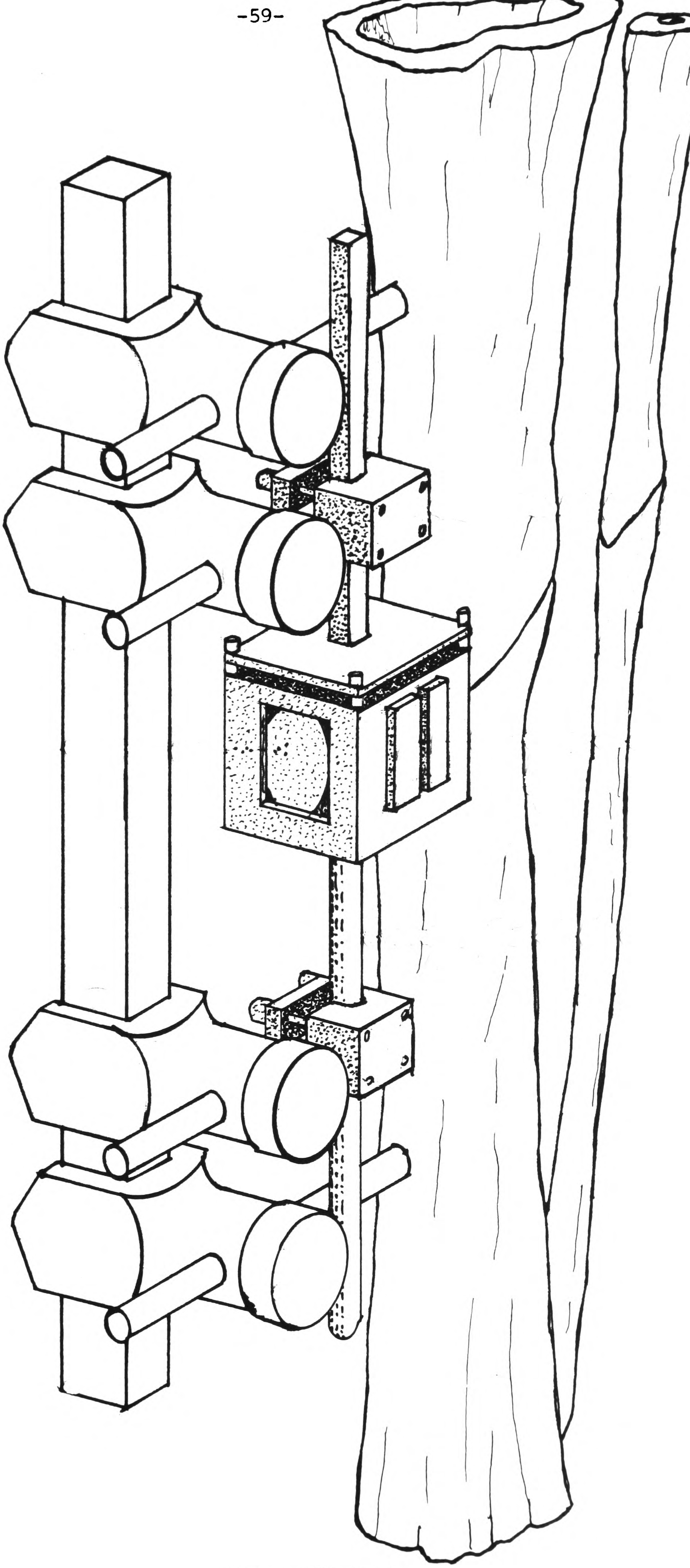

Fig 3.2.1

3.2(ii) Possible Systems of Measurement

Various methods of measuring displacement were considered:

a) Strain Gauges

b) Pot entiometers, or Linear Displacement-Voltage Transducer

c) Light Em itting Diodes with Phototransistors

d) Light Em itting Diodes with Lateral Effect Photodetectors

Strain gauges were rejected as the strain which was required to be measured, up to 20%, would be too large for conventional gauges.

Potentiometers and Linear Displacement-Voltage Transducers (LDVTs) were considered together and rejected, as the space available was not sufficiently large to accommodate six of either of these. The potentiometers would have interfered with each other, and there did not seem to be any LVDTs of sufficiently small size and sufficiently large travel on the market at the time.

The system of Light Emitting Diodes (LED's) and phototransistors would have involved six LED's coupled with six phototransistors on one half of the transducer, and in between them attached to the other half of the transducer there would have been sheets of continuously variable transmissivity. This would have required the production of the sheets, which would have been extremely difficult. There would have again been problems with the amount of space available for the detectors and LED's and six sheets of this material.

The last method considered was using LED's again, but this time shining onto Lateral Effect Photodetectors. These detectors are manufactured by United Detector Technology Inc. of California, and they produce an electrical output dependent upon the displacement in two dimensions of the centroid of the light falling upon them. Thus three of these would have been needed, mounted mutually perpendicularly, with three LED's shining onto them to produce the required six degrees of measurement. This was clearly the most practical approach, and a transducer of this type was constructed.

These detectors are availible in two different types, either Schottky barrier PIN (P-type, Intrinsic, N-type) photodiode or planar diffused PIN photodiodes. The Schottky barrier ones were available with active areas of 10 mm square in a 25 mm diameter case, 18 mm square in a 38 mm diameter case and 44.5 mm square in a 56.5 mm diameter case. The planar diffused ones were availible in two sizes, 2.5 mm square in a 9 mm diameter case and 10 mm square in a 25 mm diameter case. To measure the expected maximum displacement of $\pm$ 2.5 mm in any direction the requisite size was 10 mm square and this size was obtainable in both types in cases of diameter 25 mm, which was within the previously defined size limit even when it was mounted in a box. The Schottky barrier photodiodes required to be used photoconductively which would have required a power input, while the planar diffused type were used photovoltaicly. The spectral range of both types was similar, 350-1100 nm with a peak at 900 nm for the Schottky barrier and 850 nm for the planar diffused type. These wavelengths are in the infra-red part of the spectrum and miniature infra-red LED's are available (Texas Instruments TIL32) with a length of 5 mm with 12.7 mm long leads and a diameter of 3 mm. There was a difference in the responsivity for the two types at their maximum responsivity wavelengths, 0.35 AW^{-1} at 10V bias for the Schottky barrier compared with 0.55 AW^{-1} at 0V bias for the planar diffused. The quoted positional linearity over the central 25% was identical for both types, but for the central 75% it was 4% for the Schottky barrier compared with 3% for the planar diffused. The 10-90% rise and 90-10% fall times for the Schottky barrier were both 2 μs at 10V bias compared with 4 μs at 0V bias for the planar diffused type, and as a result the maximum frequency of usage for the Schottky barrier was 10 kHz which was double that of the planar diffused type.

The planar diffused type of photodetector was chosen in preference to the Schottky barrier primarily for its increased responsivity, but also because it did not require biassing. It was considered that if a LED had to be collimated then the amount of light availible would not be very great, and thus the increased responsivity would be advantageous and would produce a better signal-to-noise ratio. The lower frequency response of the planar diffused type would not be a disadvantage as it was not intended to use it at a frequency as high as 5 kHz. The detector used, the United Detector Technology PIN-SC/10D, is shown in Figure 3.2.2, mounted in the transducer.

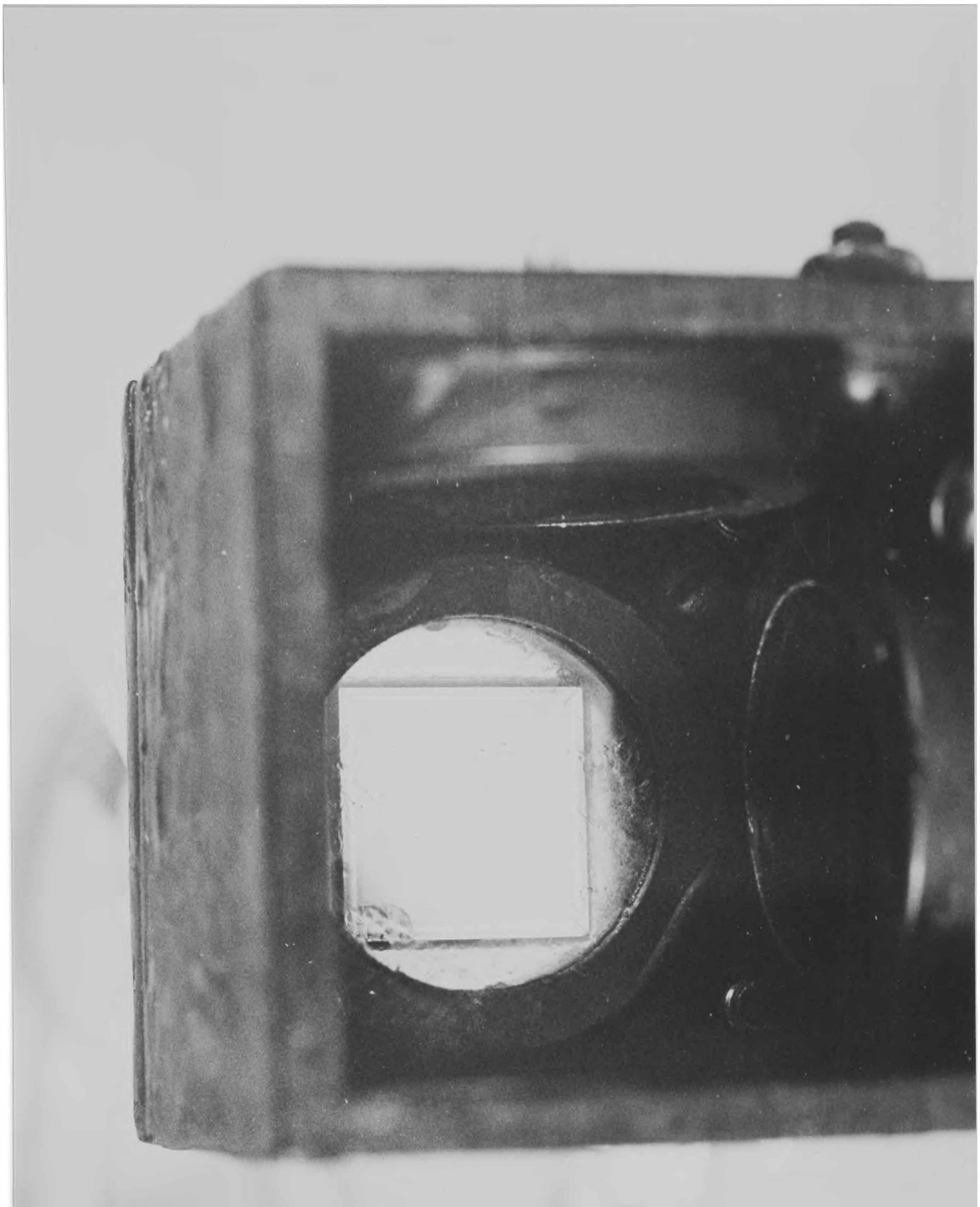

Fig. 3.2.2 Lateral Effect Photodetector

3.2(iii) Design of the Transducer

A sketch diagram of the Transducer is shown in Figure 3.2.1 with an exploded view in Figure 3.2.3. The transducer consists of two mechanically separate parts, the detector head containing the three detectors mounted in mutually perpendicularly on a rod and the LED head containing the three LED's which were also mounted mutually perpendicularly onto a rod. The three lateral effect photodetectors were mounted in a perspex box with their leads on the outside of the box, this is shown in Figure 3.2.4. In the initial electronics design the pre-amplifiers were mounted on the backs of the detectors as shown in Figure 3.2.1, and suitable sized cutouts were made in the perspex to accommodate the integrated circuits. The electronic design was subsequently modified, and in the second design the initial amplification took place remotely, so the perspex box only needed five small holes behind each detector to permit the electrical connections to be made. However, as the detectors were already mounted in a suitable box, this was not changed. The perspex box was mounted onto a plate that was fixed to a 6 mm square steel rod so that the "transducer head" could be clamped perpendicular to one of the pins of the fixator.

There were two designs for the "LED head" of the transudcer. The original one is shown in Figure 3.2.5 and as a sketch in Figure 3.2.3. Here the LED's were placed inside the head, which was hollow, with three mutually perpendicular holes drilled in it into which the three collimators were pushed. The collimators were cylindrical with flanges which sat flat on the outside of the head when in position. These collimators were a push fit both into the holes and onto the LED's so that they held the LED's mutually perpendicular. Each

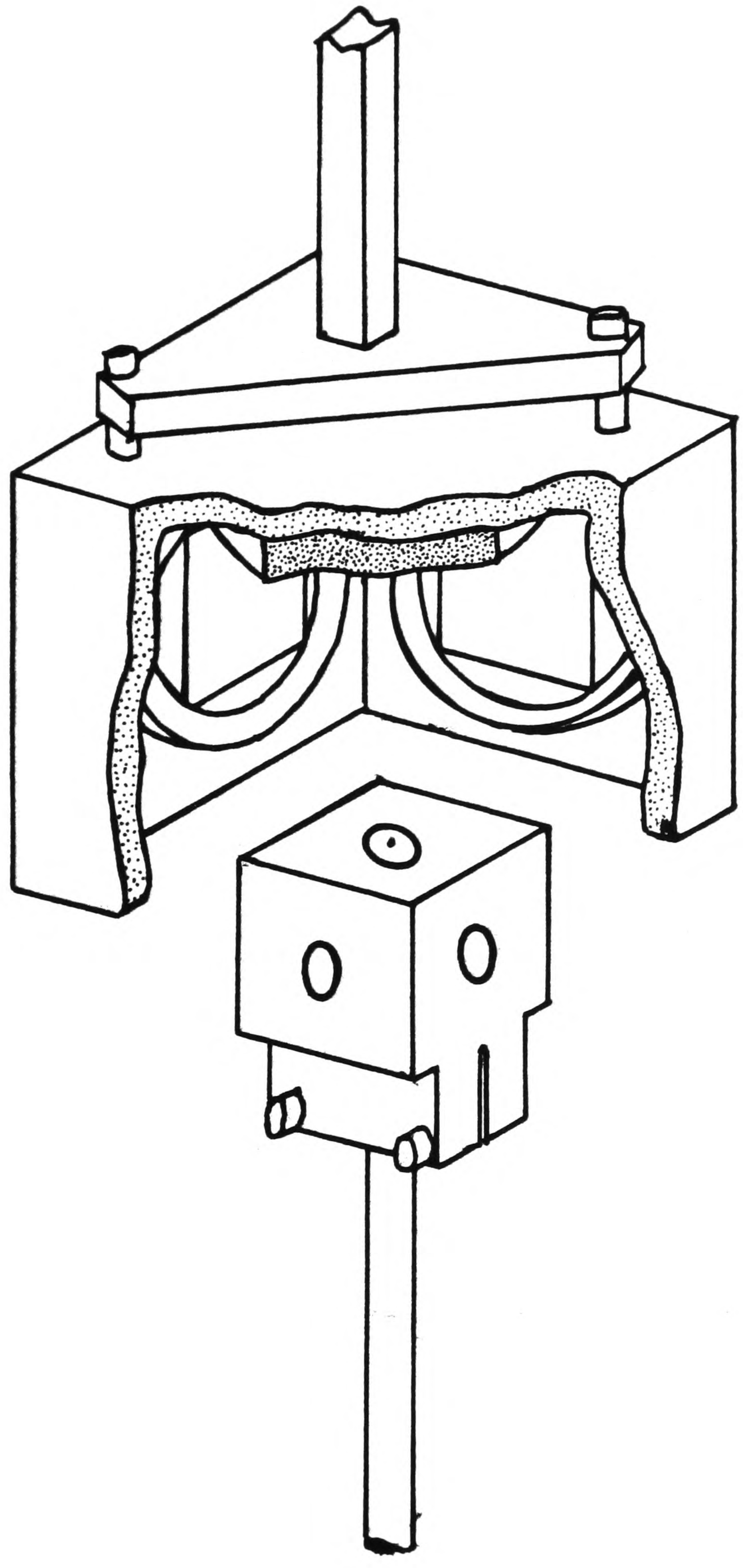

Fig 3.2.3

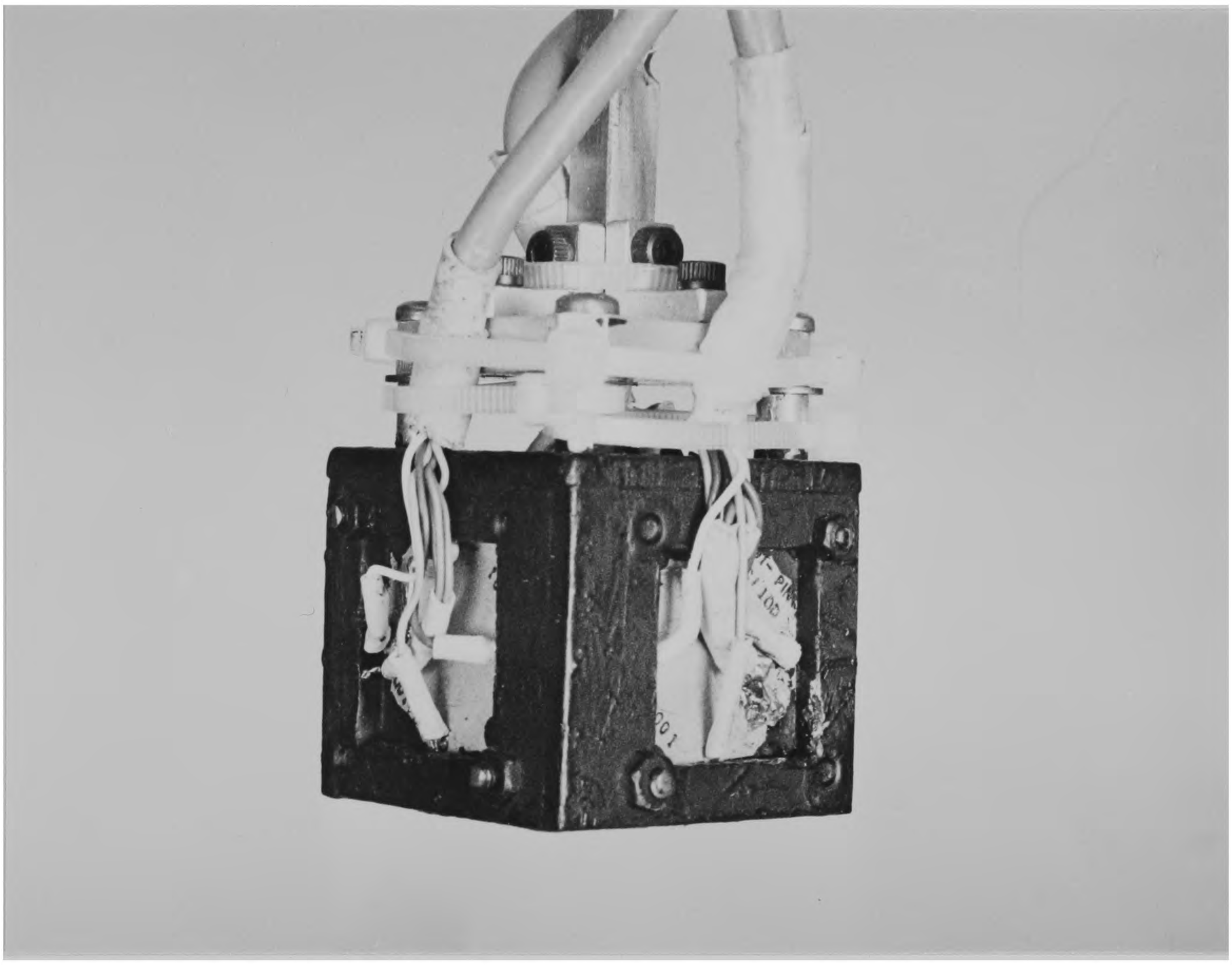

Fig. 3.2.4 Transducer Head

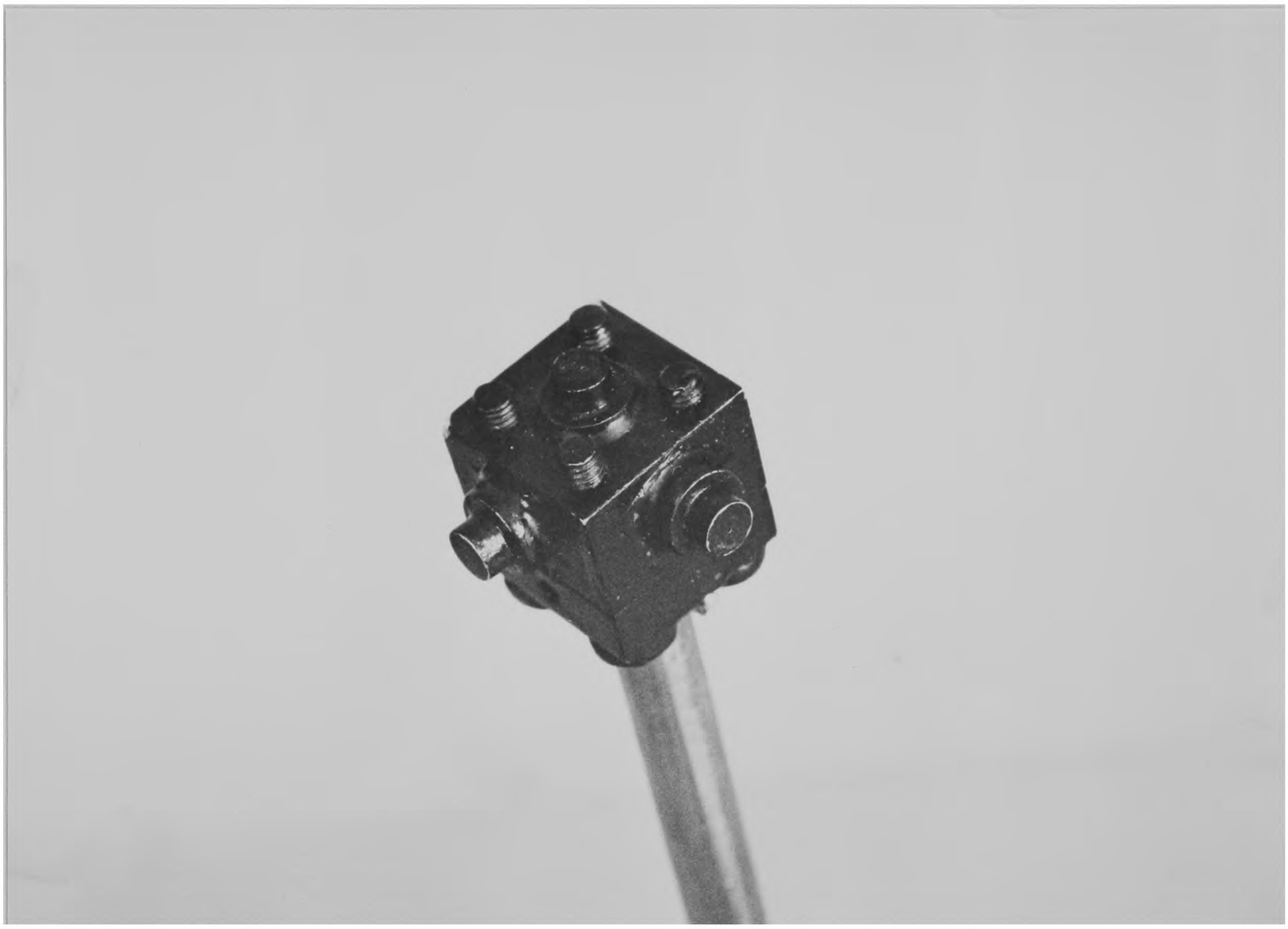

Fig. 3.2.5 First Design LED Head

collimator consisted of one long thin hole. There was a two core cable going to the LED head which passed through to the inside of the head on either side of the 6 mm diameter bar upon which the head was mounted. Both the versions of the LED head were mounted on a 6 mm round diameter bar, so that if the two fixator pins upon which the transducer was mounted were not parallel, then the detector head would be mounted square to one of the pins, with the LED head mounted square to the detector head.

The LED head was redesigned when the second set of electronics was built. In this design a solid aluminium block had three mutually perpendicular quarter inch holes drilled and reamed through it. Six collimators were then made of quarter inch aluminium stock rod, which was a push fit into the quarter inch holes, by drilling this rod to within approximately 1 mm of the end and then drilling a 0.5 mm hole through the end.

Three collimators were pushed into the holes so that their front faces were flush with the sides of the block facing the detectors (Fig 3.2.6). The remaining three collimators were then pushed into the block so that their front faces met at the centre of the block, and the three LED's then were pushed into the holes in the collimators so that their leads were then sticking out of the sides of the block. These were then connected to solder pads on a flat of the block as shown in Figure 3.2.6.

Two collimators were used per LED so that the light was collimated by passing through two small, short holes separated by a distance rather than one long hole which would be more difficult to manufacture.

The block was drilled out so that it would take the 6 mm diameter rod. A saw cut was made through this hole and the two sides parallel

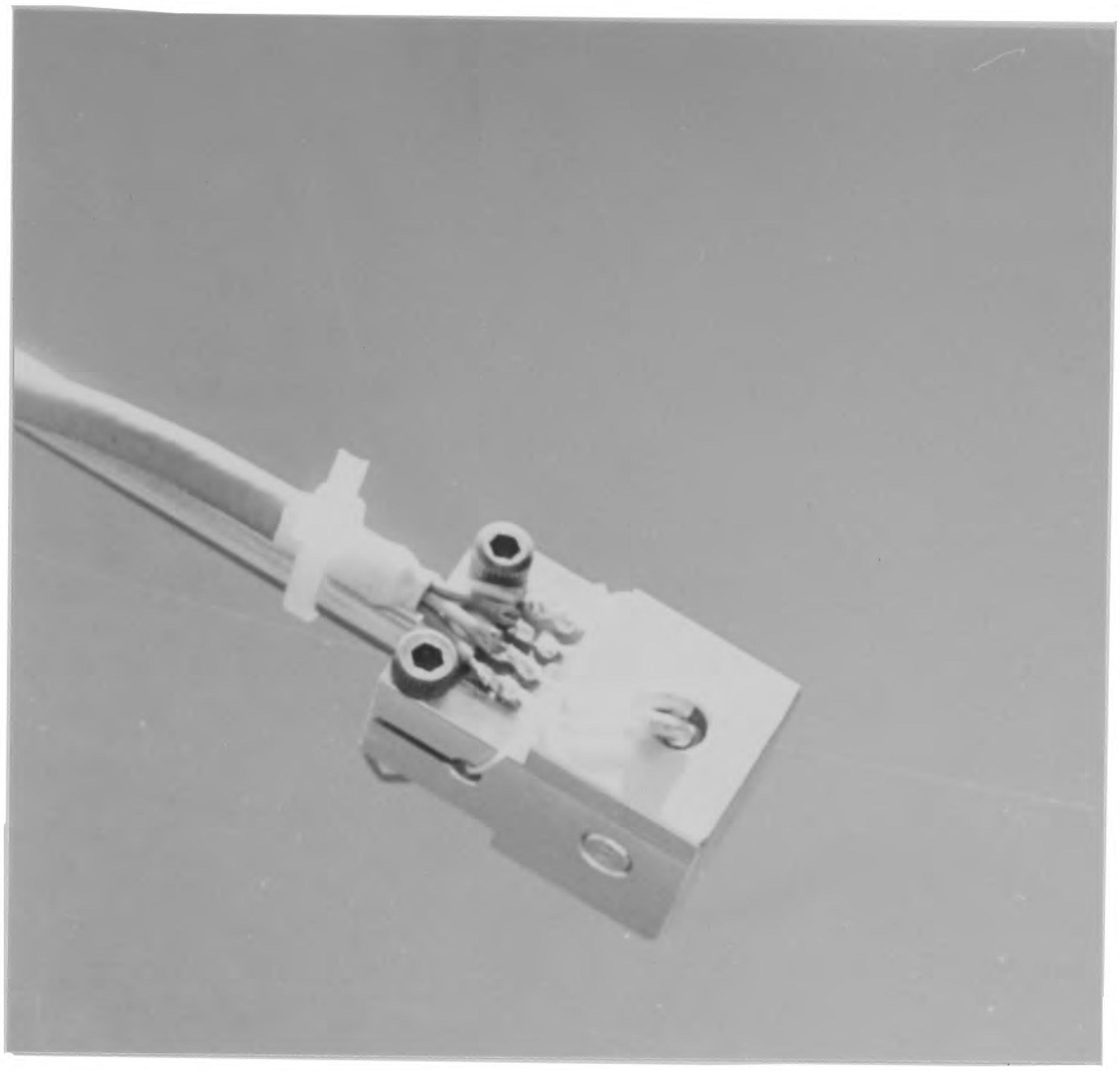

Fig 3.2.6 Second Design of LED Head

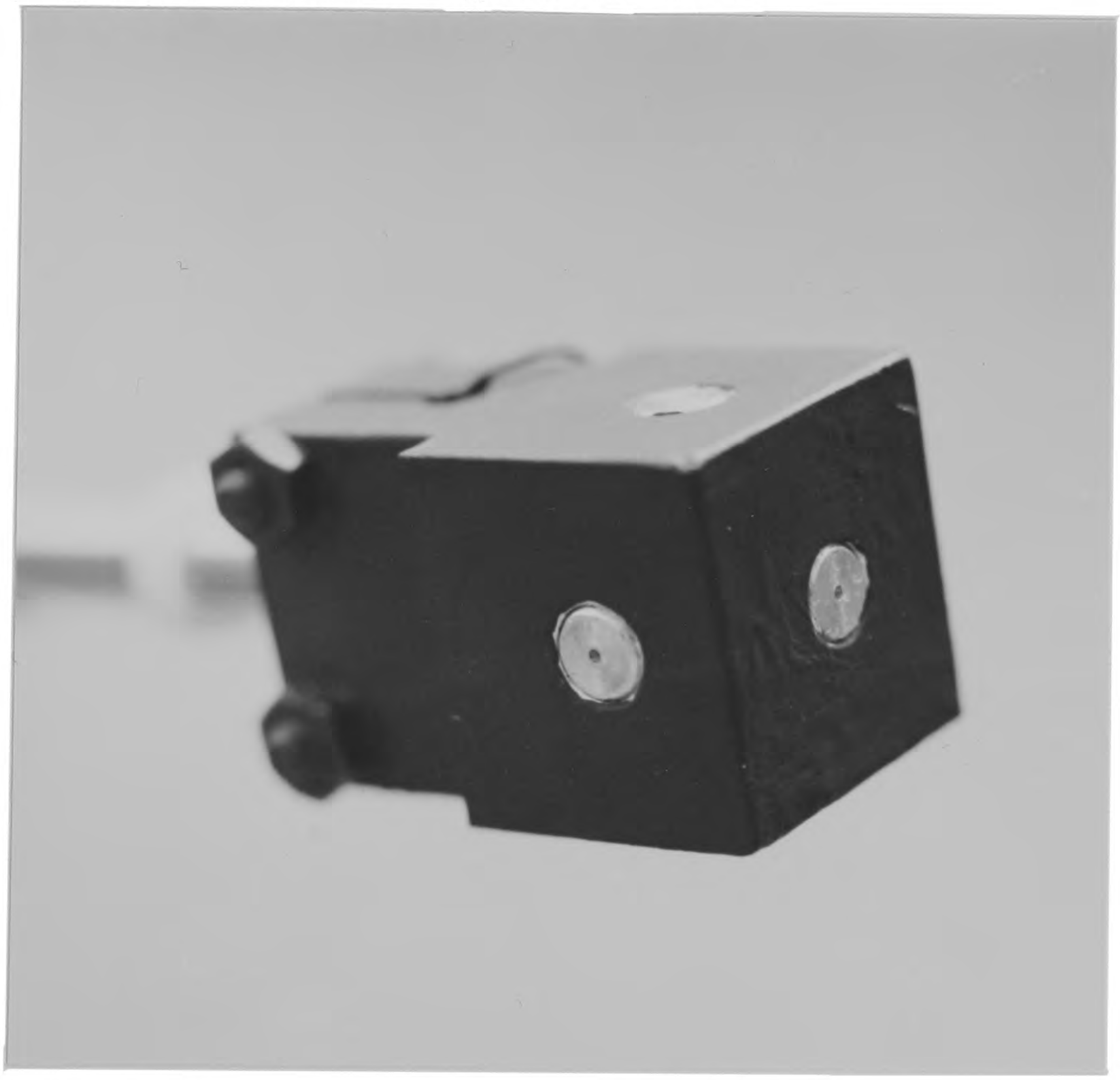

Fig 3.2.7 Second Design of LED Head

to this cut were then milled down to produce flats which could clamp the rod. The LED head could then be loosely placed on the end of the rod and the two parts of the transducer clamped up in a "set-up jig". The position of the LED head could be zeroed on the rod before being clamped onto it.

The "set-up jig" (Fig 3.2.8) was designed so that the two parts of the transducer would be in the same relative position each time the transducer was used. It was also used to hold the transducer when not in use and so reduce the risk of damage. The two arms of the jig holding the transducer each had a slot milled across them and then a steel ball bearing was mounted in the corner of the slot. Each of the support bars of the transducer had a pair of indentations made in them, one to mate with the ball bearing and the other with the end of the locking screw.

The original clamps are shown in Figures 3.2.1, 3.2.9 and 3.2.10; they were designed so that they would fit on either the round or the square rod of the transducer. They would also allow up to 12° of angulation between the direction of the perpendicular to the pin and the rod. They were, however, rather awkward to put on.

The design of these was improved, as shown in Figures 3.2.11 and 3.2.12. There was more angulation possible and only one screw to be tightened per clamp.

In both Figures 3.2.9 and 3.2.11, one complete clamp is shown dismantled along with the one component that varies between the transducer head clamp and the LED head clamp. In both Figures 3.2.10 and 3.2.12, the clamps are shown in use on the LED head.

The detectors were covered with a photographic filter so that the amount of non-infra-red light reaching the transducer was reduced.

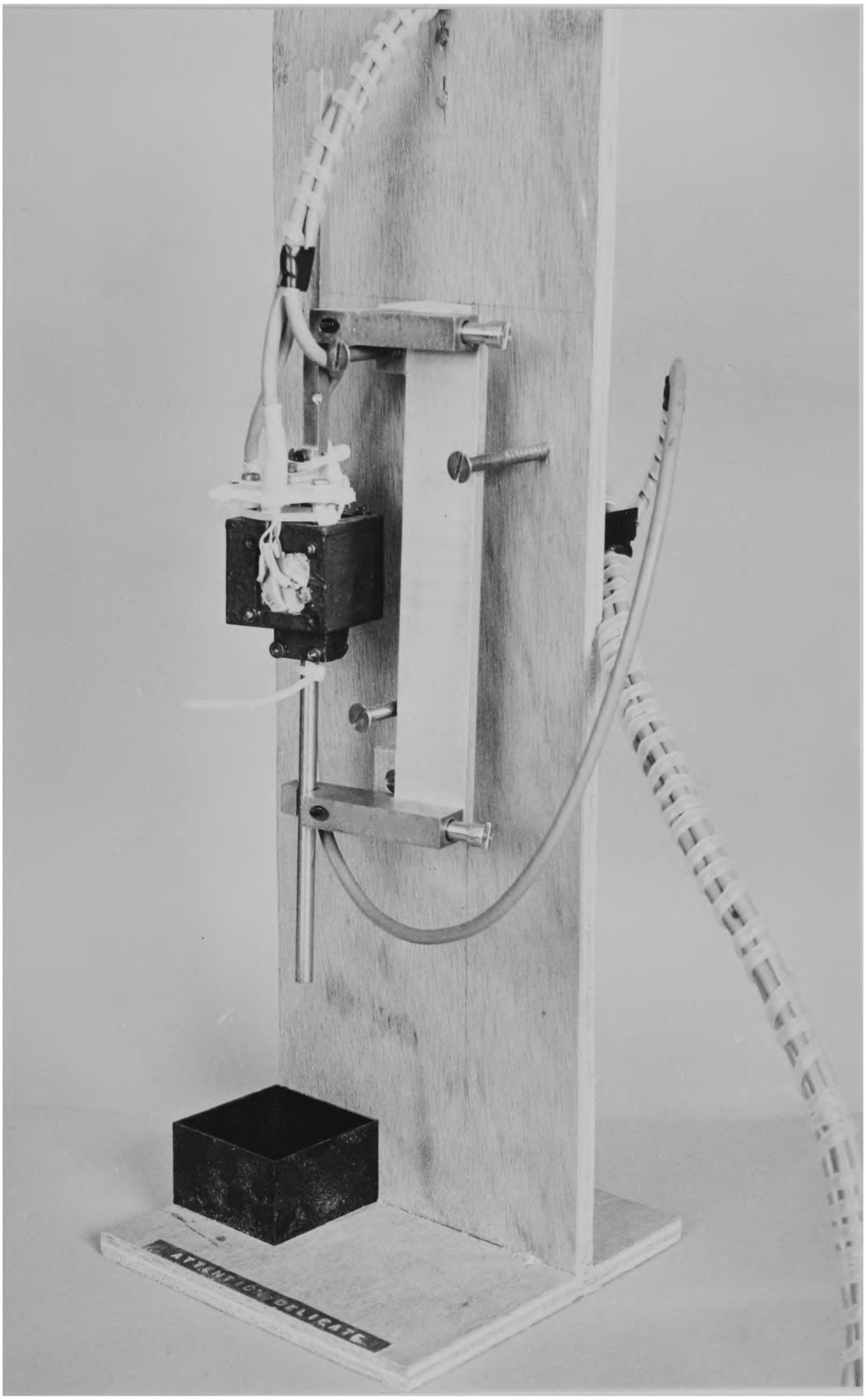

Fig. 3.2.8 Set-up Jig

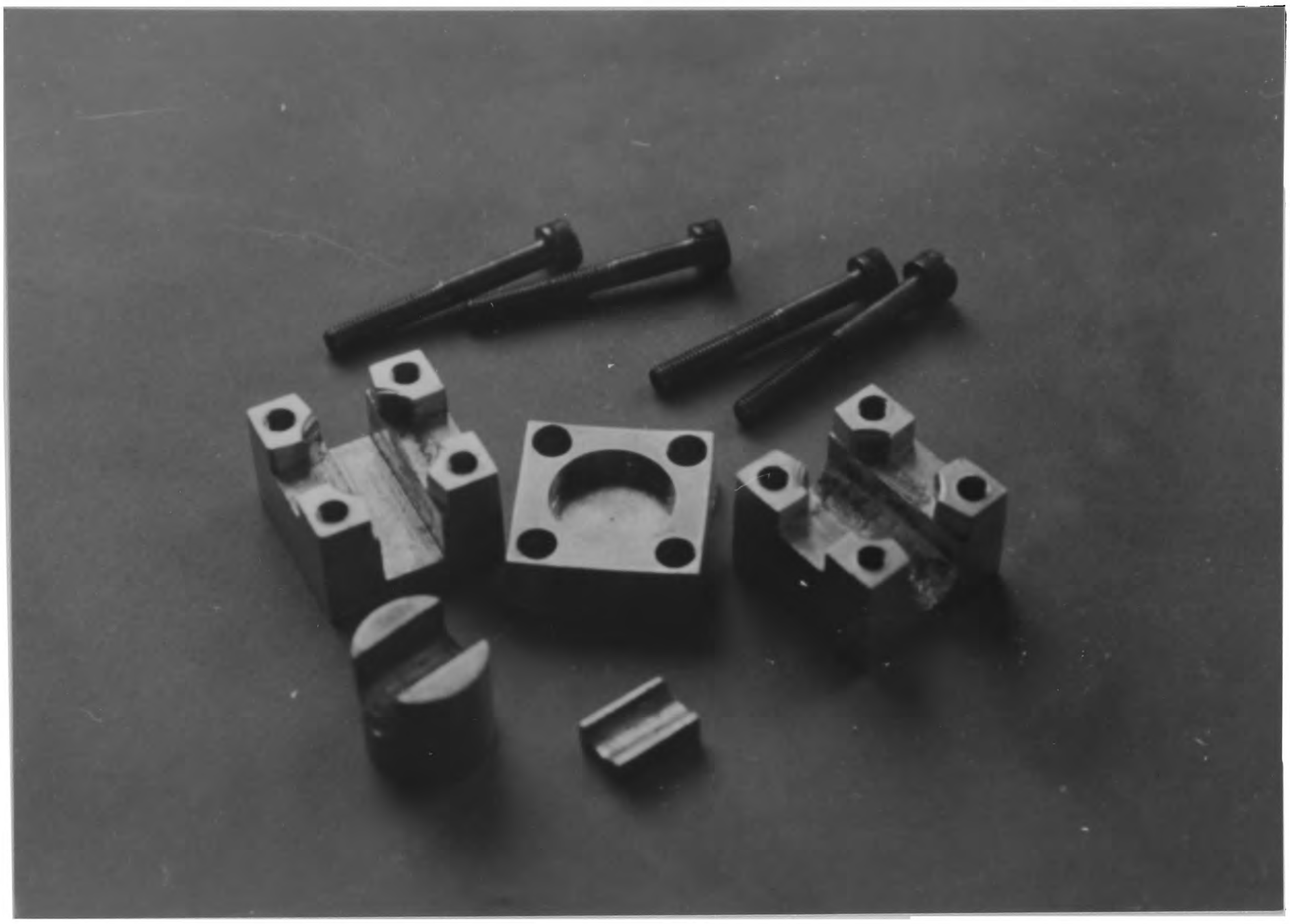

Fig 3.2.9 First Design of Transducer Clamp (Dismantled)

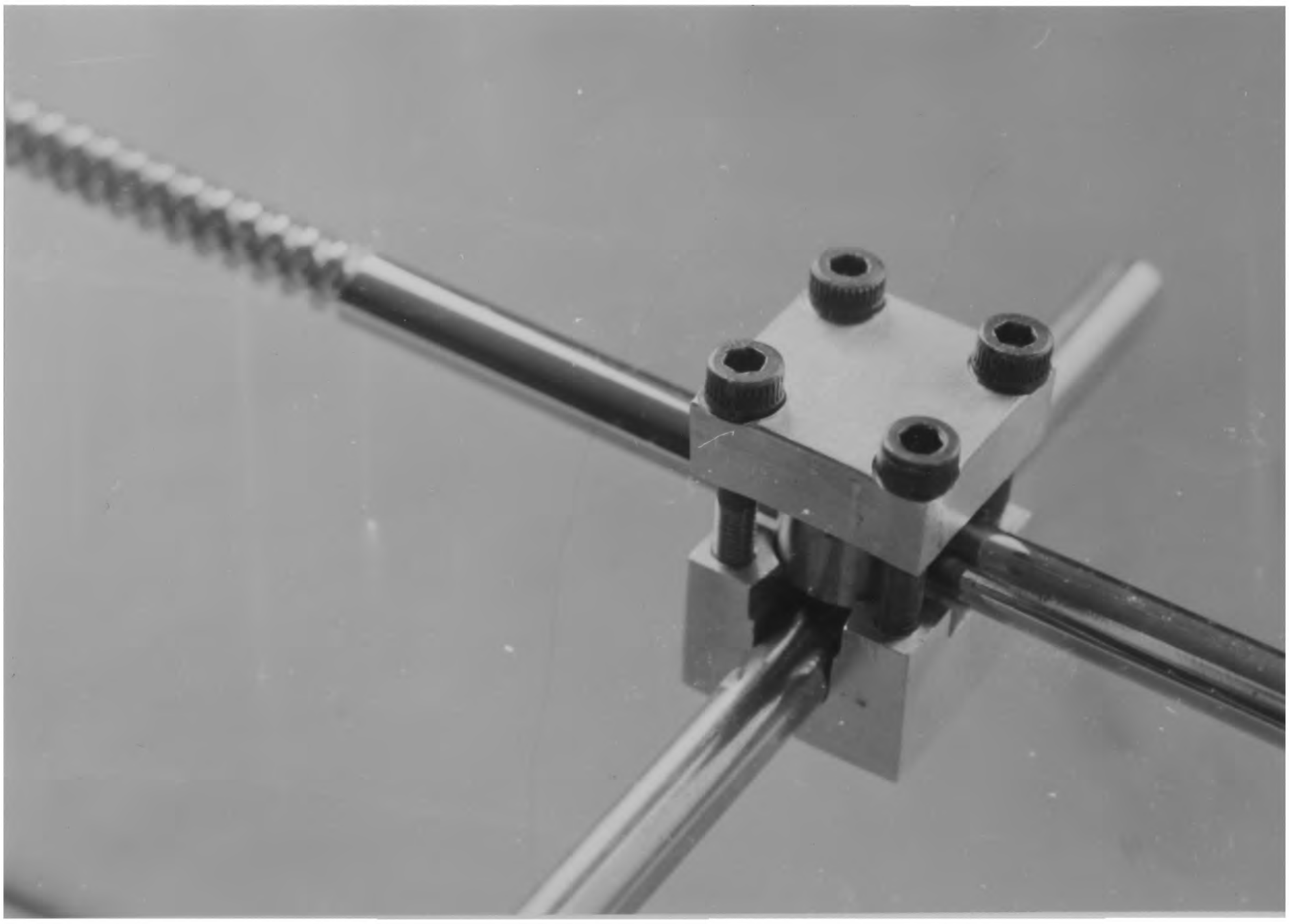

Fig 3.2.10 First Design of Transducer Clamp (In Use)

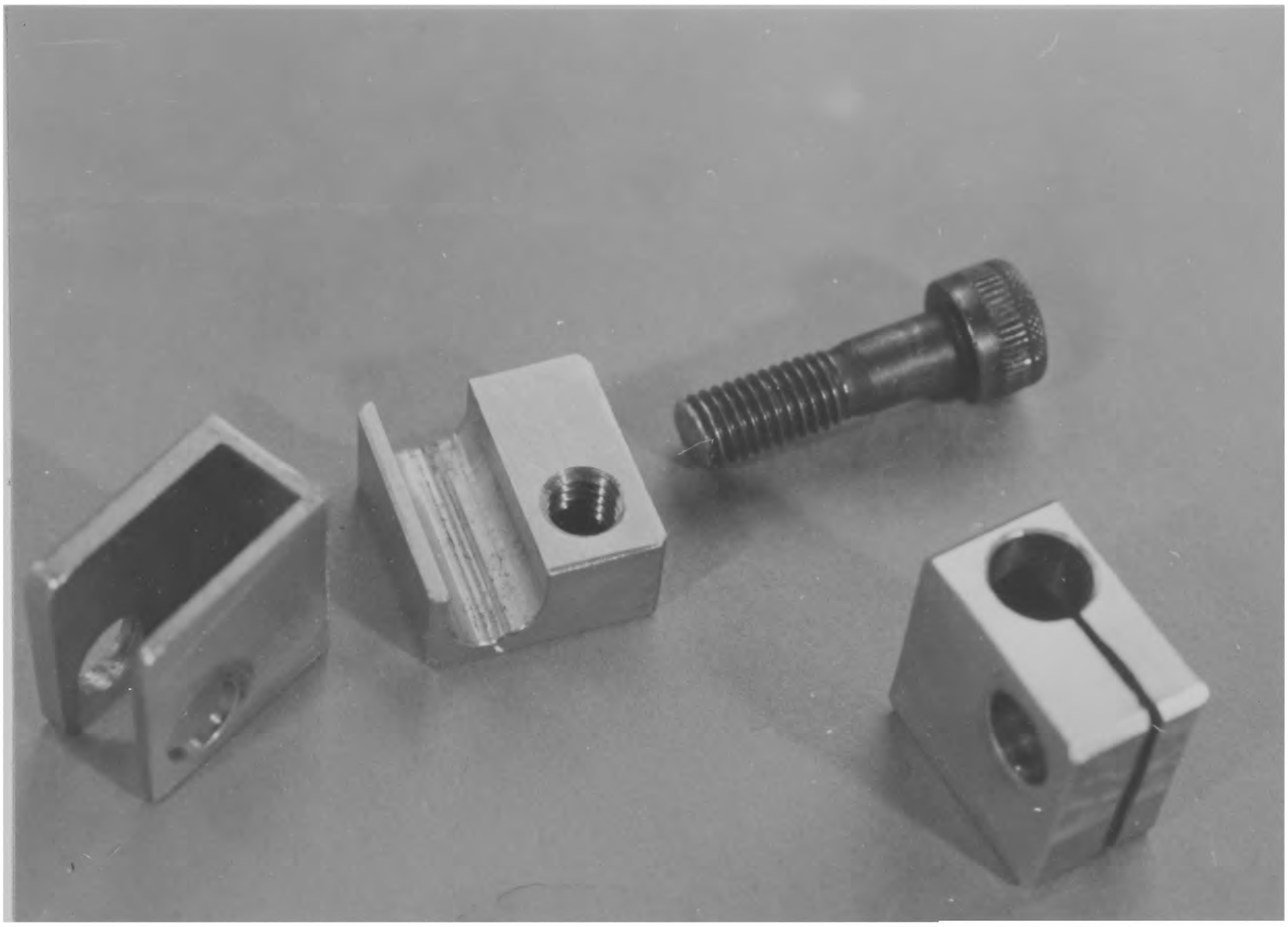

Fig 3.2.11 Second Design of Transducer Clamp (Dismantled)

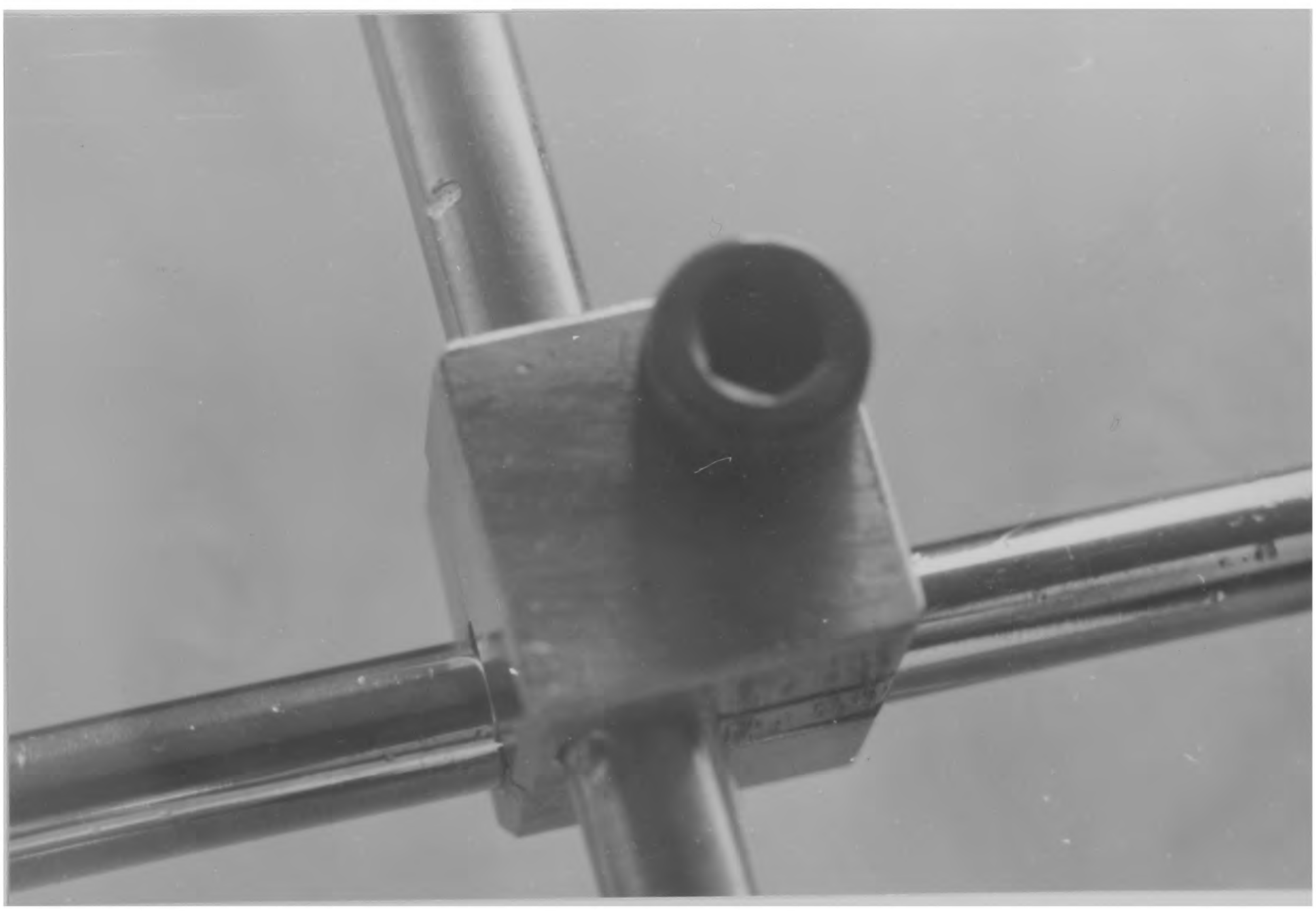

Fig 3.2.12 Second Design of Transducer Clamp (In Use)

This filter, Kodak Gelatine filter No. 87C, permitted infra-red light only, the transmissivity is shown in Table 3.2.1. Thus the amount of interference due to daylight and light from the lights in the room was reduced. In order to reduce stray light, the inside and outside of the detector box was painted with matt black paint, as shown on the LED head in Figure 3.2.2. This would also have the effect of reducing the amount of light which could be reflected inside the box. Infra-red light reflected inside the box would be picked up by other detectors and give a false reading. For the same reason the LED head was also painted with matt black paint.

Table 3.2.1: Transmissivity of Kodak No. 87C Gelatine Filter

Wave Length in nm	Percentage Transmission
790	0.55
800	3.0
810	8.3
820	16.2
830	25.7
840	38.0
850	48.4
860	57.5
870	65.3
880	72.5
890	78.5
900	80.2
910	82.2
920	83.2
930	83.2
940	83.2

3.3 Electronics

3.3(i) Lateral Effect Photodetector

When a semiconductor diode is illuminated, a voltage is produced across the junction. According to Lucovsky (1960) when light falls on the junction, electron-hole pairs are formed at the surface the light is falling on. These pairs diffuse through the region in which they are formed. If the thickness of this region is less than the minority carrier diffusion length, then some of the electron-hole pairs will diffuse as far as the junction, where the electrostatic charge will separate the pairs. If, for example, the pairs were formed in the p region then the electrons will cross the barrier and go to the n region, and the holes will remain in the p region. This will reduce the potential barrier across the junction and thus alter the Fermi Levels. In an attempt to return this barrier to its equilibrium value a current flows from the p to the n region, as electrons flow from n to p regions and holes from p to n regions. At steady state the rate of separation of electron-hole pairs is equal to the reinjection current attempting to produce equilibrium. The voltage produced by this current is known as the transverse voltage.

If, however, only one part of the junction is illuminated, or if the illumination is non-uniform, then at different point in the junction different numbers of electron-hole pairs will be produced, then separated by the electrostatic barrier at the junction. This will result in a different level of reduction in the Fermi Levels, and thus a variation in potential across the base layer.

This was first reported by Schottky in 1930, using a copper-copper oxide metal semiconductor. His base was copper, and lateral currents flowed in it due to its low resistivity. Moore and Webster (1955), while measuring the surface recombination velocity of a Germanium surface with a floating barrier, found that when a spot of light, which was producing holes, was over the barrier region, the lifetime of the holes did not agreee with the one dimensional theory which they were applying. They realized that the reason for this was that the junction was of lower resistivity than the rest of the germanium, and was acting as an equipotential region, but they did not realize the capabilities of such a system. Wallmark in 1957 used a junction between an n region and an p region; the p region was more heavily doped than the n region and was known as a p^+ region. It had a lower resistivity than the n region, and as a result higher currents flowed in the p^+ region.

There are injected holes in the p^+ region, and injected electrons in the n region. The p^+ region has a higher conductivity than the than the n region, and the holes redistribute themselves throughout the p^+ region. At points which are not illuminated, the potential difference between the two sides will be different from the Fermi level, and the majority holes in the p^+ region will be injected into the n region, where they will become minority carriers. The electrons, as majority carriers in the n region, will then move through this region to recombine with the holes, and this movement produces the lateral current.

The detectors used were United Detector Technology Inc.'s PIN SC/10D. In this type of photodetector the light falls on the p region, the electron-hole pairs are formed in the intrinsic region, the electrons go into the n region or base, while the holes go into the p region (Kelly, 1976).

Lucovsky (1960) produced a theoretical analysis of a circle of light of radius a falling on an infinite p-n junction. The radius of the spot of light was greater than the minority carrier diffusion length, and the relationship between voltage and illumination which he produced for steady-state, small signal conditions was :-

$$\frac{d^2U}{dr^2} + \frac{1}{r}\left(\frac{dU}{dr}\right) - \frac{\rho_p C}{W_p}\left(\frac{\partial U}{\partial t}\right) - \frac{\rho_p q J_s}{W_p\, k\, T}\, U = \begin{cases} q\rho_p f/W_p & r < a \\ 0 & r > a \end{cases} \tag{3.3.1}$$

or

$$\nabla^2 U - \frac{\rho_p C}{W_p}\left(\frac{\partial U}{\partial t}\right) - \frac{\rho_p\, q\, J_s}{W_p\, k\, T}\, U = q\rho_p f(\mathbf{r},t) \tag{3.3.2}$$

where U(r) is the transverse photovoltage, a is the radius of the spot of light, r is the distance of the position being considered from the centre of the spot of light, ρ_p is the resistivity of the p type region, q is the electron charge, J_s is the current density, W_p is the thickness of the p type layer, k is Boltzmann's constant, T is the absolute temperature and f is the number of electron-hole pairs separated per unit time per unit area at the point being considered. The term $\left(\frac{\rho_p J_s q}{W_p\, k\, T}\right)$ is α^2, where α is the Lucovsky fall-off parameter (Woltring, 1975). Woltring interpreted this parameter as the product of the lateral sheet resistance per unit area and the transverse conductance per unit area at zero bias.

Kelly (1976) for a similar PIN detector used the solution of the above equation

$$I_s = I_0\, \frac{\sinh(\alpha(L-s))}{\sinh(\alpha L)} \tag{3.3.3}$$

for a detector of length L and a spot of light distance s from the contact through which I_s is flowing; α is the Lucovsky fall-off parameter and I_0 is the total photoinduced current, given by

$$I_0 = \int_{\lambda=0}^{\lambda=\infty} P_d \, R_\lambda \, d\lambda \tag{3.3.4}$$

where P_d is the monochromatic light power incident perpendicularly on the detector and R_λ is the detector responsivity to light of wavelength λ. With zero termination impedance most of the current produced flows down the contacts, but some is lost due to recombination at the surface of the diode. As α approaches zero then I_s approaches I_0 (1-s/L), and the smaller α is the more nearly this is approached. Kelly considered that non-linearities in the system are solely due to variations in the light intensity.

Lucovsky's equation (3.3.2) for the time dependent small signal case is:

$$\nabla^2 U - \frac{\rho_d C}{W_d}\left(\frac{\partial U}{\partial t}\right) - \alpha^2 = \frac{-\rho_{pq}}{W_p} f(\mathbf{r},t) \tag{3.3.5}$$

according to Woltring, where C is the barrier capacitance. This is the generalised heat equation (Kreysig, 1975) and may be solved with the boundary Dirichlet conditions (i.e. U=0 at the edges) giving

$$I_{x-} = I(x=0,t) = \frac{2}{\pi} I_s \sum_{n=-\infty}^{\infty} \frac{\sin[(2n-1)\pi \, y_0/l]}{(2n-1)} \cdot \left[\frac{\sinh[a_n(1-x_0/l)]}{\sinh a_n} - \sum_{m=-\infty}^{\infty} \frac{m\pi \sin[m\pi \, x_0/l]}{a_n^2 + m^2\pi^2} \exp\left\{ -(a_n^2 + m^2\pi^2)\frac{t}{\rho l^2} \right\} \right] \tag{3.3.6}$$

where $a_n = (\alpha^2 l^2 + (2n-1)^2 \pi^2)$

The y coordinate is present in this solution, and as a result the signals output from two opposite contacts decrease when the spot of light moves out of the centre towards either of the other contacts, for constant noise and light power. For the PIN type of detector, if the outputs from the four contacts are X^+ in the positive and X^- in the negative X directions and Y^+ in the positive and Y^- in the negative Y directions, Woltring suggested three possible linearising algorithms:

(i) $$P_x = X^+ - X^- \;,\; P_y = Y^+ - Y^- \tag{3.3.7}$$

(ii) $$P_x = \frac{X^+ - X^-}{X^+ + X^- + Y^+ + Y^-} \qquad P_y = \frac{Y^+ - Y^-}{X^+ + X^- + Y^+ + Y^-} \tag{3.3.8}$$

(iii) $$P_x = \log_{10}(X^+/X^-) \quad P_y = \log_{10}(Y^+/Y^-) \tag{3.3.9}$$

Olson (1977) suggested three different electronic circuits for reading the output of the lateral effect photodetectors:

(i) Simple difference, which is equivalent to Woltring's first algorithm, i.e. $P_x = X^+ - X^-$, $P_y = Y^+ - Y^-$ (3.3.7)

(ii) Divider Intensity Normalisation, where the difference of the two signals is divided by the sum of the two signals,

i.e. $$P_x = \frac{X^+ - X^-}{X^+ + X^-} \;,\; P_y = \frac{Y^+ - Y^-}{Y^+ + Y^-} \tag{3.3.10}$$

(iii) Automatic Gain Control Intensity Normalisation, where the sum of the two sides is compared to a desired voltage level, and the light intensity is varied to make these two levels equal. The difference of the two signals is then used. However, this method is only suitable for one dimensional rather than two dimensional detector.

3.3(ii) Electronic Circuits

It was decided that the way to use the photodetectors was by illuminating them with pulsed light. This meant that if they were sampled during both the "light" and "dark" times any background light or current could be subtracted from the signal.

The original electronic circuit that was designed is shown in Figure 3.3.1. The outputs from the Lateral Effect Photodetectors were first fed into current-to-voltage preamplifiers (Analog AD510J). The output signals from opposite sides of the detector were subsequently applied to both the adder and the subtractor circuits, and then into the Sample-Hold circuits, so that the minimum could be subtracted from the maximum value of the signal. The minimum signal consisted of any background light, and any voltage offsets from other causes, including bias voltages, while the maximum signal consisted of required signal together with the offsets that were present in the minimum signal. The difference between the output signals was divided by the sum of the output signals, in an Analog AD532JD divider, so that any changes in the light intensity would be nullified (Kelly, 1976). Finally the signal was passed through a low pass filter (Sallen and Key, 1955) to remove any high frequency noise.

The LED's were driven by the circuit shown in Figure 3.3.2. Here the CMOS 555 is used in its astable manner to produce a train of pulses with a duty cycle given by

$$\frac{t_1}{t_1+t_2} = \frac{R_A+R_B}{R_A+2R_B} \times 100\% \qquad (3.3.11)$$

were $t_1 = 0.693(R_A+R_B)C$ and $t_2 = 0.693R_BC$ (Horowitz and Hill, 1980). The chosen values were R_A=1M0, R_B=680k and C = 330pF. This gave a duty cycle $t_1/(t_1 + t_2)$ of 71% at a frequency of 1.85 kHz. This signal was fed into a 4017 5-stage Johnson counter,

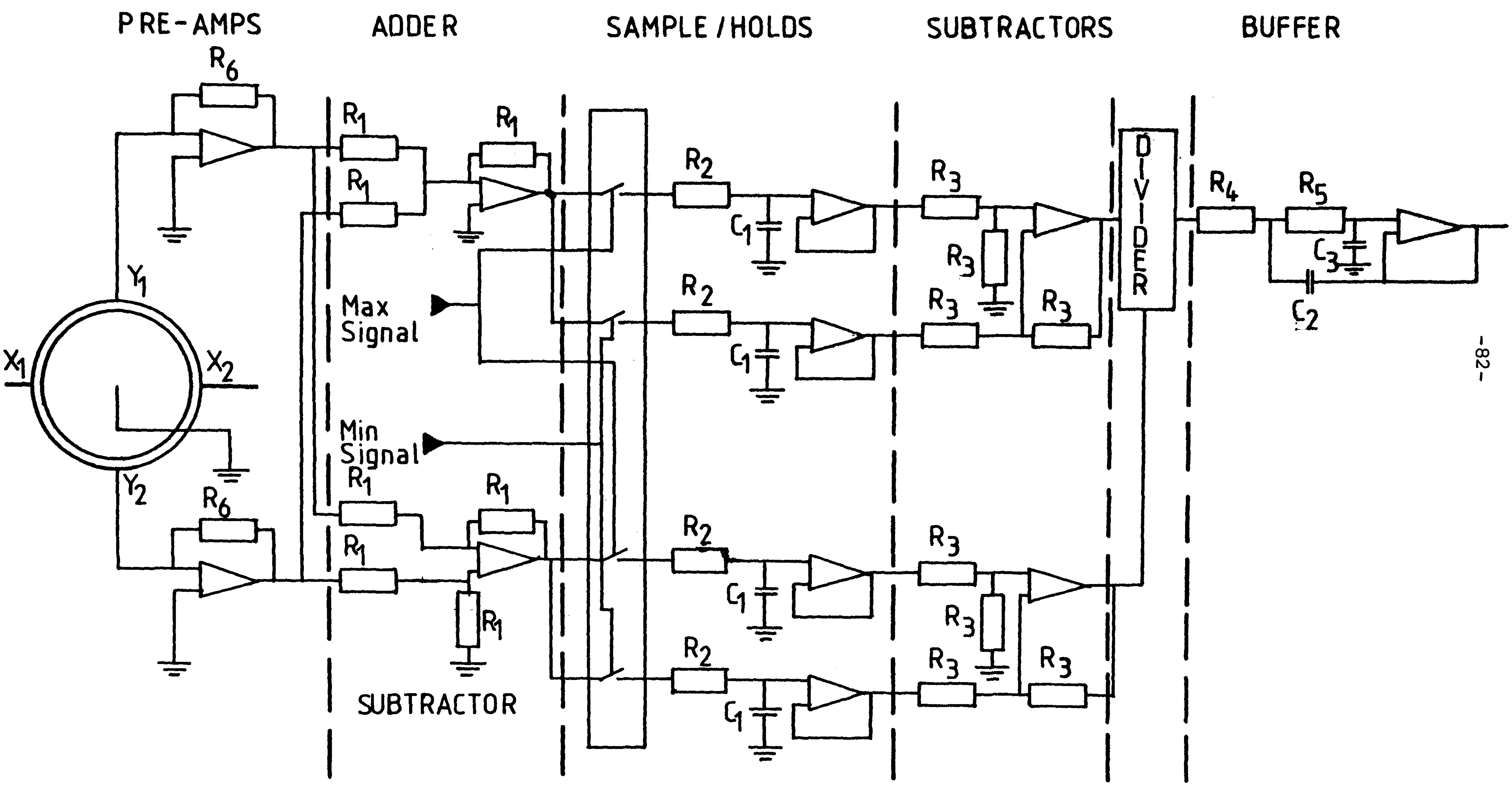

Detector Reading Circuit (Mark I(a))

Fig 3.3.1

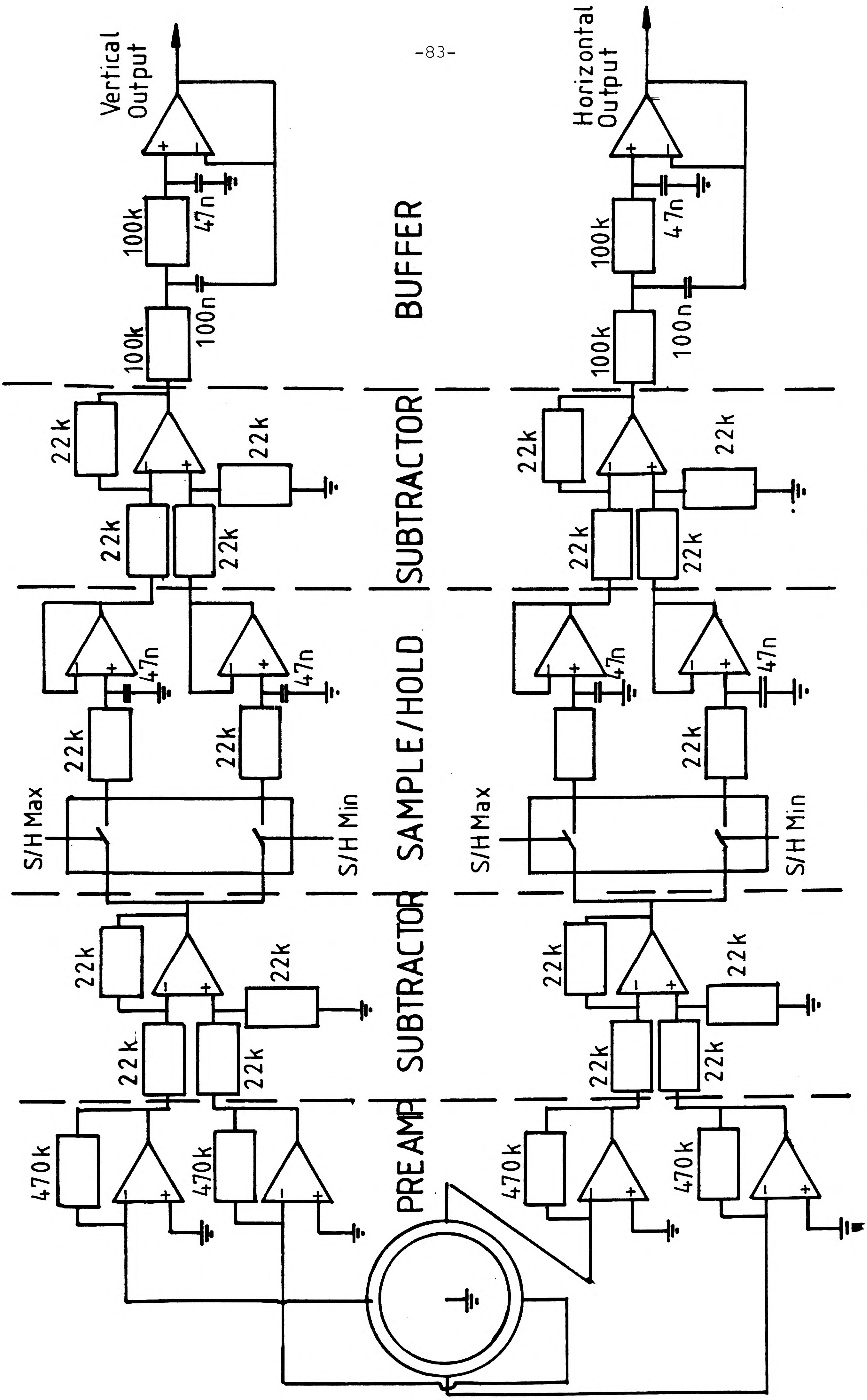

Detector Reading Circuit (Mark I(b))

Fig 3.3.3

from which outputs O_0 and O_5 were sent to a 4066 Quadruple Bilateral Switch. This produced the signals to control the sample-and-hold circuits, and to switch the LED's. The LED's (Texas Instruments TIL32) were connected in series, and supplied by an 80 mA pulsed constant current signal, with a 1 in 10 cycle. The devices are rated at 40 mA in free air at a temperature of 25°C. Since the LED's were to be placed inside a tightly fitting aluminium collimator, inside an aluminium block, inside a black box, it was considered that a safety factor was needed to prevent the LED's from overheating, and that a 1 in 10 cycle of 80 mA would provide this while still giving a frequency of sampling of 185 Hz.

When these circuits had been designed the power consumption was found to be approximately 900 mW at +/- 15 V d.c. per detector. This was to have been supplied by a 5 V battery pack, via a 5 V to +/- 15 V converter of approximately 70% efficiency. The total power requirement would therefore be 1.3 W per detector, or approximately 4 W for three detectors. This was thought to be too great to permit the patient to be monitored for a reasonable length of time.

It was decided that a significant saving in power consumption could be made by eliminating the divider circuit, half of the sample-and-holds, the adder and one of the subtractors. The output would then be sensitive to variations in LED light output. However, the LEDs were to be run off a constant current source, under which conditions the light output should be stable (Kelly, 1976; Olson, 1977). The resulting reduction in power consumption was appoximately 1.3 W or 32%, increasing the possible monitoring time by 50%, although this was still not long enough, so another circuit was designed.

The circuit decided upon is shown in Figure 3.3.3. The four

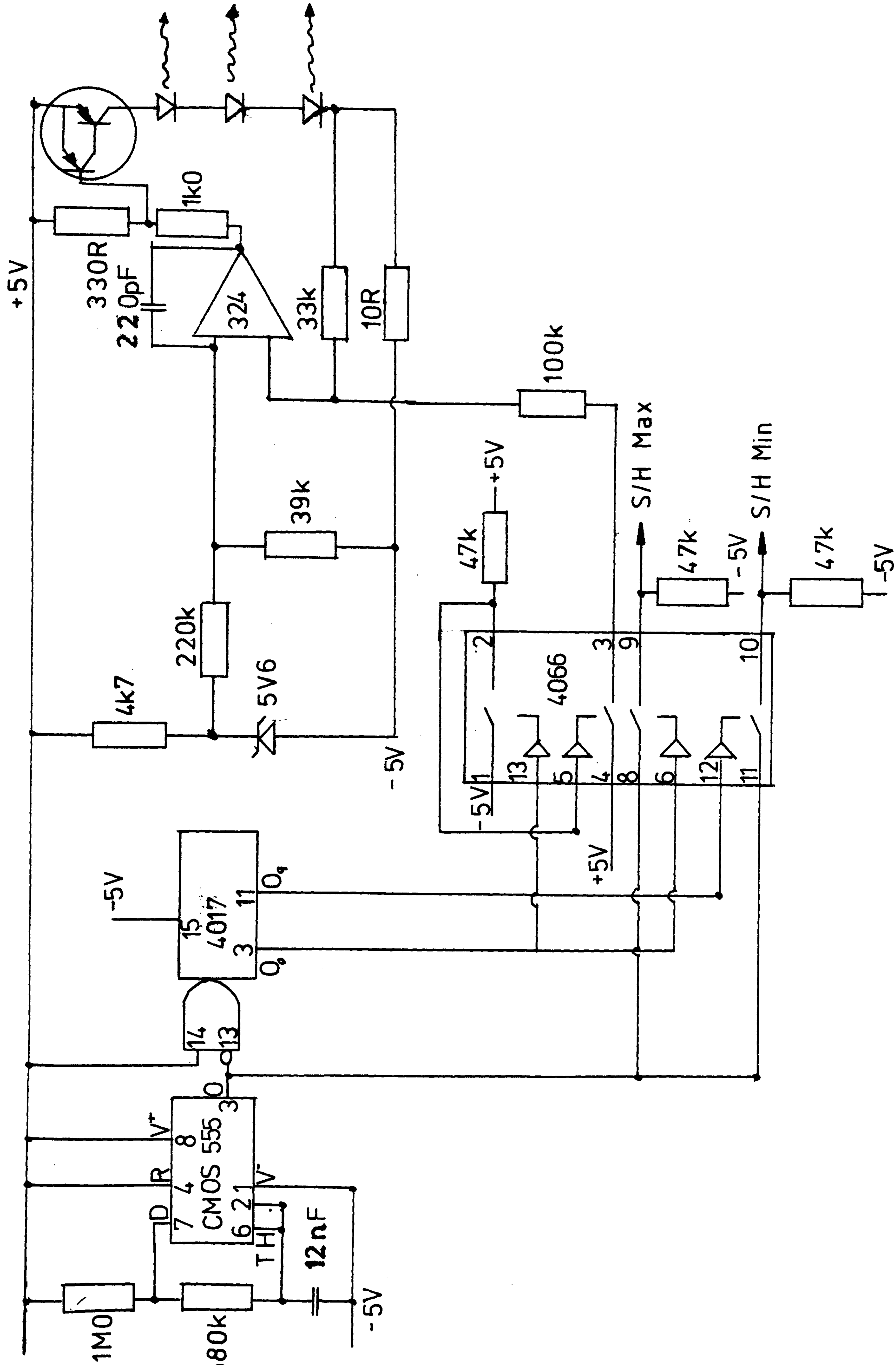

Fig 3.3.2

L.E.D. Driving Circuit (Mark I)

current outputs were fed into four pre-amplifiers, which were low power dual matched instrumentation operational amplifiers (Precision Monolithics OP10CY). These amplifiers could be run off +/- 5 V d.c. power supply, with a maximum power consumption of 8 mW, compared with a maximum power consumption of 120 mW for the Analog AD510J. The outputs from the opposing sides were then subtracted and fed into sample-and-holds, so that the "dark" current could be subtracted from the "light" current. The signal was finally passed to the Sallen and Key low pass filter. This circuit was run off +/- 5 V d.c. power supply with a total power consumption of 250 mW for the three detectors and the L.E.D. drive circuit.

3.3(iii) Linearity of the detectors

The detectors were calibrated by mounting a detector on the stage of a microscope and mounting an LED in its collimator in the lens section of the microscope. The microscope stage was arranged so that two micrometers could move it relative to the rest of the microscope in two perpendicular directions. The micrometers were were marked in divisions of 0.01 mm, and each had a travel of 25 mm. The detector was mounted so that as far as possible the axes of the detector were aligned with the directions of movement of the stage. However, as the detector was mounted in a circular case by the manufacturer, this alignment had to be done by eye. A similar problem was encountered in mounting the LED and its collimator perpendicular to the stage. This resulted in the effects shown in Figure 3.2.22 where as the LED was raised, theoretically perpendicular to the plane of the detector, the point of light moved over the detector.

The system consisting of the LED in a collimator, driven by the circuit shown in Figure 3.3.2, and the photodetector, read by the circuit shown in Figure 3.3.3, was calibrated. The voltages produced by the X and Y circuits were measured in steps of 0.25 mm in one direction and steps of 2.00 mm in the perpendicular direction. The relationship between displacements and voltages are shown in Figures 3.3.4 to 3.3.7. As the spot of light was moved parallel to one of the axes, the output in the direction perpendicular to the direction of motion did not remain constant, which it should have done according to Kelly (1976) and Olson (1977). Instead it varied in an approximately parabolic manner so that as the light moved away from the centre line of the detector the output in the perpendicular direction fell. The change in output perpendicular to the direction of motion was not

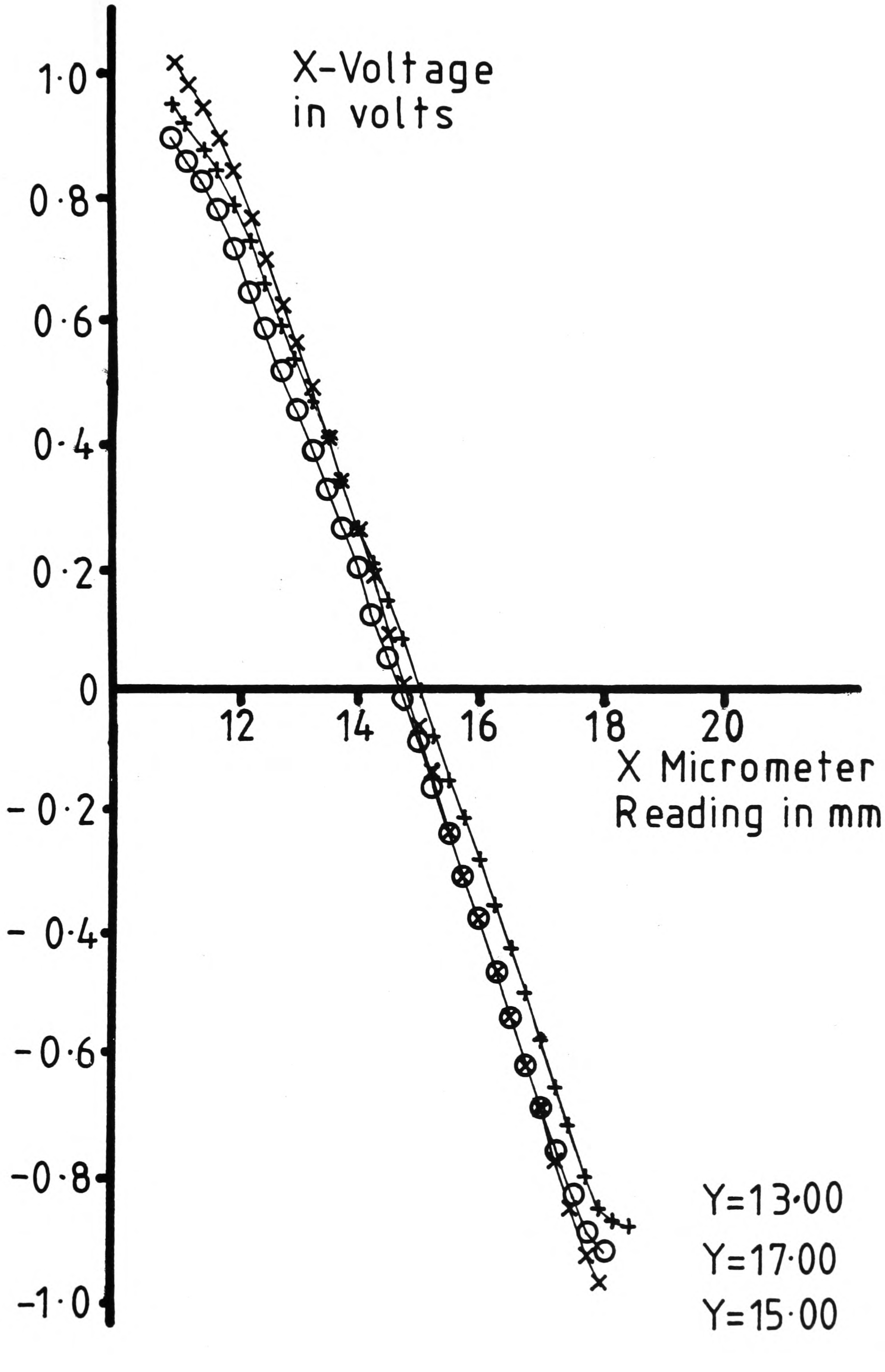
X-Voltage
in volts
1·0
0·8
0·6
0·4
0·2
0
- 0·2
- 0·4
-0·6
-0·8
-1·0
12
14
16
18
20
X Micrometer
Reading in mm
Y=13·00
Y=17·00
Y=15·00

Fig 3.3.4

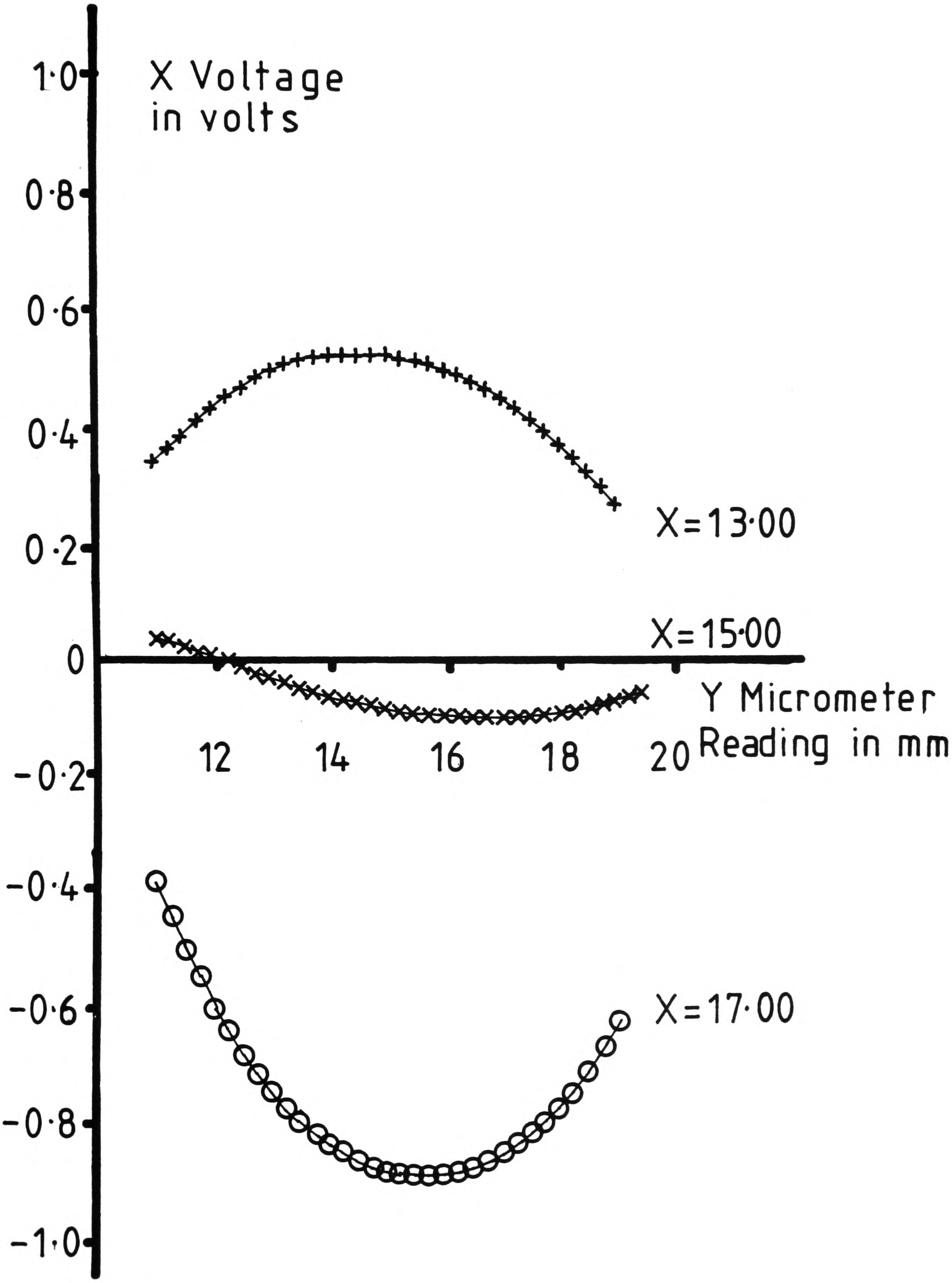
X Voltage
in volts
1·0
0·8
0·6
0·4
0·2
0
-0·2
-0·4
-0·6
-0·8
-1·0
12
14
16
18
20
Y Micrometer
Reading in mm
X=13·00
X=15·00
X=17·00

Fig 3.3.5

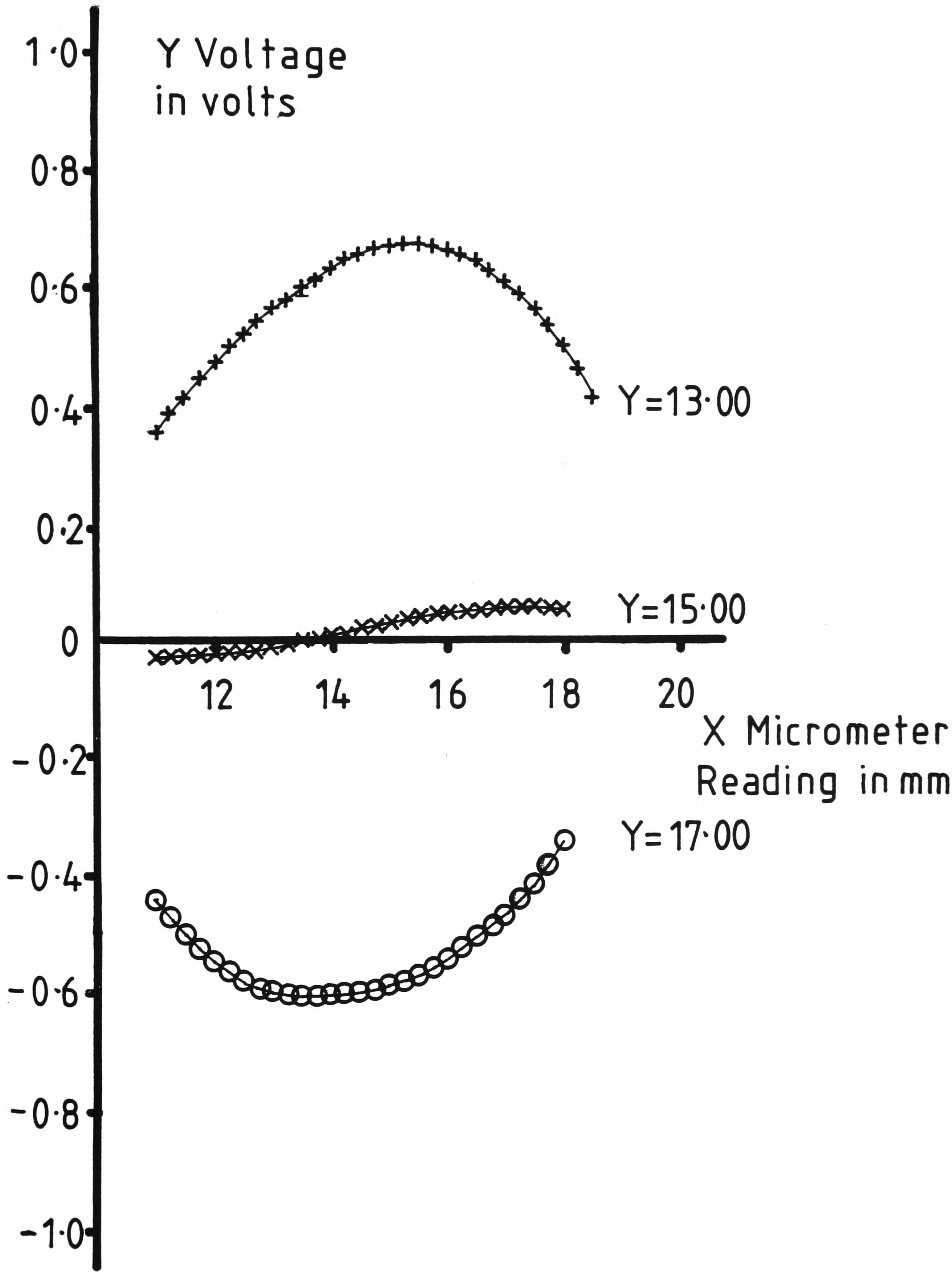
1·0
0·8
0·6
0·4
0·2
0
-0·2
-0·4
-0·6
-0·8
-1·0
Y Voltage
in volts
Y=13·00
Y=15·00
Y=17·00
12
14
16
18
20
X Micrometer
Reading in mm

Fig 3.3.6

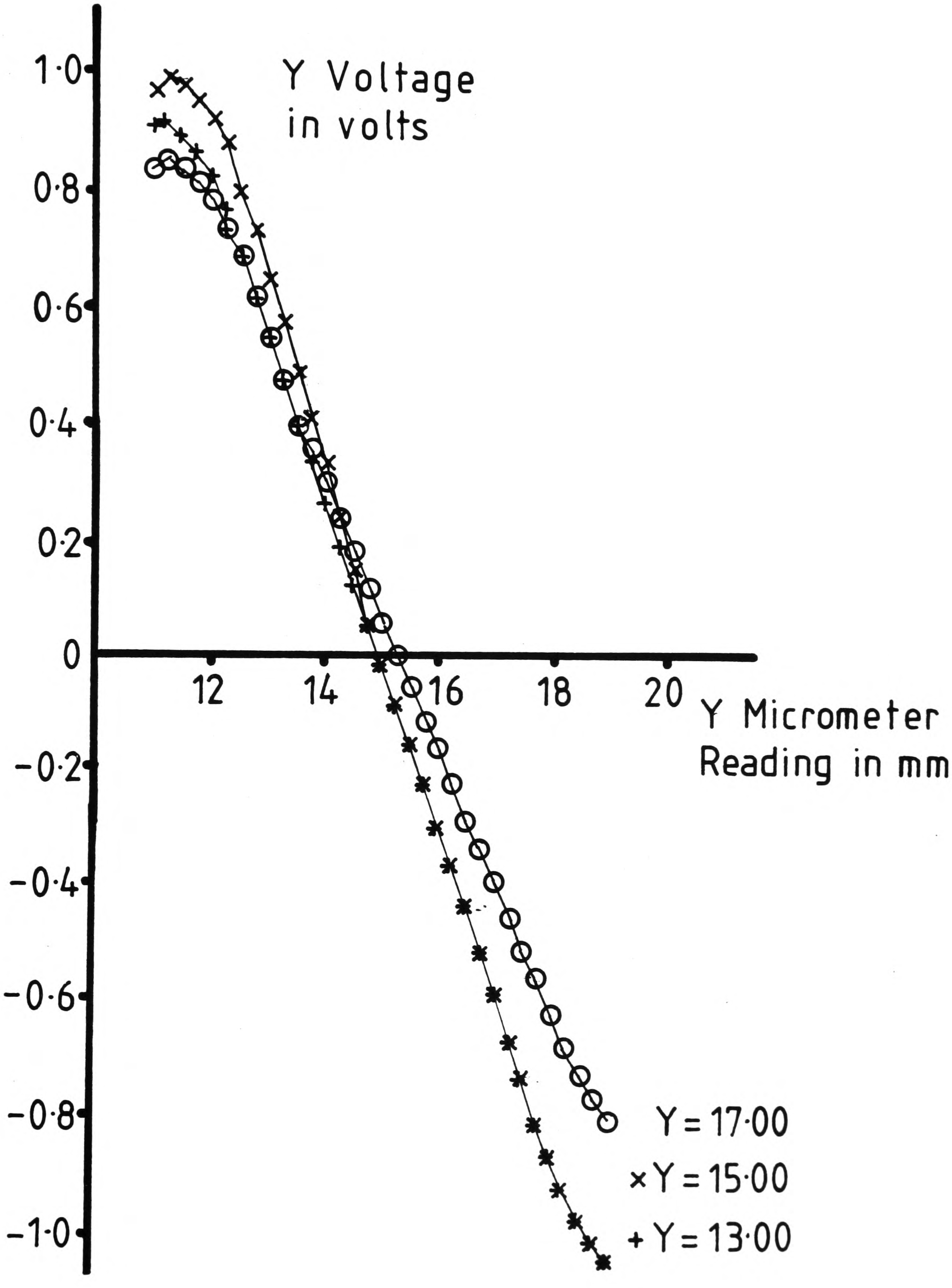
Y Voltage
in volts
1·0
0·8
0·6
0·4
0·2
0
−0·2
−0·4
−0·6
−0·8
−1·0
12
14
16
18
20
Y Micrometer
Reading in mm
Y = 17·00
× Y = 15·00
+ Y = 13·00

Fig 3.3.7

predicted by Olson (1977) or Kelly (1976), but it does agree with the theory of Woltring (1975). The output parallel to the direction of movement, however was found to be linear, over the range $\pm$ 3 mm from the centre of the detector. The falloff in the signal outside this range was presumably because the some of the light was not falling on the detector and the number of electron-hole pairs being produced was reduced. The spot of light was designed to have a diameter of approximately 2 mm, which would result in a falloff in signal strength at a distance of 3 mm away from the centre of the detector.

Various methods were tried to remove the non-linearity of the detectors. Reverse biassing the detector with 5 V and 12 V, did not have the desired effect. When the two sides which were not being measured were disconnected, the non-linearity was still present, as can be seen in figure 3.3.8, showing the voltage in the direction perpendicular to the direction of movement.

It was decided to perform the linearisation mathematically, using a digital computer, rather than by electronic circuitry. It was thus necessary to modify the circuit to output the signal from the preamplifiers, eliminating the sample-and-hold and subtraction stages, as shown in Figure 3.3.9. A separate signal was provided to send timing signals to the computer 'A/D start' line, as shown in Figure 3.2.10. The detector output signals were conneted to the AR11 analog/digital interface on a Digital Equipment Corporation PDP11/34 computer. The 12 channels were each sampled twice during the cycle, once in the "light" pulse and once during the "dark" phase. The sampling was performed by the subroutine LSAMPL.MAC, and the timing pulses were detected by the subroutine MSTART.MAC, both of which were called by the program LINPUT.FOR. (The programs and subroutines are

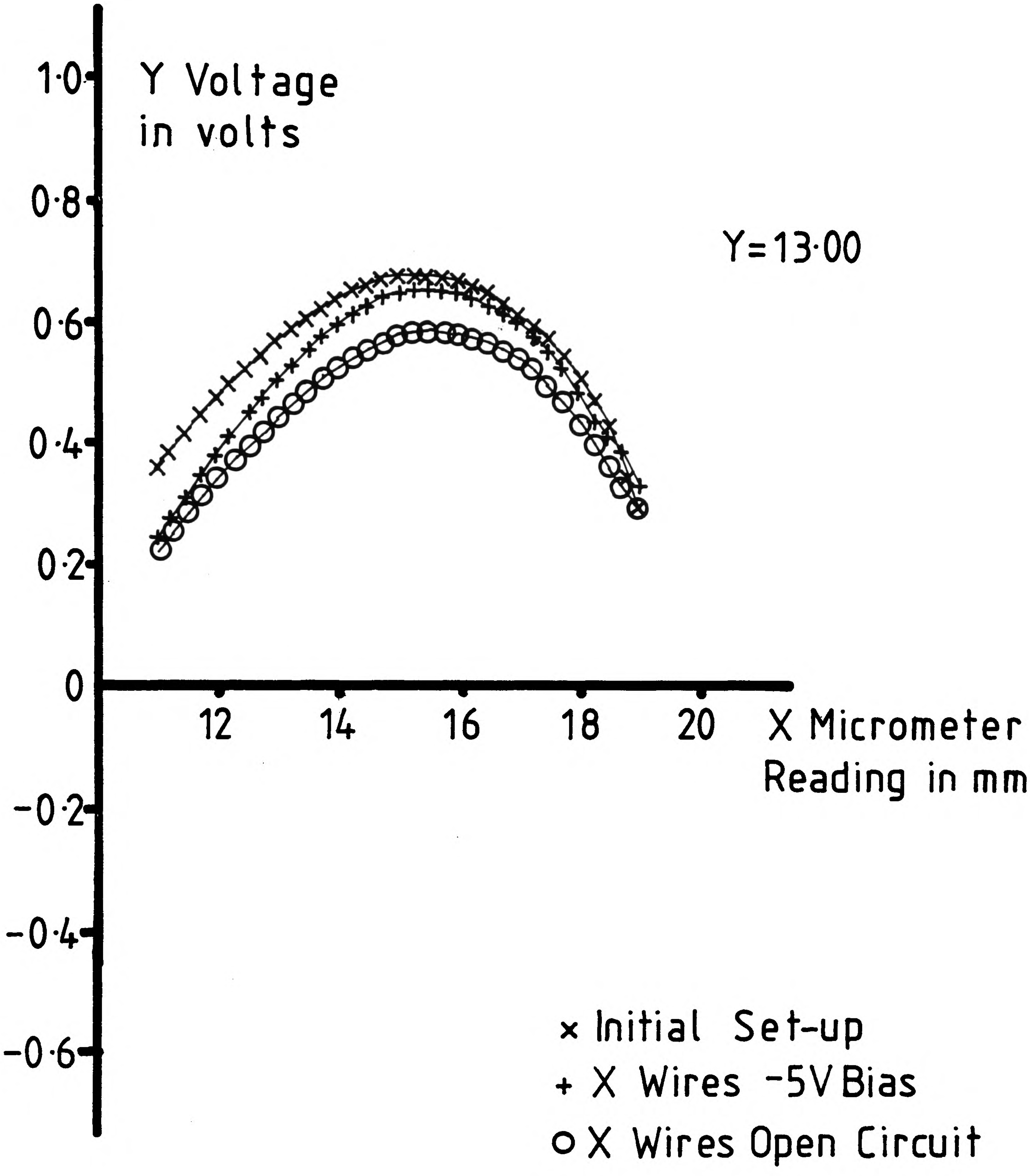

1·0
0·8
0·6
0·4
0·2
0
-0·2
-0·4
-0·6
Y Voltage
in volts
Y=13·00
12
14
16
18
20
X Micrometer
Reading in mm
× Initial Set-up
+ X Wires -5V Bias
o X Wires Open Circuit

Fig 3.3.8

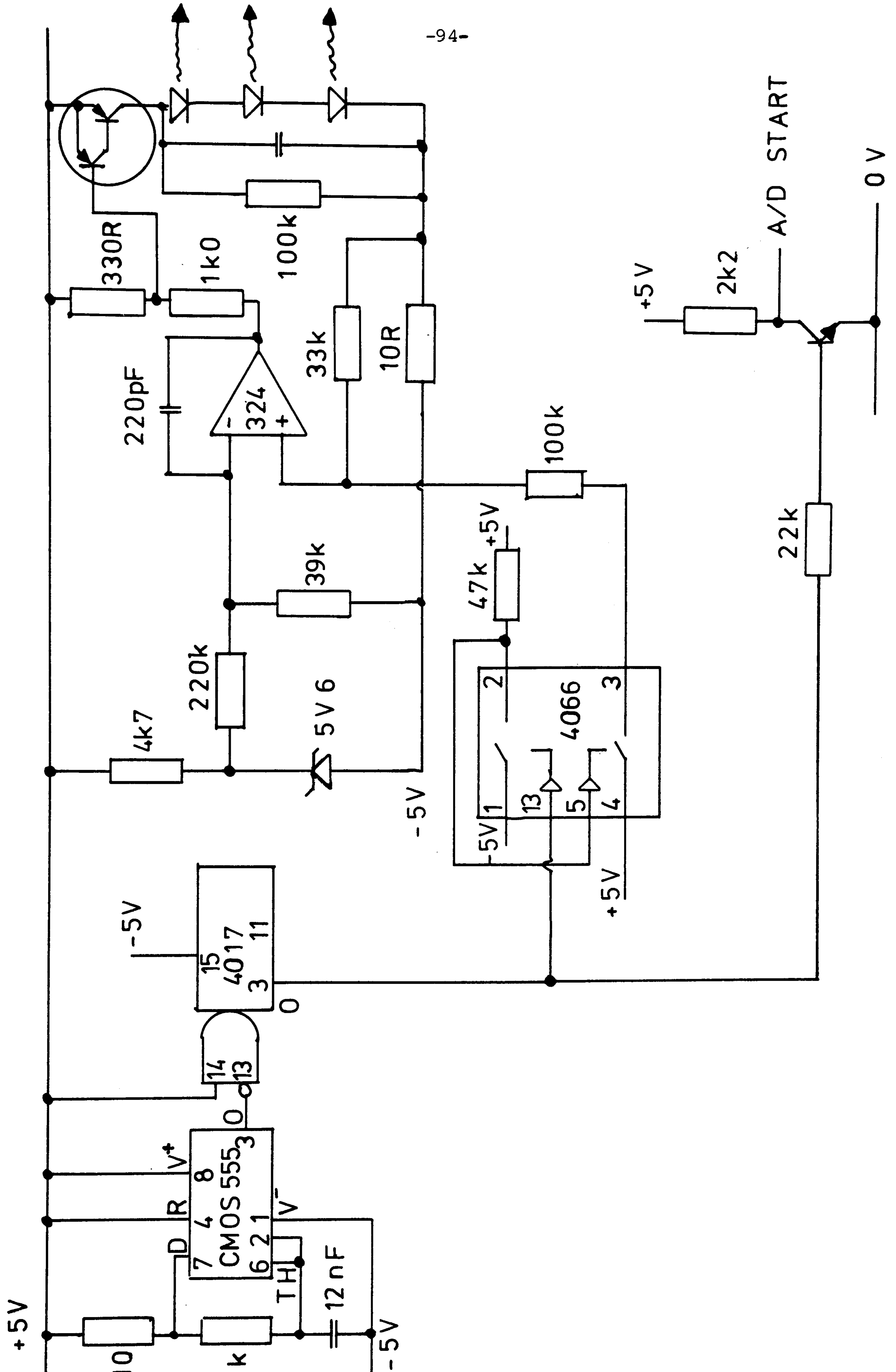

L.E.D. Drive Circuit (Mark II)

Fig 3.3.10

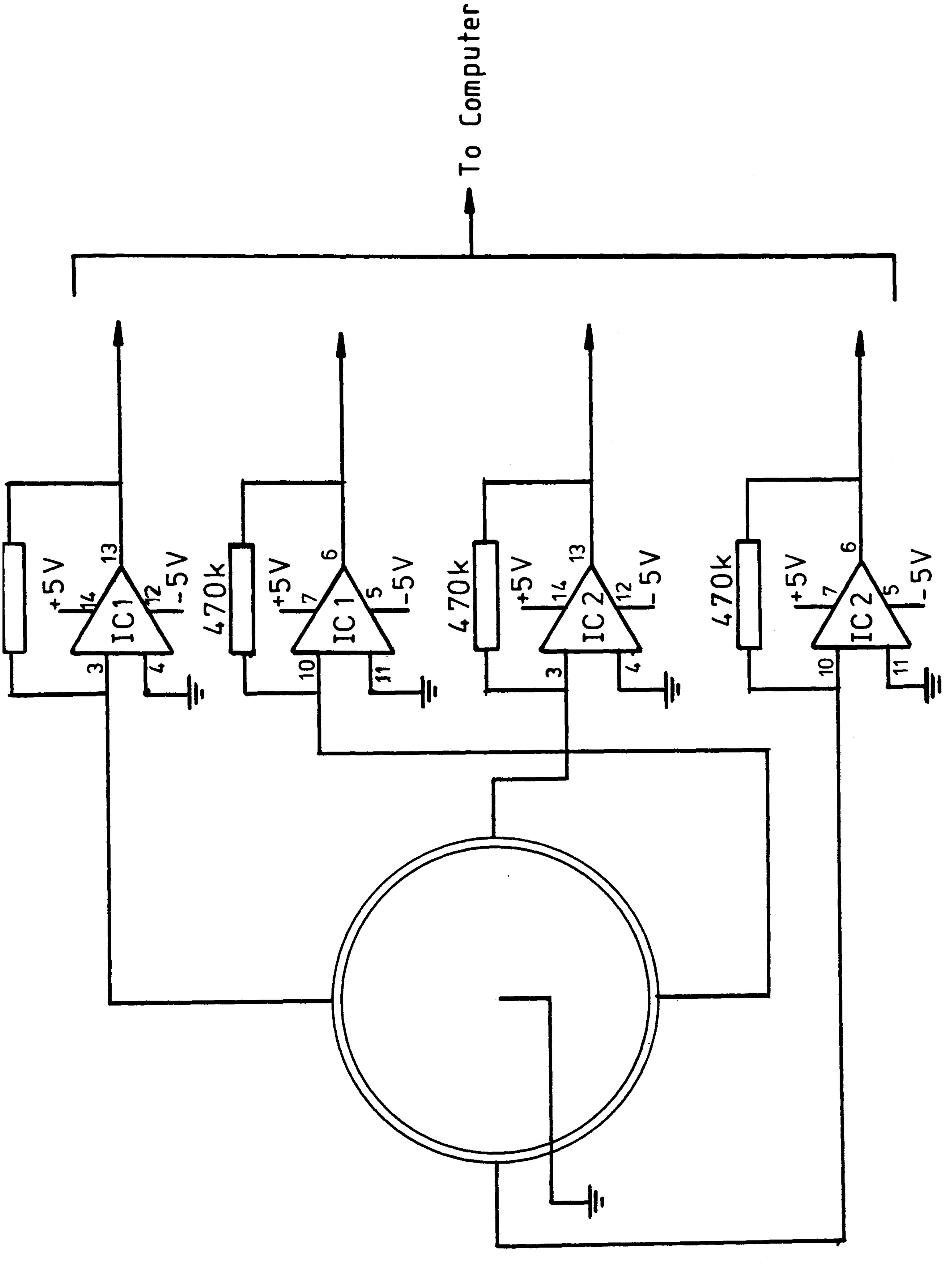

Detector Reading Circuit. (Mark II)

Fig 3.3.9

listed in the Microfische in the back cover of this thesis.)

Three linearising algorithms were compared:

$$\text{(i)} \quad D_X = \frac{X^+-X^-}{X^++X^-+Y^++Y^-} \qquad D_Y = \frac{Y^+-Y^-}{X^++X^-+Y^++Y^-} \tag{3.3.12}$$

$$\text{(ii)} \quad D_X = \log_{10}(X^-/X^+) \qquad D_Y = \log_{10}(Y^-/Y^+) \tag{3.3.13}$$

suggested by Woltring (1975) and

$$\text{(iii)} \quad D_x = \frac{X^+-X^-}{X^++X^-} \qquad D_y = \frac{Y^+-Y^-}{Y^++Y^-}$$

which is the mathematical equivalent of the circuitry suggested by Olson (1977) where X^+ and X^-, and Y^+ and Y^- are the outputs in the positive and negative X and Y directions. Woltring's third algorithm, $D_X = X^++X^-$, $D_Y = Y^++Y^-$, was not tried as it was the mathematical equivalent of the circuit which had previously been tested and rejected.

Figures 3.2.11 to 3.2.14 show the results from Woltring's first algorithm (equation 3.2.12). The D_X versus X micrometer movement and D_Y versus Y micrometer movement graphs are linear, however, the D_X versus Y micrometer and D_Y versus X micrometer are parabolic. Figures 3.2.15 to 3.2.18 show the results from Woltring's second algorithm, the logarithmic relationship (equation 3.2.13). The D_X versus X micrometer movement and D_Y versus Y micrometer movement are linear as are the D_Y versus X micrometer movement and D_X versus Y micrometer movement graphs. Figures 3.2.19 to 3.2.22 show the results of Olson's algorithm equation 3.2.14. All four graphs are linear. The two algorithms, $D_X = \ln (X^-/X^+)$ and $D_X = \dfrac{X^+ - X^-}{X^+ + X^-}$ give

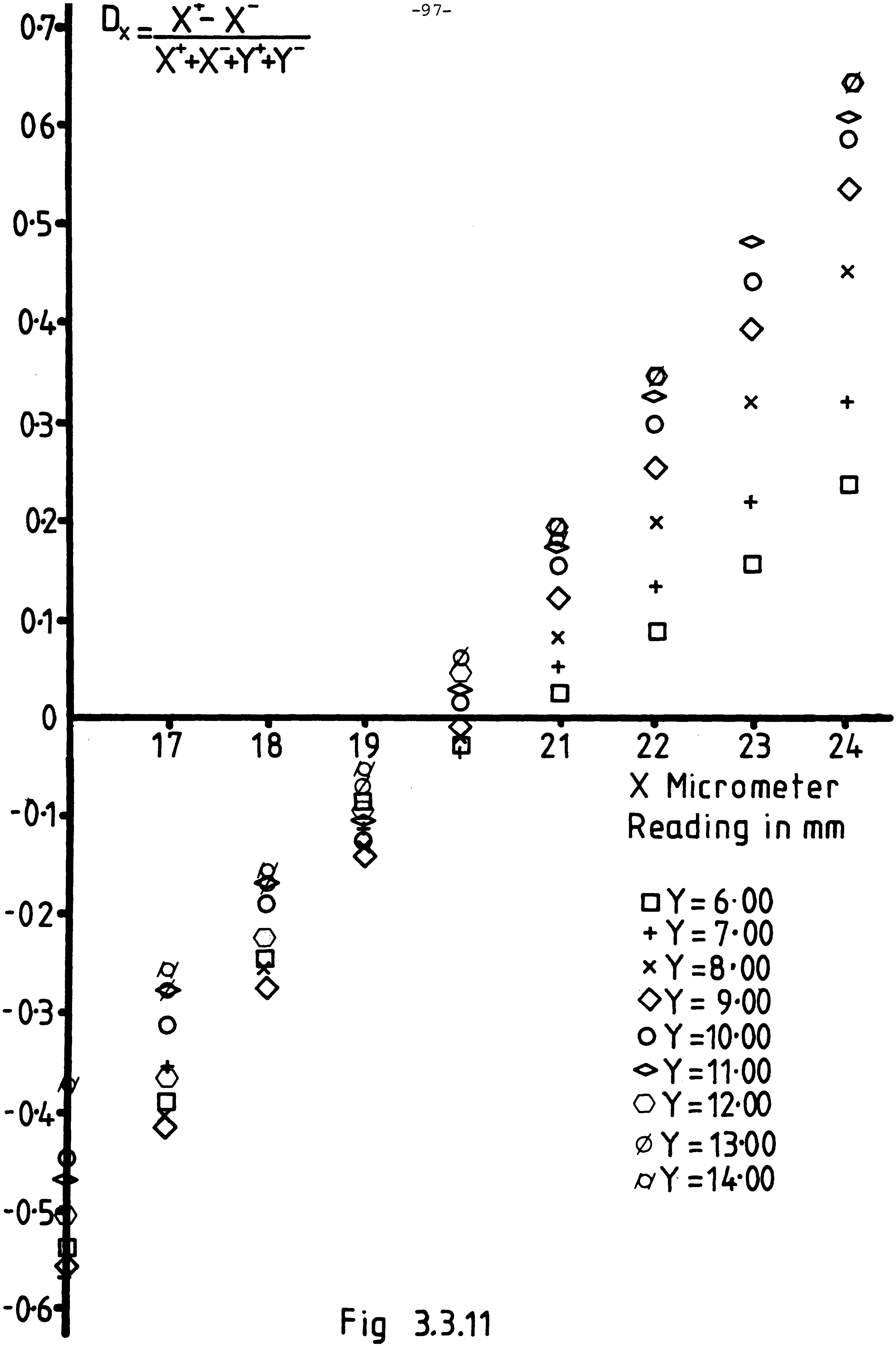

$D_x = \frac{X^+ - X^-}{X^+ + X^- + Y^+ + Y^-}$
0·7
0·6
0·5
0·4
0·3
0·2
0·1
0
-0·1
-0·2
-0·3
-0·4
-0·5
-0·6
17
18
19
21
22
23
24
X Micrometer Reading in mm
Y = 6·00
Y = 7·00
Y = 8·00
Y = 9·00
Y = 10·00
Y = 11·00
Y = 12·00
Y = 13·00
Y = 14·00

Fig 3.3.11

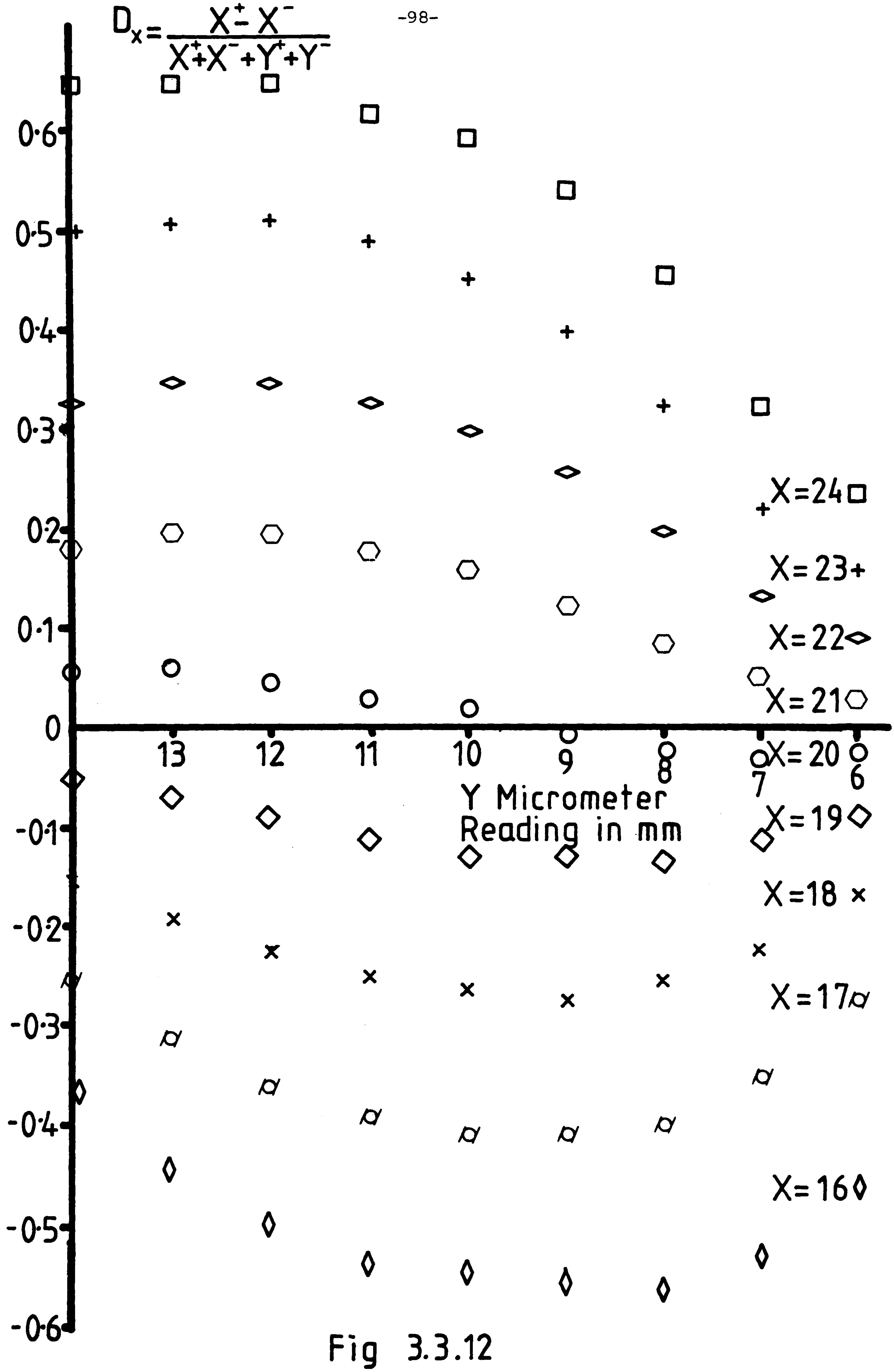
$D_x = \frac{X^+ - X^-}{X^+ + X^- + Y^+ + Y^-}$
0·6
0·5
0·4
0·3
0·2
0·1
0
-0·1
-0·2
-0·3
-0·4
-0·5
-0·6
13
12
11
10
9
8
7
6
Y Micrometer
Reading in mm
X=24
X=23
X=22
X=21
X=20
X=19
X=18
X=17
X=16

Fig 3.3.12

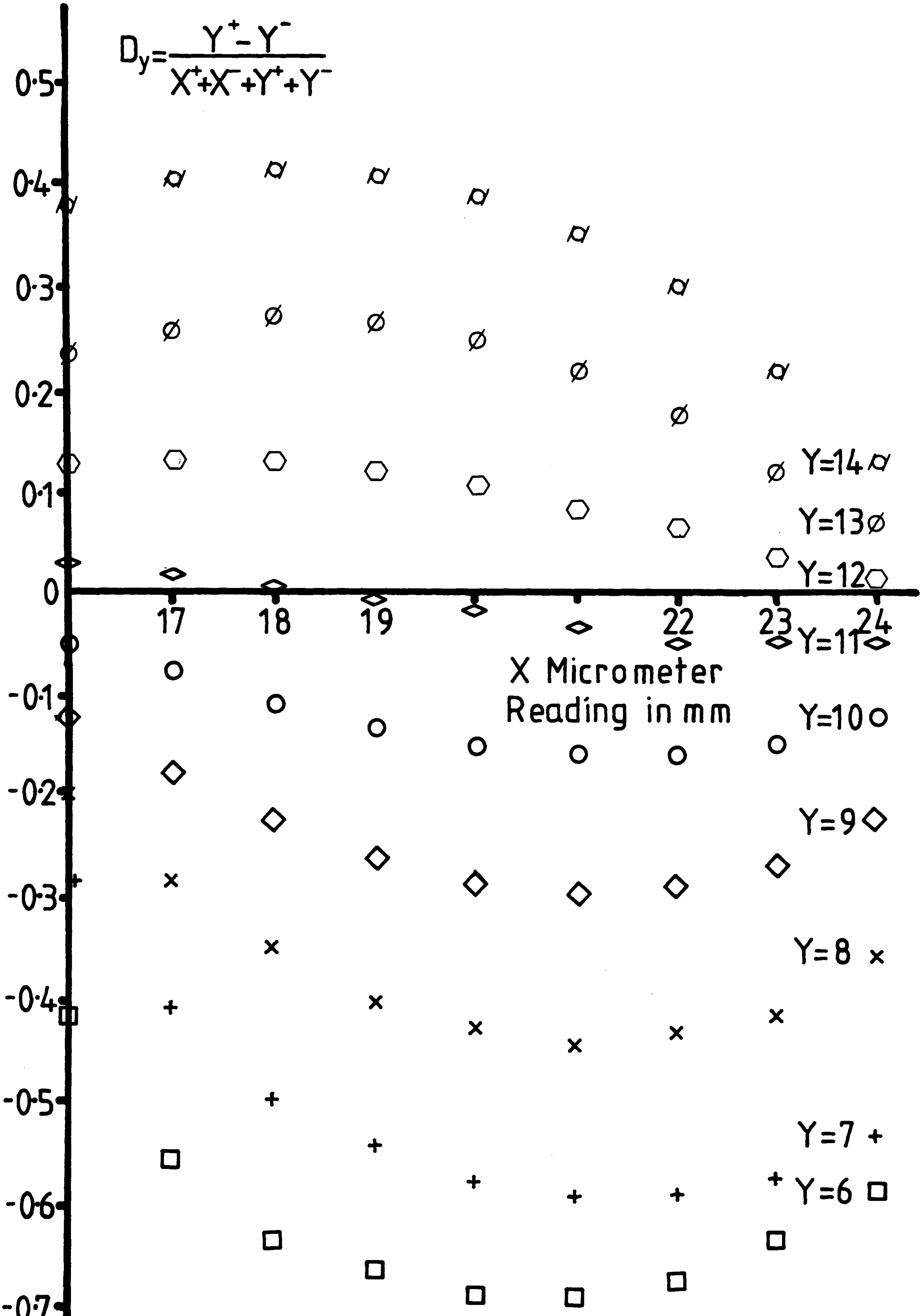
$D_y = \frac{Y^+ - Y^-}{X^+ + X^- + Y^+ + Y^-}$
0·5
0·4
0·3
0·2
0·1
0
-0·1
-0·2
-0·3
-0·4
-0·5
-0·6
-0·7
17
18
19
22
23
24
X Micrometer
Reading in mm
Y=14
Y=13
Y=12
Y=11
Y=10
Y=9
Y=8
Y=7
Y=6

Fig 3.3.13

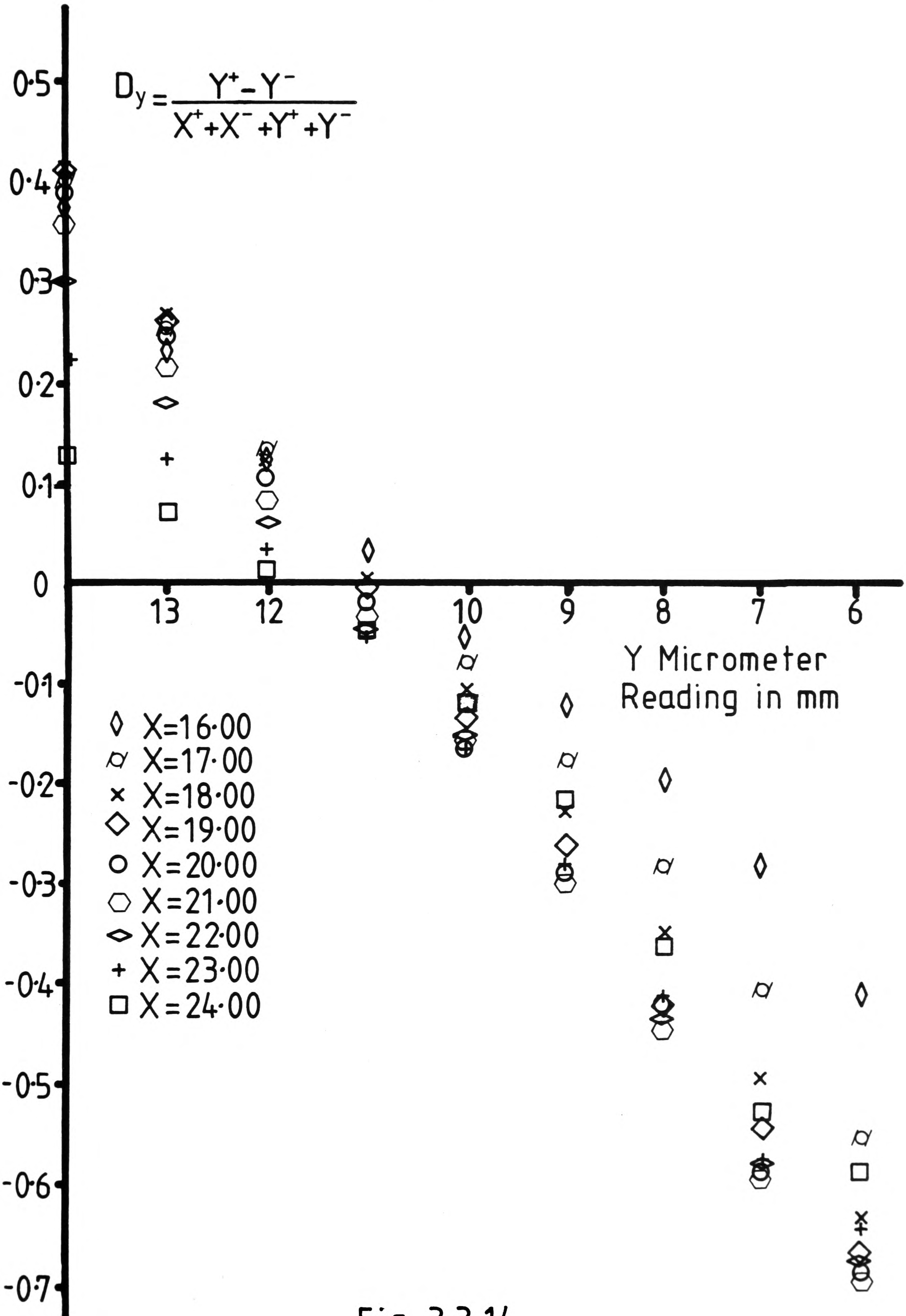

$D_y = \frac{Y^+ - Y^-}{X^+ + X^- + Y^+ + Y^-}$
0·5
0·4
0·3
0·2
0·1
0
-0·1
-0·2
-0·3
-0·4
-0·5
-0·6
-0·7
13
12
10
9
8
7
6
Y Micrometer
Reading in mm
X=16·00
X=17·00
X=18·00
X=19·00
X=20·00
X=21·00
X=22·00
X=23·00
X=24·00

Fig 3.3.14

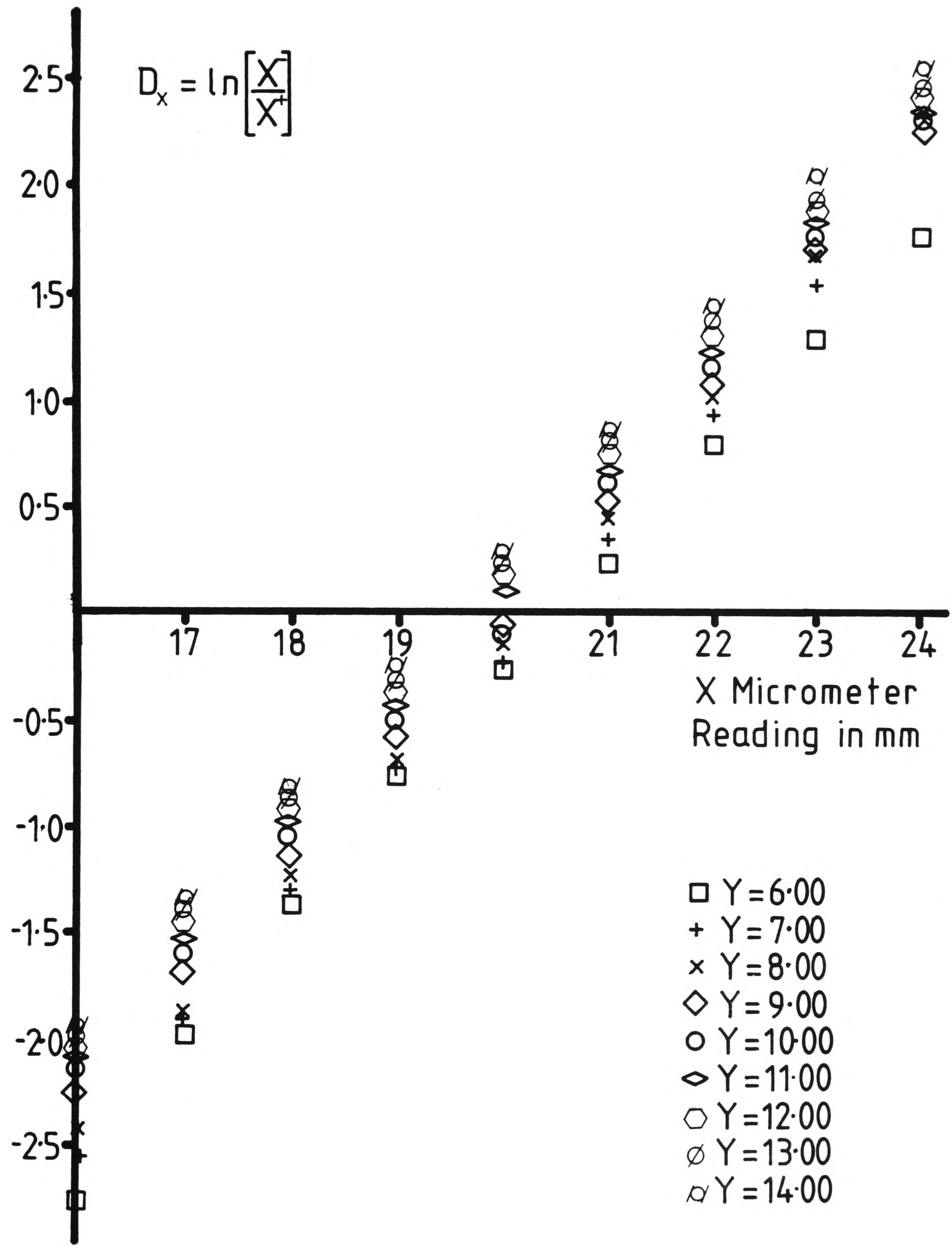

$D_x = \ln\left[\frac{X}{X^+}\right]$
2·5
2·0
1·5
1·0
0·5
-0·5
-1·0
-1·5
-2·0
-2·5
17
18
19
21
22
23
24
X Micrometer
Reading in mm
Y = 6·00
Y = 7·00
Y = 8·00
Y = 9·00
Y = 10·00
Y = 11·00
Y = 12·00
Y = 13·00
Y = 14·00

Fig 3.3.15

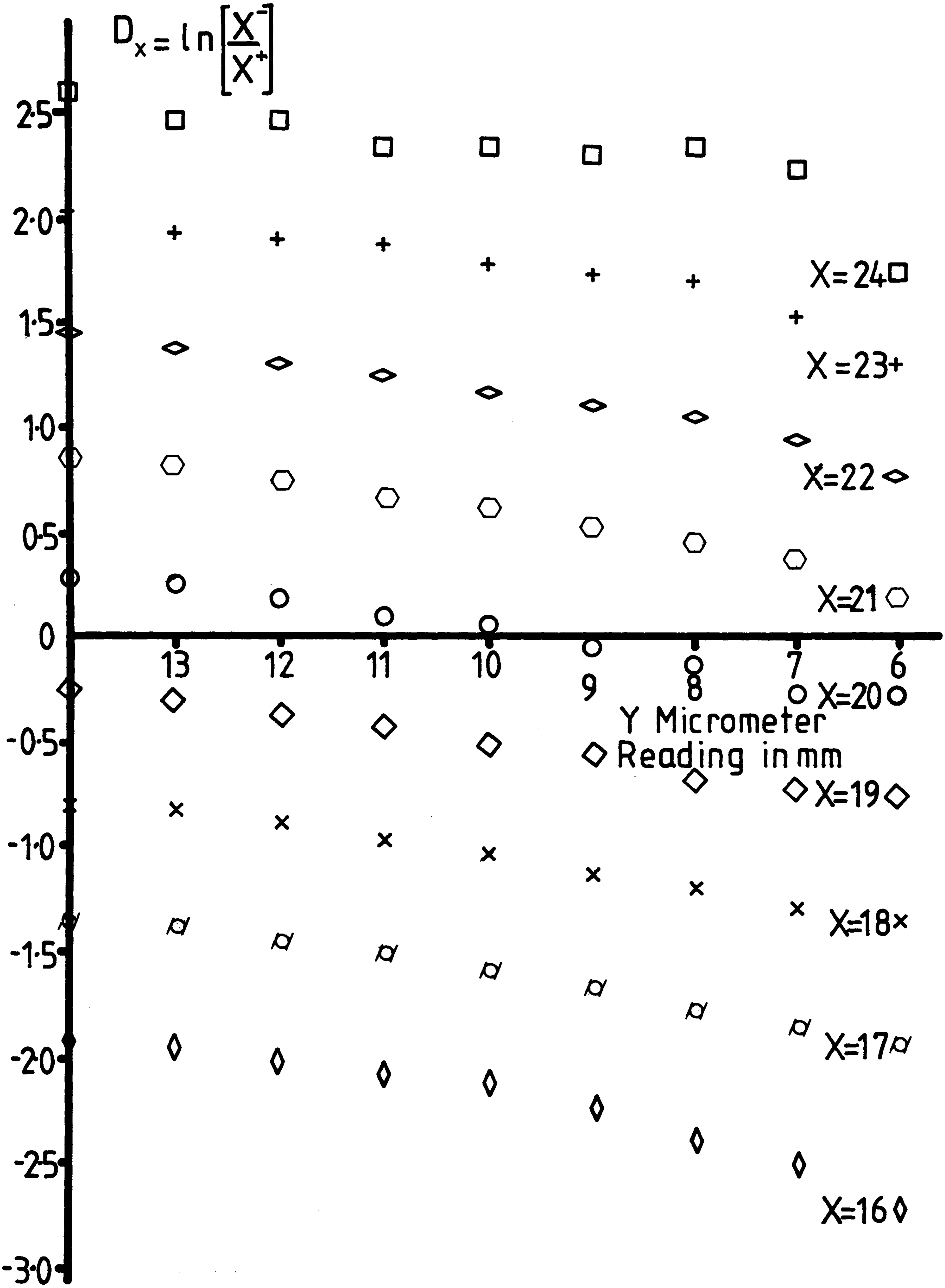
$D_x = \ln\left[\frac{X^-}{X^+}\right]$
2·5
2·0
1·5
1·0
0·5
0
-0·5
-1·0
-1·5
-2·0
-2·5
-3·0
13
12
11
10
9
8
7
6
Y Micrometer
Reading in mm
X=24
X=23+
X=22
X=21
X=20
X=19
X=18×
X=17
X=16

Fig 3.3.16

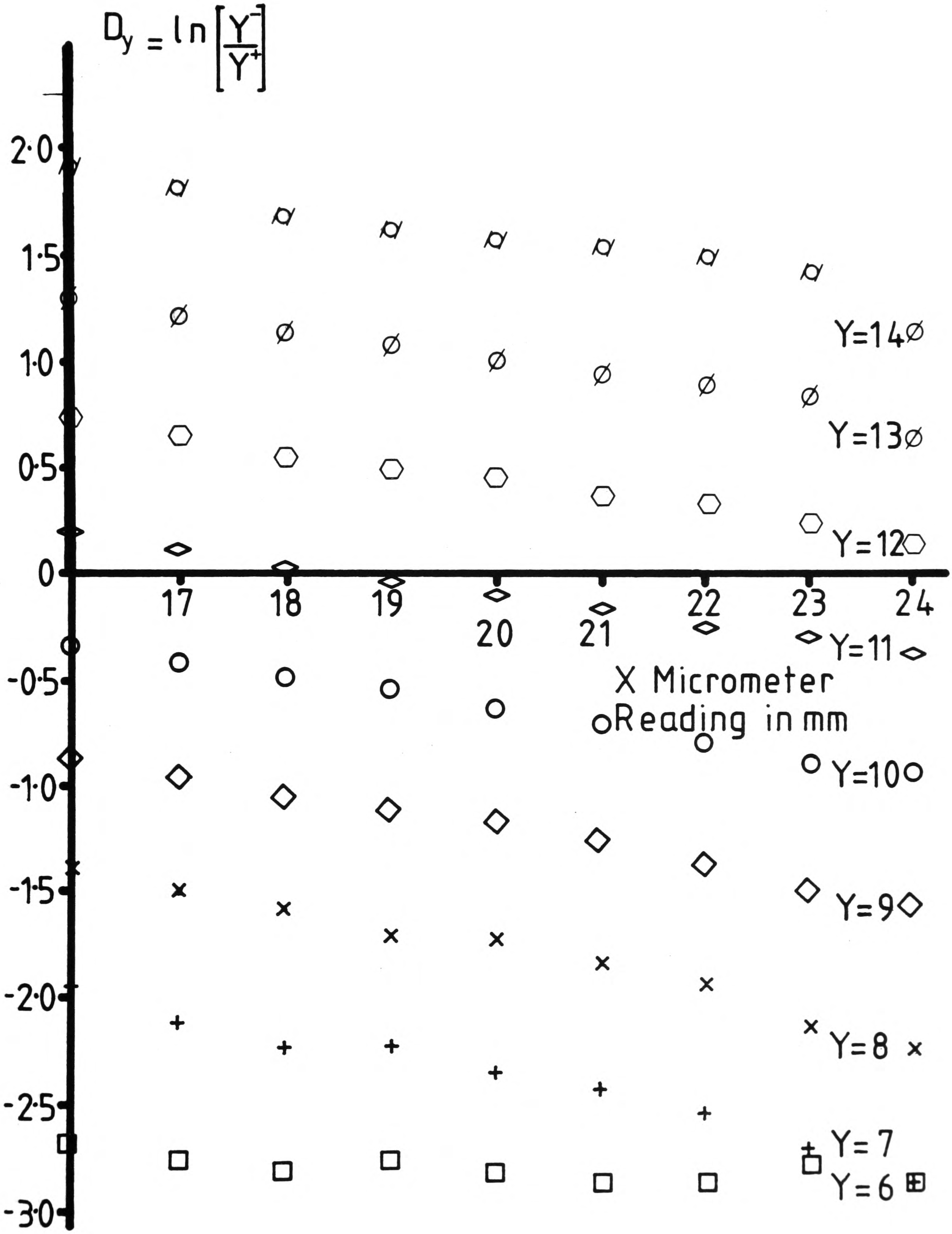

$D_y = \ln\left[\frac{Y^-}{Y^+}\right]$
2·0
1·5
1·0
0·5
0
-0·5
-1·0
-1·5
-2·0
-2·5
-3·0
17
18
19
20
21
22
23
24
X Micrometer
Reading in mm
Y=14
Y=13
Y=12
Y=11
Y=10
Y=9
Y=8
Y=7
Y=6

Fig 3.3.17

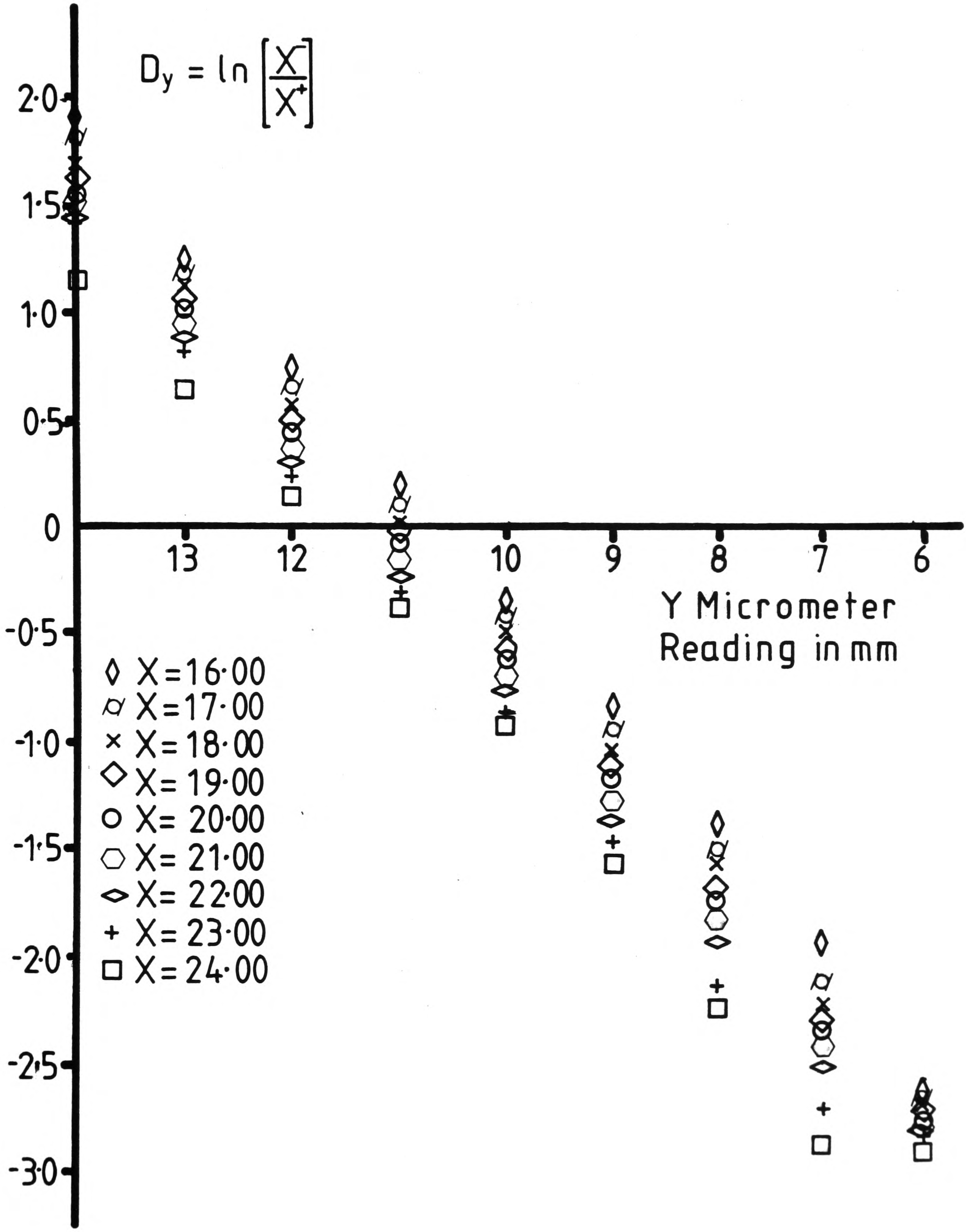

$D_y = \ln\left[\frac{X^-}{X^+}\right]$
2·0
1·5
1·0
0·5
0
-0·5
-1·0
-1·5
-2·0
-2·5
-3·0
13
12
10
9
8
7
6
Y Micrometer
Reading in mm
X=16·00
X=17·00
X=18·00
X=19·00
X= 20·00
X= 21·00
X= 22·00
X= 23·00
X= 24·00

Fig 3.3.18

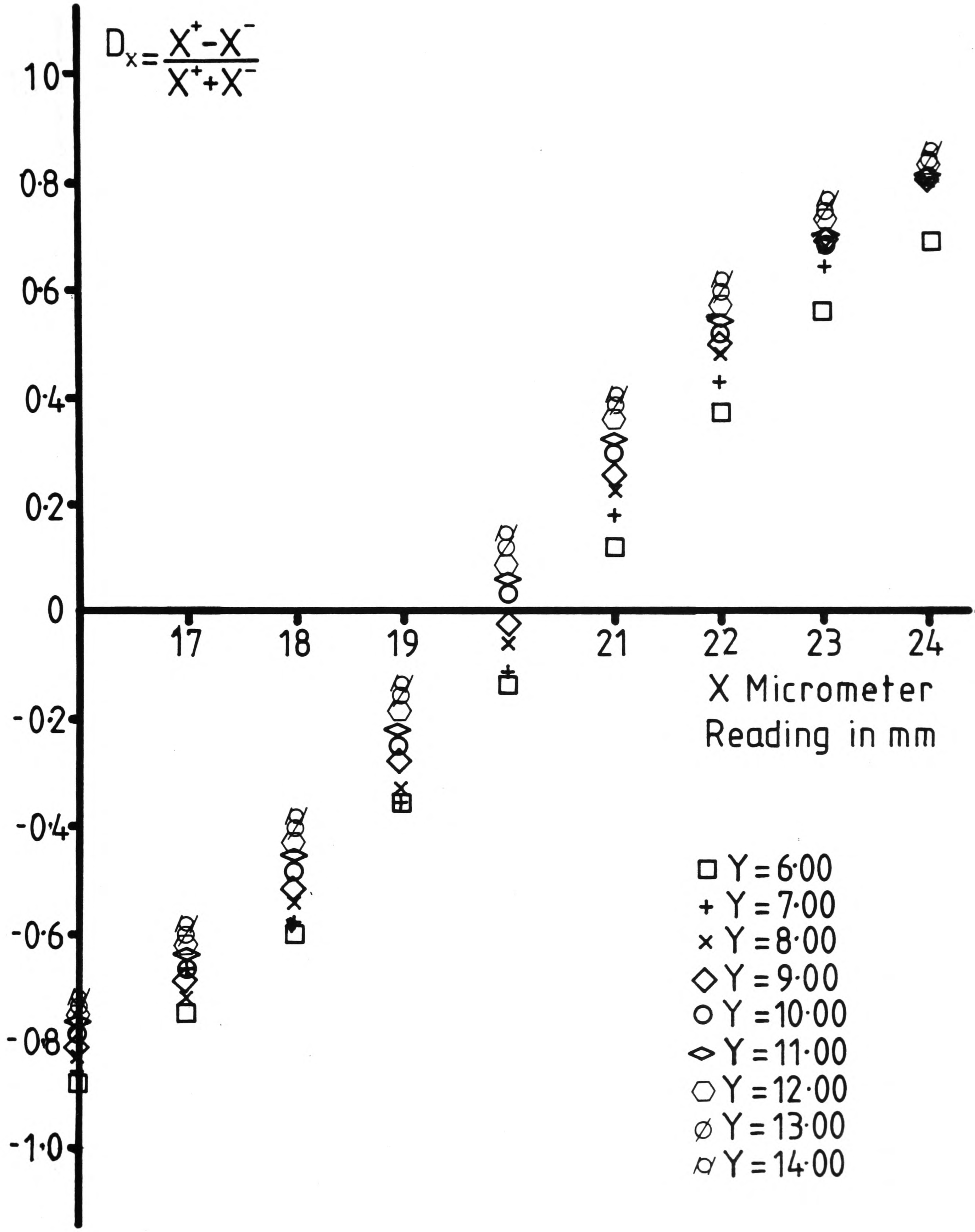
$D_x = \frac{X^+ - X^-}{X^+ + X^-}$
1.0
0.8
0.6
0.4
0.2
0
-0.2
-0.4
-0.6
-0.8
-1.0
17
18
19
21
22
23
24
X Micrometer
Reading in mm
Y = 6·00
Y = 7·00
Y = 8·00
Y = 9·00
Y = 10·00
Y = 11·00
Y = 12·00
Y = 13·00
Y = 14·00

Fig 3.3.19

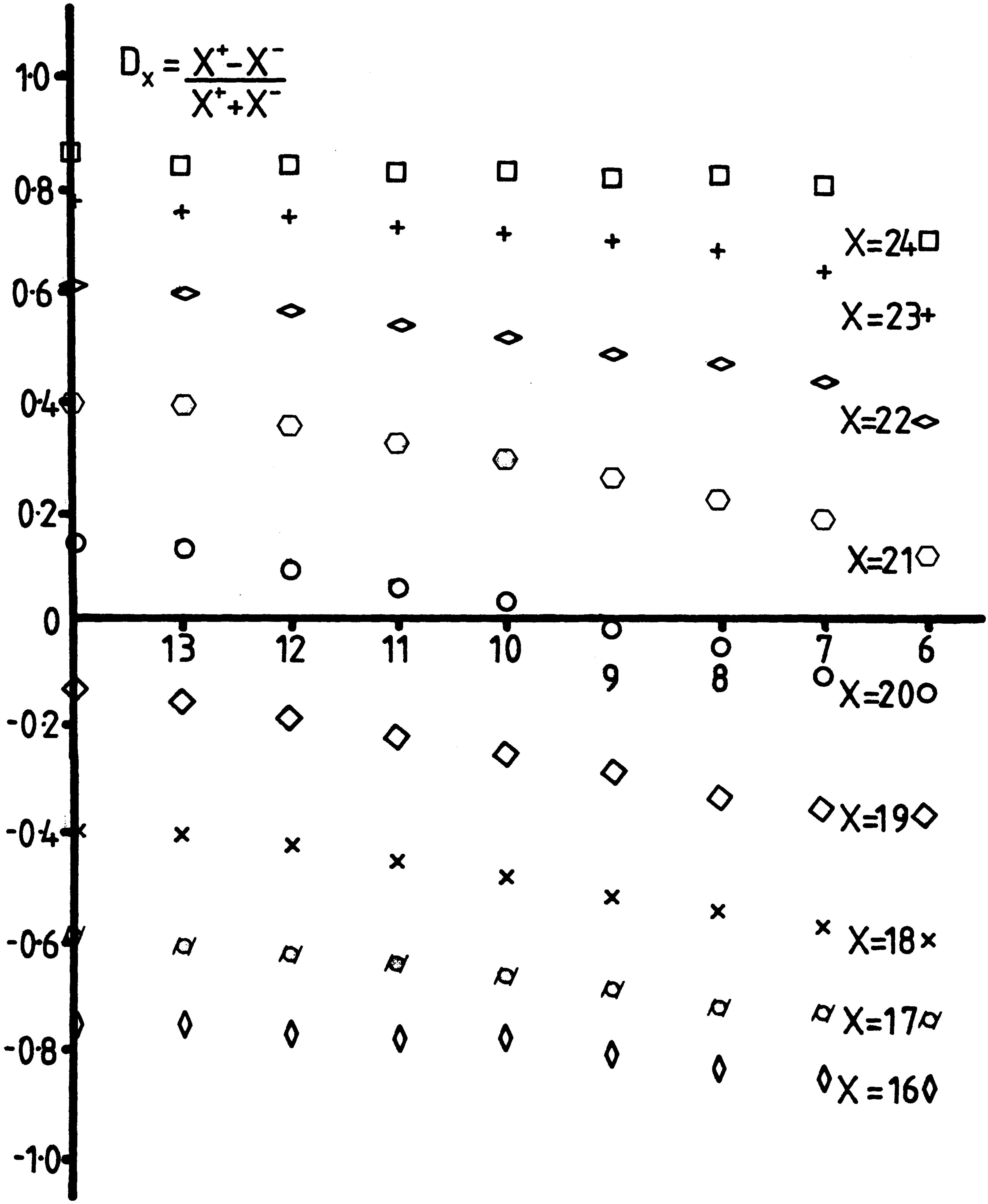

$D_x = \frac{X^+ - X^-}{X^+ + X^-}$
1·0
0·8
0·6
0·4
0·2
0
-0·2
-0·4
-0·6
-0·8
-1·0
13
12
11
10
9
8
7
6
X=24
X=23
X=22
X=21
X=20
X=19
X=18
X=17
X=16

Fig 3.3.20

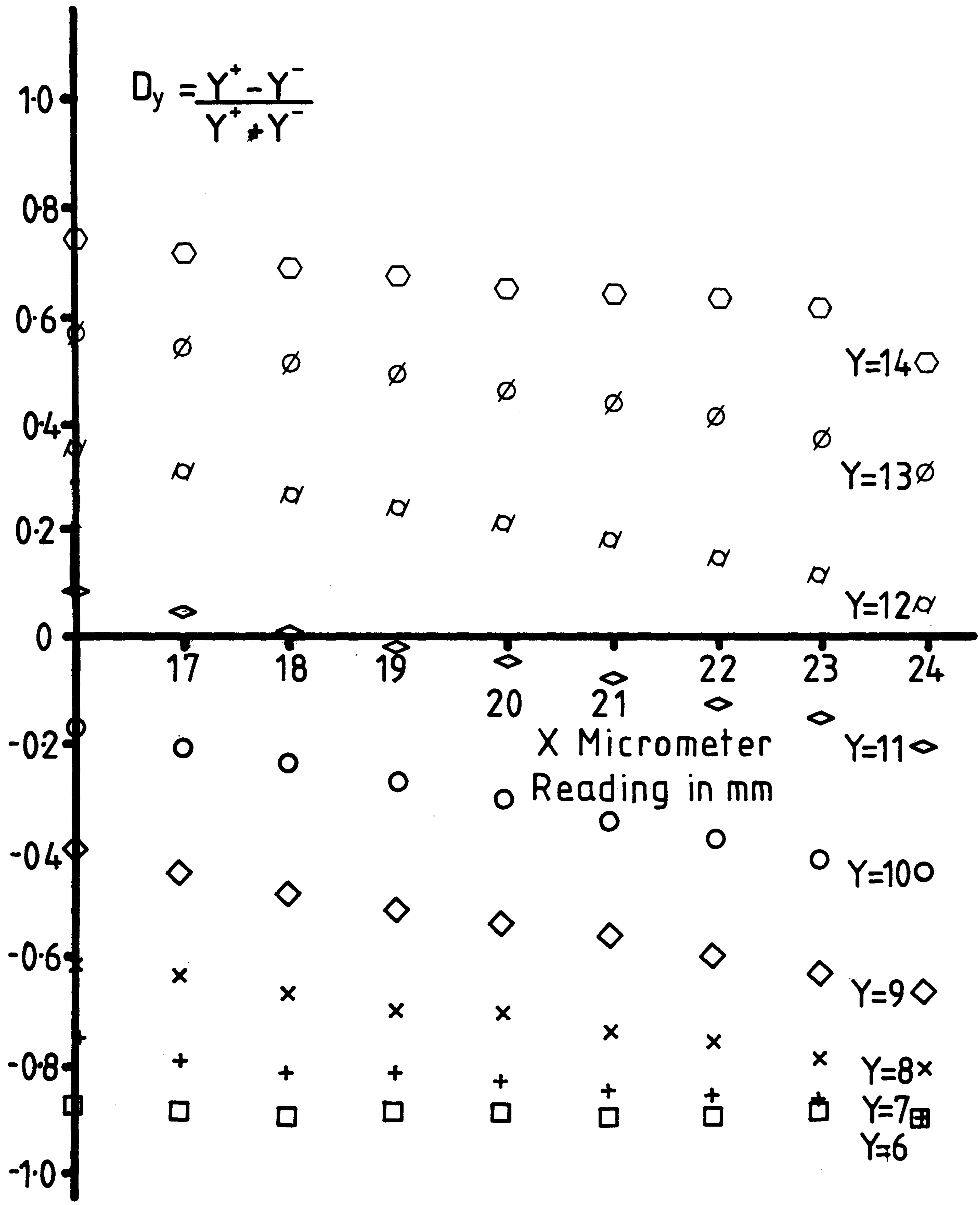

$D_y = \frac{Y^+ - Y^-}{Y^+ + Y^-}$
1·0
0·8
0·6
0·4
0·2
0
-0·2
-0·4
-0·6
-0·8
-1·0
17
18
19
20
21
22
23
24
X Micrometer Reading in mm
Y=14
Y=13
Y=12
Y=11
Y=10
Y=9
Y=8
Y=7
Y=6

Fig 3.3.21

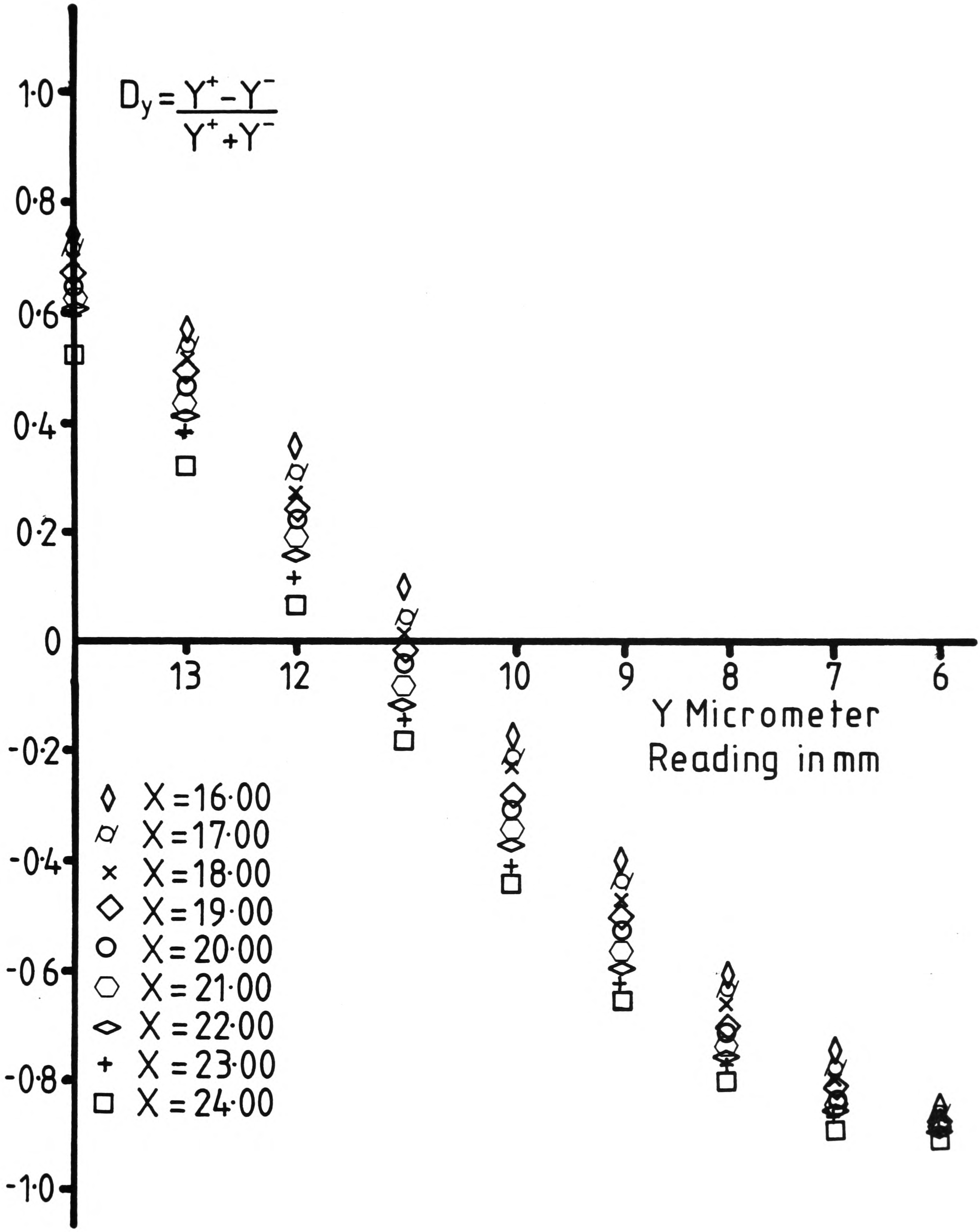

$D_y = \frac{Y^+ - Y^-}{Y^+ + Y^-}$
1·0
0·8
0·6
0·4
0·2
0
-0·2
-0·4
-0·6
-0·8
-1·0
13
12
10
9
8
7
6
Y Micrometer
Reading in mm
X = 16·00
X = 17·00
X = 18·00
X = 19·00
X = 20·00
X = 21·00
X = 22·00
X = 23·00
X = 24·00

Fig 3.3.22

equally good results, but it was decided to use $D_X = \frac{X^+ - X^-}{X^+ + X^-}$,

as the logarithmic relationship is more susceptible to quantization errors at the extremes of movement, as can be seen by comparing the X = 16.0 and X = 24.0 lines in Figure 3.3.16 and the Y = 6.0 and Y = 14.0 lines in Figure 3.3.17 with the equivalent lines in Figures 3.3.20 and 3.3.21.

Figure 3.2.22 shows the effect of altering the distance between the LED and the detector. The direction of the light beam was not absolutely perpendicular, so that as the LED was raised the positions at which the spot of light hit the detector changed. However, the diferences between these positions was constant over the vertical displacements of the order expected in the final system.

One consequence of feeding the detector output directly into the computer was that the patient was then connected to a piece of equipment with a supply voltage of 240 V a.c. This meant that electrical isolation had to be provided by means of optical isolation amplifiers, to prevent any leakage currents reaching the patients from the computer. This problem is considered in greater detail in the section on Patient Isolation (section 3.4).

Due to the low frequency response of the Isolation Amplifiers, 1 kHz, the time between the start of the LED pulse and the start of the A/D sampling had to be increased to allow the full signal value to be reached. In order to meet this requirement the length of the pulse had to be increased, and the LEDs were pulsed 1 in 5.

A suitable length of cable to allow the patients to walk about during data acquisition was found to be about 20 m. The previously designed circuitry was unable to drive this length of cable due to its capacitance, which was 190 pF m^{-1}, giving a total capacitance of

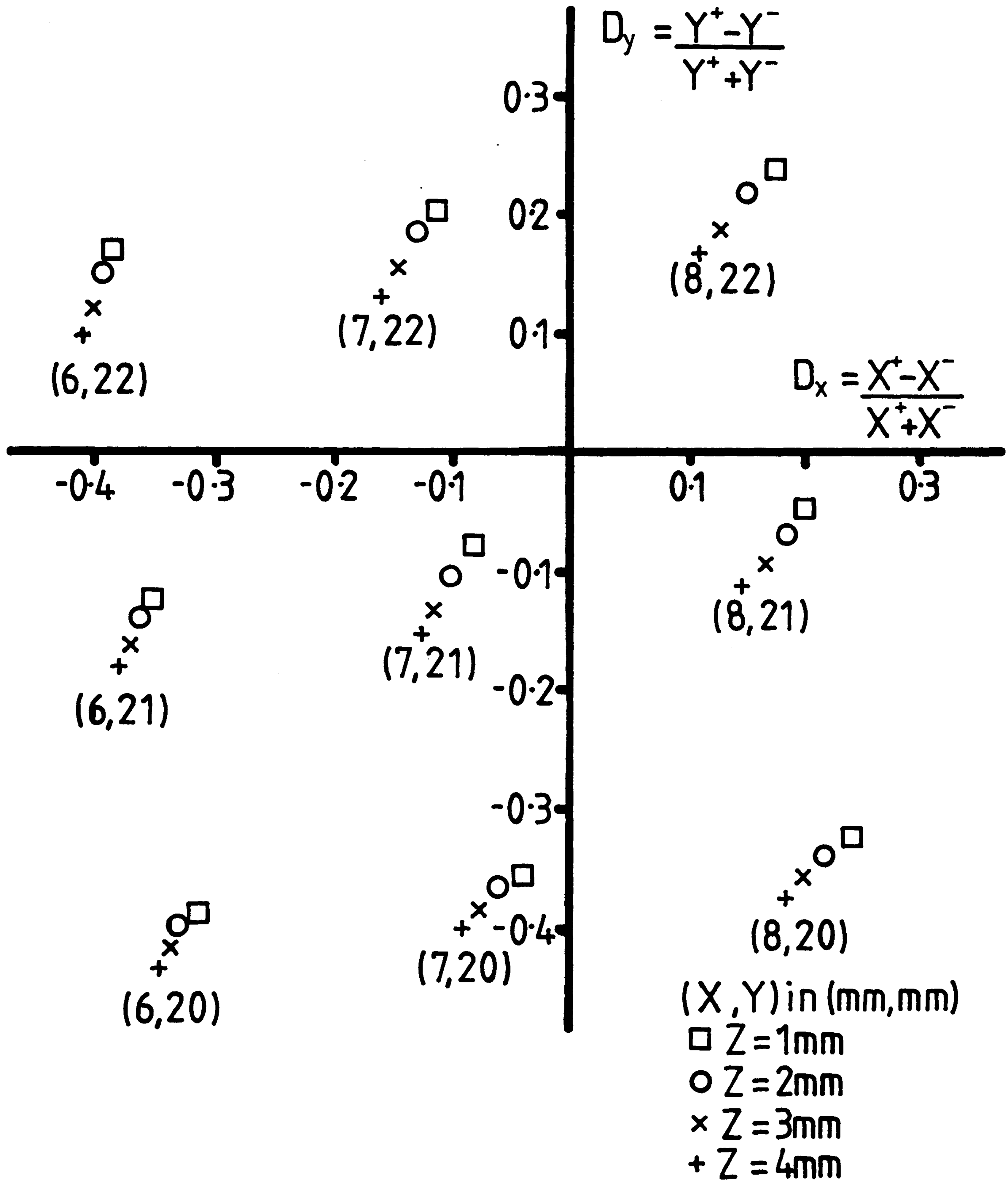

$D_y = \frac{Y^+ - Y^-}{Y^+ + Y^-}$
$D_x = \frac{X^+ - X^-}{X^+ + X^-}$
0·3
0·2
0·1
-0·1
-0·2
-0·3
-0·4
-0·4
-0·3
-0·2
-0·1
0·1
0·3
(6,22)
(7,22)
(8,22)
(6,21)
(7,21)
(8,21)
(6,20)
(7,20)
(8,20)
(X,Y) in (mm,mm)
□ Z=1mm
○ Z=2mm
× Z=3mm
+ Z=4mm

Fig 3.3.23

approximately 4 nF for the whole cable.

It was also found that the input impedance of the operational amplifiers used was too low to give a linear output when used to provide a current to voltage gain of 50,000. A further problem which had been found was that the power supply voltage across the detector circuit varied as the LEDs were turned on and off.

3.3(iv) Redesign of the Transducer Electronics

The entire electronic circuitry was thus redesigned to meet the following requirements:

(i) There should be two totally separate power supplies, one for the operational amplifiers and one for the LEDs and associated circuitry.

(ii) The operational amplifiers used for the preamplification of the signals should either have a much higher input impedance than the OP 10 CYs used previously, or a smaller feedback resistance should be used, with a second stage of amplification.

(iii) As the sample/hold circuitry had been removed the LED driver circuit could be much simpler, as all it would be required to do would be to pulse three LEDs and to produce a TTL logic pulse to control the A/D start. The LEDs were to be pulsed 1 in 5 at a frequency of 50 Hz.

(iv) The LED currents were to be adjustable so that despite any differences between the individual LEDs, or between their collimators, the amount of light produced by each LED-collimator combination would be the same.

It was decided to power the preamplifiers from the isolation amplifiers, by means of the connecting cable. The Isolation Amplifiers have a $\pm$ 15 V power supply with a maximum current of $\pm$ 10 mA giving a maximum power of 300 mW. This was used to power three TL064CN's which are quadrilateral Bifet Operational Amplifiers with low power consumption, typically $\pm$ 200μA at $\pm$ 15 V per amplifier, and with wide input voltage range, $\pm$ 2 V to $\pm$ 18 V. These were used as the preamplifiers as shown in Figure 3.3.24. The typical total power consumption of three of these quads (12 operational amplifiers) is 72 mW, which is well within the maximum power supply of one of the Isolation Amplifiers

The pulsing circuit was Transistor Transistor Logic (TTL), powered by PP3 8.4 V battery via a 5 V regulator. This circuit is shown in Figure 3.3.25. This circuit again was based on a 555, although this was a TTL 555 rather than a CMOS 555, acting astably, with R_B = 1M5, R_B = 470k and C = 12nF. The duty cycle is given by $t_1/(t_1+t_2) = (R_A+R_B)/(R_A+2R_B) = 81\%$ and the pulse durations by $t_1 = 0.693(R_A+R_B) = 16$ msec and $t_2 = 0.693R_BC = 4$ msec. The output signal from this was fed into three halves of two SN75453B dual peripheral positive-or drivers. These consist of an NAND gate controlling the base of an n-p-n transistor, with the emitter grounded. Both inputs of the gates were connected to the output of the 555, and as can be seen from the logic table (Table 3.3.1) when they are both low the output is low and the transistor conducts, and when they are both high the transistor does not conduct. The LED was connected as the collector load of the transistor, and it was illuminated when the transistor was conducting, i.e. when the 555 output was low. The variable resistor provided an adjustment on the light output of the LEDs.

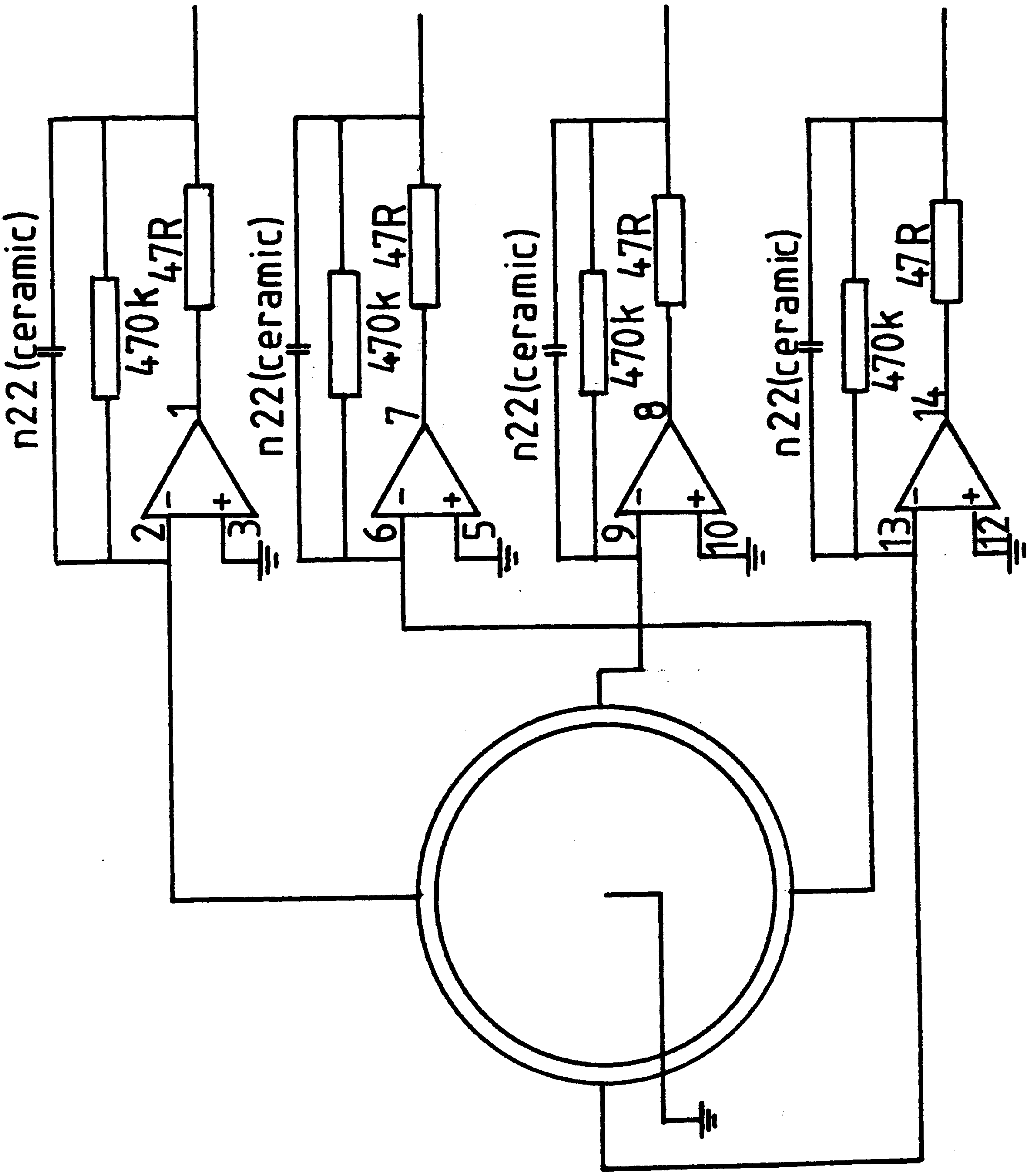

Detector Reading Circuit (Mark III)

Fig 3.3.24

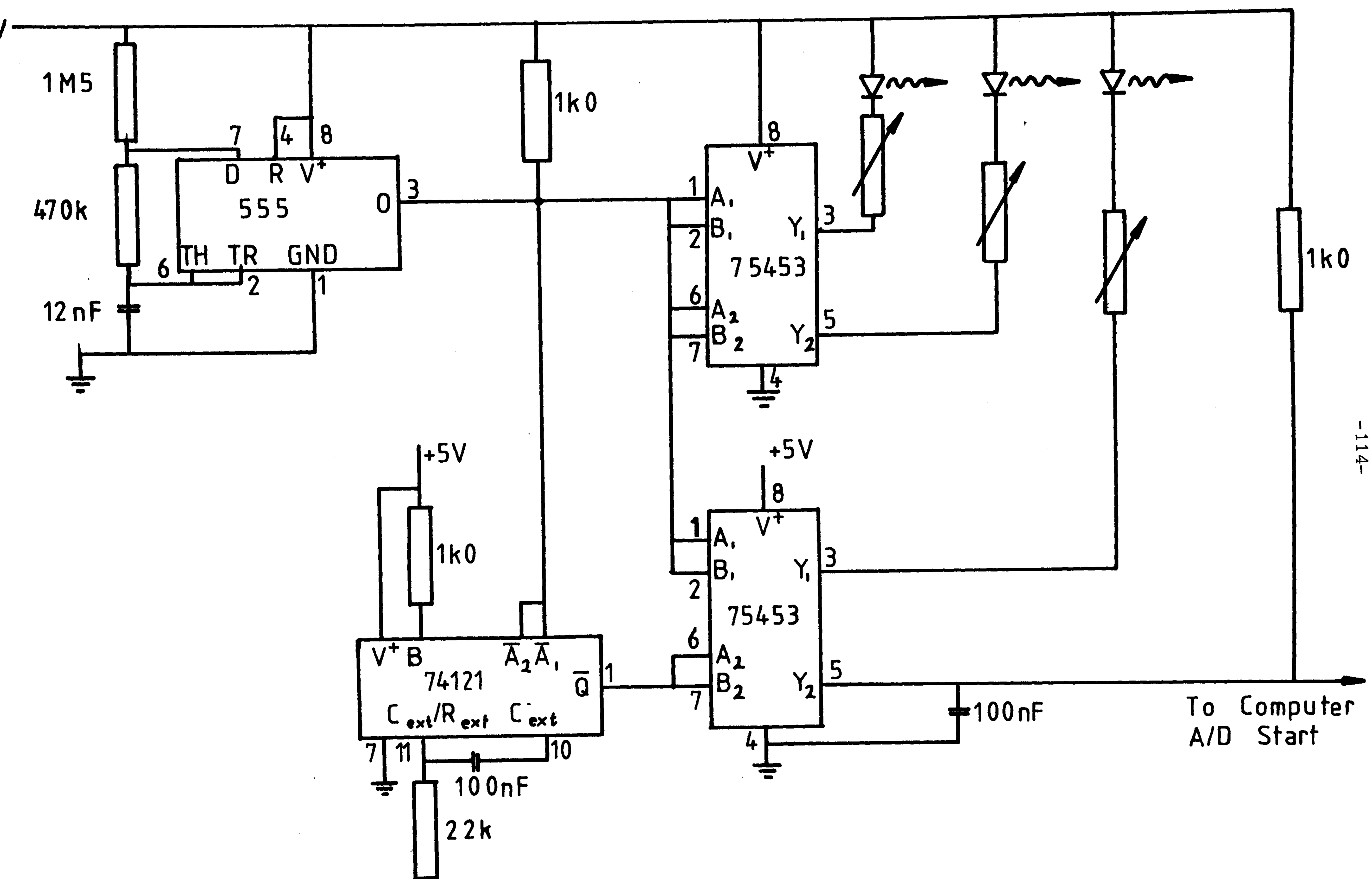

LED Drive Circuit (Mark III)

Fig 3.3.25

Table 3.3.1: Logic Table for SN74121

INPUTS			OUTPUTS	
A1	A2	B	Q	$\bar{Q}$
L	X	H	L	H
X	L	H	L	H
X	X	L	L	H
H	L	X	L	H
H	↓	H	⊓	⊔
↓	H	H	⊓	⊔
↓	↓	H	⊓	⊔
L	X	↑	⊓	⊔
X	L	↑	⊓	⊔

The output of the 555 was also applied to the input of a 74121 monostable multivibrator, which provided a delay to permit the LED'S to stabilise before sampling took place. The input B was set permanently high, and the output of the 555 was fed into A_1 and A_2, the inputs of a NAND gate which is connected to a Schmitt trigger. As can be seen from Table 3.3.1, when B is high and A_1 and A_2 are both falling, then a positive pulse is produced at Q and a negative pulse is produced at $\bar{Q}$. The length of this pulse is controlled by the external resistor and capacitor applied to the 74121. The pulse width is $0.7C_{ext}R_{ext}$ (from the specifications of this device) and when R_{ext} = 22k and C_{ext} = 100 nF then t = 1.5 msec so that the A/D start pulse was produced 1.5 msec after the LEDs were illuminated. The pulse produced by the 74121 was then fed into the two inputs of the remaining SN75453, to buffer the 74121, so that the signal could be driven down the long cable back to the computer. The two circuits were packed into the box shown in Figure 3.3.26.

Particular thought was given to the earthing and wiring of these circuits, as there were twelve signals of 10^{-5} A being produced by the detectors, which had to travel approximately 1 m to the preamplifiers, before they were amplified and sent down 25 m of cable to the computer. The cable to the transducer would also be carrying the three LED drive pulses, which could easily interfere with the signals from the detectors. The cable to the computer would also be carrying the A/D start pulse. The length of cable in use produced a significant risk of picking up any stray electromagnetic radiation around the laboratory or the Patient Assessment Area. An earth star point was provided at each detector, as can be seen in Figure 3.3.27, from which there were 5 ground wires. Four of these went to the noninverting input of the differential preamplifiers, so that the inputs to the preamplifiers were pseudo-twisted pairs. The remaining wire from the earth star point went to the zero volts of the $\pm$ 15 V power supply. The same arrangement was used at each of the detectors, to reduce the cross talk between them. Ideally, the output from each detector would have been carried by a twisted pair, but this would have resulted in 12 shielded twisted pairs. It was felt that such a cable would have been impractible for a piece of equipment to be carried by a patient. Shielding was also applied around and between the LED driver circuit and the preamplifier circuit, to minimise cross-talk. High force energy transients from the A/D start signal were reduced by means of a capacitor. The timing of the A/D start

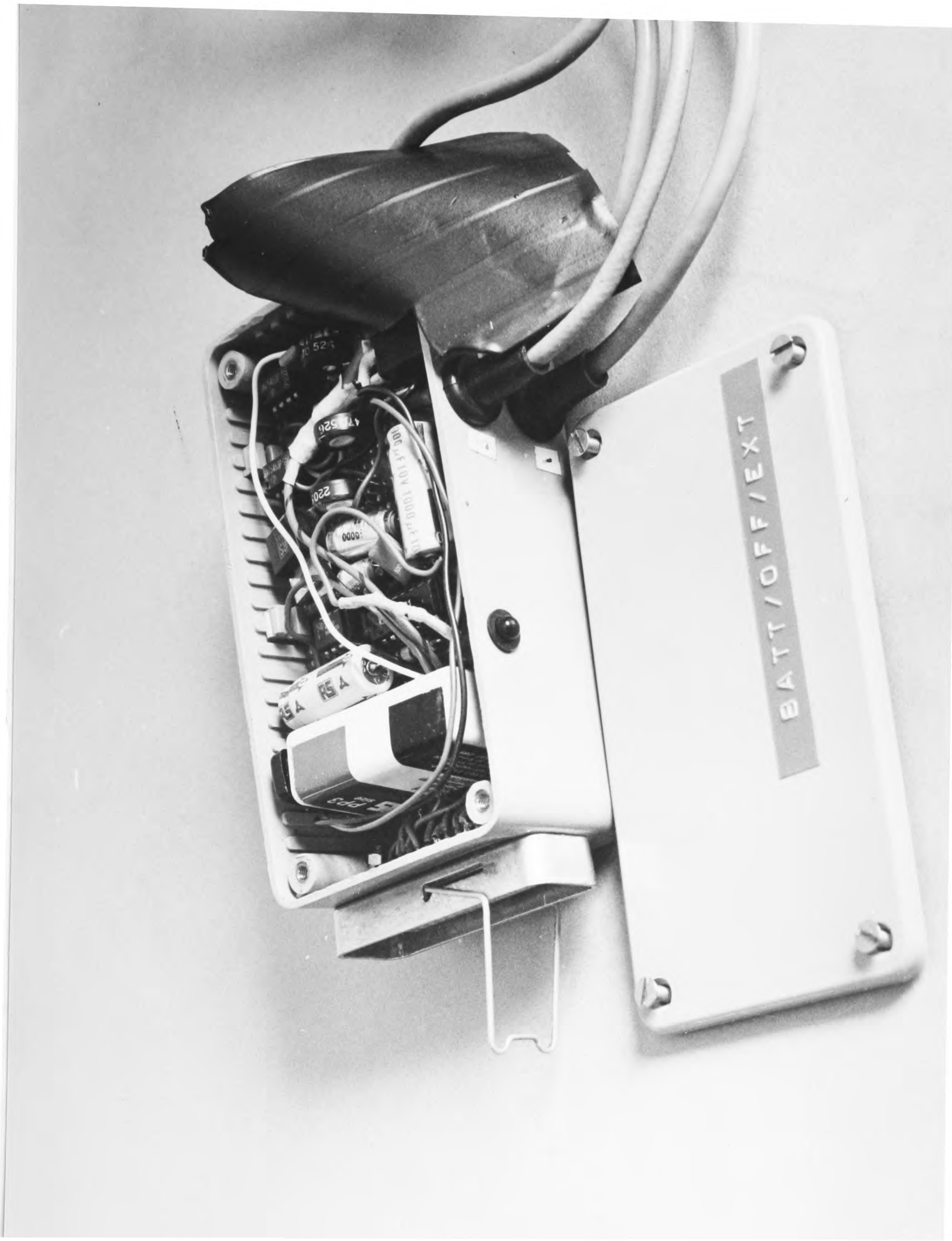

Fig. 3.3.26 Box carried by Patients

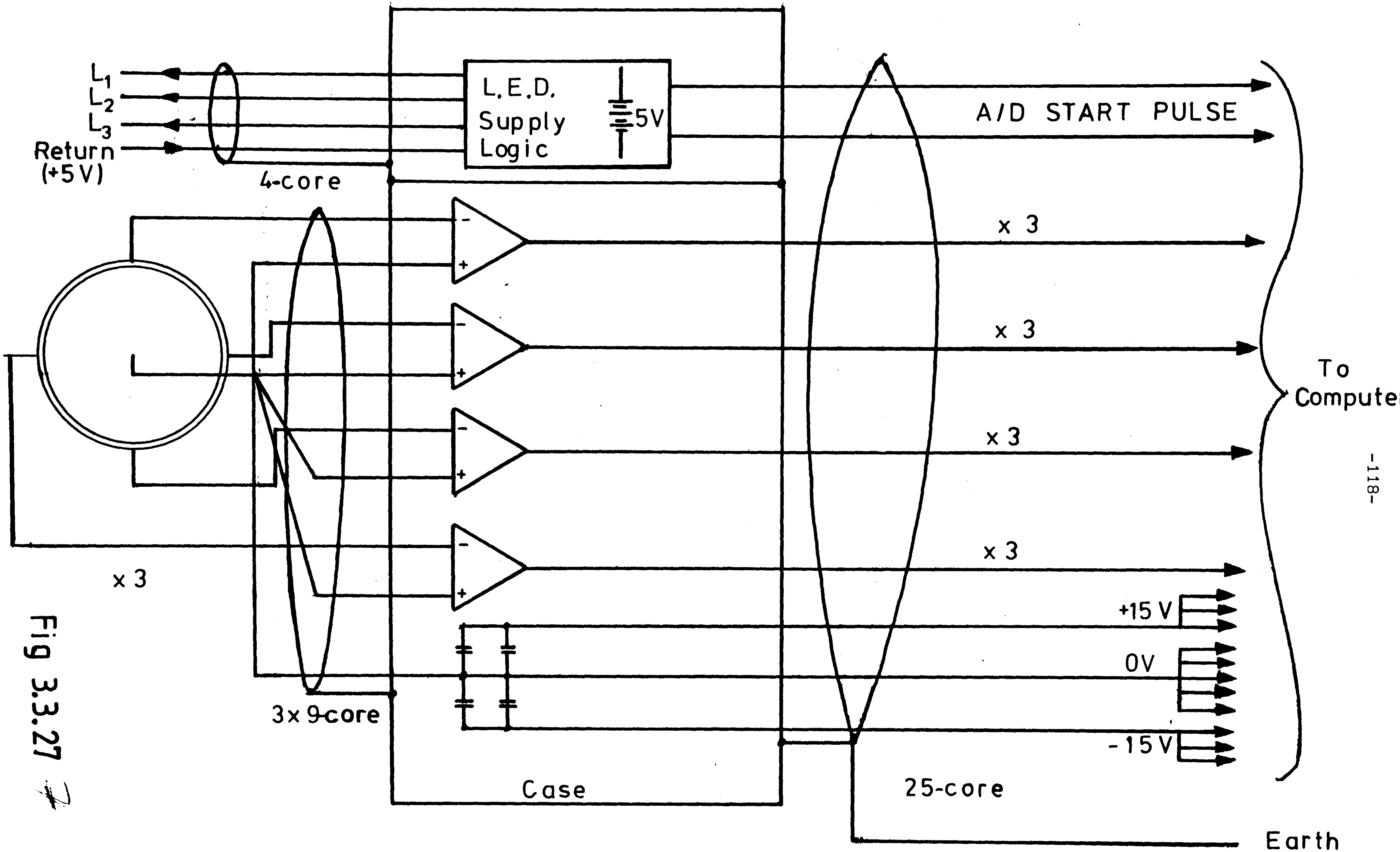

Fig 3.3.27

Details of Earthing Circuit

pulse was not critical and was not deleteriously affected by this smoothing.

A 22 nF capacitor in parallel with a 470 k resistor was added to the preamplifier feedback, to eliminate a 28 kHz oscillation which was present on the line, presumably arising from the detector. According to its specification, the typical detector capacitance at 0 V bias is 1200 pF, and the typical value of the series resistance of the base is 5 kΩ These two values in an R-C circuit would produce oscillation at a frequency of 26 kHz.

The entire transducer was then calibrated , using the algorithm

$$D_X = \frac{X^+ - X^-}{X^+ + X^-} \qquad D_Y = \frac{Y^+ - Y^-}{Y^+ + Y^-} \tag{3.3.14}$$

and this is discussed in section 5.1.

3.4 Patient Isolation

3.4(i) Isolation Requirements

According to Health Technical Memoradum No. 8 (HTM 8), Safety Code for Electro-medical Apparatus (1969) for an alternating current flowing to and from the body via external contacts, e.g. hand to hand, the threshold of feeling is 1 mA. Muscular paralysis is produced by 15 mA and ventricular fibrillation by 70 mA. For a direct current these values are higher, 5 mA being the threshold of feeling, and muscular paralysis and ventricular fibrillation being produced by 75 mA and 300 mA respectively. However if direct contact is made with the heart then ventricular fibrillation can occur with currents as low as 0.5 mA. Therefore British Standard 5724 (Specifications for the safety of Medical Electrical Equipment) (1979) which has superseded HTM8 has two sets of maximum patient leakage currents. One is for equipment "which may come into Direct Conductive Contact with the Patient's heart" (section 2.2.7), and the other for equipment which does not. For the first type of equipment the "maximum Patient Leakage Current" in normal use is 0.01 mA and in the single fault condition is 0.05 mA. For the second type of equipment these currents are 0.1 mA and 0.5 mA respectively (section 19.1c). B.S.5724 defines 50 V d.c. or 24 V a.c. maximum rated supply voltage as "Medical Safety Extra-Low Voltage" (section 2.4.3) and circuits working at or below these voltages must be isolated from the "Mains Supply", and also are subjected to lower insulation and earthing requirements.

There are two convenient methods of electrical isolation: optical and electro-magnetic. The former uses a light emitting diode and either a phototransistor or a photodetector inside the same light proof box. If a current is flowing in the LED then light is given out which is received by the photodetector or the phototransistor, and an identical signal to the input signal is produced. If a signal is applied at the output end nothing happens. In the second (magnetic) method, which was the one used in this case, the input signals modulated to an a.c. signal which then passed through a transformer to a demodulator to give the output signal, as current cannot flow from the demodulator to the transformer.

3.4(ii) Isolation Amplifiers

The isolation amplifier chosen was the Intronics Inc. IA 184. This has a maximum leakage current of 1.2 μA r.m.s. at 115 V, 60 Hz with a frequency response of 1 kHz, and a breakdown voltage of 2500 V. The input impedance is $10^8 \Omega$ in parallel with 3 pF. If more than one of these amplifiers is used then they may be synchronized to prevent beats, and they also produce an isolated power supply of $\pm$10 mA maximum current at $\pm$ 15 Vd.c. This gives an isolated power supply of 300 mW.

There were 12 signals from the detectors and one A/D start signal which had to be transmitted to the computer. The isolation amplifiers were built in boxes containing four isolation amplifiers with a 64 way edge connector so that they could be plugged into a 19" rack in the analog input computer rack along with a 15 V power supply and a syncronizing circuit. It was arranged that the inputs to each unit of isolation could either be via one plug with four signals with a common ground signal and +15 V power supply, or via four plugs for four signals, each with its own signal ground and $\pm$15 V power supply. The circuit inside each unit is shown in Figure 3.4.1.

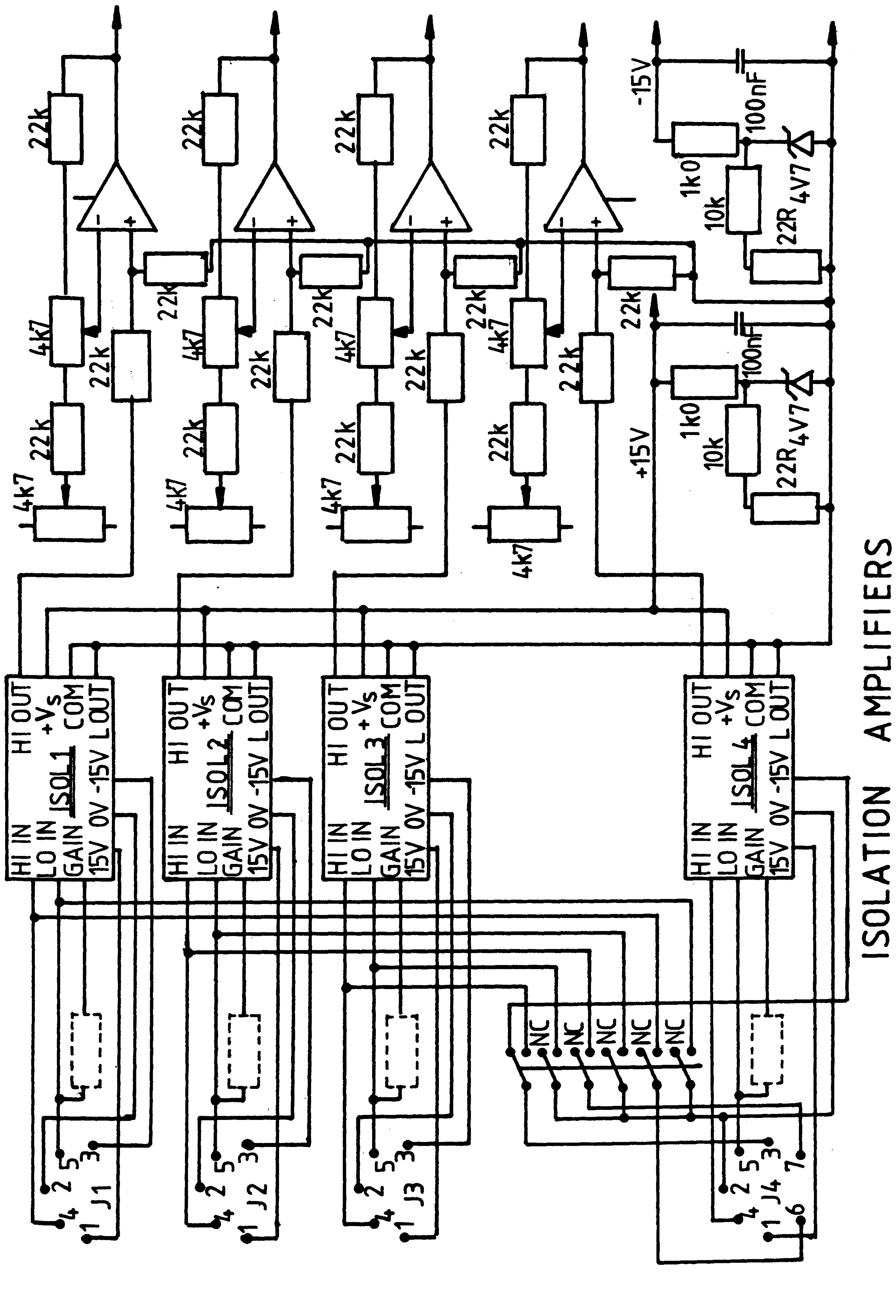
ISOLATION AMPLIFIERS
ISOL1
ISOL2
ISOL3
ISOL4
HI OUT
+Vs
COM
L OUT
HI IN
LO IN
GAIN
15V
0V
-15V
22k
4k7
1k0
10k
22R
4V7
100nF
+15V
-15V
NC
J1
J2
J3
J4

Fig 3.4.1

3.5 The Strain Gauge Transducer

3.5(i) The Strain Gauge Transducer

The output from the fracture movement transducer was compared with that of a strain gauge transducer (Fig. 3.5.1) which was designed by Evans (1979) specifically for use on the Oxford External Fixator. It is a removable device which clamps onto the fixator support bar, measuring the two bending strains and the torsional strain about the major axis of the fixator support bar, the axial strain is not measured. There are two strain gauged semi-circular bridges mounted onto anchor blocks which are then clamped onto the support bar. The output from the strain gauges was fed into a purpose build three channel strain gauge amplifier which was connected to the input of the A/D converter of the DEC PDP 11/34 computer. The two sets of tests, those with the displacement transducer, and those with the strain gauge transducer, were performed separately.

The strain gauge amplifier had no scaling in it to allow for the geometrical amplification of the support bar strain, as discussed in Churches et al (1985b), but the same transducer was used for all the tests, and thus the scale factor does not affect the trend in results.

The tests performed for the two transducers were identical and are discussed in the section "Patient Testing"

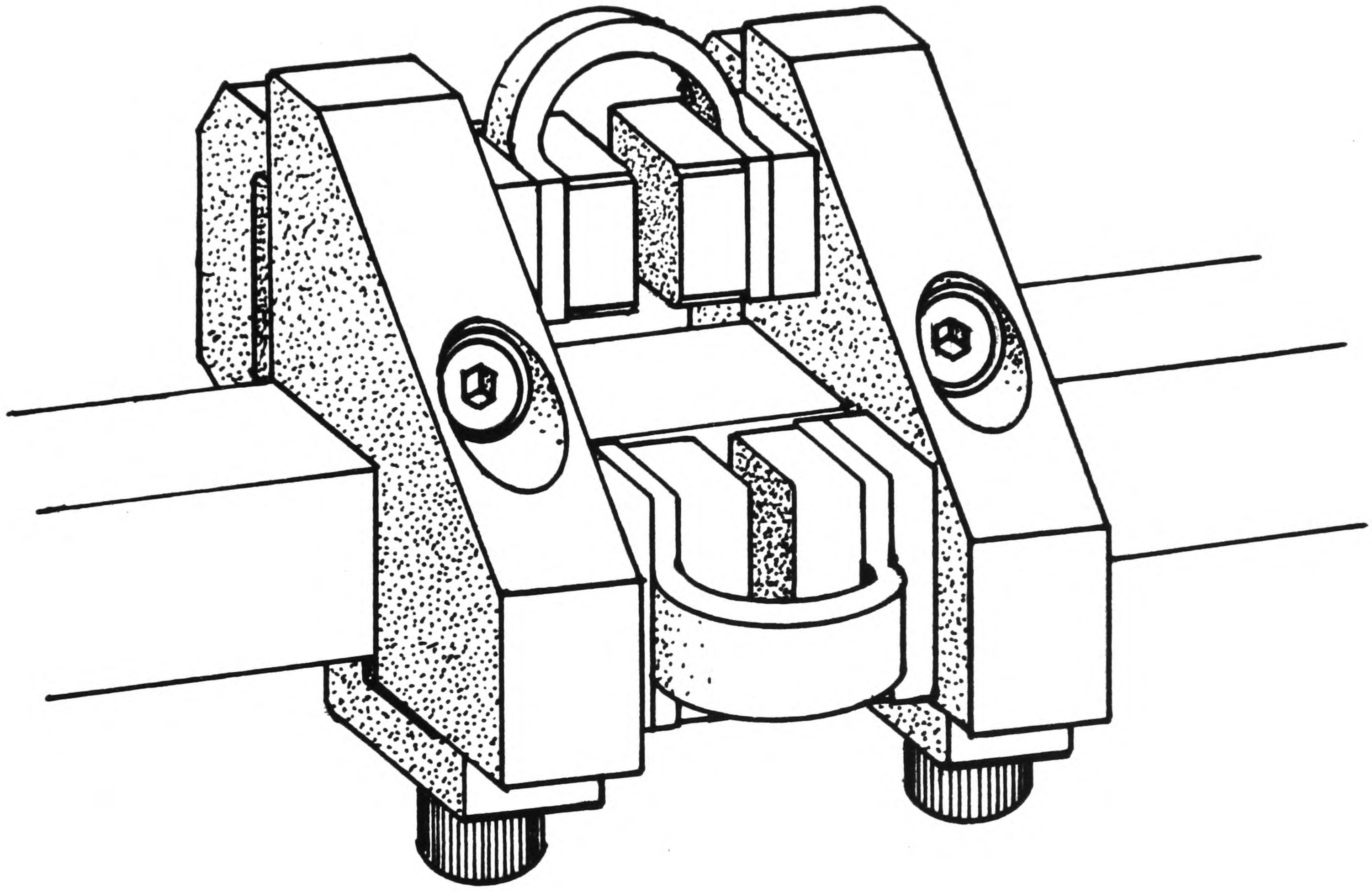

Strain Gauge Transducer

Fig 3.5.1

3.5(ii) Calibration of the strain gauge transducer

This has been discussed in various papers by Evans (1982). The two bending channels give an output of $3.625\mu\varepsilon\ N^{-1}m^{-1}$ applied bending moment in the support column with a cross talk of less than 7% torsion and 4% bending. The torsion channel gives an output of $4.65\mu\varepsilon\ N^{-1}m^{-1}$ of applied torsion to the support bar with a maximum of 15% cross talk on the bending channels.

CHAPTER 4

GEOMETRICAL AND MECHANICAL ANALYSIS OF FIXATOR AND TRANSDUCER

4 GEOMETRICAL AND MECHANICAL ANALYSIS OF FIXATOR

4.1 Photodetector Outputs to Transducer Displacements

When the three PIN photodetectors had been mounted as described in section 3.3 and the signals from the outputs of these detectors had been amplified as described in section 3.4, it was required to calculate the relative positions of the two parts of the transducer. First the two dimensional position of each spot of light on the detectors was calculated. The "dark" current was subtracted from the "light" current; as the LEDs were pulsed, the data input program LPATIN sampled each detector output twice per pulse, once when the LEDs were illuminated, the "light" signal, and once when the LEDs were not illuminated, the "dark" current. The differences between these "light" and "dark" currents were used with the algorithm from section 3.2, to find the positions of the spots of light. The beams of light were known to be mutually perpendicular, so the problem of finding the relative positions of the two sections of the detectors are that of finding the point of intersection of three mutually perpendicular lines which pass through three known points in space. The locus of a point from which two mutually perpendicular lines may be dropped through two fixed points is a sphere with the two fixed points as diameter. Therefore the point of intersection of three mutually perpendicular lines passing through three known points is the point of intersection of three spheres with, as diameters, the lines joining the three points.

If, the three points A, B and C are $2\underline{a}$, $2\underline{b}$, $2\underline{c}$ in a system of vectors with origin and axes as yet undefined, (Figure 4.1.1), then the spheres with radii AC and BC meet in a circle. This circle must

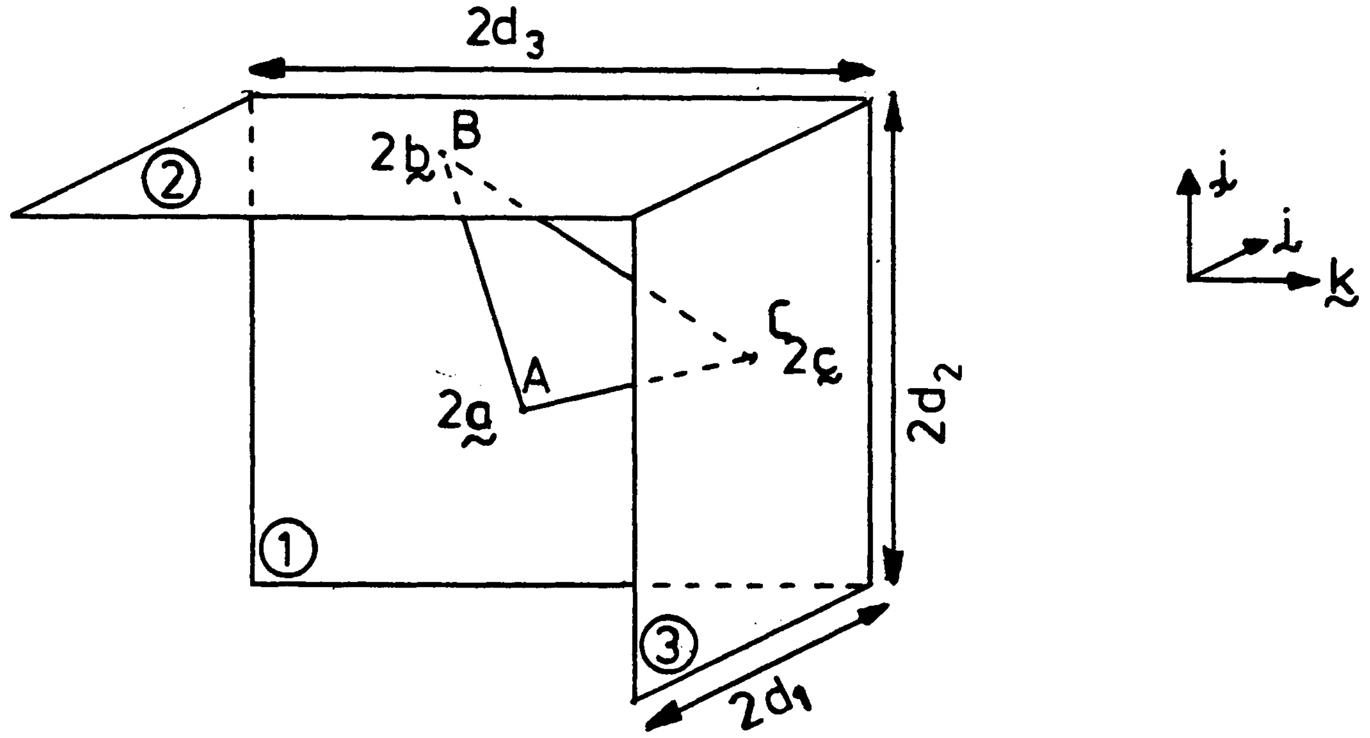

Fig 4.1.1

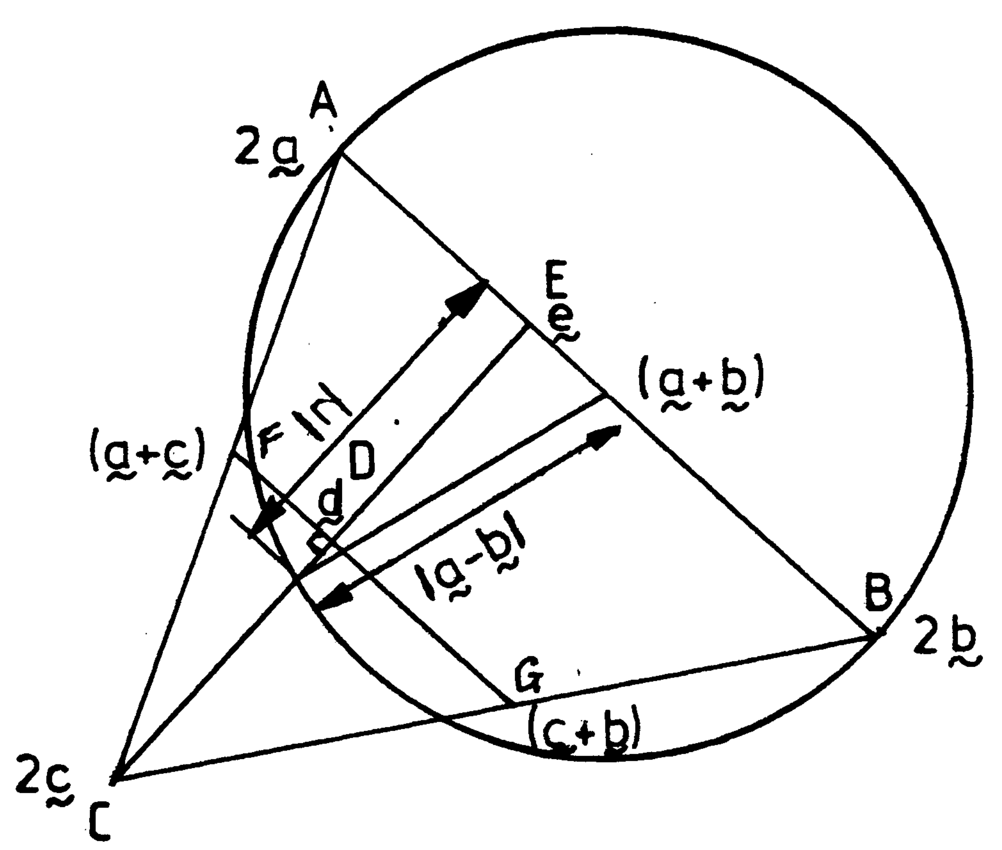

Fig 4.1.2.

pass through the point C, as the point of intersection of both spheres. Also the circle produced by the intersection of a plane and a sphere must have its centre on and be perpendicular to a radius of the sphere. Thus the circle which is the intersection of the spheres diameter AC and BC must have its centre on the line joining the centres of the two spheres, which are at the points F and G with postion vectors $(\underline{a}+\underline{c})$ and $(\underline{b}+\underline{c})$ (Figure 4.1.2.) Let the centre of this circle be $\underline{D}$ with position vector $\underline{d}$ then

$$\underline{d} = \underline{a} + \underline{c} + \lambda(\underline{a}-\underline{b}) \tag{4.1.1}$$

D is on a line joining F and G

and $$(\underline{a}-\underline{b})\cdot(\underline{d}-2\underline{c})=0 \tag{4.1.2}$$

i.e. a radius $(\underline{d}-2\underline{c})$ is perpendicular to the direction of the line joining the points with position vectors $(\underline{a}+\underline{c})$ and $(\underline{b}+\underline{c})$.
Substituting 4.1.1 into 4.1.2 gives:

$$(\underline{a}-\underline{b})\cdot(\underline{a}+\underline{c}+\lambda(\underline{a}-\underline{b})-2\underline{c})=0$$

Thus $$\lambda = \frac{(\underline{a}-\underline{b})\cdot(\underline{c}-\underline{a})}{(\underline{a}-\underline{b})^2} \tag{4.1.3}$$

and $$\underline{d} = \underline{a} + \underline{c} + \left[\frac{(\underline{a}-\underline{b})\cdot(\underline{c}-\underline{a})}{(\underline{a}-\underline{b})^2}\right](\underline{a}-\underline{b}) \tag{4.1.4}$$

The point of intersection of the vectors $\underline{d}-2\underline{c}$ and $2\underline{b}-2\underline{a}$, has position vector $\underline{e}$, and a consideration of similar triangles shows that $\underline{e} - \underline{d}$ is a radius of the circle centre D. Thus

$$\underline{d} - 2\underline{c} = \underline{e} - \underline{d} \tag{4.1.5}$$

This circle lies in the plane shown in figure 4.1.3 and from

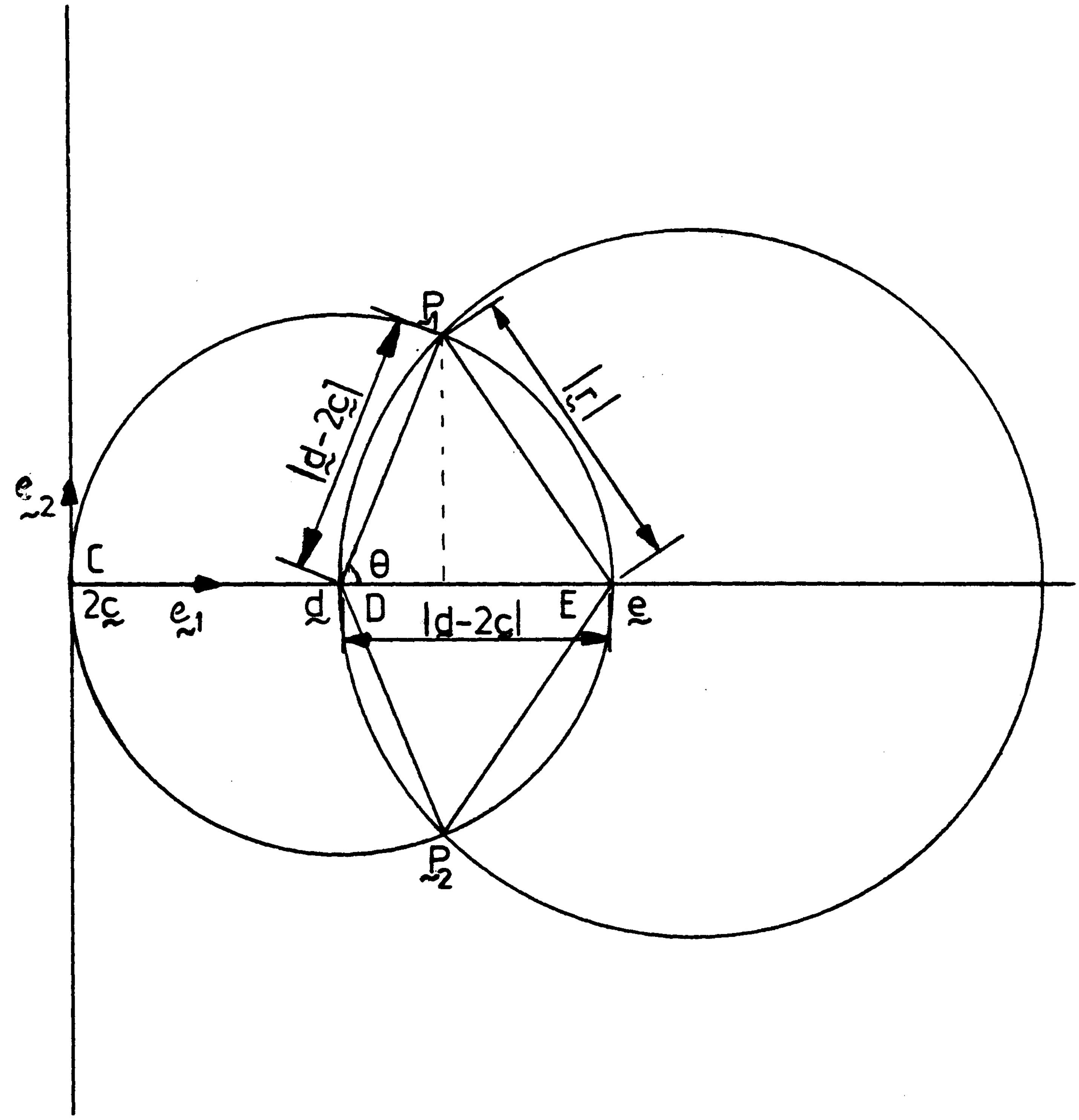

Fig 4.1.3

figure 4.1.2 this plane cuts the sphere with diameter AB in a circle centre E and radius $|\underline{r}|$, an application of Pythagoras' theorem gives

$$|\underline{a}-\underline{b}|^2 = |\underline{r}|^2 - |\underline{e}-(\underline{a}+\underline{b})|^2 \qquad (4.1.6)$$

Now $\underline{e} = (2\underline{d}-2\underline{c})$ from (4.1.5)

$$\underline{e} = 2\underline{a} + 2\underline{c} + 2\lambda(\underline{a}-\underline{b}) - 2\underline{c} \qquad \text{from (4.1.1)}$$

$$= 2\underline{a} + 2\lambda(\underline{a}-\underline{b}) \quad \text{(substituting for } \underline{d} \text{ from 4.1.1)}$$

Thus $\underline{e} - (\underline{a}+\underline{b}) = (\underline{a}-\underline{b})(1+2\lambda)$ (4.1.7)

Then from 4.1.6
$$|\underline{r}|^2 = |\underline{a}-\underline{b}|^2 - |(\underline{a}-\underline{b})(1+2\lambda)|^2$$
$$= |\underline{a}-\underline{b}|^2(1-(1+4\lambda+4\lambda^2)$$
$$= -4\lambda(1+\lambda)|\underline{a}-\underline{b}|^2 \qquad (4.1.8)$$

and from figure 4.1.3

$$P_1, P_2 = \underline{d} + |\underline{d}-2\underline{c}|\cos\theta\ \underline{e_1} \pm |\underline{d}-2\underline{c}|\sin\theta\ \underline{e_2} \qquad (4.1.9)$$

where $\underline{e_1} = \dfrac{\underline{d}-2\underline{c}}{|\underline{d}-2\underline{c}|}$ $\quad \underline{e_2} = \dfrac{(\underline{a}-\underline{c})_\wedge(\underline{b}-\underline{c})}{|(\underline{a}-\underline{c})_\wedge(\underline{b}-\underline{c})|}$

i.e. $\underline{e_2}$ is perpendicular to both $(\underline{a}-\underline{c})$ and $(\underline{b}-\underline{c})$

On substitution in 4.1.9. for $\underline{e_1}$ and $\underline{e_2}$ gives:

Position vectors of points P_1 and P_2

$$P_1, P_2 = \underline{d} + (\underline{d}-2\underline{c})\cos\theta \pm \frac{|\underline{d}-2\underline{c}|\ (\underline{a}-\underline{c})_\wedge(\underline{b}-\underline{c})\sin\theta}{|(\underline{a}-\underline{c})_\wedge(\underline{b}-\underline{c})|} \qquad (4.1.10)$$

Now from the cosine theorem

$$|\underline{r}|^2 = |\underline{d}-2\underline{c}|^2 + |\underline{d}-2\underline{c}|^2 - 2|\underline{d}-2\underline{c}|\,|\underline{d}-2\underline{c}|\cos\theta$$

and therefore $\cos\theta = \dfrac{2\left|\underline{d}-2\underline{c}\right|^2-\left|\underline{r}\right|^2}{2\left|\underline{d}-2\underline{c}\right|^2}$

$$= 1 - \frac{\left|\underline{r}\right|^2}{2\left|\underline{d}-2\underline{c}\right|^2}$$

$$= 1 + \frac{2\lambda(1+\lambda)\ \left|\underline{a}-\underline{b}\right|^2}{\left|\underline{d}-2\underline{c}\right|^2} \qquad \text{(from 4.1.8)} \qquad (4.1.11)$$

If the origin of the system is now defined as the "zero" position of the transducer, with axes along the original directions of the beams of light, then the displacements of the spots of light from their "zero" positions give directly the position vectors of the three points A, B and C. Now if the displacements given by the detectors are Y_1,Z_1, X_2,Z_2, X_3,Y_3 on the detectors 1,2 and 3 respectively and in the X, Y and Z directions (Figure 4.1.4), then

$$\begin{aligned} 2\underline{a} &= d_1\ \underline{i} + Y_1\ \underline{j} + Z_1\ \underline{k} \\ 2\underline{b} &= X_2\ \underline{i} + d_2\ \underline{j} + Z_2\ \underline{k} \qquad (4.1.12) \\ 2\underline{c} &= X_3\ \underline{i} + Y_3\ \underline{j} + d_3\ \underline{k} \end{aligned}$$

In equation 4.1.10 both positive and negative signs occur since the three spheres will meet in two points, one inside the transducer box and the other outside this box, depending on which side the points are of the plane ABC. It is necessary to know which sign in equation 4.1.9 should be used to give the required position. If the zero positions of the points A,B and C ($\underline{a}_0$, $\underline{b}_0$, $\underline{c}_0$) are used in the equation 4.1.12, the point P_1 or P_2 should be the origin if the required sign is used.

$$2a=d_1\ \underline{i} \qquad a_0 = (d_1/2)\ \underline{i}$$

$$2b=d_2\ \underline{j} \qquad b_0 = (d_2/2)\ \underline{j}$$

$$2c=d_3\ \underline{k} \qquad c_0 = (d_3/2)\ \underline{k}$$

From (4.1.3) $\lambda = \left(\dfrac{-d_1^2}{d_1^2+d_2^2}\right)$

Therefore $\underset{\sim}{d} = \dfrac{d_1}{2}\underset{\sim}{i} + \dfrac{d_3}{2}\underset{\sim}{k} - \left(\dfrac{d_1^2}{d_1^2+d_2^2}\right)\left(\dfrac{d_1}{2}\underset{\sim}{i} - \dfrac{d_2}{2}\underset{\sim}{j}\right)$

$$= \frac{1}{2}\left(\frac{d_1 d_2^2}{d_1^2+d_2^2}\right)\underset{\sim}{i} + \frac{1}{2}\left(\frac{d_1^2 d_2}{d_1^2+d_2^2}\right)\underset{\sim}{j} + \frac{d_3}{2}\underset{\sim}{k} \qquad (4.1.13)$$

Now $(\underset{\sim}{a}-\underset{\sim}{c})\wedge(\underset{\sim}{b}-\underset{\sim}{c}) = \left(\dfrac{d_1}{2}\underset{\sim}{i} - \dfrac{d_3}{2}\underset{\sim}{k}\right)\wedge\left(\dfrac{d_2}{2}\underset{\sim}{j} - \dfrac{d_3}{2}\underset{\sim}{k}\right)$

$$= \frac{1}{4}\left(d_2 d_3\underset{\sim}{i} + d_1 d_3\underset{\sim}{k} + d_1 d_2\underset{\sim}{k}\right) \qquad (4.1.14)$$

and $\left|(\underset{\sim}{a}-\underset{\sim}{c})\wedge(\underset{\sim}{b}-\underset{\sim}{c})\right| = {}^1\!/_4\left(d_2^2 d_3^2 + d_1^2 d_3^2 + d_1^2 d_2^2\right)^{1/2}$ (4.1.15)

Also $\underset{\sim}{d} - 2\underset{\sim}{c} = \dfrac{1}{2}\left[\dfrac{d_1 d_2^2}{d_1^2+d_2^2}\right]\underset{\sim}{i} + \dfrac{1}{2}\left[\dfrac{d_1^2 d_2}{d_1^2+d_2^2}\right]\underset{\sim}{j} - \dfrac{d_3}{2}\underset{\sim}{k}$ (4.1.16)

$$\left|\underset{\sim}{d} - 2\underset{\sim}{c}\right| = \frac{1}{2}\left[\frac{d_1^2 d_2^2 + d_2^2 d_3^2 + d_3^2 d_1^2}{d_1^2+d_2^2}\right]^{1/2} \qquad (4.1.17)$$

$$\underset{\sim}{a} - \underset{\sim}{b} = \frac{d_1}{2}\underset{\sim}{i} - \frac{d_2}{2}\underset{\sim}{j} \qquad (4.1.18)$$

$$\left|\underset{\sim}{a} - \underset{\sim}{b}\right| = {}^1\!/_2\left(d_1^2 + d_2^2\right)^{1/2}$$

$$\cos\theta = 1 + \frac{2\left(\frac{d_1^2}{d_1^2+d_2^2}\right)\left(\frac{d_2^2}{d_1^2+d_2^2}\right).\,4\left(d_1^2+d_2^2\right).\,{}^1\!/_4\left(d_1^2+d_2^2\right)}{\left(d_1^2 d_2^2 + d_2^2 d_3^2 + d_1^2 d_3^2\right)}$$

$$= 1 - \frac{2 d_1^2 d_2^2}{\left(d_1^2 d_2^2 + d_2^2 d_3^2 + d_1^2 d_3^2\right)}$$

$$1 + \cos\theta = 2 - \frac{2 d_1^2 d_2^2}{d_1^2 d_2^2 + d_2^2 d_3^2 + d_1^2 d_3^2}$$

$$= \frac{2 d_3^2\left(d_1^2 + d_2^2\right)}{d_1^2 d_2^2 + d_1^2 d_3^2 + d_2^2 d_3^2} \qquad (4.1.19)$$

$$\sin\Theta = (1-\cos^2\Theta)^{1/2}$$

$$= \left[1 - \left(1 - \frac{4\,d_1^2 d_2^2}{d_1^2 d_2^2 + d_2^2 d_3^2 + d_1^2 d_3^2} + \frac{4\,d_1^4 d_2^4}{(d_1^2 d_2^2 + d_1^2 d_3^2 + d_2^2 d_3^2)^2}\right)\right]^{1/2}$$

$$= \frac{2\,d_1 d_2 d_3\,(d_1^2 + d_2^2)^{1/2}}{d_1^2 d_2^2 + d_1^2 d_3^2 + d_2^2 d_3^2} \qquad (4.1.20)$$

Substituing for equations 4.1.13 to 4.1.20 into equation 4.1.9

$$P_1, P_2 = \left[\frac{1}{2}\left(\frac{d_1 d_2^2}{d_1^2 + d_2^2}\right)\underset{\sim}{i} + \frac{1}{2}\left(\frac{d_1^2 d_2}{d_1^2 + d_2^2}\right)\underset{\sim}{j} + \frac{d_3}{2}\underset{\sim}{k}\right]\frac{2 d_3^2 (d_1^2 + d_2^2)}{d_1^2 d_2^2 + d_2^2 d_3^2 + d_1^2 d_3^2}$$

$$- 2\,\frac{d_3}{2}\,\underset{\sim}{k}\left[1 - \frac{2 d_1^2 d_2^2}{d_1^2 d_2^2 + d_1^2 d_3^2 + d_2^2 d_3^2}\right]$$

$$\pm \frac{1}{2}\left[\frac{d_1^2 d_2^2 + d_1^2 d_3^2 + d_2^2 d_3^2}{d_1^2 + d_2^2}\right]^{1/2}\frac{4}{\left[d_1^2 d_2^2 + d_1^2 d_3^2 + d_2^2 d_3^2\right]^{1/2}}\cdot\frac{1}{4}\left[d_2 d_3\,\underset{\sim}{i}\right.$$

$$\left. + d_1 d_3\,\underset{\sim}{j} + d_1 d_2\,\underset{\sim}{k}\right]\frac{2\,d_1 d_2 d_3\,(d_1^2 + d_2^2)^{1/2}}{d_1^2 d_2^2 + d_1^2 d_3^2 + d_2^2 d_3^2}$$

$$= \frac{\left[d_1 d_2^2 d_3^2\,\underset{\sim}{i} + d_1^2 d_2 d_3^2\,\underset{\sim}{j} + d_1^2 d_2^2 d_3\,\underset{\sim}{k}\right]}{(d_1^2 d_2^2 + d_1^2 d_3^2 + d_2^2 d_3^2)} \qquad (4.1.21)$$

$$\pm \frac{\left[d_1 d_2^2 d_3^2\,\underset{\sim}{i} + d_1^2 d_2 d_3^2\,\underset{\sim}{j} + d_1^2 d_2^2 d_3\,\underset{\sim}{k}\right]}{d_1^2 d_2^2 + d_1^2 d_3 + d_2^2 d_3^2}$$

If the negative sign is used in equation 4.1.22 then P_2 is the origin of the axis system. This calculation was then used in the second part of the programs LTRANS.FTN and LTRFOR.FTN (appendix A).

4.2 Transducer Displacements to Fracture Site Displacements

4.2(i) With Fixator Support Bar in Position

The work of Evans et al (1979), and Churches at al (1985a) on the analysis of the "Oxford" Fixator concludes that movement at the fracture site is mainly due to the bending of the pins, the relative movement both between the pins and the bone, and between the pins and the fixator clamps. Therefore it is assumed that the support bar and the clamps are a rigid entity, and that the bone is also totally rigid. However, the Schanz pins are considered to be elastic, with an instantaneous transition from the unthreaded portion to the threaded portion of the pins.

The threaded portion, of the pin whose total length is l, is assumed to commence at a distance d from the support bar (Figure 4.2.1), with a part of the thread outside the bone, i.e. d is less than l. MacCauley's method using singularity functions (MacCauley, 1919) is used in the region $0 < x < d$ and gives

$$EI_1 \left(\frac{d^2v}{dx^2}\right) = -F_y\ [x]^1 + (M_z + F_y l)\ [x]^0$$

$$EI_1 \left(\frac{dv}{dx}\right) = -F_y \frac{[x]^2}{2} + (M_z + F_y l)\ [x]^1 + A_1 \qquad (4.2.1)$$

$$EI_1\ v = -F_y \frac{[x]^3}{6} + (M_z + F_y l) \frac{[x]^2}{2} + A_1 x + B_1 \qquad (4.2.2)$$

Where a force F_y and a moment M_z act at a distance l from the support, v is the displacement from the initial position, E is Young's Modulus and I_1 is the second moment of area of the shank of the pin. A_1 and B_1 are the constants of inte gration. The distance between the transducer clamp and the support is assumed to be a, and the singularity function is described in the glossary.

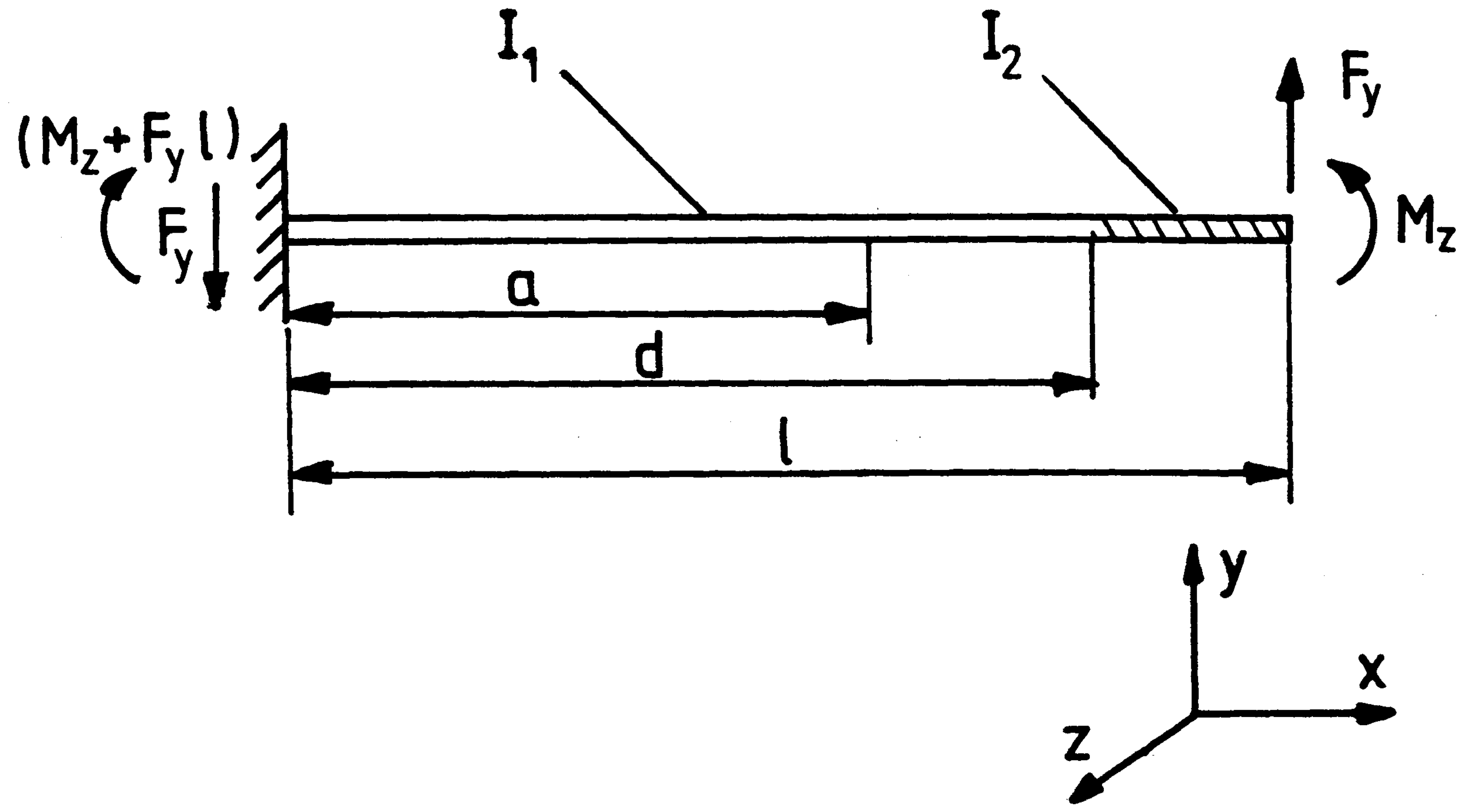

Fig 4.2.1

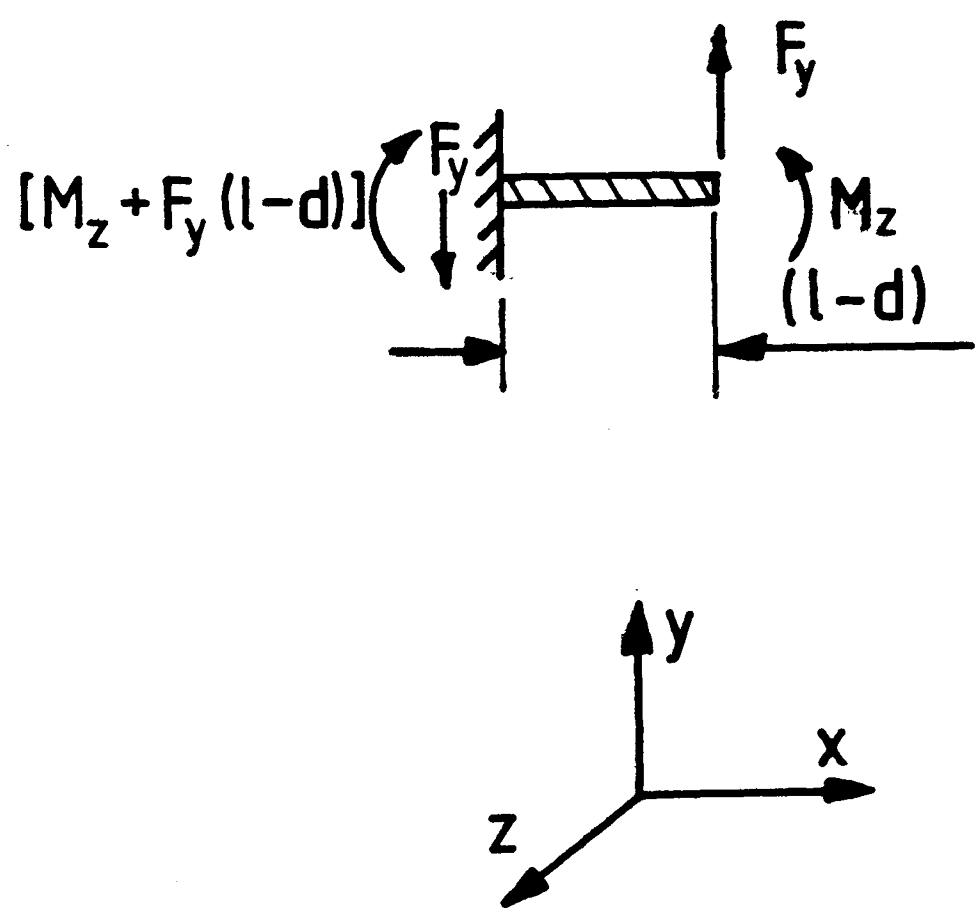

Fig 4.2.2

When $x = 0$ $\frac{dv}{dx} = 0$ and therefore $A_1 = 0$

When $x = 0$ $v = kNF_y$ and therefore $B_1 = kNF_yEI_1$

where k is the stiffness of the fixator spring in use and N is the number of springs (the fixator is either a Mark I, where there are no springs, or a Mark II, using either a pack of disc springs or a helical spring, as discussed in section 3.1).

When $x = a$ let $\frac{dv}{dx} = \alpha_z$, and $v = \delta_y$

so that from 4.2.1

$$\alpha_z = \frac{-F_y a^2}{2EI_1} + \frac{(M_z + F_y l)a}{EI_1}$$

$$= \frac{M_z a}{EI_1} + \frac{F_y a(2l - a)}{EI_1} \qquad (4.2.3)$$

and from 4.2.2

$$\delta_y = \frac{1}{EI_1}\left[\frac{-F_y a^3}{6} + \frac{(M_z + F_y l)a^2}{2}\right] + EI_1 kNF_y$$

$$= \frac{M_z a}{2EI_1} + \frac{F_y a^2(3l-a)}{6EI_1} + F_y kN \qquad (4.2.4)$$

When $x = d$ (i.e. at the junction of the threaded and unthreaded portions of the Schanz pin)

$$\frac{dv}{dx} = \frac{M_z d}{EI_1} + \frac{F_y d(2l-d)}{2EI_1}, \qquad (4.2.5)$$

and

$$v = \frac{M_z d^2}{2EI_1} + \frac{F_y d^2(3l-d)}{6EI_1} + kNF_y \qquad (4.2.6)$$

For the threaded portion of the pin in figure 4.2.2, again using MacCauley's method

$$EI_2\left(\frac{d^2y}{dx^2}\right) = -F_y\,[x]^1 + (M_z + F_y(1-d))\,[x]^0 \qquad (4.2.7)$$

$$EI_2\left(\frac{dv}{dx}\right) = -F_y\,\frac{[x]^2}{2} + (M_z + F_y(1-d))\,[x]^1 + A_2 \qquad (4.2.8)$$

$$EI_2\ v = -F_y\,\frac{[x]^3}{6} + (M_z + F_y(1-d))\,\frac{[x]^2}{2} + A_2x + B_2 \qquad (4.2.9)$$

Where A_2 and B_2 are the new constants of inte gration, and I_2 is the second moment of area for the threaded portion of the pin.

From 4.2.5 when $x = 0$ $\dfrac{dv}{dx} = \dfrac{M_zd}{EI_1} + \dfrac{F_yd(21-d)}{2EI_1}$

therefore $A_2 = \left(\dfrac{I_2}{I_1}\right)\left[M_zd + \dfrac{F_yd(21-d)}{2}\right]$

From 4.2.6 when $x = 0$ $v = \dfrac{M_zd^2}{2EI_1} + \dfrac{F_yd^2(31-d)}{6EI_1} + kNF_y$

Therefore $B_2 = \left(\dfrac{I_2}{I_1}\right)\left[\dfrac{M_zd^2}{2} + \dfrac{F_yd^2(31-d)}{6}\right] + kNF_yEI_1$

When $x = (1-d)$

$$EI_2\left(\frac{dv}{dx}\right) = \frac{-F_y(1-d)^2}{2} + [M_z + F_y(1-d)](1-d)$$

$$+\left(\frac{I_2}{I_1}\right)\left[M_zd + \frac{F_yd(21-d)}{2}\right]$$

$$\text{i.e}\left(\frac{dv}{dx}\right) = M_z\left[\frac{d}{EI_1} + \frac{(1-d)}{EI_2}\right] + F_y\left[\frac{d(21-d)}{2EI_1} + \frac{(1-d)^2}{2EI_2}\right] \qquad (4.2.10)$$

also $EI_2v = \dfrac{-F_y(1-d)^3}{6} + [M_z + F_y(1-d)]\dfrac{(1-d)^2}{2}$

$$+ \left(\frac{I_2}{I_1}\right)\left[M_z d + \frac{F_y d(1-d)}{2}\right] (1-d)$$

$$+ \left(\frac{I_2}{I_1}\right)\left[\frac{M_z d^2}{2} + \frac{F_y d^2(31-d)}{6} + kNF_y EI_1\right]$$

$$v = F_y\left[\frac{d(31^2-31d+d^2)}{3EI_1} + \frac{(1-d)^3}{3EI_2} + kN\right] + M_z\left[\frac{d(21-d)}{2EI_1} + \frac{(1-d)^2}{2EI_2}\right] \tag{4.2.11}$$

However, $\frac{dv}{dx}$ and v are the angulation and displacement respectively of the pin at the point where it enters the bone, whereas, what is actually required is the displacement and angulation of the bone relative to the fixator clamp, at the point where the pin enters the bone. Since the pin-bone connection is not absolutely rigid, there will be angulation of the bone on the pin due to the moment at the pin-bone interface, modulus T rad $N^{-1}m^{-1}$, and there will be translation of the bone perpendicular to the length of the pin, modulus S mm N^{-1}, due to the force in that direction. These two moduli relating the forces/moments to the displacements and angulations will be variable (Evans et al, 1979), but an average value will be used in these calculations.

Thus from 4.2.10 and 4.2.11

$$\beta_z = M_z\left[\frac{d}{EI_1} + \frac{(1-d)}{EI_2} + T\right] + F_y\left[\frac{d(21-d)}{2EI_1} + \frac{(1-d)^2}{2EI_2}\right] \tag{4.2.12}$$

$$\Delta_y = M_z\left[\frac{d(21-d)}{2EI_1} + \frac{(1-d)^2}{2EI_2}\right] + F_y\left[\frac{d(31^2-31d+d^2)}{3EI_1} + \frac{(1-d)^3}{3EI_2} + S + kN\right] \tag{4.2.13}$$

Eliminating M_z and F_y from these equations gives:

$$\beta_z = \frac{1}{(a^3 + 12EI_1kN)}\left[\left(\frac{I_1}{I_2}\right)(l-d)\left\{6\delta_y(a-l-d) - a\alpha_z(2a-3l-3d)\right\}\right.$$
$$+ d\left\{6(a-d)\delta_y - a\alpha_z(2a-3d)\right\} + \frac{12EI_1kN\alpha_z}{a}\left\{d + \left(\frac{I_1}{I_2}\right)(l-d)\right\}$$
$$\left. + 2EI_1T\left\{\alpha_z\left[a(3l-a) + \frac{6EI_1kN}{a}\right] - 3\delta_y(2l-a)\right\}\right] \quad (4.2.14)$$

$$\Delta_y = \frac{1}{(a^3 + 12EI_1kN)}\left[\delta_y\left\{d(6al - 6ld - 3ad + 4d^2) + \left(\frac{I_1}{I_2}\right)(l-d)(3a-3l-4d)\right\}\right.$$
$$- a\alpha_z\left\{d(2al - 3ld - 3ad + 2d^2) + \left(\frac{I_1}{I_2}\right)(l-d)^2(a-l-2d)\right\} + 6EI_1S\left[2\delta_y - a\alpha_z\right]$$
$$\left. + 6EI_1kN\left[2\delta_y + \frac{\alpha_z}{a}\left\{2ld - d^2 - a^2 + \left(\frac{I_1}{I_2}\right)(l-d)^2\right\}\right]\right] \quad (4.2.15)$$

Similar calculations are performed for α_y δ_z β_y and Δ_z but since there are no springs in the direction of F_z, N = 0, and the moduli S and T will be replaced by the moduli U and V, different values being necessary due to the anistrophic behaviour of bone, so that,

$$\alpha_y = \frac{M_y a}{EI_1} + \frac{F_z a(21-a)}{EI_2} \quad (4.2.16)$$

$$\delta_z = \frac{M_y a^2}{2EI_1} + \frac{F_z d^2(31-a)}{6EI_1} + kNF_z \quad (4.2.17)$$

and

$$\beta_y = M_y\left[\frac{d}{EI_1} + \frac{(1-d)}{EI_2} + U\right] + F_z\left[\frac{d(21-d)}{2EI_1} + \frac{(1-d)^2}{2EI_2}\right] \quad (4.2.18)$$

$$\Delta_z = M_y\left[\frac{d(21-d)}{2EI_1} + \frac{(1-d)^2}{2EI_2}\right] + F_y\left[\frac{d(31^2-31d+d^2)}{3EI_1} + \frac{(1-d)^3}{3EI_2} + V\right] \quad (4.2.19)$$

Similarly from 4.2.16, 4.2.17, 4.2.18 and 4.2.19

$$\beta_y = \frac{1}{a^3}\left[\left(\frac{I_1}{I_2}\right)(l-d)\left[6\delta_z(a-l-d) - a\alpha_y(2a-3(l+d))\right]\right.$$
$$+ d\left\{6(a-d)\delta_z - a\alpha_y(2a-3d)\right\}$$
$$\left. + 2EI_1V\left\{a\alpha_y(3l-a) - 3\delta_z(2l-a)\right\}\right] \quad (4.2.20)$$

$$\Delta_z = \frac{1}{a_3}\Big[\delta_z\Big\{d(6al - 6ld - 3ad + 4d^2) + \left(\frac{I_1}{I_2}\right)(l-d)^2(3a - 2l - 4d)\Big\}$$
$$- a\alpha_y\Big\{d(2al - 3ld - ad + 2d^2) + \left(\frac{I_1}{I_2}\right)(l-d)^2(a - l - 2d)\Big\}$$
$$+ 6EI_1 u(2\delta_z - a\alpha_y)\Big] \qquad (4.2.21)$$

Also, according to Evans et al (1979), the extension of the pin is sufficiently small to be ignored, and the displacements along the line of the pin are due to the movement of the pin in the bone and in the clamp (Figure 4.2.3), where the modulus of extension of the pin in the clamp is A mm N^{-1} and that of the pin in bone is B mm N^{-1}, thus,

$$\delta_x = A\,F_x$$
$$\Delta_x = (A + B)\,F_x$$

Thus $$\Delta_x = \left(\frac{A + B}{A}\right)\delta_x \qquad (4.2.22)$$

For torsion about the length of the pin figure (4.2.4), where the modulus of rotation relating the torque applied to the pin to the rotation of the pin in the clamp is R rad $N^{-1}m^{-1}$ and that for the rotation of the pin in the bone is Q rad $N^{-1}m^{-1}$, thus

$$\alpha_x = \frac{M_x a}{GJ_1} + M_x R$$
$$= M_x\left(R + \frac{a}{GJ_1}\right)$$
$$= M_x\left(\frac{RGJ_1 + a}{GJ_1}\right)$$

and $$\beta_x = \frac{M_x}{G}\left(\frac{d}{J_1} + \frac{(l-d)}{J_2}\right) + M_x(Q + R)$$

Thus $$\beta_x = \alpha_x\left(\frac{d}{GJ_1} + \frac{(l-d)}{GJ_2} + Q + R\right)\frac{(GJ_1)}{(RGJ_1 + a)} \qquad (4.2.23)$$

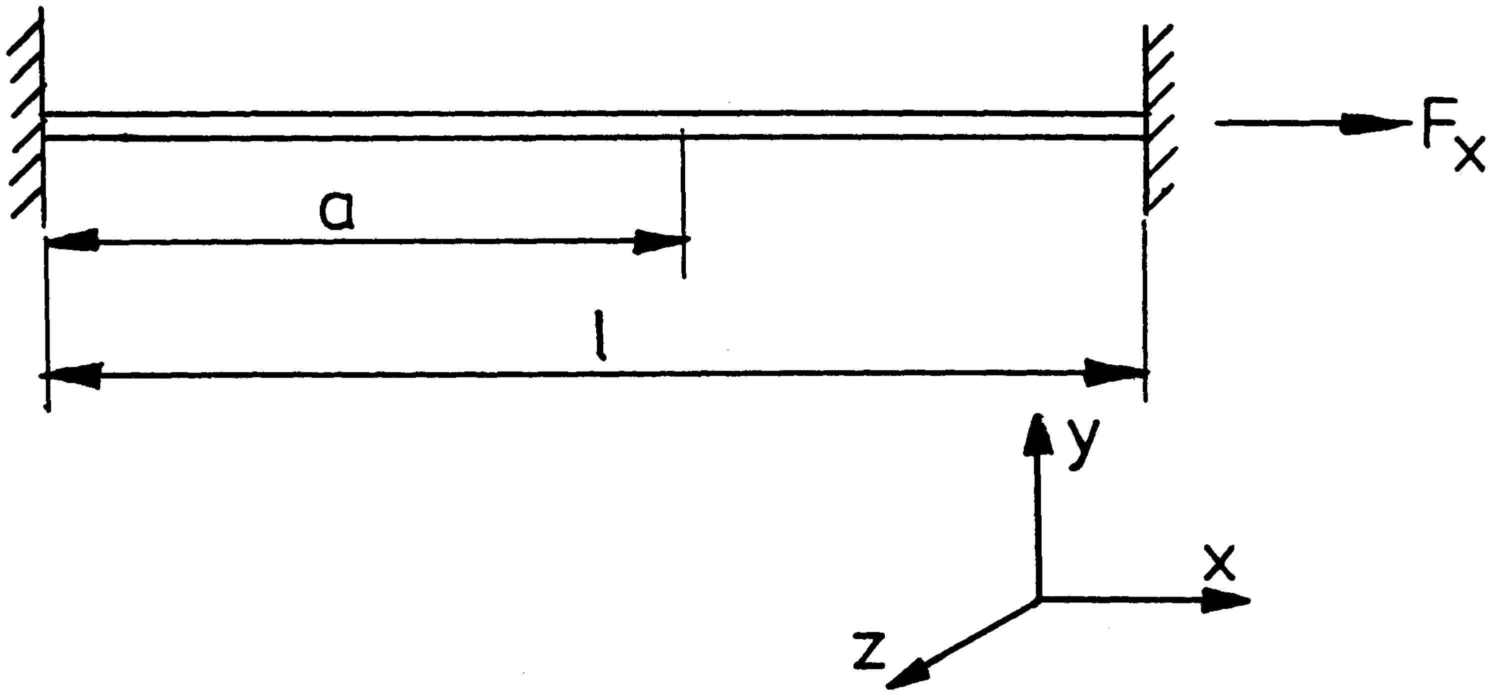

Fig 4.2.3

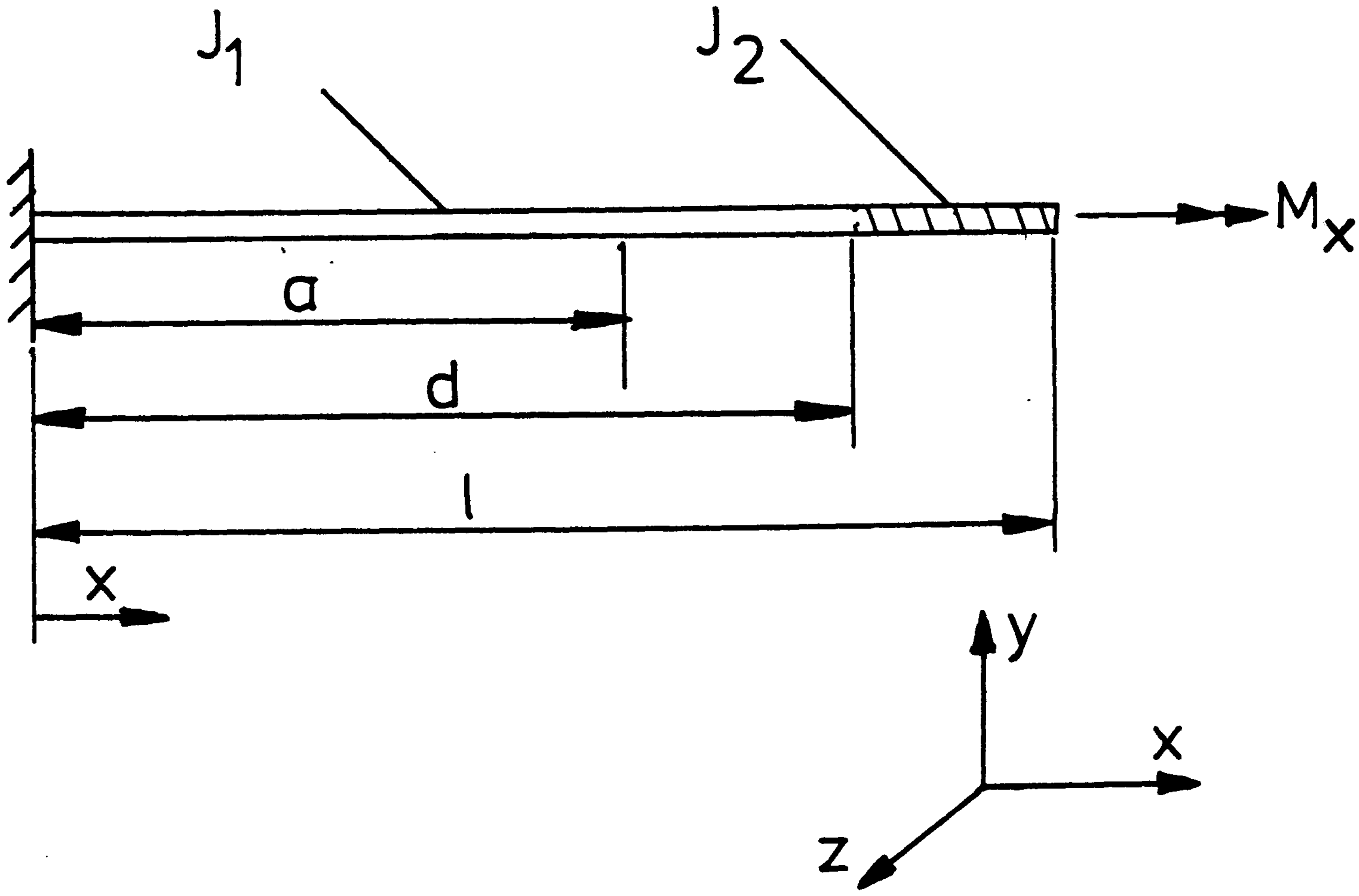

Fig 4.2.4

These, β_x, β_y, β_z, Δ_x, Δ_y and Δ_z, are the movements of the bone at the end of the pin related to the movement at the point on the pin where the transducer is attached, however what is really required is the movement at the fracture site in terms of the movement at the transducer.

Figure 4.2.5 shows a diagram of a left leg with the fixator placed on the anterio-medial side of the tibia, the transducer placed on the anterior side of the fixator. A similar arrangement would occur on a right leg with the fixator placed on the lateral side of the femur. (Usually single-sided fixators are applied to the anterio-medial face of the tibia and the lateral side of the femur). In Figure 4.2.6 the fixator is on the anterio-medial side of a right tibia or the lateral side of a left femur, with, again the transducer on the anterior side of the fixator.

The co-ordinates system used is defined as follows; the X axis is in the direction pointing towards the bone, perpendicular to the long axis of the bone in the plane of the pins, the Y axis lies in the long axis of the bone in the proximal (upwards) direction, and the Z axis is mutually perpendicular to both the X and Y axes forming a right handed orthogonal system. The origin of this set of axes will be defined at the midpoint between the clamps of pin 1 and pin 2. In this system the only difference between Figures 4.2.5 and 4.2.6 is that in Figure 4.2.6 f is in the negative $\underline{k}$ direction rather than the positive direction as in Figure 4.2.5, and so the calculations may be done for a left tibia/right femur and will apply for a right tibia/left femur providing f is negative in the second case.

The subscripts X,Y,Z relate to the X,Y,Z fixator axes as defined, and the subscripts x_1,y_1,z_1 and x_2,y_2,z_2 are related to the x_1,y_1,z_1

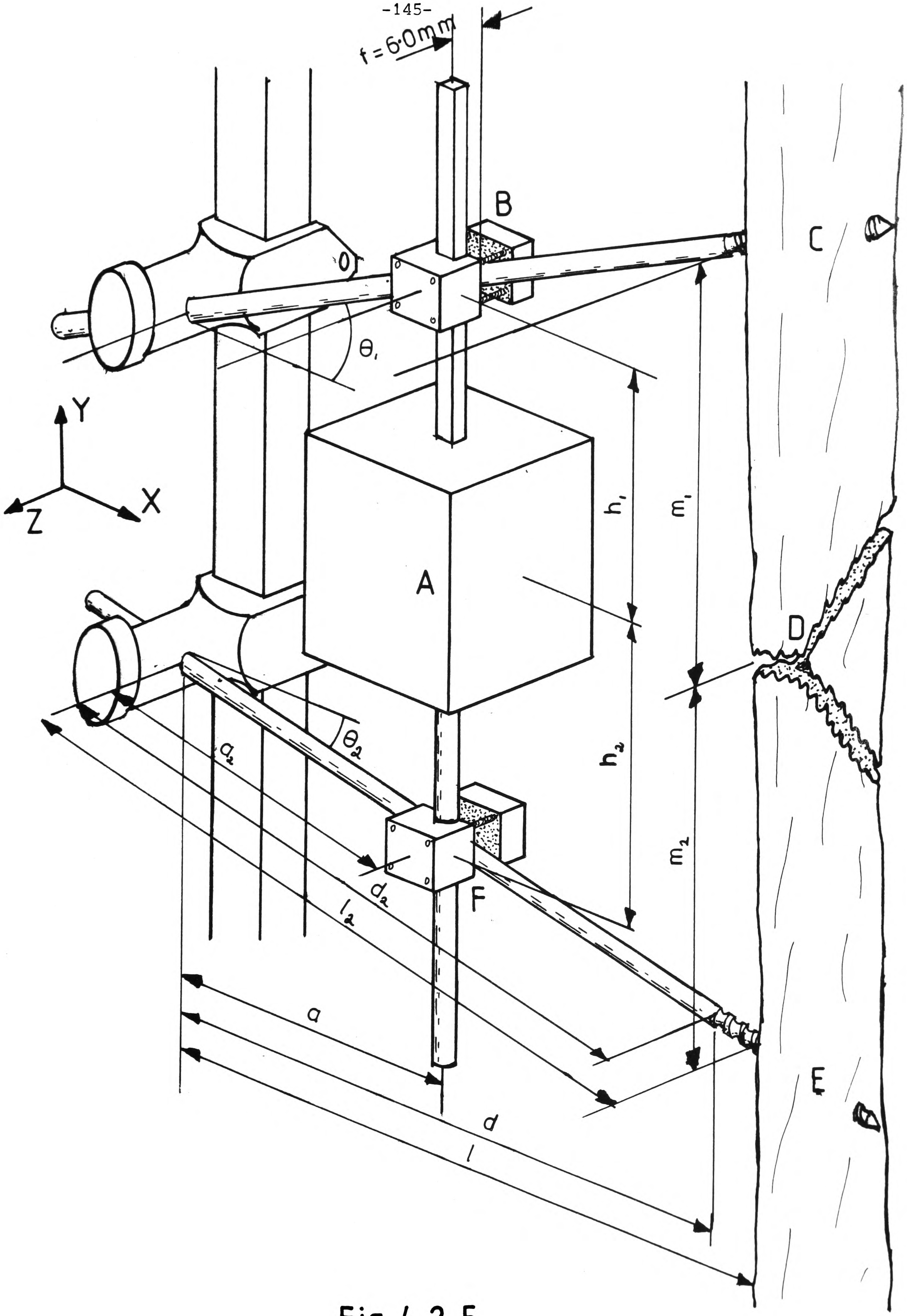

Fig 4.2.5

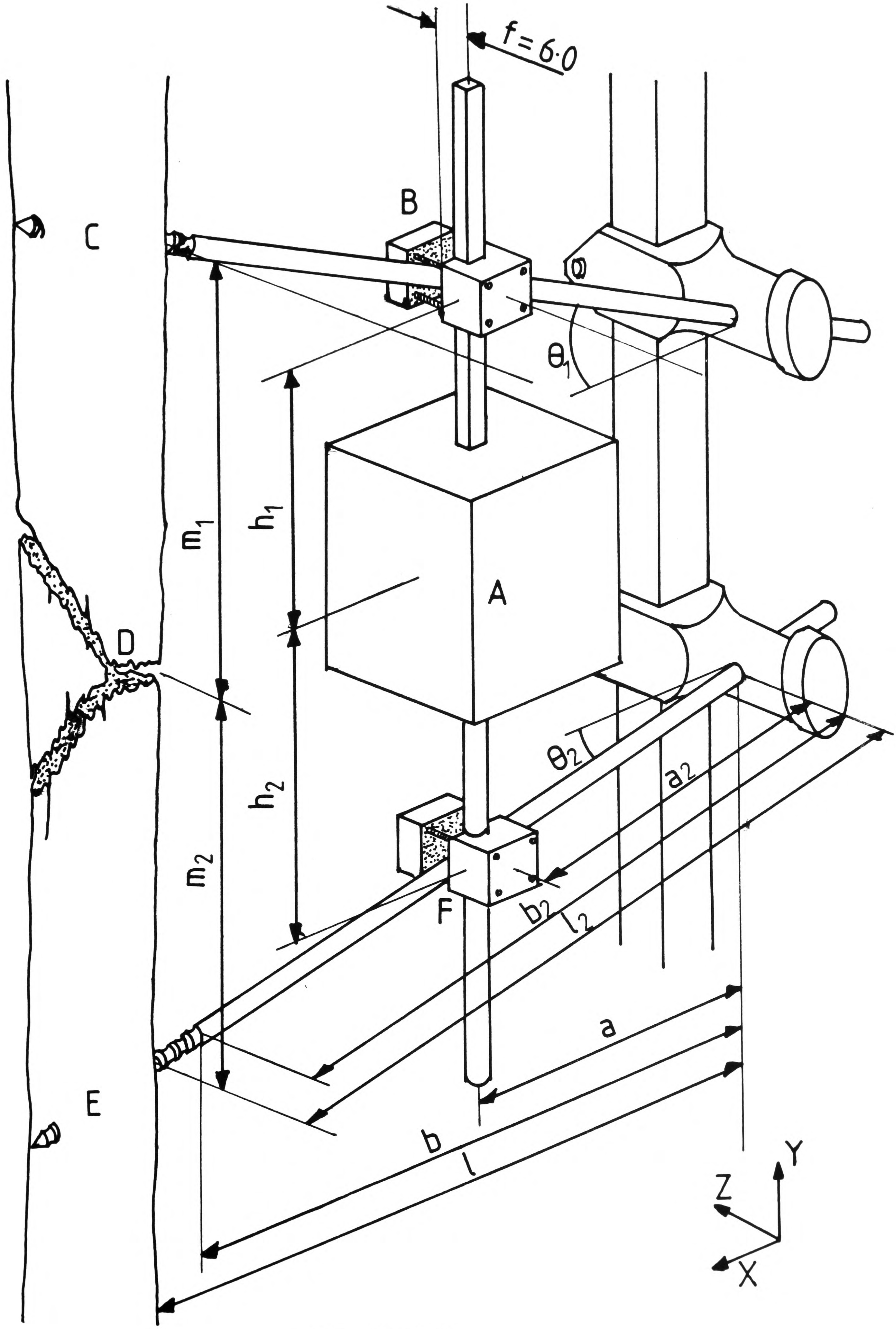

Fig 4.2.6

and x_2, y_2, z_2 directions of the pins. Pin 1 is proximal to the fracture and pin 2 is distal to the fracture. The x axis of each pin is directed along its length towards the bone, and the z axis coincides with the Z axis of the fixator and the y axis is orthogonal to these two axes. The unit vectors relating to pin 1 will be $\underline{i}'$, $\underline{j}'$ and $\underline{k}'$, those to pin 2, $\underline{i}^*$, $\underline{j}^*$ and $\underline{k}^*$ while those for the fixator axes will be $\underline{i}$, $\underline{j}$ and $\underline{k}$. The origins of these two sets of pin axes are at the points that each pin leaves the clamp that holds it.

The transducer head and the fracture are off-set from the pins, and thus the relationship between the transducer outputs and the fracture site movements will be needed.

Using the axes defined previously, prior to deformation of the pins the position vectors of the various marked points are

$a_1\underline{i}'$ corresponding to B

$l_1\underline{i}'$ corresponding to C

$l_2\underline{i}^*$ corresponding to E

$a_2\underline{i}^*$ corresponding to F

$a\underline{i} + (c/2 + a_1\sin\theta_1 - h_1)\underline{j} + f\underline{k}$ corresponding to A_1

$a\underline{i} + (-c/2 - a_2\sin\theta_2 - h_2)\underline{j} + f\underline{k}$ correspond to A_2

$(l + t)\underline{i} + (c/2 + l_1\sin\theta_1 - m_1)\underline{j}$ corresponding to D_1

$(l + t)\underline{i} + (-c/2 - l_2\sin\theta_2 + m_2)\underline{j}$ corresponding to D_2

where a_1 is the distance from the clamp to the transducer clamp along pin 1, a_2 is the similar distance along pin 2, l_1 is the total length of pin 1, l_2 is the total length of pin 2, l is the distance from the support bar to the bone, c is the distance between the two clamps and 2t is the thickness of the bone, h_1 is the distance from the centre of the transducer to pin 1 along the transducer bar, h_2 is the similar distance to pin 2, m_1 is the distance from the fracture to pin 1 along to bone, and m_2 from the fracture to pin 2.

A_1 is on the upper part of the transducer, and A_2 is on the lower part of the transducer. D_1 is on the proximal bone fragment and D_2 is on the distal bone fragment. Prior to deformation of the pins the position vectors of the points A_1 and A_2 and those of D_1 and D_2 are identical, i.e.

$$c/2 + a_1\sin\theta_1 - h_1 = -c/2 - a_2\sin\theta_2 + h_2$$

and

$$c/2 + l_1\sin\theta_1 - m_1 = -c/2 - l_2\sin\theta_2 + m_2$$

After deformation all these points have moved, so that their new position vectors are

$$B \text{ at } (a_1 + \delta_{x1})\underline{i}' + \delta_{y1}\underline{j}' + \delta_{z1}\underline{k}'$$
$$C \text{ at } (l_1 + \Delta_{x1})\underline{i}' + \Delta_{y1}\underline{j}' + \Delta_{z1}\underline{k}'$$
$$E \text{ at } (l_2 + \Delta_{x2})\underline{i}^* + \Delta_{y2}\underline{j}^* + \Delta_{z2}\underline{k}^*$$
$$F \text{ at } (a_2 + \delta_{x2})\underline{i}^* + \Delta_{y2}\underline{j}^* + \delta_{z2}\underline{k}^*$$

Also, the vector equations of the members BA_1, CD_1, ED_2 and EA_2 in the pin systems are found to be

$$BA_1 = -h_1\sin\theta_1\underline{i}' - h_1\cos\theta_1\underline{j}' + f\underline{k}' \qquad (4.2.24)$$
$$CD_1 = (-m_1\sin\theta_1 + t\cos\theta_1)\underline{i}' + (-m_1\cos\theta_1 - t\sin\theta_1)\underline{j}' \qquad (4.2.25)$$
$$ED_1 = (m_2\sin\theta_2 + t\cos\theta_2)\underline{i}^* + (m_2\cos\theta_2 + t\sin\theta_2)\underline{j}^* \qquad (4.2.26)$$
$$FA_2 \text{ is } -h_2\sin\theta_2\underline{i}^* + h_2\cos\theta_2\underline{j}^* + f\underline{k}^* \qquad (4.2.27)$$

When the pins are loaded, the deformations are the resultants of small linear displacements and small angulations. Although finite rotations do not conform to the laws of vector algebra, being non-commutative, infinitesimally small rotations do, so that considering pin 1 the net displacement at the fracture due to the three angulations (βx_1, βy_1, βz_1) at C is

$$(\beta x\underline{i}' + \beta y\underline{j}' + \beta z\underline{k}') \wedge (t\underline{i} - m_1\underline{j}).$$

Thus point D_1 may be calculated and its new position is

$$(1 + t)\underline{i} + (c/2 + l_1\sin\theta_1 - m_1)\underline{j} + \Delta_{x1}\underline{i}' + \Delta_{y1}\underline{j}' + \Delta_{z1}\underline{k}'$$

$$(\beta_{x1}\underline{i}' + \beta_{y1}\underline{j}' + \beta_{z1}\underline{k}') \wedge (t\underline{i} - m_1\underline{j})$$

$$= (1 + t + \Delta_{x1}\cos\theta_1 - \Delta_{y1}\sin\theta_1)\underline{i} + (c/2 + l_1\sin\theta_1 - m_1 + \Delta_{x1}\sin\theta_1$$
$$+ \Delta_{y1}\cos\theta_1)\underline{j} + \Delta_{z1}\underline{k} - \beta_{x1}t\sin\theta_1\underline{k} + \beta_{y1}t\cos\theta_1\underline{k} + \beta_{z1}t\underline{j}$$
$$- \beta_{x1}m_1\cos\theta_1\underline{k} + \beta_{y1}m_1\sin\theta_1\underline{k} + \beta_{z1}m_1\underline{i}$$
$$= (1 + t + \Delta_{x1}\cos\theta_1 - \Delta_{y1}\sin\theta_1 + \beta_{z1}m_1)\underline{i} + (c/2 + l_1\sin\theta_1 - m_1$$
$$+ \Delta_{x1}\sin\theta_1 + \Delta_{y1}\cos\theta_1 + \beta_{z1}t)\underline{j} + (\Delta_{z1} - \beta_{x1}(m_1\cos\theta_1 + t\sin\theta_1)$$
$$+\beta_{y1}(m_1\sin\theta_1 - t\cos\theta_1))\underline{k} \qquad (4.2.28)$$

and D_2 moves to $(1 + t)\underline{i} + (-c/2 - l_2\sin\theta_2 + m_2)\underline{j} + \Delta_{x2}\underline{i}^* + \Delta_{y2}\underline{j}^* + \Delta_{z2}\underline{k}^*$

$$+ (\beta_{x2}\underline{i}^* + \beta_{y2}\underline{j}^* + \beta_{z2}\underline{k}^*) \wedge (t\underline{i} + m_2\underline{j})$$
$$= (1 + t + \Delta_{x2}\cos\theta_2 + \Delta_{y2}\sin\theta_2)\underline{i} + (-c/2 - l_2\sin\theta_2 + m_2$$
$$- \Delta_{x2}\sin\theta_2 + \Delta_{y2}\cos\theta_2)\underline{j} + \Delta_{z2}\underline{k} + \beta_{x2}t\sin\theta_2\underline{k} - \beta_{y2}t\cos\theta_2\underline{k}$$
$$+ \Delta_{z2}t\underline{j} + \beta_{x2}m_2\cos\theta_2\underline{k} + \beta_{y2}m_2\sin\theta_2\underline{k} - \beta_{z2}m_2\underline{i}$$
$$= (1 + t + \Delta_{x2}\cos\theta_2 + \Delta_{y2}\sin\theta_2 - \beta_{z2}m_2)\underline{i} + (-c/2 - l_2\sin\theta_2 + m_2$$
$$- \Delta_{x2}\sin\theta_2 + \Delta_{y2}\cos\theta_2 + \beta_{z2}t)\underline{j} + (\Delta_{z2} + \beta_{x2}(t\sin\theta_2 + m_2\cos\theta_2)$$
$$+\beta_{y2}(-t\cos\theta_2 + m_2\sin\theta_2))\underline{k} \qquad (4.2.29)$$

The movement at the fracture site $\mathbf{D_2D_1}$ can now be calculated from 4.2.28 and 4.2.29.

$$= (\Delta_{x1}\cos\theta_1 - \Delta_{x2}\cos\theta_2 - \Delta_{y1}\sin\theta_1 - \Delta_{y2}\sin\theta_2 + \beta_{z1}m_1 + \beta_{z2}m_2)\underline{i}$$
$$+ (\Delta_{x1}\sin\theta_1 + \Delta_{x2}\sin\theta_2 + \Delta_{y1}\cos\theta_1 - \Delta_{y2}\cos\theta_2 + t(\beta_{z1} - \beta_{z2}))\underline{j}$$
$$+ (\Delta_{z1} - \Delta_{z2} + t(-\beta_{x1}\sin\theta_1 - \beta_{x2}\sin\theta_2 - \beta_{y1}\cos\theta_1 + \beta_{y2}\cos\theta_2)$$
$$+ m_1(-\beta_{x1}\cos\theta_1 + \beta_{z2}\sin\theta_2) - m_2(\beta_{x2}\cos\theta_2 + \beta_{y2}\sin\theta_2))\underline{k}$$
$$(4.2.30)$$

And the angulations at the fracture site shall be those between the projections of D_1C and ED_2 onto the YZ and ZX planes as defined by the original position of the fixator and the rotation about the bone. If displacements $d_{x1}\underline{i} + d_{y1}\underline{j} + d_{z1}\underline{k}$ occur at A with rotations $\gamma_{x1}\underline{i} + \gamma_{y1}\underline{j} + \gamma_{z1}\underline{k}$ producing displacements at a distance $h_1\underline{j} - f\underline{k}$ given by

$$
\begin{aligned}
& d_{x1}\underset{\sim}{i} + d_{y1}\underset{\sim}{j} + d_{z1}\underset{\sim}{k} + (\gamma_{x1}\underset{\sim}{i} + \gamma_{y1}\underset{\sim}{j} + \gamma_{z1}\underset{\sim}{k})\wedge(h_1\underset{\sim}{j} - f\underset{\sim}{k}) \\
&= d_{x1}\underset{\sim}{i} + d_{y1}\underset{\sim}{j} + d_{z1}\underset{\sim}{k} + h_1\gamma_{x1}\underset{\sim}{k} - h_1\gamma_{z1}\underset{\sim}{i} + f\gamma_{x1}\underset{\sim}{j} - f\gamma_{y1}\underset{\sim}{i} \\
&= \left[(d_{x1} - h_1\gamma_{z1} - f\gamma_{y1})\cos\theta_1 + (d_{y1} + f\gamma_{x1})\sin\theta_1\right]\underset{\sim}{i}' \qquad (4.2.31) \\
&\quad + \left[-(d_{x1} - h_1\gamma_{z1} - f\gamma_{y1})\sin\theta_1 + (d_{y1} + f\gamma_{x1})\cos\theta_1\right]\underset{\sim}{j}' + (d_{z1} + h_1\gamma_{x1})\underset{\sim}{k}'
\end{aligned}
$$

But this is $\delta_{x1}\underset{\sim}{i}' + \delta_{y1}\underset{\sim}{j}' + \delta_{z1}\underset{\sim}{k}'$

$$
\begin{aligned}
\text{ie}\quad \delta_{x1} &= d_{x1}\cos\theta_1 + d_{y1}\sin\theta_1 + f\gamma_{x1}\sin\theta_1 - f\gamma_{y1}\cos\theta_1 - h_1\gamma_{z1}\cos\theta_1 \\
\delta_{y1} &= -d_{x1}\sin\theta_1 + d_{y1}\cos\theta_1 + f\gamma_{x1}\cos\theta_1 + f\gamma_{y1}\sin\theta_1 + h_1\gamma_{z1}\cos\theta_1 \\
\delta_{z1} &= d_{z1} + h_1\gamma_{x1} \qquad (4.2.32)
\end{aligned}
$$

And the rotations at B $\gamma_{x1}\underset{\sim}{i} + \gamma_{y1}\underset{\sim}{j} + \gamma_{z1}\underset{\sim}{k}$ are $\alpha_{x1}\underset{\sim}{i}' + \alpha_{y1}\underset{\sim}{j}' + \alpha_{z1}\underset{\sim}{k}'$

$$
\left.
\begin{aligned}
\alpha_{x1} &= \gamma_{x1}\cos\theta_1 + \gamma_{y1}\sin\theta_1 \\
\alpha_{y1} &= -\gamma_{x1}\quad\theta_1 + \gamma_{y1}\cos\theta_1 \\
\alpha_{z1} &= \gamma_{z1}
\end{aligned}
\right\} \qquad (4.2.33)
$$

Similarily at F

$$
\begin{aligned}
& \delta_{x2}\underset{\sim}{i}^* + \delta_{y2}\underset{\sim}{j}^* + \delta_{z2}\underset{\sim}{k}^* = d_{x2}\underset{\sim}{i} + d_{y2}\underset{\sim}{j} + d_{z2}\underset{\sim}{k} + (\gamma_{x2}\underset{\sim}{i} + \gamma_{y2}\underset{\sim}{j} + \gamma_{z2}\underset{\sim}{k})\wedge(-h_2\underset{\sim}{j} - f\underset{\sim}{k}) \\
&= d_{x2}\underset{\sim}{i} + d_{y2}\underset{\sim}{j} + d_{z2}\underset{\sim}{k} - h_2\gamma_{x2}\underset{\sim}{k} + h_2\gamma_{z2}\underset{\sim}{i} + f\gamma_{x2}\underset{\sim}{j} - f\gamma_{y2}\underset{\sim}{i} \\
&= \left[(d_{x2} - f\gamma_{y2} + h_2\gamma_{z2})\cos\theta_2 - (d_{y2} + f\gamma_{x2})\sin\theta_2\right]\underset{\sim}{i}^* \qquad (4.2.34) \\
&\quad + \left[(d_{x2} - f\gamma_{y2} + h_2\gamma_{z2})\sin\theta_2 + (d_{y2} + f\gamma_{x2})\cos\theta_2\right]\underset{\sim}{j}^* + \left[d_{z2} - h_2\gamma_{x2}\right]\underset{\sim}{k}^*
\end{aligned}
$$

$$
\begin{aligned}
\delta_{x2} &= d_{x2}\cos\theta_2 - d_{y2}\sin\theta_2 - f\gamma_{x2}\sin\theta_2 - f\gamma_{y2}\cos\theta_2 + h_2\gamma_{z2}\cos\theta_2 \\
\delta_{y2} &= d_{x2}\sin\theta_2 + d_{y2}\cos\theta_2 + f\gamma_{x2}\cos\theta_2 - f\gamma_{y2}\sin\theta_2 + h_2\gamma_{z2}\sin\theta_2 \\
& \qquad (4.2.35) \\
\delta_{z2} &= d_{z2} - h_2\gamma_{x2}
\end{aligned}
$$

and

$$
\left.
\begin{aligned}
\alpha_{x2} &= \gamma_{x2}\cos\theta_2 - \gamma_{y2}\sin\theta_2 \\
\alpha_{y2} &= \gamma_{x2}\sin\theta_2 + \gamma_{y2}\cos\theta_2 \\
\alpha_{z2} &= \gamma_{z2}
\end{aligned}
\right\} \qquad (4.2.36)
$$

Using $\tan(A - B) = \dfrac{\tan A - \tan B}{1 + \tan A \tan B}$

and that the projection of $a\underline{i} + b\underline{j} + c\underline{k}$ onto the YZ is $b\underline{j} + c\underline{h}$ and similarly for $x\underline{i} + y\underline{j} + z\underline{k}$ is $y\underline{j} + z\underline{k}$ and so the angle between the projections of these two vectors onto the YZ plane, i.e. ϕ_x is given by:

$$\tan \phi_x = \frac{b/c - y/z}{1 + b/c \; y/z} = \frac{bz - yc}{by + cz}. \tag{4.2.37}$$

Thus the angles between the vector from pin 2 along the edge of the bone to fracture site $(-\beta_{z2}m_2\underline{i} + m_2\underline{j} + (\beta_{x2}m_2\cos\theta_2 + \beta_{y2}m_2\sin\theta_2)\underline{k})$ and the vector from the fracture site to pin 1 is

$(-\beta_{z1}m_1\underline{i} + m_1\underline{j} + (\beta_{x1}m_1\cos\theta_1 - \beta_{y1}m_1\sin\theta_1)\underline{k})$

$$\phi_x = \tan^{-1}\left[\frac{m_1 m_2(\beta_{x1}\cos\theta_1 - \beta_{y1}\sin\theta_1) - m_1 m_2(\beta_{x2}\cos\theta_2 + \beta_{y2}\sin\theta_2)}{m_1 m_2 + (\beta_{x1}m_1\cos\theta_1 - \beta_{y1}m_1\sin\theta_1)(\beta_{x2}m_2\cos\theta_2 + \beta_{y2}m_2\sin\theta_2)}\right]$$

$$= \tan^{-1}\left[\frac{(\beta_{x1}\cos\theta_1 - \beta_{x2}\cos\theta_2) - (\beta_{y1}\sin\theta_1 + \beta_{y2}\sin\theta_2)}{1 + (\beta_{x1}\cos\theta_1 - \beta_{y1}\sin\theta_1)(\beta_{x2}\cos\theta_2 + \beta_{y2}\sin\theta_2)}\right] \tag{4.2.38}$$

and

$$\phi_z = \tan^{-1}\left[\frac{-\beta_{z2}\, m_1 m_2 + \beta_{z1}\, m_1 m_2}{\beta_{z2} m_2 \beta_{z1} m_1 + m_1 m_2}\right]$$

$$= \tan^{-1}\left[\frac{\beta_{z1} - \beta_{z2}}{1 + \beta_{z1}\beta_{z2}}\right] \tag{4.2.39}$$

However, for the earlier calculations assume that all the angulations are small so tan $\beta \simeq \beta$ for $\beta < 5°$ so that

$$\phi_x = \beta_{x1}\cos\theta_1 - \beta_{y1}\sin\theta_1 - (\beta_{x2}\cos\theta_2 + \beta_{y2}\sin\theta_2)$$

$$= \beta_{x1}\cos\theta_1 - \beta_{x2}\cos\theta_2 - \beta_{y1}\sin\theta_1 - \beta_{y2}\sin\theta_2$$

$$\phi_z = \beta_{z1} - \beta_{z2}$$

The two angles ϕ_x, ϕ_z can be found using this method, but this does not give the rotation about the line of the vectors. Thus to find the relative rotation between the two bone segments, the projection after deformation, onto the XZ plane of the two vectors initially at C and E with direction $\underline{i}$, is required. The vector at C is then given by

$$\underline{i} + (\beta_{x1}\underline{i}' + \beta_{y1}\underline{j}' + \beta_{z1}\underline{k}') \wedge \underline{i}$$
$$= \underline{i} - \beta_{x1}\sin\theta_1\underline{k} - \beta_{y1}\cos\theta_1\underline{k} + \beta_{z1}\underline{j} \tag{4.2.42}$$

And that at E becomes

$$\underline{i} + (\beta_{x2}\underline{i}^* + \beta_{y2}\underline{j}^* + \beta_{z2}\underline{k}^*) \wedge \underline{i}$$
$$= \underline{i} + \beta_{x2}\sin\theta_2\underline{k} - \beta_{y2}\cos\theta_2\underline{k} + \beta_{z2}\underline{j} \tag{4.2.43}$$

and thus

$$\phi_y = \tan^{-1}\left[\frac{(\beta_{x2}\sin\theta_2 - \beta_{y2}\cos\theta_2) + (\beta_{x1}\sin\theta_1 + \beta_{y1}\cos\theta_1)}{1 - (\beta_{x2}\sin\theta_2 - \beta_{y2}\cos\theta_2)(\beta_{x1}\sin\theta_1 + \beta_{y1}\cos\theta_1}\right]$$

or assuming small angles (4.2.44)

$$\phi_y = \beta_{x1}\sin\theta_1 + \beta_{x2}\sin\theta_2 + \beta_{y1}\cos\theta_1 - \beta_{y2}\cos\theta_2$$

However, what is required is the movement at the fracture site in terms of the measured movements at the transducer.

Considering D_x from 4.2.30:

$$D_x = \Delta_{x1}\cos\theta_1 - \Delta x_2 \cos\theta_2 - \Delta_{y2}\sin\theta_2 - \Delta_{y1}\sin\theta_1 + \beta_{31}m_1 + \beta_{32}m_2$$

$$= \left(\delta_{x1}\cos\theta_1 - \delta_{x2}\cos\theta_2\right)\left(\frac{A+B}{A}\right) - \frac{\sin\theta_1}{(a_1^3 + 12EI_1kN)}\Big[\delta_{y1}\Big\{d_1(6a_1l_1 - 6l_1d_1$$

$$-3a_1d_1 + 4d_1^2) + \left(\frac{I_1}{I_2}\right)(l_1-d_1)^2(3a_1-l_1-4d_1)\Big\} - a_1\alpha_{31}\Big[d_1(2a_1l_1 - 3l_1d_1 - a_1d_1 + 2d_1^2)$$

$$+\left(\frac{I_1}{I_2}\right)(l_1-d_1)^2(a_1-l_1-d_1)\Big] + 6EI_1S\left[2\delta_{y1} - a_1\alpha_{31}\right] + 6EI_1kN\Big[2\delta_{y1}$$

$$+\frac{\alpha_{31}}{a_1}\left[2l_1d_1 - d_1^2 - a_1^2 + \left(\frac{I_1}{I_2}\right)(l_1-d_1)^2\right]\Big]\Big] - \frac{\sin\theta_2}{(a_2^3 + 12EI_1kN)}\Big[\delta_{y2}\Big\{d_2(6a_2l_2 - 6l_2d_2$$

$$-3a_2d_2 + 4d_2^2) + \left(\frac{I_1}{I_2}\right)(l_2-d_2)^2(3a_2-l_2-4d_2)\Big\} - a_2\alpha_{32}\Big\{d_2(2a_2l_2 - 3l_2d_2$$

$$-a_2d_2 + 2d_2^2) + \left(\frac{I_1}{I_2}\right)(l_2-d_2)^2(a_2-l_2-d_2)\Big\} + 6EI_1S\left\{2\delta_{y2} - a_2\alpha_{32}\right\}$$

$$+6EI_1kN\left\{2\delta_{y2} + \frac{\alpha_{32}}{a_2}\left(2l_2d_2 - d_2^2 - a_2^2 + \left(\frac{I_1}{I_2}\right)(l_2-d_2)^2\right)\right\}\Big]$$

$$+\frac{m_1}{(a_1^3 + 12EI_1kN)}\Big\{\delta_{y1}\left(6d_1(a_1-d_1) + 6\left(\frac{I_1}{I_2}\right)(l_1-d_1)(a_1-l_1-d_1)\right) - a_1\alpha_{31}\Big\{d_1(2a_1-3d_1)$$

$$+\left(\frac{I_1}{I_2}\right)(l_1-d_1)(2a_1-3l_1-3d_1)\Big\} + \frac{12EI_1kN\alpha_{31}}{a_1}\left\{a_1 + (l_1-d_1)\left(\frac{I_1}{I_2}\right)\right\} + 2EI_1T\Big(\alpha_{31}(a_1(3l_1-a_1)$$

$$+\frac{6EI_1kN}{a_1}\Big) - 3\delta_{y1}(2l_1-a_1)\Big)\Big] + \frac{m_2}{a_2^3 + 12EI_1kN}\Big[\delta_{y2}\Big[6d_2(a_2-d_2) + 6\left(\frac{I_1}{I_2}\right)(l_2-d_2)(a_2-l_2-d_2)\Big]$$

$$-a_2\alpha_{32}\left[d_2(2a_2-3d_2) + \left(\frac{I_1}{I_2}\right)(l_2-d_2)(2a_2-3l_2-3d_2)\right] + \frac{12EI_1kN\alpha_{32}}{a_2}\left[a_2 + \left(\frac{I_1}{I_2}\right)(l_2-d_2)\right]$$

$$+2EI_1T\left(\alpha_{32}\left\{a_2(3l_2-a_2) + \frac{6EI_1kN}{a_2}\right\} - 3\delta_{y2}(2l_2-a_2)\right)\Big]$$

But considering figures 4.2.5, 4.2.6

$$l_1 = \frac{l}{\cos\Theta_1}, \quad a_1 = \frac{a}{\cos\Theta_1}, \quad d_1 = \frac{d}{\cos\Theta_1}, \quad l_2 = \frac{l}{\cos\Theta_2} \quad a_2 = \frac{a}{\cos\Theta_2} \quad d_2 = \frac{d}{\cos\Theta_2}$$

$$D_x = \left(\frac{A+B}{A}\right)\left(\delta x_1 \cos\Theta_1 - \delta x_2 \cos\Theta_2\right) - \frac{\sin\Theta_1}{a_3 + 12EI_1 kN\cos^3\Theta_1}\left[\delta_{y1}\left\{d(6al - 6ld\right.\right.$$

$$\left.- 3ad + 4d^2) + \left(\frac{I_1}{I_2}\right)(l-d)^2(3a - 2l - 4d)\right\} - \frac{a\alpha_{31}}{\cos\Theta_1}\left\{d(2al - 3ld - ad + 2d^2)\right.$$

$$\left.+ \left(\frac{I_1}{I_2}\right)(l-d)^2(a - l - 2d)\right\} + 6EI_1 S\left[2\cos^3\Theta_1 \delta_{y1} - a\cos^2\Theta_1 \alpha_{31}\right] + 6EI_1 kN\left[2\cos^3\Theta_1 \delta_{y1}\right.$$

$$\left.\left. + \frac{\alpha_{31}\cos^2\Theta_1}{a}\left\{2ld - d^2 - a^2 + \left(\frac{I_1}{I_2}\right)(l-d)^2\right\}\right]\right] - \frac{\sin\Theta_2}{a^3 + 12EI_1 kN\cos^3\Theta_2}\left[\delta_{y2}\left\{d(6al - 6ld\right.\right.$$

$$\left.- 3ad + 4d^2) + \left(\frac{I_1}{I_2}\right)(l-d)^2(3a - 2l - 4d)\right\} - \frac{a\,\alpha_{32}}{\cos\Theta_2}\left\{d(2al - 3ld - ad + 2d^2)\right.$$

$$+ \left(\frac{I_1}{I_2}\right)(l-d)^2(a - l - 2d) + 6EI_1 S\left[2\cos^3\Theta_2\, \delta_{y2} - a\cos^2\Theta_2\, \alpha_{32}\right] + 6EI_1 kN\left[2\cos^3\Theta_2 \delta_{y2}\right.$$

$$\left.\left. + \frac{\alpha_{32}\cos^2\Theta_2}{a}\left\{2ld - d^2 - a^2 + \left(\frac{I_1}{I_2}\right)(l-d)^2\right\}\right]\right] + \frac{m_1}{a^3 + 12EI_1 kN\cos^3\Theta_1}\left[\delta_{y1}\cos\Theta_1\left\{6d(a-d)\right.\right.$$

$$\left.+ 6\left(\frac{I_1}{I_2}\right)(l-d)(a-l-d)\right\} - a\alpha_{31}\left[d(2a - 3d) + \left(\frac{I_1}{I_2}\right)(l-d)(2a - 3l - 3d)\right] +$$

$$+ \frac{12EI_1 kN\cos^3\Theta_1\alpha_{31}}{a}\left\{a + \left(\frac{I_1}{I_2}\right)(l-d)\right\} + 2EI_1 T\left\{\alpha_{31}\left(a(3l-a)\cos\Theta_1 + \frac{6EI_1 kN\cos^4\Theta_1}{a}\right)\right.$$

$$\left.\left. - 3\delta_{y1}\cos^2\Theta_1(2l-a)\right\}\right] + \frac{m_2}{a^3 + 12EI_1 kN\cos^3\Theta_2}\left[\delta_{y2}\cos\Theta_2\left\{6d(a-d) + 6\left(\frac{I_1}{I_2}\right)(l-d)(a-l-d)\right\}\right.$$

$$- a\alpha_{32}\left[d(2a - 3d) + \left(\frac{I_1}{I_2}\right)(l-d)(2a - 3l - 3d)\right] + \frac{12EI_1 kN\cos^3\Theta_2\alpha_{32}}{a}\left\{a + \left(\frac{I_1}{I_2}\right)(l-d)\right\}$$

$$\left. + 2EI_1 T\left\{\alpha_{32}\left[a(3l-a)\cos\Theta_2 + \frac{6EI_1 kN\cos^4\Theta_2}{a}\right] - 3\delta_{y2}\cos^2\Theta_2(2l-a)\right\}\right]$$

$$\Rightarrow \quad D_x = \left(\frac{A+B}{A}\right)\left(\delta x_1 \cos\theta_1 - \delta x_2 \cos\theta_2\right) -$$

$$- \left[\frac{\delta y_1 \sin\theta_1}{a^3+12EI_1kN\cos^3\theta_1} + \frac{\delta y_2 \sin\theta_2}{a^3+12EI_1kN\cos^3\theta_2}\right]\left[d(6al-6ld-3ad+4d^2)\right.$$

$$\left. + \left(\frac{I_1}{I_2}\right)(l-d)^2(3a-2l-4d)\right] - \left[\frac{\delta y_1 \sin\theta_1\cos^3\theta_1}{a^3+12EI_1kN\cos^3\theta_1} + \frac{\delta y_2 \sin\theta_2\cos^3\theta_2}{a^3+12EI_1kN\cos^3\theta_2}\right]\left[12EI_1(S\right.$$

$$\left. + kN)\right] + \left[\frac{\alpha_{z1}\tan\theta_1}{a^3+12EI_1kN\cos^3\theta_1} + \frac{\alpha_{z2}\tan\theta_2}{a^3+12EI_1kN\cos^3\theta_2}\right]\left[ad(2al-3ld-ad+2d^2\right.$$

$$\left. + \left(\frac{I_1}{I_2}\right)(l-d)^2(a-l-2d)\right] + \left[\frac{\alpha_{z1}\sin\theta_1\cos^2\theta_1}{a^3+12EI_1kN\cos^3\theta_1} + \frac{\alpha_{z2}\sin\theta_2\cos^2\theta_2}{a^3+12EI_1kN\cos^3\theta_2}\right]\left[-6EI_1Sa\right.$$

$$\left. + \frac{6EI_1kN}{a}\left[2ld-d^2-a^2+\left(\frac{I_1}{I_2}\right)(l-d)^2\right]\right]$$

$$+ \left[\frac{\delta y_1 m_1\cos\theta_1}{a^3+12EI_1kN\cos^3\theta_1} + \frac{\delta y_2 m_2\cos\theta_2}{a^3+12EI_1kN\cos^3\theta_2}\right]\left[6d(a-d)+6\left(\frac{I_1}{I_2}\right)(l-d)(a-l-d)\right]$$

$$- \left[\frac{\delta y_1 m_1\cos^2\theta_1}{a^3+12EI_1kN\cos^3\theta_1} + \frac{\delta y_2 m_2\cos^2\theta_2}{a^3+12EI_1kN\cos^3\theta_2}\right]\left[6EI_1T(2l-a)\right]$$

$$- \left[\frac{m_1\alpha_{z1}}{a^3+12EI_1kN\cos^3\theta_1} + \frac{m_2\alpha_{z2}}{a^3+12EI_1kN\cos^3\theta_2}\right]\left[ad(2a-3d)+a\left(\frac{I_1}{I_2}\right)(l-d)(2a-3l-3d)\right]$$

$$+ \left[\frac{m_1\alpha_{z1}\cos\theta_1}{a^3+12EI_1kN\cos^3\theta_1} + \frac{m_2\alpha_{z2}\cos\theta_2}{a^3+12EI_1kN\cos^3\theta_2}\right]\left[\frac{12EI_1kN}{a}\left(a+\left(\frac{I_1}{I_2}\right)(l-d)\right)\right]$$

$$+ \left[\frac{m_1\alpha_{z1}\cos^4\theta}{a^3+12EI_1kN\cos\theta_1} + \frac{m_2\alpha_{z2}\cos^4\theta_2}{a^3+12EI_1kN\cos\theta_2}\right]\left[\frac{12E^2I_1^2TkN}{a}\right]$$

Substituting for δ_x, δ_y etc.

$$D_x = \left(\frac{A+B}{A}\right)\Big[d_{x1}\cos^2\theta_1 - d_{x2}\cos^2\theta_2 + d_{y2}\sin\theta_1\cos\theta_1 + d_{y2}\sin\theta_2\cos\theta_2 + f\theta_{x1}\sin\theta_1\cos\theta_1$$

$$+ f\theta_{x2}\sin\theta_2\cos\theta_2 - f\theta_y\cos^2\theta_1 + f\theta_{y2}\cos^2\theta_2 - h_1\theta_{z1}\cos^2\theta_1 - h_2\theta_{z2}\cos^2\theta_2\Big]$$

$$-\Bigg[\frac{-d_{x1}\sin^2\theta_1 + d_{y1}\sin\theta_1\cos\theta_1 + f\theta_{x1}\sin\theta_1\cos\theta_1 + f\theta_{y1}\sin^2\theta_1 + h_1\theta_{z1}\sin^2\theta_1}{a^3 + 12EI_1kN\cos^3\theta_1}$$

$$+\frac{d_{x2}\sin^2\theta_2 + d_{y2}\sin\theta_2\cos\theta_2 + f\theta_{x2}\sin\theta_2\cos\theta_2 - f\theta_{y2}\sin^2\theta_2 + h_2\theta_{z2}\sin^2\theta_2}{a^3 + 12EI_1kN\cos^3\theta_2}\Bigg]\Big[d(6al - 6ld - 3ad$$

$$+4d^2) + \left(\frac{I_1}{I_2}\right)(l-d)^2(3a - 2l - 4d)\Big]$$

$$+\Bigg[\frac{-d_{x1}\sin^2\theta_1\cos^3\theta_1 + d_{y1}\sin\theta_1\cos^4\theta_1 + f\theta_{x1}\sin\theta_1\cos^4\theta_1 + f\theta_{y1}\sin^2\theta_1\cos^3\theta_1 + h_1\theta_{z1}\sin^2\theta_1\cos^3\theta_1}{a^3 + 12EI_1kN\cos^3\theta_1}$$

$$+\frac{d_{x2}\sin^2\theta_2\cos^3\theta_2 + d_{y2}\sin\theta_2\cos^4\theta_2 + f\theta_{x2}\sin\theta_2\cos^4\theta_2 - f\theta_{y2}\sin^2\theta_2\cos^3\theta_2 + h_2\theta_{z1}\sin^2\theta_2\cos^3\theta_2}{a^3 + 12EI_1kN\cos^3\theta_2}\Bigg]$$

$$\times\Big(12EI_1(kN + S)\Big)$$

$$-a\left[\frac{\gamma_{z1}\tan\theta_1}{a^3 + 12EI_1kN\cos^3\theta_1} + \frac{\gamma_{z2}\tan\theta_2}{a^3 + 12EI_1kN\cos^3\theta_2}\right]\left[d(2al - 3ld - ad + 2d^2) + \left(\frac{I_1}{I_2}\right)(l-d)(a-l-d)\right]$$

$$+\left[\frac{\gamma_{z1}\sin\theta_1\cos^2\theta_1}{a^3 + 12EI_1kN\cos^3\theta_1} + \frac{\gamma_{z2}\sin\theta_2\cos^2\theta_2}{a^3 + 12EI_1kN\cos^3\theta_2}\right]\left[-6EI_1Sa + \frac{6EI_1kN}{a}\left(2ld - d^2 - a^2 + \left(\frac{I_1}{I_2}\right)(l-d)^2\right)\right]$$

$$+\Bigg[\frac{-m_1d_{x1}\sin\theta_1\cos\theta_1 + m_1d_{y1}\cos^2\theta_1 + m_1f\gamma_{x1}\cos^2\theta_1 + m_1f\gamma_{y1}\sin\theta_1\cos\theta_1 + m_1h_1\gamma_{z1}\sin\theta_1\cos\theta_1}{a^3 + 12EI_1kN\cos^3\theta_1}$$

$$+\frac{m_2d_{x2}\sin\theta_2\cos\theta_2 + m_2d_{y2}\cos^2\theta_2 + m_1f\gamma_{x2}\cos^2\theta_2 \quad m_2f\gamma_{y2}\sin\theta_2\cos\theta_2 + m_2h_2\gamma_{z2}\sin\theta_2\cos\theta_2}{a^3 + 12EI_1kN\cos^3\theta_2}\Bigg]\Big[6a(a-d)$$

$$+6\left(\frac{I_1}{I_2}\right)(l-d)(a-l-d)\Big]$$

(continued on next page)

$$-\left[\frac{-m_1 d_{x1}\sin\Theta_1\cos^2\Theta_1 + m_1 d_{y1}\cos^3\Theta_1 + m_1 f\gamma_{x1}\cos^3\Theta_1 + m_1 f\gamma_{y1}\sin\Theta_1\cos^2\Theta_1 + h_1 m_1\gamma_{z1}\sin\Theta_1\cos^2\Theta_1}{a^3 + 12EI_1 kN\cos^3\Theta_1}\right.$$

$$\left.+\frac{m_2 d_{x2}\sin\Theta_2\cos^2\Theta_2 + m_2 d_{y2}\cos^3\Theta_2 + m_2 f\gamma_{x2}\cos^3\Theta_2 - m_2 f\gamma_{y2}\sin\Theta_2\cos^2\Theta_2 + h_2 m_2\gamma_{z2}\sin\Theta_2\cos^2\Theta_2}{a^3 + 12EI_1 kN\cos^3\Theta_2}\right]$$

$$\times\left[6EI_1 T(2l-a)\right] - \left[\frac{m_1\gamma_{z1}}{a^3+12EI_1 kN\cos^3\Theta_1} + \frac{m_2\gamma_{z2}}{a^3+12EI_1 kN\cos^3\Theta_2}\right]\left[ad(2a-3d) + \left(\frac{I_1}{I_2}\right)(l-d)(2a-3l-3d)\right]$$

$$+\left[\frac{m_1\gamma_{z1}\cos^3\Theta_1}{a^3+12EI_1 kN\cos^3\Theta_1} + \frac{m_2\gamma_{z2}\cos^3\Theta_2}{a^3+12EI_1 kN\cos^3\Theta_2}\right]\left[\frac{12EI_1 kN}{a}\left(a + \left(\frac{I_1}{I_2}\right)(l-d)\right)\right]$$

$$+\left[\frac{m_1\gamma_{z1}\cos\Theta_1}{a^3+12EI_1 kN\cos^3\Theta_1} + \frac{m_2\gamma_{z2}\cos^3\Theta_2}{a^3+12EI_1 kN\cos^3\Theta_2}\right]\left[2EI_1 Ta(3l-a)\right]$$

$$+\left[\frac{m_1\gamma_{z1}\cos^4\Theta_1}{a^3+12EI_1 kN\cos^3\Theta_1} + \frac{m_2\gamma_{z2}\cos\Theta_2}{a^3+12EI_1 kN\cos^3\Theta_1}\right]\left[\frac{12E^2I_1^2 kNT}{a}\right]$$

If $\theta_1 = \theta_2 = \theta$ and $d_x = d_{x1} - d_{x2}$ etc. then

$$D_x = \left(\frac{A+B}{A}\right)\Big[d_x\cos^2\theta + (d_{y1}+d_{y2})\sin\theta\cos\theta + f(\gamma_{x1}+\gamma_{x2})\sin\theta\cos\theta - f\gamma_y\cos^2\theta - (h_1\gamma_{z1}+h_2\gamma_{z2})\cos^2\theta\Big]$$

$$- \left[\frac{-d_x\sin^2\theta + (d_{y1}+d_{y2})\sin\theta\cos\theta + f(\gamma_{x1}+\gamma_{x2})\sin\theta\cos\theta + f\gamma_y\sin^2\theta + (h_1\gamma_{z1}+h_2\gamma_{z2})\sin^2\theta}{a^3 + 12EI_1kN\cos^3\theta}\right]\Big[d(6al$$

$$- 6ld - 3ad + 4d^2) + \left(\frac{I_1}{I_2}\right)(l-d)^2(3a-2l-4d) - 12EI_1(kN+S)\cos^2\theta\Big]$$

$$- \left[\frac{(\gamma_{z1}+\gamma_{z2})}{a^3 + 12EI_1kN\cos^3\theta}\right]\Big[\tan\theta.\, ad(2al-3ld-ad+2d^2) + \left(\frac{I_1}{I_2}\right)(l-d)^2(a-l-d)a\tan\theta$$

$$+ 6EI_1Sa\sin\theta\cos\theta + \frac{6EI_1kN\sin\theta\cos\theta}{a}\left(2ld - d^2 - a^2 + \left(\frac{I_1}{I_2}\right)(l-d)\right)\Big]$$

$$+ \Bigg[\frac{(-m_1d_{x1}+m_2d_{x2})\sin\theta\cos\theta + (m_1d_{y1}+m_2d_{y2})\cos^2\theta + f(m_1\gamma_{x1}+m_2\gamma_{x2})\cos^2\theta}{a^3 + 12EI_1kN\cos^3\theta}$$

$$+ \frac{f(m_1\gamma_{y1} - m_2\gamma_{y2})\sin\theta\cos\theta + (m_1h_1\gamma_{z1} + m_2h_2\gamma_{z2})\sin\theta\cos\theta}{a^3 + 12EI_1kN\cos^3\theta}\Bigg]\Big[6a(a-d)$$

$$+ 6\left(\frac{I_1}{I_2}\right)(l-d)(a-l-d) - 6EI_1T(2l-a)\cos\theta\Big] - \left[\frac{m_1\gamma_{z1} + m_2\gamma_{z2}}{a^3 + 12EI_1kN\cos^3\theta}\right]\Big[ad(2a-3d)$$

$$+ a\left(\frac{I_1}{I_2}\right)(l-d)(2a-3l-3d) - \frac{12EI_1kN\cos^3\theta}{a}\left(a + \left(\frac{I_1}{I_2}\right)(l-d)\right) - 2EI_1T(3l-a)\cos\theta$$

$$- \frac{12E^2I_1^2TkN\cos^4\theta}{a}\Big] \qquad (4.2.45)$$

If $\theta_1 = \theta_2 = 0$ then

$$D_x = \left(\frac{A+B}{A}\right)\Big[d_x - f\gamma_y - (h_1\gamma_{z1} + h_2\gamma_{z2})\Big]$$

$$+ \left[\frac{(m_1d_{y1} + m_2d_{y2}) + f(m_1\gamma_{x1} + m_2\gamma_{x2})}{a^3 + 12EI_1kN}\right]\Big[6a(a-d) + 6\left(\frac{I_1}{I_2}\right)(l-d)(a-l-d) - 6EI_1T(2l-a)\Big]$$

$$- \left[\frac{m_1\gamma_{x1} + m_2\gamma_{x2}}{a^3 + 12EI_1kN}\right]\Big[ad(2a-3d) + a\left(\frac{I_1}{I_2}\right)(l-d)(2a-3l-3d) - \frac{12EI_1kN}{a}\left(a + \left(\frac{I_1}{I_2}\right)(l-d)\right)$$

$$- 2EI_1Ta(3l-a) - \frac{12E^2I_1^2kNT}{a}\Big] \qquad (4.2.46)$$

From equation 4.2.25

$D_Y = \Delta_{x1}\sin\theta_1 + \Delta_{x2}\sin\theta_2 + \Delta_{y1}\cos\theta_1 - \Delta_{y2}\cos\theta_2 + t(\beta_{z1} - \beta_{z2})$

And by similar calculations

When $\theta_1 = \theta_2 = \theta$

$$D_y = \left(\frac{A+B}{A}\right)\Big[(d_{x1}+d_{x2})\sin\theta\cos\theta + d_y\sin^2\theta + f\gamma_x\sin^2\theta - f(\gamma_{y1}+\gamma_{y2})\sin\theta\cos\theta - (h_1\gamma_{z1} - h_2\gamma_{z2})\sin\theta\cos\theta\Big]$$

$$\left[\frac{-(d_{x1}+d_{x2})\sin\theta\cos\theta + d_y\cos^2\theta + f\gamma_x\cos^2\theta + f(\gamma_{y1}+\gamma_{y2})\sin\theta\cos\theta + (h_1\gamma_{z1}-h_2\gamma_{z2})\sin\theta\cos\theta}{a^3 + 12EI_1 kN\cos^3\theta}\right]$$

$$\times\Big[d(6al - 6ld - 3ad + 4d^2) + \left(\frac{I_1}{I_2}\right)(l-d)(3a-2l-4d) + 6t\left(\frac{I_1}{I_2}\right)(l-d)(a-l-d) + 6td(a-d) - 6EI_1T\cos\theta(2l-a) + 12EI_1(S+kN)\cos^3\theta\Big]$$

$$-\frac{\gamma_z}{a^3 + 12EI_1kN\cos^3\theta}\Big[ad(2al-3ld-ad+2d^2) + a\left(\frac{I_1}{I_2}\right)(l-d)^2(a-l-2d) + at\left(\frac{I_1}{I_2}\right)(l-d)(2a-3l-3d) + adt(2a-3d) - 2EI_1Tat(3l-a)\cos\theta + 6EI_1\cos^3\theta\left[Sa - \frac{kN}{a}\left(2ld - a^2 - d^2 + \left(\frac{I_1}{I_2}\right)(l-d)\right)\right]$$

$$+\frac{12E^2I_1^2kNT\cos^4\theta}{a} + \frac{12EIkNt\cos^3\theta}{a}\left\{d + \left(\frac{I_1}{I_2}\right)(l-d)\right\}\Big] \qquad (4.2.47)$$

And when $\theta_1 = \theta_2 = 0$

$$D_y = \left[\frac{d_Y + f\gamma_x}{a^3 + 12EI_1kN}\right]\Big[d(6al - 6ld - 3ad + 4d^2) + \left(\frac{I_1}{I_2}\right)(l-d)^2(3a-2l-4d) + 6dt(a-d) + 6t\left(\frac{I_1}{I_2}\right)(l-d)(a-l-d) - 6EI_1T(2l-a)t + 12EI_1(S+kN)\Big]$$

$$-\left[\frac{\gamma_z}{a^3+12EI_1kN}\right]\Big[ad(2al-3ld-ad+2d^2) + a\left(\frac{I_1}{I_2}\right)(l-d)^2(a-l-2d) + adt(2a-3d) + at\left(\frac{I_1}{I_2}\right)(l-d)(2a-3l-3d) - 2EI_1Tat(3l-a) + 6EI_1\left[Sa - \frac{kN}{a}\left\{2ld - a^2 - d^2 + \left(\frac{I_1}{I_2}\right)(l-d)^2\right\}\right]$$

$$+\frac{12E^2I_1^2kNTt}{a} + \frac{12EIkNt}{a}\left\{d + \left(\frac{I_1}{I_2}\right)(l-d)\right\}\Big] \qquad (4.2.48)$$

From 4.2.25

$$D_Z = \Delta_{z1} - \Delta_{z2} + t(-\beta_{x1}\sin\theta_1 - \beta_{x2}\sin\theta_2 - \beta_{y1}\cos\theta_1 + \beta_{y2}\cos\theta_2)$$
$$+m_1(-\beta_{x1}\cos\theta_1 + \beta_{y1}\sin\theta_1) - m_2(\beta_{x2}\cos\theta_2 + \beta_{y2}\sin\theta_2)$$

By similar calculations to those for D_X

When $\theta_1 = \theta_2 = \theta$

$$D_z = \left[\frac{dz + h_1\gamma_{x1} + h_2\gamma_{x2}}{a^3}\right]\left[d(6al - 6ld - 3ad + 4d^2) + \left(\frac{I_1}{I_2}\right)(l-d)^2(3a - 2l - 4d)\right.$$
$$\left. -6\left(\frac{I_1}{I_2}\right)(l-d)(a-l-d)\cos^2\theta - 6d(a-d)\cos^2\theta + 12EI_1U\cos^3\theta + 6EI_1V(2l-a)t\cos^3\theta\right]$$
$$+\left[\frac{(m_1 dz_1 - m_2 dz_2)\sin\theta\cos\theta + (m_1h_1\gamma_{x1} + m_2h_2\gamma_{x2})\sin\theta\cos\theta}{a^3}\right]\left[6\left(\frac{I_1}{I_2}\right)(l-d)(a-l-d)\right.$$
$$\left. +6d(a-d) + 6EI_1V(2l-a)\cos\theta\right] - \left[\frac{-(\gamma_{x1}+\gamma_{x2})\tan\theta + \gamma_y}{a}\right]\left[d(2al - 3ld - ad + 2d^2)\right.$$
$$+\left(\frac{I_1}{I_2}\right)(l-d)^2(a-l-2d) - 6EI_1U\cos^3\theta + 2EI_1V(3l-a)t\cos\theta + dt(2a-3d)\cos^2\theta$$
$$\left. +\left(\frac{I_1}{I_2}\right)(l-d)(2a-3l-3d)t\cos^2\theta\right]$$
$$+\left[\frac{-(m_1\gamma_{x1} + m_2\gamma_{x2})\sin^2\theta + (m_1\gamma_{y1} - m_2\gamma_{y2})\sin\theta\cos\theta}{a^2}\right] 2EI_1V(3l-a).$$
$$-\left[(m_1\gamma_{x1} + m_2\gamma_{x2})\cos^2\theta + (m_1\gamma_{y1} - m_2\gamma_{y2} + t\gamma_{x1} + \gamma_{x2})\sin\theta\cos\theta + t\gamma_y\sin^2\theta\right]\left[\frac{d}{GJ_1} + \frac{(l-d)}{GJ_2}\right.$$
$$\left. +(Q+R)\cos\theta\right]\left[\frac{GJ_1}{RGJ_1\cos\theta + a}\right] \qquad (4.2.49)$$

And When $\theta_1 = \theta_2 = 0$

$$D_z = \left[\frac{dz + h_1\gamma_{x1} + h_2\gamma_{x2}}{a^3}\right]\left[d(6al - 6ld - 3ad + 4d^2) + \left(\frac{I_1}{I_2}\right)(l-d)^2(3a - 2l - 4d) - 6dt(a-d)\right.$$
$$\left. -6t\left(\frac{I_1}{I_2}\right)(l-d)(a-l-d) + 12EI_1U + 12EI_1V(2l-a)t\right] - \left(\frac{\gamma_y}{a^2}\right)\left[d(2al - 3ld - ad + 2d^2)\right.$$
$$\left. +\left(\frac{I_1}{I_2}\right)(l-d)^2(a-l-2d) - 6EI_1U + 2EI_1Vt(3l-a) + \left(\frac{I_1}{I_2}\right)(l-d)(2a-3l-3d)t + dt(2a-3d)\right]$$
$$-(m_1\gamma_{x1} + m_2\gamma_{x2})\left[\frac{d}{GJ_1} + \frac{(l-d)}{GJ_2} + Q + R\right]\left[\frac{GJ_1}{RGJ_1 + a}\right] \qquad (4.2.50)$$

And

$$\phi_X = \beta_{x1}\cos\theta_1 - \beta_{x2}\cos\theta_2 - \beta_{y1}\sin\theta_1 - \beta_{y2}\sin\theta_2$$

When $\theta_1 = \theta_2 = \theta$

$$\phi_x = \left(\gamma_x\cos\theta + (\gamma_{y1}+\gamma_{y2})\sin\theta\right)\left[\frac{d}{GJ_1} + \frac{l-d}{GJ_2} + (Q+R)\cos\theta\right]\left[\frac{GJ_1\cos\theta}{RGJ_1\cos\theta + a}\right]$$
$$-\left[\frac{(dz_1+dz_2+(h_1\gamma_{x1}-h_2\gamma_{x2}))\sin\theta\cos\theta}{a^3}\right]\left[6\left(\frac{I_1}{I_2}\right)(l-d)(a-l-d)-6(a-d)-6EI_1V(2l-a)\cos\theta\right]$$
$$-\left[\frac{\gamma_x\sin^2\theta-(\gamma_{y1}+\gamma_{y2})\sin\theta\cos\theta}{a^2}\right]\left[\left(\frac{I_1}{I_2}\right)(l-d)(2a-3l-3d)+d(2a-3d)+2EI_1V(3l-a)\cos\theta\right]$$

(4.2.51)

And when $\theta_1 = \theta_2 = 0$

$$\phi_x = \gamma_x\left[\frac{d}{GJ_1} + \frac{l-d}{GJ_2} + Q + R\right]\left[\frac{GJ_1}{RGJ_1 + a}\right] \tag{4.2.52}$$

And

$$\phi_Y = \beta_{x1}\sin\theta_1 + \beta_{x2}\sin\theta_2 + \beta_{y1}\cos\theta_1 - \beta_{y1}\cos\theta_2$$

When $\theta_1 = \theta_2 = \theta$

$$\phi_y = \left[(\gamma_{x1}+\gamma_{x2})\sin\theta + \gamma_y\sin\theta\tan\theta\right]\left[\frac{d}{GJ_1} + \frac{l-d}{GJ_2} + (Q+R)\cos\theta\right]\left[\frac{GJ_1\cos\theta}{RGJ_1\cos\theta + a}\right]$$
$$+\left[\frac{dz\cos^2\theta + (h_1\gamma_{x1}+h_2\gamma_{x2})\cos^2\theta}{a^3}\right]\left[6\left(\frac{I_1}{I_2}\right)(l-d)(a-l-d)+6d(a-d)-6EI_1V(2l-a)\cos\theta\right]$$
$$-\left[\frac{\gamma_y\cos^2\theta-(\gamma_{x1}+\gamma_{x2})\sin\theta\cos\theta}{a^2}\right]\left[\left(\frac{I_1}{I_2}\right)(l-d)(2a-3l-3d)+d(2a-3d)+2EI_1V(3l-a)\cos\theta\right]$$

(4.2.53)

When $\theta_1 = \theta_2 = 0$

$$\phi_y = \left[\frac{dz + h_1\gamma_{x1}+h_2\gamma_{x2}}{a^3}\right]\left[6\left(\frac{I_1}{I_2}\right)(l-d)(a-l-d)+6d(a-d)-6EI_1V(2l-a)\cos\theta\right]$$
$$-\left(\frac{\gamma_y}{a^2}\right)\left[\left(\frac{I_1}{I_2}\right)(l-d)(2a-3l-3d)+d(2a-3d)-2EI_1V(3l-a)\right] \tag{4.2.54}$$

Finally

$\phi_z = \beta_{z1} - \beta_{z2}$

When $\theta_1 = \theta_2 = \theta$

$$\phi_z = \left[\frac{-(d_{x1}+d_{x2})\sin\theta\cos\theta + d_y\cos^2\theta + f\gamma_x\cos^2\theta + f(\gamma_{y1}+\gamma_{y2})\sin\theta\cos\theta}{a^3+12EI_1kN\cos^3\theta}\right.$$

$$\left.+\frac{(h_1\gamma_{z1}-h_2\gamma_{z2})\sin\theta\cos\theta}{a^3+12EI_1kN\cos^3\theta}\right]\left[6a(a-d)+6\left(\frac{I_1}{I_2}\right)(l-d)(a-l-d)-6EI_1T(2l-a)\cos\theta\right]$$

$$+\left[\frac{\gamma_z}{a^3+12EI_1kN\cos^3\theta}\right]\left[-ad(2a-3d)-a\left(\frac{I_1}{I_2}\right)(l-d)(2a-3l-3d)+2EI_1Ta(3l-a)\cos\theta\right.$$

$$\left.+\frac{12EI_1kN\cos^3\theta}{a}\left\{d+\left(\frac{I_1}{I_2}\right)(l-d)\right\}+\frac{12E^2I_1^2kNT\cos^4\theta}{a}\right] \qquad (4.2.55)$$

If $\theta_1 = \theta_2 = 0$

$$\phi_z = \left[\frac{d_y+f\gamma_x}{a^3+12EI_1kN}\right]\left[6a(a-d)+\left(\frac{I_1}{I_2}\right)(l-d)(a-l-d)-6EI_1T(2l-a)\right]$$

$$+\frac{\gamma_z}{a^3+12EI_1kN}\left[-ad(2a-3d)-a\left(\frac{I_1}{I_2}\right)(l-d)(2a-3l-3d)+2EI_1Ta(3l-a)\right.$$

$$\left.+\frac{12EI_1kN}{a}\left\{d+\left(\frac{I_1}{I_2}\right)(l-d)\right\}+\frac{12E^2I_1^2kNT}{a}\right] \qquad (4.2.56)$$

These are the equations which are used in the appropiate points in the programs LTRANS, LTRFOR, LINCA2 etc..

4.2(ii) Without the Fixator Support Bar

If the fixator support bar is removed, the pins are free to move without bending or displacing, and the relationship between the transducer movements and the fracture movements depends entirely upon the geometrical offsets from the fracture to the transducer. The problem becomes that of the relative movement between two bodies. The axes are the same as those in the previous section, i.e. the X axis is perpendicular to the long axis of the bone in the plane of the pins and pointing towards the bone, the Y axis is directed along the long axis of the bone pointing in the proximal direction and the Z forms the third axis of the orthogonal system as in section 4.2(i). In Figure 4.2.7, the fixator is on the anterio-medial aspect of the left tibia/right femur with the transducer anterior to the pins. The displacement at the fracture is $(\mathbf{D_1D_2}) = D_x\underline{i} + D_y\underline{j} + D_z\underline{k}$,the measured displacement $(\mathbf{A_1A_2}) = d_x\underline{i} + d_y\underline{j} + d_z\underline{k}$ and the measured small angulations at A are $\theta_x\underline{i} + \theta_y\underline{j} + \theta_z\underline{k}$ where θ_x is the rotation about the x axis in the y-z plane, similarly for θ_y and θ_z. In this case,

$D_x\underline{i} + D_y\underline{j} + D_z\underline{k}$

$$= d_x\underline{i} + d_y\underline{j} + d_z\underline{k} + (\theta_x\underline{i} + \theta_y\underline{j} + \theta_z\underline{k}) \wedge ((c+t)\underline{i} - f\underline{k})$$

$$= (d_x - f\theta_y)\underline{i} + (d_y + f\theta_x + (c+t)\theta_z)\underline{j} + (d_z - (c+t)\theta_y)\underline{k} \quad (4.2.58)$$

Since the rotation of every point in a rigid body is the same then

$$\phi_x = \theta_x$$
$$\phi_y = \theta_y$$
$$\phi_z = \theta_z$$

where ϕ_x, ϕ_y and ϕ_z are the angulations at the fracture site corresponding to θ_x, θ_y and θ_z at A.

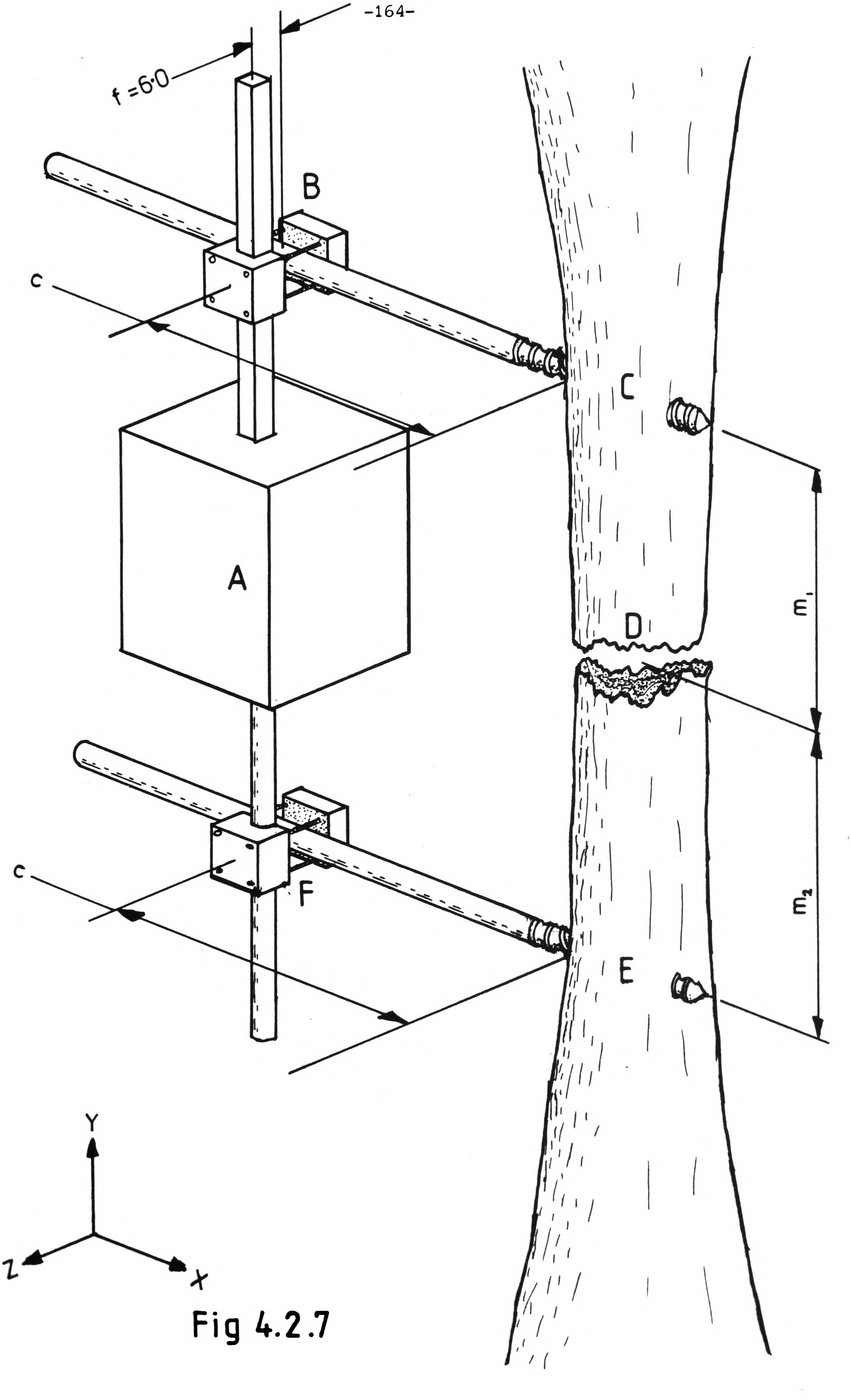

Fig 4.2.7

If the fixator is on the right tibia/left femur then f is in the negative z direction, and the same calculations may be used but with f negative (Figure 4.2.8).

The applications of the calculations in sections 4.1, 4.2(i) and 4.2(ii) are further discussed in section 6.1, Data Processing.

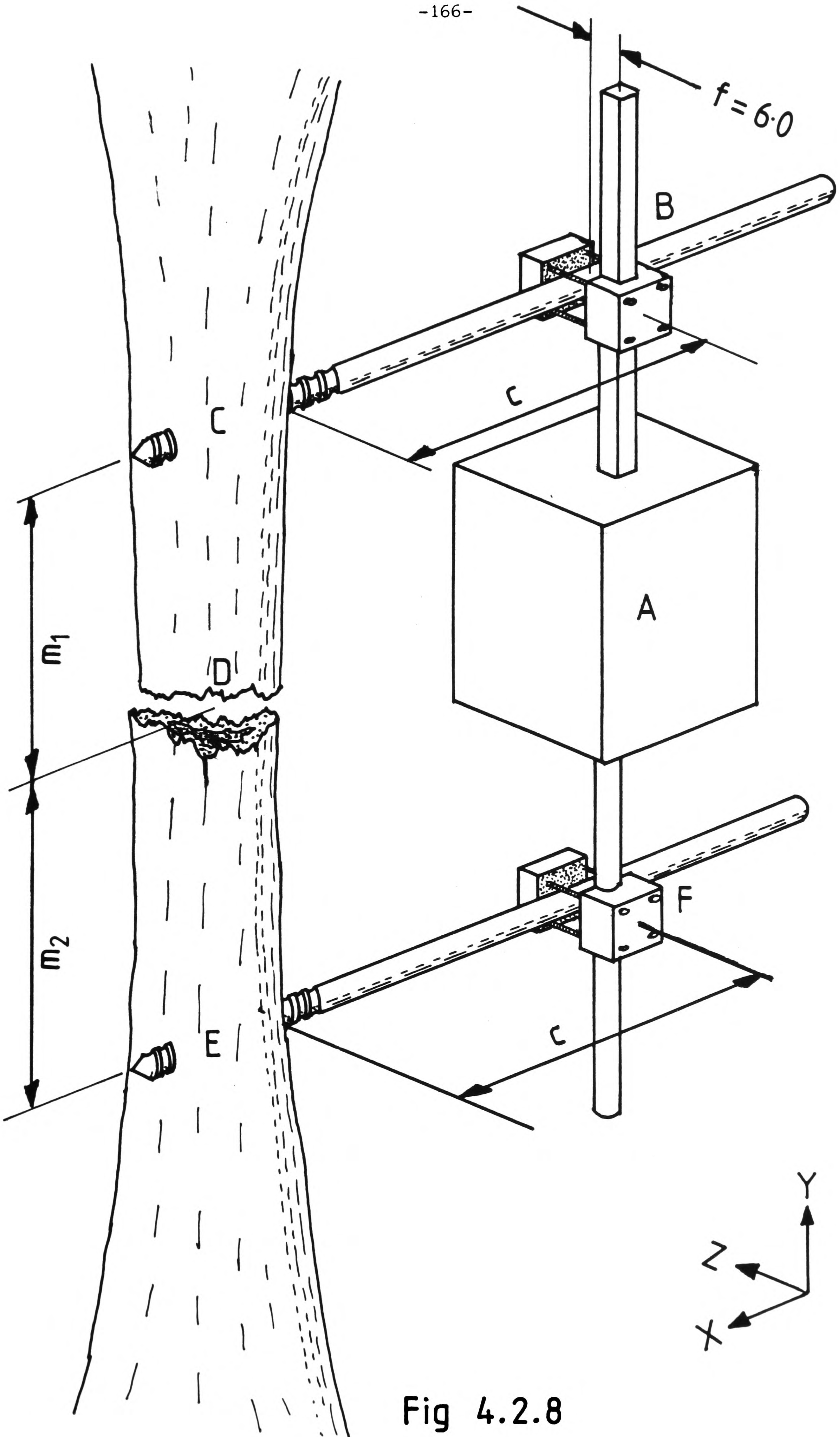

Fig 4.2.8

4.3 Mechanical Analysis of the Fixator

The initial analysis of the Oxford External Fixator was by Evans et al (1979). This just considered loading in the axial direction for the case with all the pins parallel. This assumed that the pin-bone and pin-clamp connections were absolutely rigid, and made various assumptions about symmetry. The forces in the various parts of the fixator were calculated. Once the forces and moments had been calculated, the experimentally determined relaxations were reinserted in the system and the displacement and angulation were calculated. Two errors were made in this publication; a) the axial load in each pin was stated to be FL/B where F was applied load, L the pin length and B the pin separation, whereas it should be FL/2B; b) in the first figure of that paper the bending moments at each end of the pins have been drawn in opposing directions whereas they should be in the same direction as shown in Figure 4.3.1.

Tanner (1979) performed an experimental study of the effect of non-parallel pins on the Oxford fixator, inserting the pins at angles of 10, 20 and 30° to the normal to the bone in the plane of the fixator. The distance between where the pins entered the bone substitute was kept as one of the constants. When the angulation of the pins was such that the distance between the fixator clamps was increased then the axial stiffness was increased, and when clamp separation was decreased then the axial stiffness was similarly decreased. There have been many other solely experimental studies of fixator stiffnesses and methods of increasing these particularly from the A.O. group for example (Egker et al, 1980).

Churches et al (1985a,b) extended, and corrected, the work of

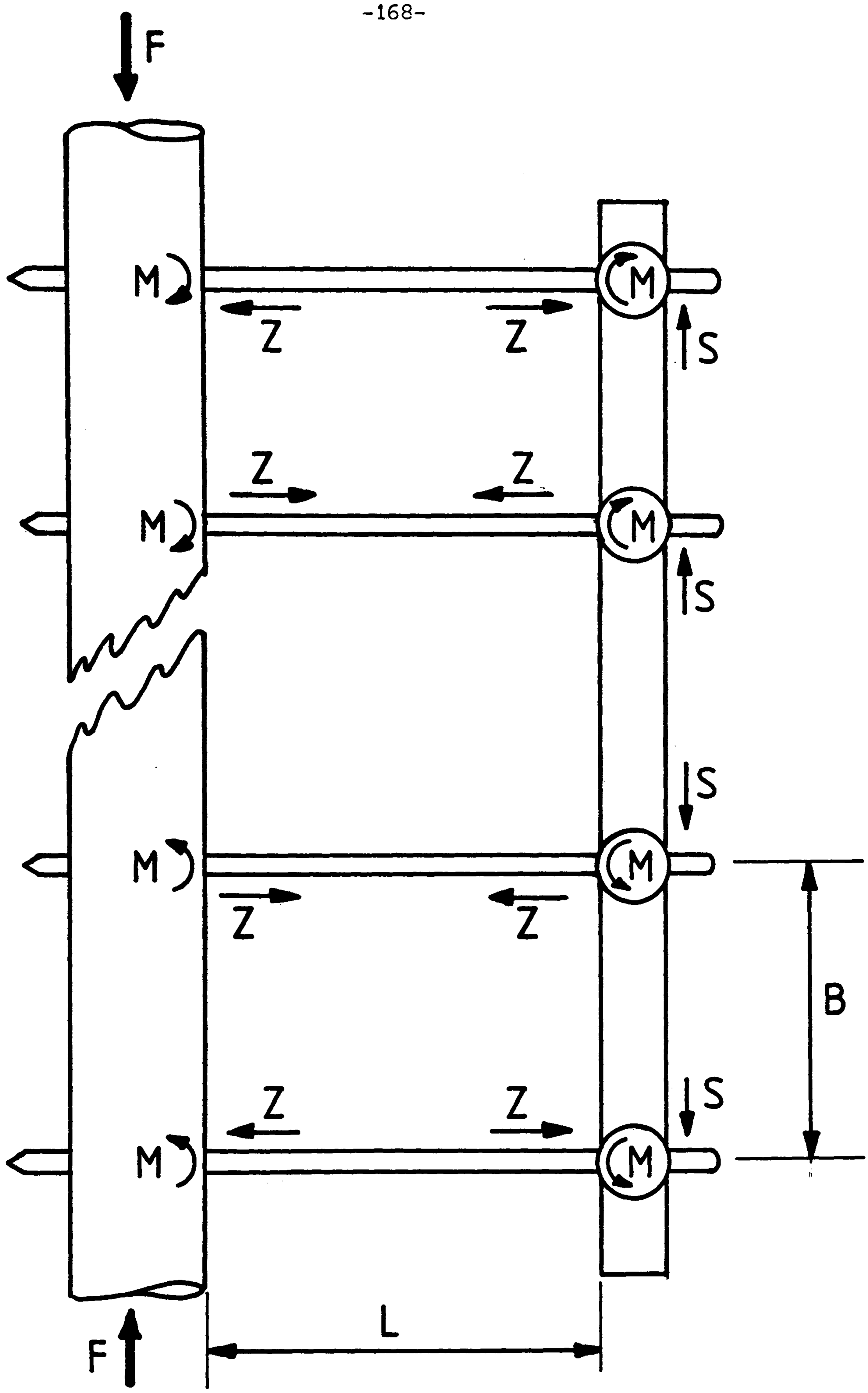

$$Z = \frac{FL}{2B} \qquad S = \frac{F}{2} \qquad M = \frac{FL}{4}$$

Fig 4.3.1

Evans et al (1979), and considered not only the axial stiffness but also the torsional and the two perpendicular bending stiffnesses. This analysis used a similar simple approach to that of Evans et al of estimating the forces in the various parts of the fixator, and then considering how they would deform under these loads. If this is done for example with a fixator with pin separation of 33 mm and pin length of 55 mm then the calculated stiffness was 917 Nmm^{-1} for all pins tight, compared with an experimental stiffness of 129 Nmm^{-1}.

Another method considered was that of using standard formula (Roach and Young, 1975) for various combinations of tight and loose pins. The fixator can be modelled by two portal frames with equal and opposite loads and moments applied as shown in Figure 4.3.2. This method has an advantage over the previous method as the finite width of the support bar can be accounted for by applying the load at the ends of the pins, and a bending moment produced by the offset of the load by one half of the width of the support bar. Once the loads had been calculated the deflections were found from standard deflection theory (Todd, 1974). Thus from Figure 4.3.3

$$C_{HH} = \left(\frac{2l_1^3}{3EI_1}\right) + \left(\frac{l_1^2 l_3}{2EI_3}\right) = 2.665\ 10^3$$

$$C_{HV} = C_{VH} = \left(\frac{l_1^2 l_3}{2EI_1}\right) + \left(\frac{l_1 l_3^2}{3EI_3}\right) = 1.041\ 10^3$$

$$C_{HM} = C_{MH} = \left(\frac{l_1^2}{EI_1}\right) + \left(\frac{l_1 l_3}{EI_3}\right) = 63.10$$

$$C_{VV} = \left(\frac{l_1 l_3^2}{EI_1}\right) + \left(\frac{l_3^3}{3EI_3}\right) = 1.0882\ 10^3$$

$$C_{VM} = C_{MV} = \left(\frac{l_1 l_3}{EI_1}\right) + \left(\frac{l_3^2}{2EI_3}\right) = 32.86$$

$$C_{MM} = \left(\frac{2l_1}{EI_1}\right) + \left(\frac{l_3}{EI_3}\right) = 1.992 \qquad (4.3.1)$$

These are the stiffness factors and for a framework built in at each end $\delta_{HA} = \delta_{VA} = \theta_A = 0$ and the relation between the stiffness

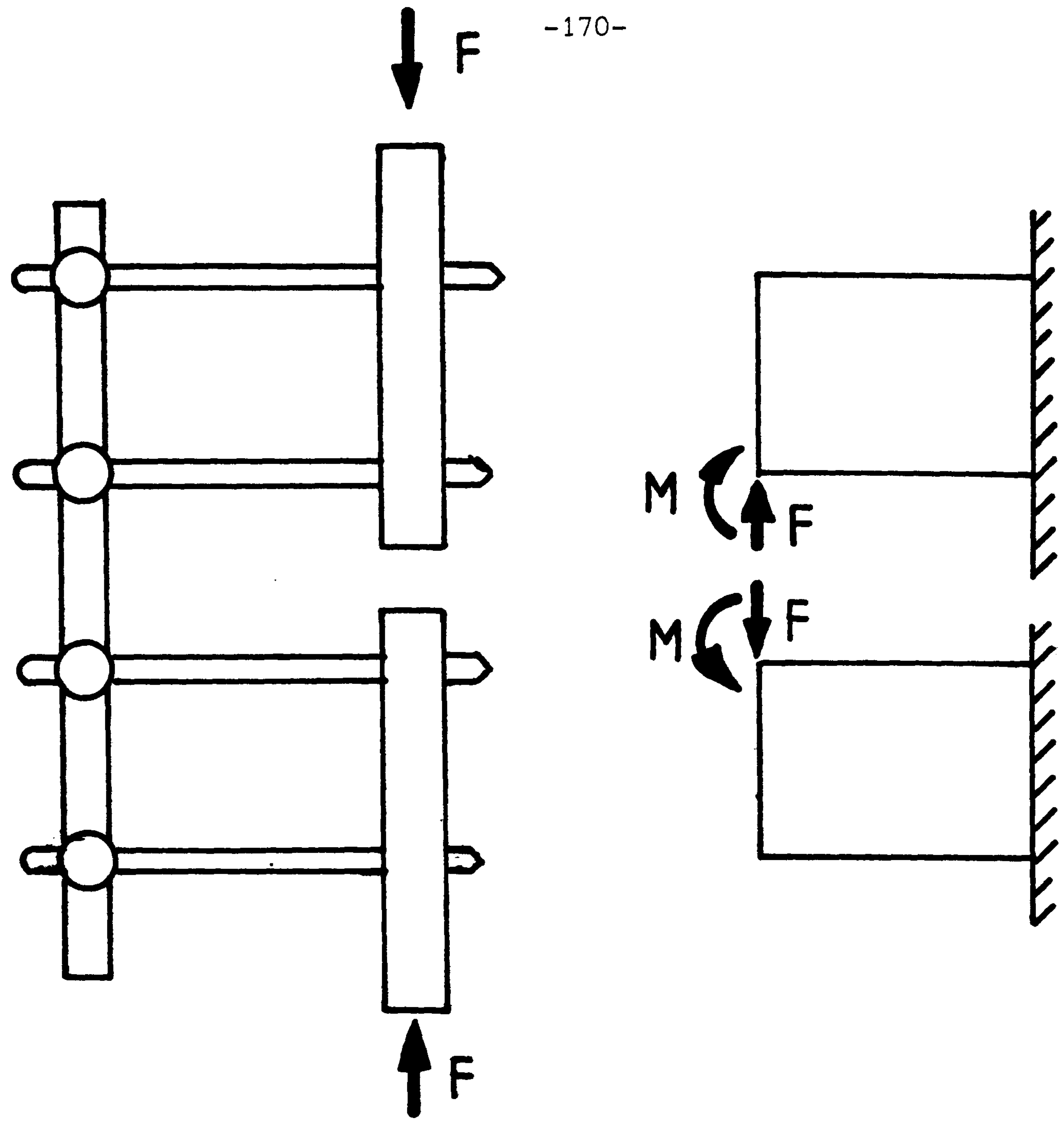

Fig 4.3.2

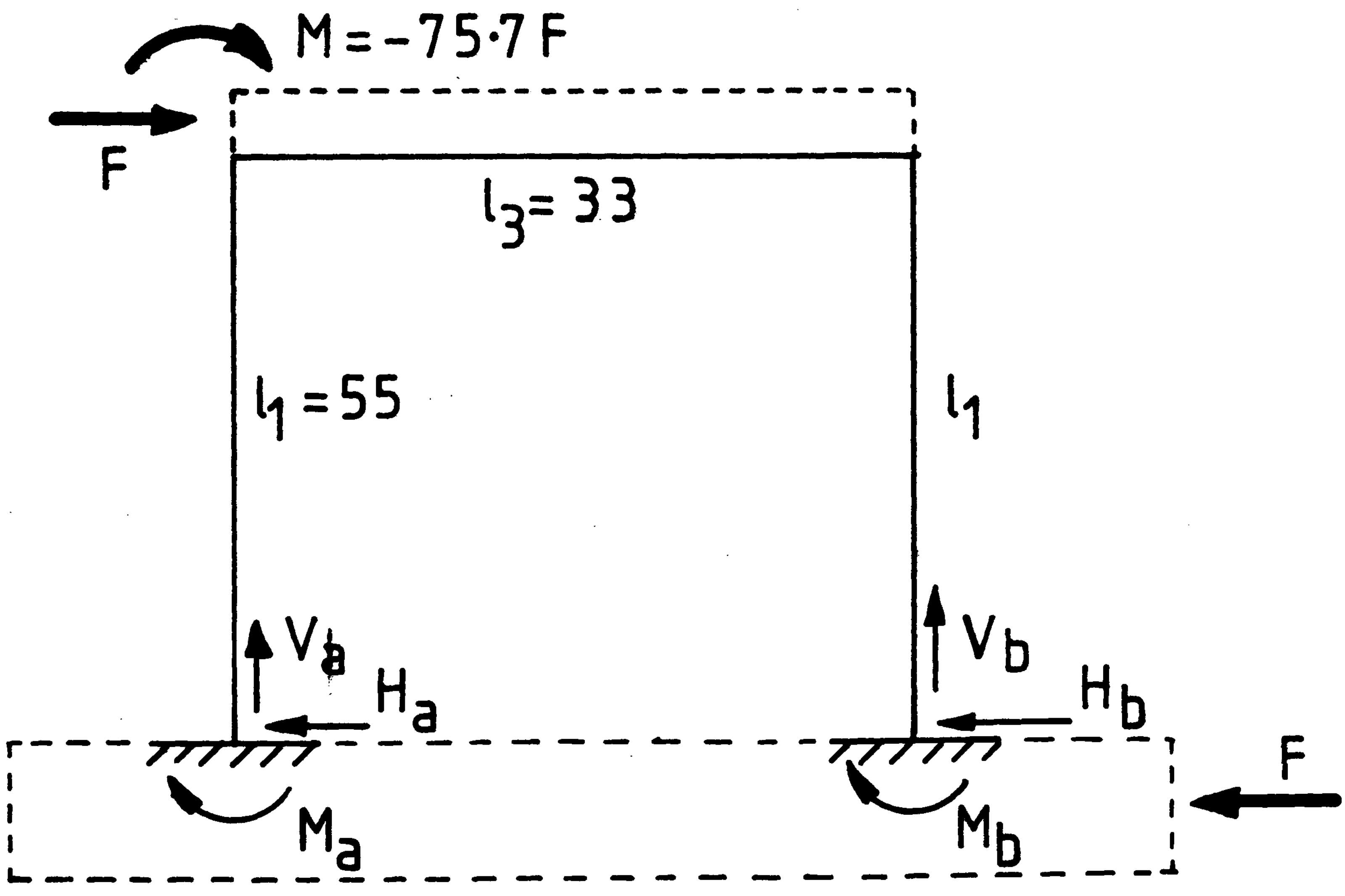

Fig 4.3.3

factors and the reactions at the point are given by

$$\begin{bmatrix} C_{HH} & C_{HV} & C_{HM} \\ C_{VH} & C_{VV} & C_{VM} \\ C_{MH} & C_{MV} & C_{MM} \end{bmatrix} \begin{bmatrix} H_A \\ V_A \\ M_A \end{bmatrix} = \begin{bmatrix} LF_H \\ LF_V \\ LF_M \end{bmatrix} \tag{4.3.2}$$

and for the loading conditions appropriate for this case

$$\begin{aligned} LF_H &= M_0\left[\frac{-l_1^2}{2EI_1} - \frac{l_1 l_2}{EI_3} \right] + W\left[C_{HH} - l_1 C_{HM} + \frac{l_1^3}{6EI_1} \right] \\ LF_V &= M_0\left[-C_{VM} \right] + W\left[C_{VH} - l_1 C_{VM} \right] \\ LF_M &= M_0\left[\frac{-l_1}{EI_1} - \frac{l_3}{EI_3} \right] + W\left[C_{MH} - l_1 C_{MM} + \frac{l_1^2}{2EI_1} \right] \end{aligned} \tag{4.3.3}$$

and with $M_0 = -75.7\ F$

$W = F$

gives

$$\begin{aligned} LF_H &= 1.759\ 10^3 \\ LF_V &= 1.456\ 10^3 \\ LF_M &= 44.61 \end{aligned} \tag{4.3.4}$$

And applying Cramer's Rule for the solution of simultaneous equations:

$$\begin{aligned} H_A &= 0.5190\ F \\ V_A &= 1.334\ F \\ M_A &= -16.05\ F \end{aligned} \tag{4.3.5}$$

Giving from conditions of equilibrium

$$\begin{aligned} H_B &= 0.481\ F \\ V_B &= -1.334\ F \\ M_B &= -15.27\ F \end{aligned} \tag{4.3.6}$$

giving $k = 1351\ Nmm^{-1}$ for half the fixator or for the whole fixator an axial stiffness of $676\ Nmm^{-1}$. This is less stiff than that produced by estimates of the forces solely, but as discussed in Churches et al (1985a) the experimentally determined stiffness is 129 Nmm^{-1}.

The other approach to the mechanical analysis of external fixators, and the only one applicable to double sided fixators due to their high degree of structural redundancy, is finite element analysis. This has been used by Chao and his colleagues. Their initial work (Chao et al, 1979) used the ANSYS STIF3 program developed by Swanson Analysis Systems Incorporated; this is a two dimensional program. They assumed absolute rotational rigidity at the clamps and their theoretical results were 40% higher than their experimental results. However, their papers in 1982 (Chao et al, 1982; Briggs and Chao, 1982) included three-dimensional analysis and significant flexibilities at the clamps. These corrections gave good correlations between the experimental and theoretical results and permitted the use of the finite element analysis for considering the effect of replacing various stainless steel components of the fixator by titanium.

Thus due to the complexity of the finite element analyses the stiffnesses of the fixators used on the various patients will be estimated from the graphs given in Churches et al (1985a,b,c). These sitffnesses will be needed to estimate the stiffnesses of the fractures from the readings obtained from both the movement transducer and the strain gauge transducer.

4.4 Fixator loading systems

As discussed in the work of Churches et al (1985b,c) the transducer readings are dependent on the relative stiffnesses of the fracture fixator system, and the loading applied. In the patient tests two different loading systems were applied. The first, consists of axial loading along the line of the fractured bone, and the second, of applying two opposing bending moments at the fracture site in a "straight leg raise". These approaches will be considered separately.

i) Axial Loading

Figure 4.4.1 shows a force F applied to the fracture fixator system, so that F_{fix}, the fixator force, passes through the fixator, and F_{fr} passes through the fracture.

Thus $$F = F_{fix} + F_{fr} \qquad (4.4.1)$$

If k_{fix} and k_{fr} are the stiffnesses of the fixator and fracture respectively, then k, the total stiffness, is

$$k = k_{fix} + k_{fr} \qquad (4.4.2)$$

and $$F_{FR}/F_{FIX} = k_{fr}/k_{fix} \qquad (4.4.3)$$

The force through the fixator produces bending moments in the fixator support bar,

$$M_1 = F_{fix}\, g \qquad\qquad M_2 = F_{fix}\, l^* \qquad (4.4.4)$$

where g is the distance along the z axis from the centre of the cross section of the support bar to the centre line of the pin, and l^* is the distance along the x axis from the line of action of the applied force, that is the centre of the bone, and the centre of that part of the pin held in the clamp.

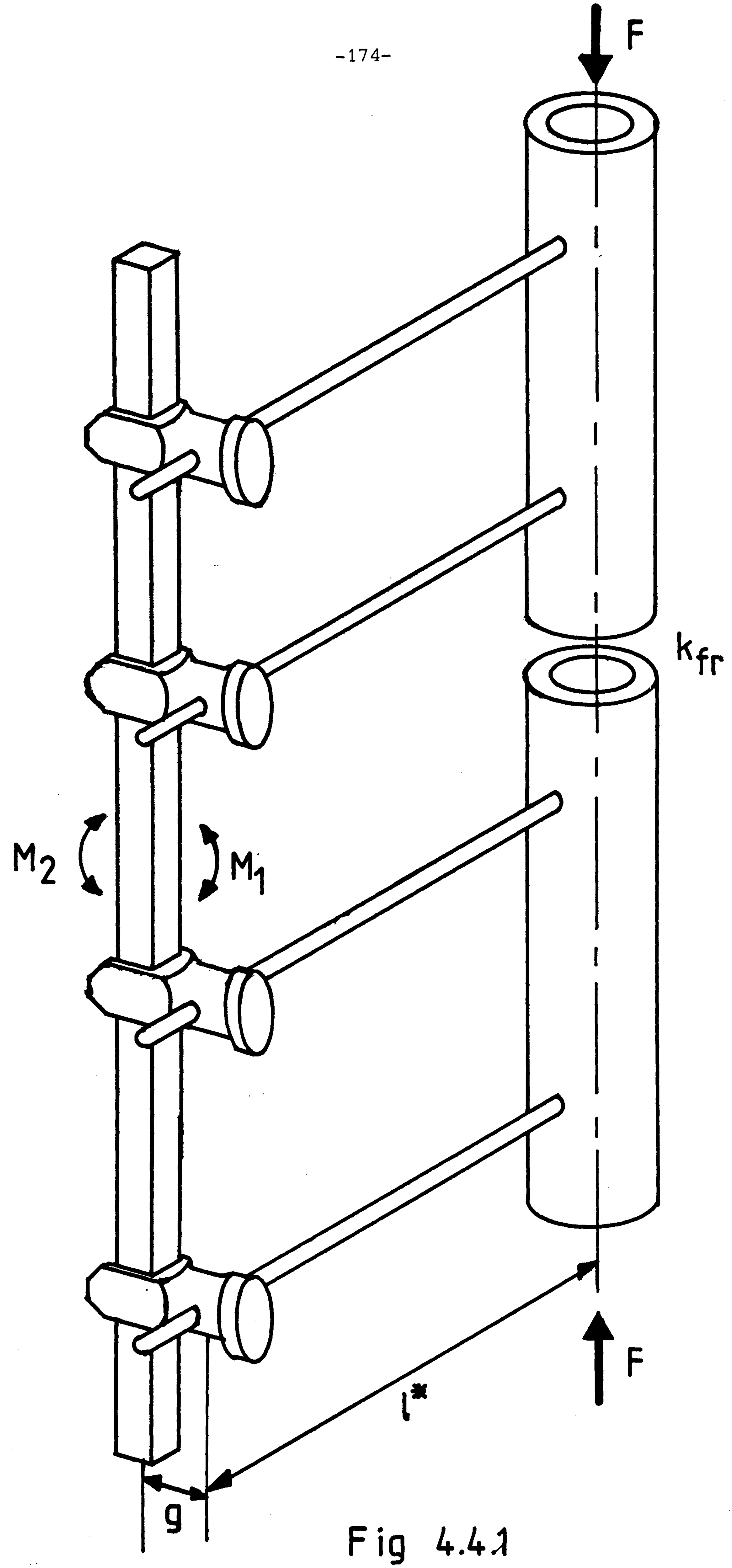

Fig 4.41

For the stiffness calculations, the force applied to the bone is unknown, but the force applied by the patient's foot to the floor is know. This force is not the same as the force in the bone, as muscle forces will also be acting on the bone. However, F_{floor} will be used instead of F for the calculations with the displacement transducer as well as the strain gauge transducer, so the errors should be similar, and will enable comparisons to be made.

ii) Straight Leg Raise

The second test, the straight leg raise, applies two bending moments in opposing directions, to the fracture-fixation system. The first of these occurs when the heel is lifted, as in Figure 4.4.2, and the leg muscles are relaxed. This is modelled in Figure 4.4.3 by a beam simply supported at each end, with a variable weight distributed linearly along the length, simulating the variation of mass distribution along the leg. The weight per unit length at the hip is w_a falling linearly to w_B at the ankle and varying such that the total leg weight is W_L. The centre of gravity of the leg is a distance l' from the hip, and the distance from the hip to the ankle is l. In addition there is also a concentrated weight W_F attributable to the foot. The weight of the portion of the leg below the fracture is W_Z, with centre of gravity a distance z from the fracture, as shown in Figure 4.4.4.

The second part of the test, in which the leg was held off the examining couch by the patient, as shown in Figure 4.4.5, may be modelled by a cantilever with weight of the lower leg varying linearly together with the concentrated weight of the foot (Figure 4.4.6) as previously. The weight of the portion of the leg below the fracture site is again W_Z with centre of gravity at a distance z from the fracture, as in Figure 4.4.7.

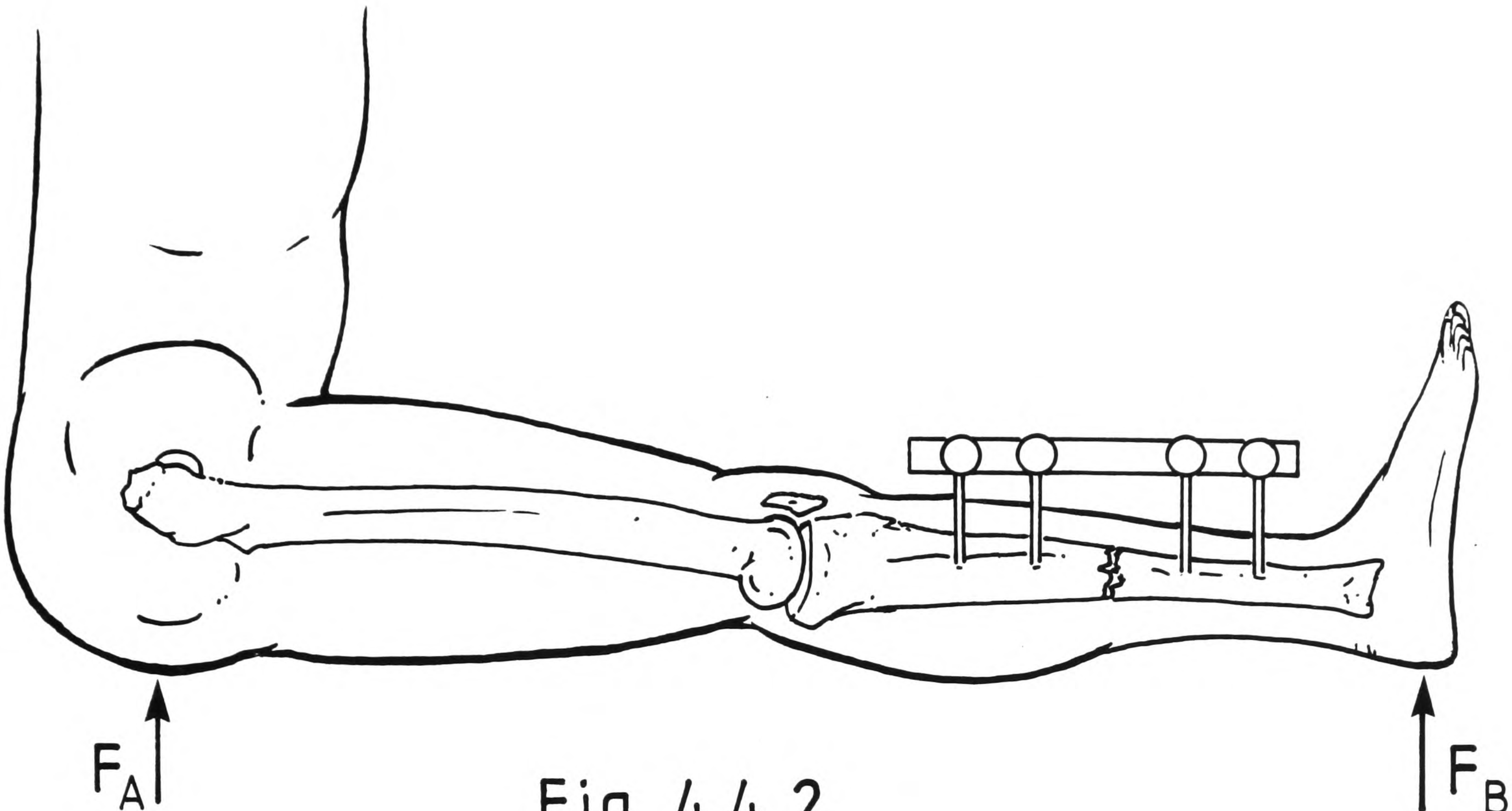

Fig 4.4.2

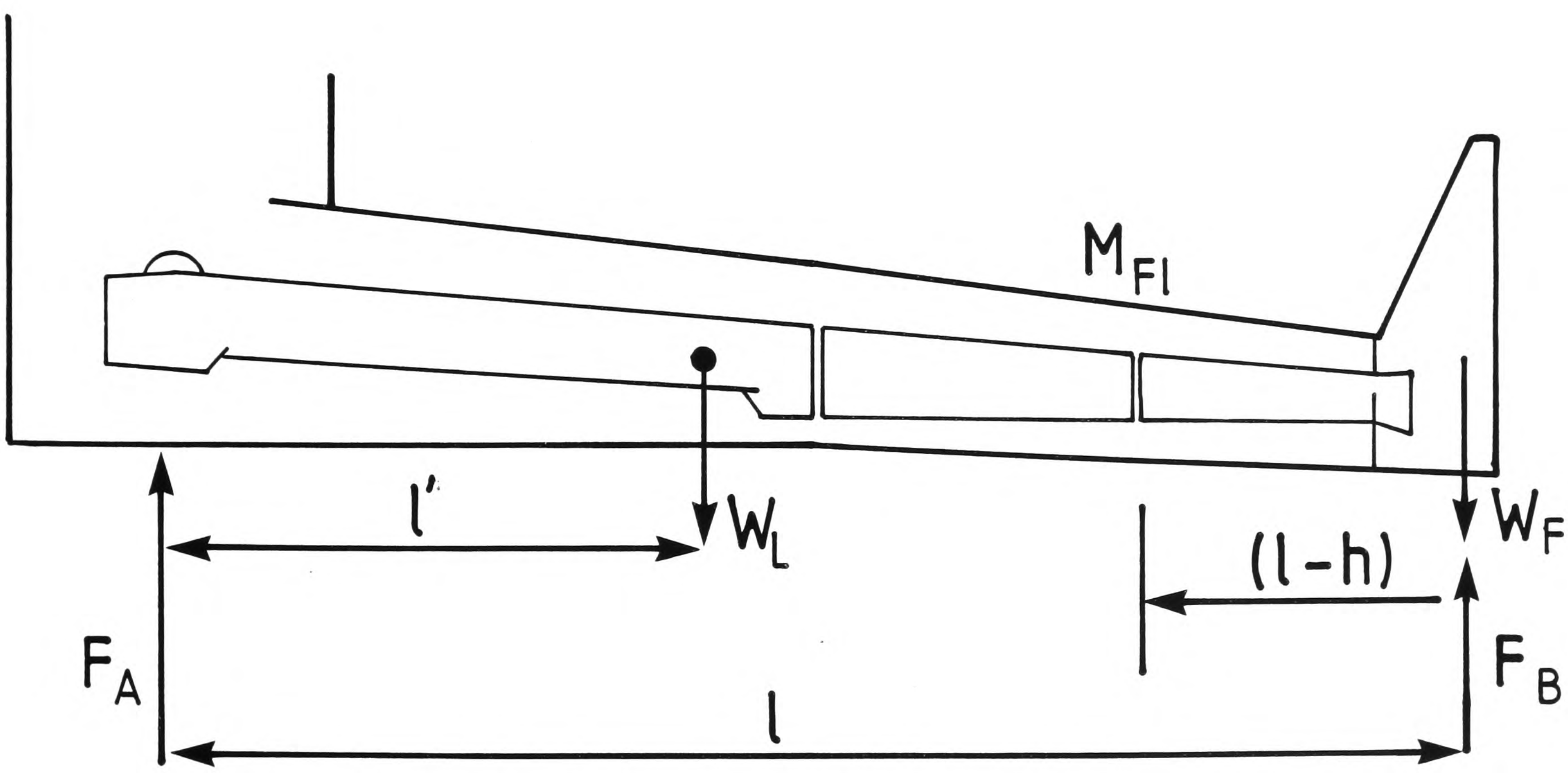

Fig 4.4.3

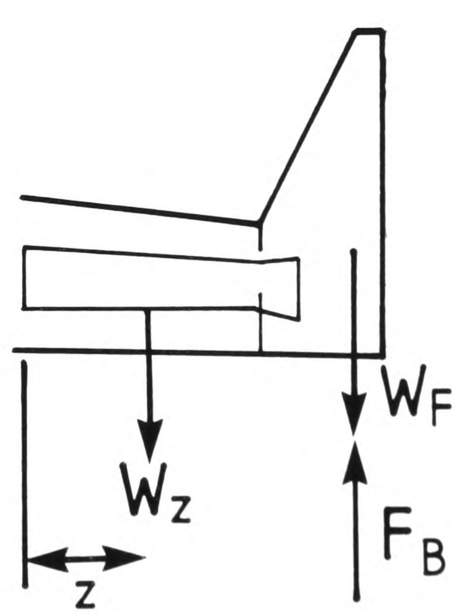

Fig 4.4.4

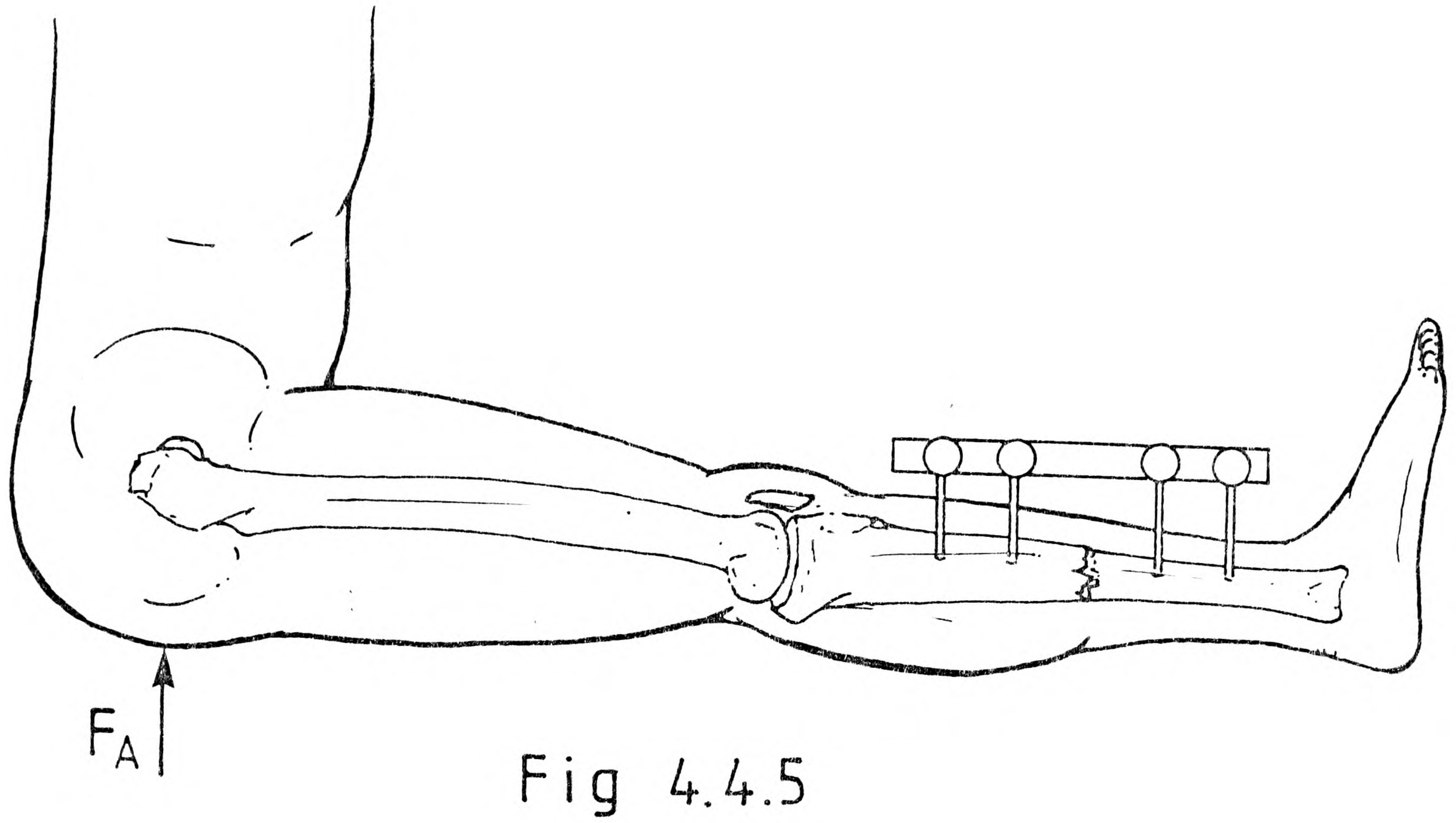

Fig 4.4.5

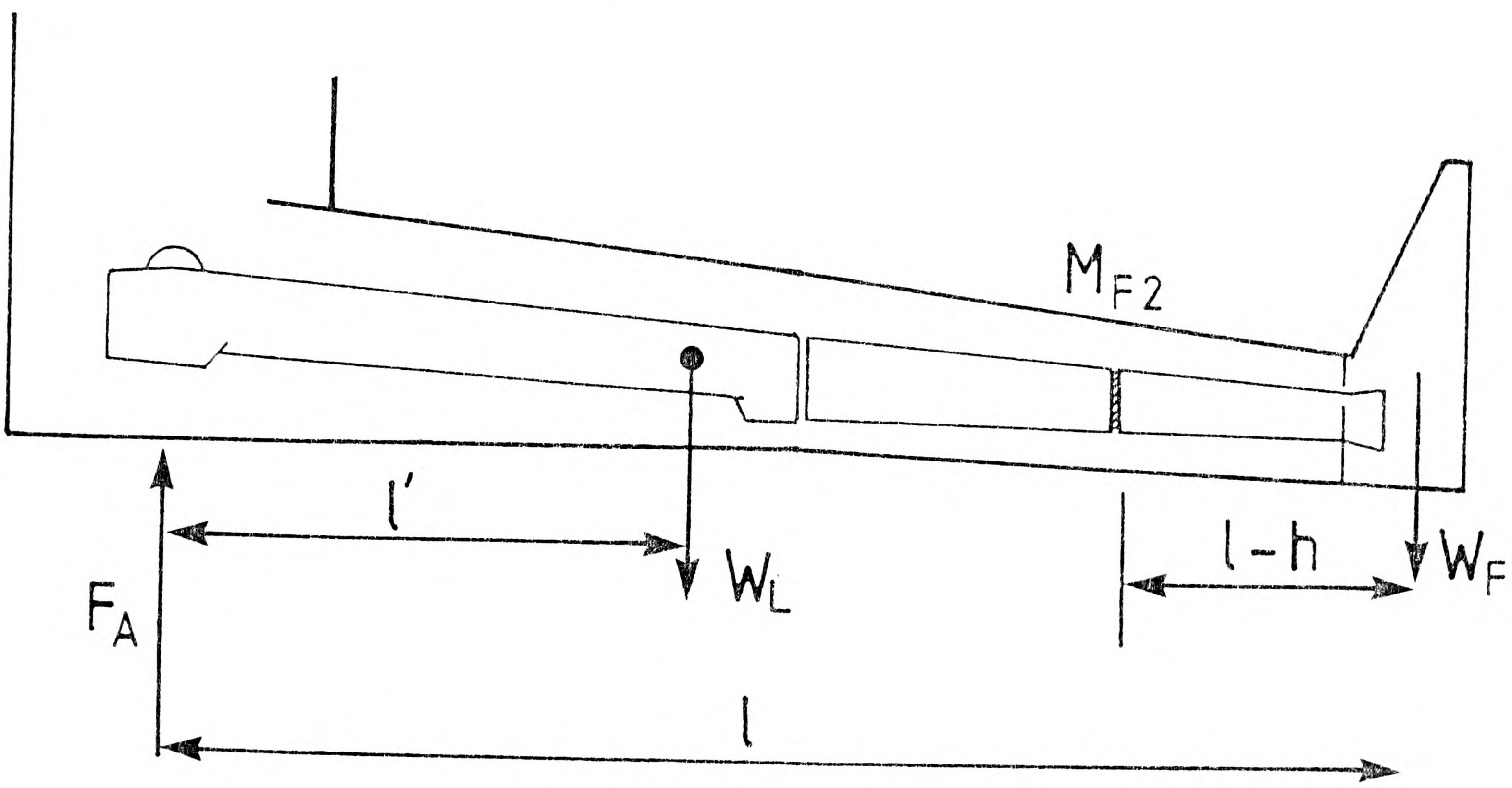

Fig 4.4.6

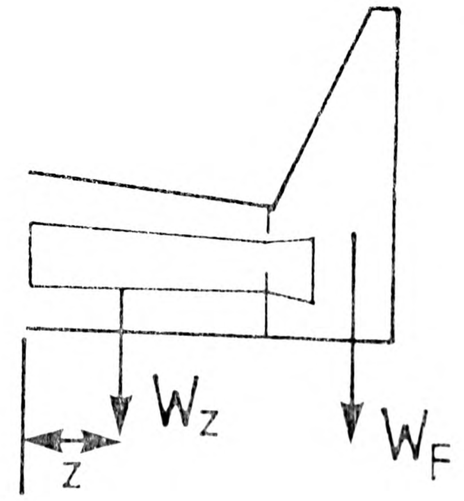

Fig 4.4.7

For the first part of the rest, resolution of forces gives:

$$F_A + F_B = W_L + W_F \tag{4.4.5}$$

where F_A is the reaction force between the couch and the leg and F_B is the reaction force between the leg and the examiner's hand while holding the leg raised.

Taking moments about A (Figure 4.4.4) gives:

$$W_L l' + W_F l = F_B l$$

$$F_B = W_L \left(\frac{l'}{l}\right) + W_F \tag{4.4.6}$$

and the bending moment at the fracture site is

$$M_{F1} = W_F\,(l-h) - F_B\,(l-h) + W_z \cdot z \tag{4.4.7}$$

For the second part of the straight leg raise test (Figures 4.4.5 to 4.4.7) the bending moment at the fracture site (Figure 4.5.7) is

$$M_{F2} = W_F\,(l-h) + W_z \cdot z \tag{4.4.8}$$

For both the displacement transducer and the strain gauge transducer, resting values were not used as a basis for comparison since the muscle forces at rest were likely to be both high and variable.

For both of the transducers the difference between the passive and active leg raising was used which is given by M_F, the difference between M_{F2} and M_{F1}.

$$\begin{aligned} M_F &= M_{F2} - M_{F1} \\ &= W_F\,(l-h) + W_Z\,Z - W_F\,(l-h) + F_B\,(l-h) - W_Z\,z \\ &= F_B\,(l-h) \end{aligned} \tag{4.4.9}$$

So that substituting for F_B from equation (4.4.5) we have:

$$M_F = \left[W_L \left(\frac{l'}{l} \right) + W_F \right] (1-h) \qquad (4.4.10)$$

Drillis and Contini (1966) give W_L = 15.05% of body weight, W_F = 1.6% of body weight, and l'/l= 41.5%; (1-h) is dependent on the position of the fracture.

$$\begin{aligned} M_F &= (\ 0.1505\ .\ 0.415 + 0.016\ )\ (1-h)\ BW \\ &= 0.07846\ (1-h)\ BW \qquad (4.4.11) \end{aligned}$$

where BW is the patient's body weight.

This moment is applied about an axis parallel to the ground, but an angle to the axes of fixator, so that it can be resolved into two components, parallel and perpendicular to the pin direction. Thus from Figure 4.4.8:

$$M_{pin} = M_F \cos \theta \qquad (4.4.12)$$

where M_{pin} is the moment applied to the fracture-fixator system about the lines of the pins and

$$M_{perp} = M_F \sin \theta \qquad (4.4.13)$$

where M_{perp} is the moment about the axis perpendicular to the plane of the pins.

then:

$$k_1 = k_{pin} + k_{FR1} \qquad k_2 = k_{perp} + k_{FR2} \qquad (4.4.14)$$

$$M_{pin} = M_1 + M_{FR1} \qquad M_{perp} = M_2 + M_{FR2} \qquad (4.4.15)$$

where M_1 and M_2 are the moments measured by the strain gauge transducer, k_{FR1} is the bending stiffness of the fracture when

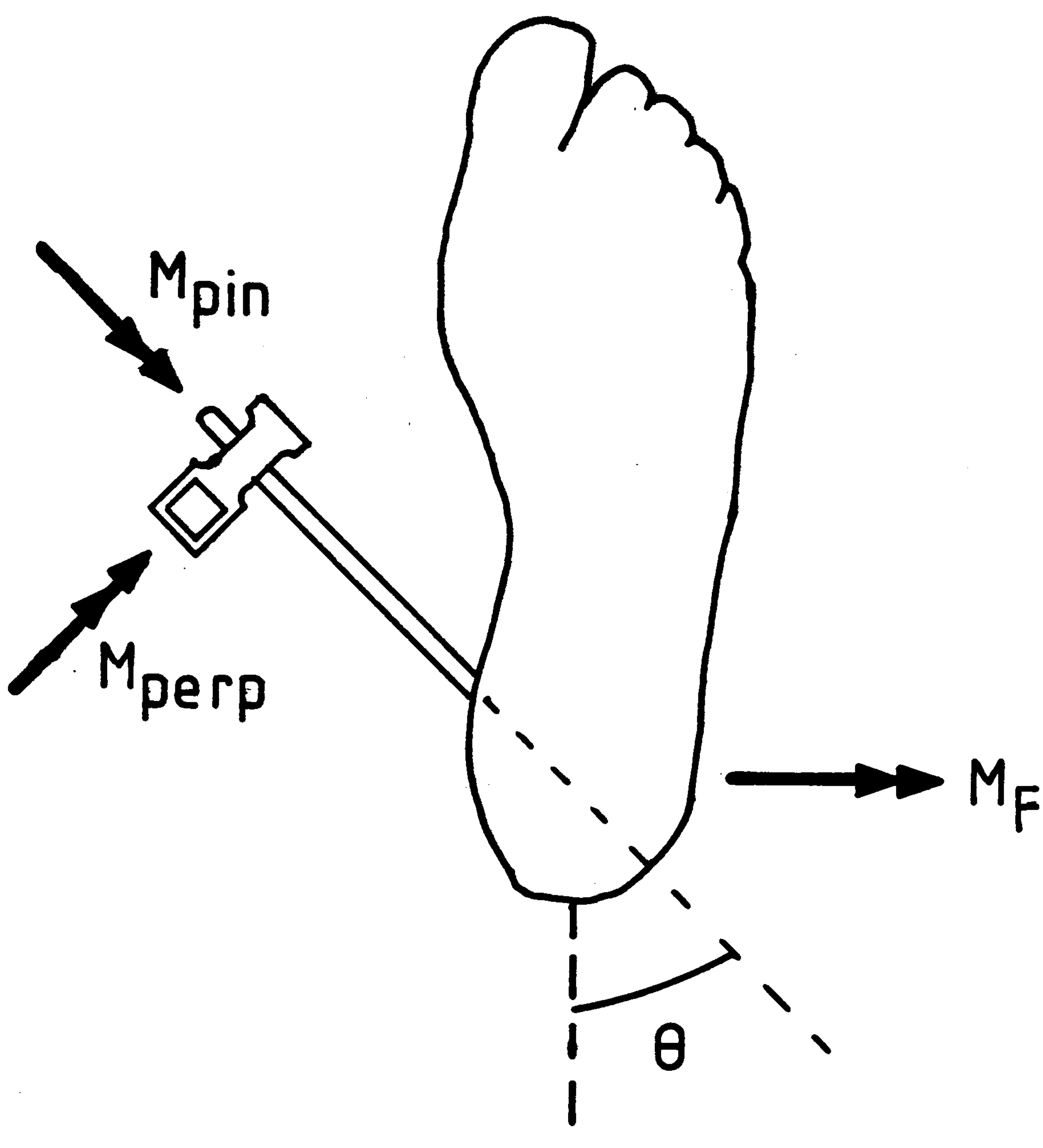

Fig 4.4.8

measured in the axis of the pins, and k_1 is the bending stiffness of the fracture and fixator in that axis. k_{FR2} and k_2 are similarly defined about the axis perpendicular to the plane of the pins. M_{FR1} and M_{FR2} are the moments applied to the fracture about the pin axis and the axis perpendicular to the plane of the pins respectively.

Also $\dfrac{M_1}{M_{FR1}} = \dfrac{k_{pin}}{k_{FR1}}$ and $\dfrac{M_2}{M_{FR2}} = \dfrac{k_{perp}}{k_{FR2}}$

Therefore
$$M_{pin} = M_1 \left[1 + \frac{k_{FR1}}{k_{pin}} \right]$$

$$M_{perp} = M_2 \left[1 + \frac{k_{FR2}}{k_{perp}} \right] \qquad (4.4.16)$$

4.5 Calculation of Fracture Stiffness from Displacement Transducer Data

The displacement transducer enables the total stiffness of the fixator-fracture system to be found directly from the data

i) Axial Loading

From (4.4.2)

$$k_T = k_{FR} + k_{fix}$$

$$k_{FR} = k_T - k_{fix} \qquad (4.5.1)$$

but k_T is F_{floor} divided by the axial displacement dy.

$$k_{FR} = \left(\frac{F_{floor}}{d_y}\right) - k_{fix} \qquad (4.5.2)$$

(ii) Straight Leg Raise

As discussed in section 4.4(ii) the bending moment applied to the fracture is 0.07846 (l-h) BW where (l-h) is the distance from the fracture to the ankle mortice and BW is the patient's total body weight.

Also as shown in section 4.4(ii)

$$M_{pin} = M_F \cos\theta \qquad\qquad M_{perp} = M_F \sin\theta$$

and

$$k_1 = k_{pin} + k_{FR1} \qquad\qquad k_2 = k_{perp} - k_{FR2}$$

$$k_{FR1} = k_1 - k_{pin} \qquad\qquad k_{FR2} = k_2 - k_{perp} \qquad (4.5.3)$$

But k_1 and k_2 can be found from M_F

$$k_1 = \frac{M_F \cos\theta}{\theta_x} \qquad \text{and} \qquad k_2 = \frac{M_F \sin\theta}{\theta_z}$$

Therefore

$$K_{FR1} = \left(\frac{M_F \cos\theta}{\theta_x}\right) - k_{pin}$$

$$k_{FR2} = \left(\frac{M_F \sin\theta}{\theta_z}\right) - k_{perp}$$

4.6 Calculation of Fracture Stiffness from Strain Gauge Data

The strain gauge transducer measures the torsion about the long axis, and the bending moments about the other two axes of the support bar.

(i) Axial Loading

As given by equation 4.4.3

$$M_1 = F_{fix}\, g \qquad M_2 = F_{fix}\, l^*,$$

in the analysis of the strain gauge transducer data, M_1 and M_2 are vector added to give M where:

$$M = (M_1{}^2 + M_2{}^2)^{\frac{1}{2}} = F_{fix}\,(l^{*2} + g^2)^{\frac{1}{2}} \qquad (4.6.1)$$

For the stiffness calculations, M is divided by F_{floor}, the force applied to the floor, rather than F the force applied to the fracture-fixator system for reasons explained in section 4.4(i).

$$\frac{M}{F_{floor}} = \left(\frac{F_{fix}}{F_{fix} + F_{FR}}\right)(\, l^{*2} + g^2\,)^{\frac{1}{2}}$$

$$= \left(\frac{1}{1 + F_{FR}/F_{fix}}\right)(\, l^{*2} + g^2\,)^{\frac{1}{2}}$$

and from equation (4.4.6):

$$\frac{F_{FR}}{F_{fix}} = \frac{k_{FR}}{k_{fix}}$$

then

$$\frac{M}{F_{floor}} = \frac{1 \qquad (\, l^{*2} + g^2\,)^{\frac{1}{2}}}{1 + k_{FR}/k_{fix}}$$

$$\frac{k_{FR}}{k_{fix}} = \frac{F_{floor}\,(\,1^{*2} + g^2\,)^{\frac{1}{2}}}{M} - 1$$

$$k_{FR} = \left(\frac{F_{floor}}{M}\right) \cdot k_{fix}\,(\,1^{*2} + g^2\,)^{\frac{1}{2}} - k_{fix}$$

But F_{floor}/M is known as the stiffness index S.I., i.e.

$$k_{FR} = \text{S.I.}\; k_{fix}\,(1^{*2} + g^2)^{\frac{1}{2}} - k_{fix} \qquad (4.6.3)$$

Thus from knowledge of the stiffness index, 1^*,g and k_{fix}, the fracture stiffness k_{FR} may be estimated.

(ii) Straight Leg Raise

From equations (4.4.10a and b):

$$M_{pin} = M_1 \left[1 + \left(\frac{k_{FR1}}{k_{pin}}\right)\right] \qquad M_{perp} = M_2 \left[1 + \left(\frac{k_{FR2}}{k_{perp}}\right)\right] \qquad (4.6.5)$$

where M_{pin} and M_{perp} are given by equations 4.4.12 and 4.4.13, that is:

$$M_{pin} = M_F \cos\theta \quad (4.4.12) \qquad M_{perp} = M_F \sin\theta \quad (4.4.13)$$

However the results are again given in terms of

$$M = (M_1{}^2 + M_2{}^2)^{\frac{1}{2}}$$

i.e. $$M = \left[\frac{M_{pin}{}^2}{\left(1 + k_{FR1}/k_{pin}\right)^2} + \frac{M_{perp}{}^2}{\left(1 + k_{FR2}/k_{perp}\right)^2}\right]^{\frac{1}{2}}$$

$$= \left[\frac{M_F{}^2 \cos^2\theta\; k_{pin}{}^2}{(\,k_{pin} + k_{FR1})^2} + \frac{M_F{}^2 \sin^2\theta\; k_{perp}{}^2}{(\,k_{perp} + k_{FR2})^2}\right]^{1/2}$$

CHAPTER 5

CALIBRATION OF THE DISPLACEMENT TRANSDUCER

5.1 Static calibration of the detectors and transducer

After the lateral effect photodetectors had been linearized as described in section 3.3(iii), they were mounted in the transducer head, as described in section 3.2(iii). The calculations of section 4.1 needed the positions of the spots of light on the detectors in the axes of the transducers as defined in section 4.2. Thus any misalignment of the detectors relative to the transducer axes must be taken into consideration. Such misalignment seemed likely as the detectors' axes could only be judged by eye when the detectors were mounted in the transducer.

The calibration apparatus is shown in figure 5.1.1. Two micrometer controlled linear displacement stages were screwed together, so that their directions of movement were mutually perpendicular, and they were then screwed onto a steel plate. The circular rod of the transducer (carrying the LED head) was clamped to the upper of these stages. The plate used had a slot machined in it so that the support bar was aligned with one of the axes of movement of the translation stages. At the opposite end of the steel plate, a micrometer controlled rotation stage was attached to hold the square rod of the detector head of the transducer. The two parts of the transducer were clamped in place while held in their set-up jig. In this way the correct alignment of the two heads was maintained.

The electronics were switched on and 50 samples of zero data were collected over a 1 second period. These were averaged to give the zero position of the transducer,using the program LIZERO (appendix A). Then the program LCALIB (Appendix A) was used to store the readings of the X, Y, and θ micrometers (two translation and one rotation), together with ten sets of data. Next the micrometers were used to

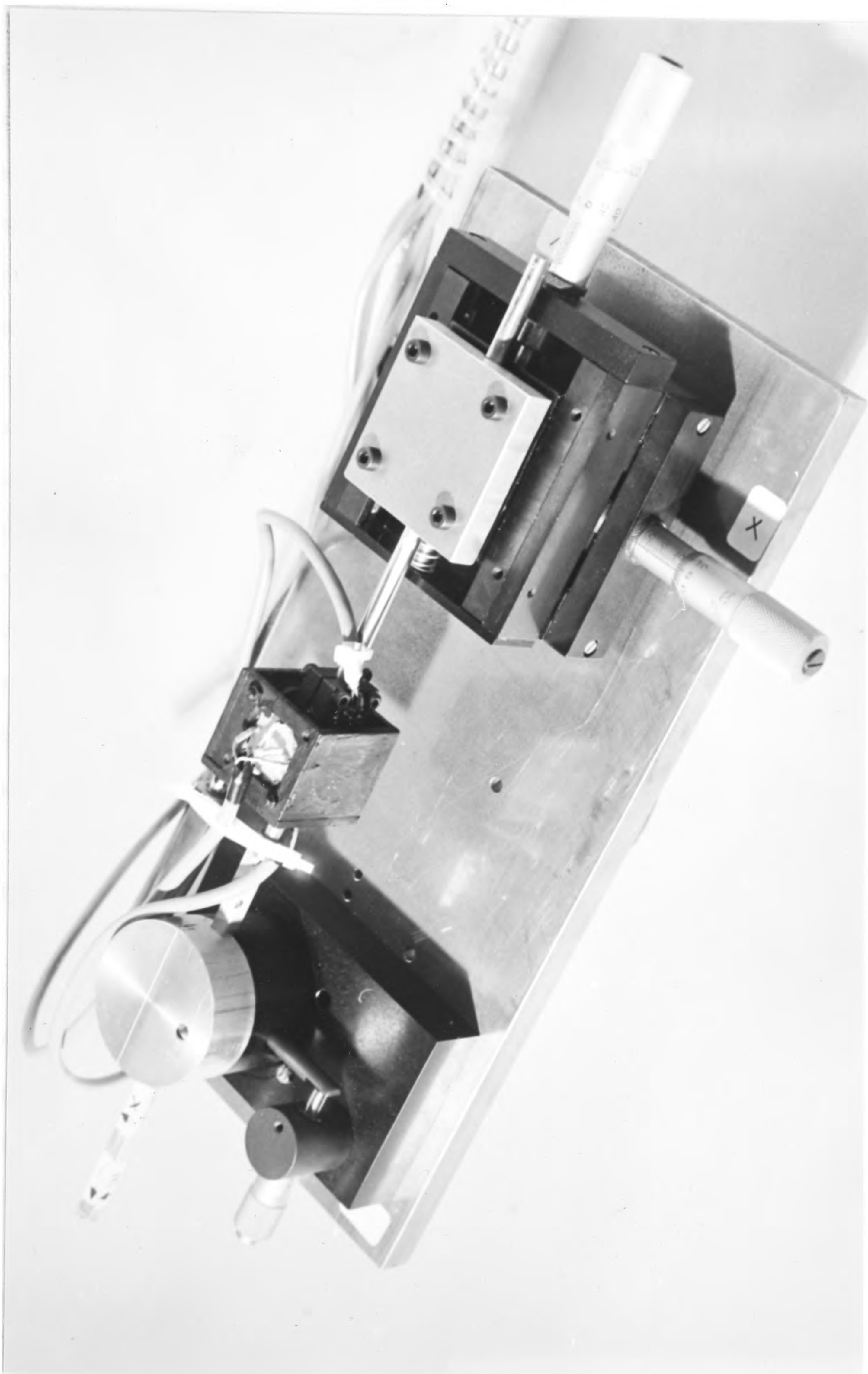

Fig. 5.1.1 Linear Displacement Calibration System

move the stages through a series of different displacements, and at each position the X, Y and θ readings followed by ten sets of data were taken and stored. The program LCAPS3 was used to read the X, Y and θ micrometer readings and then the ten sets of stored data. For each set of data the dark values were subtracted from the light values and the linearizing algorithm was used to obtain six unscaled measures of the positions of the spots of light on the detectors. The values of six unscaled factors were averaged over the ten sets of data and then the appropriate zero values, obtained by the program LIZERO, were subtracted. The scale factors and axial misalignment correction factors were then applied to the six averaged values, and the resulting displacements of the spots of light were used in the calculations of the transducer displacement from its zero position (section 4.1). Finally the program stored the X,Y and θ values, the corrected displacements of the spots of light on the detectors and the calculated transducer displacements. The program LWDATA was used to print out these values as hard copy.

This procedure was then repeated with the transducer rotated through 90^{0} about its long axis so that the third translation axis and the second rotational axis could be calibrated. Thus calculation was performed for the three translational axes and the two rotations about axes perpendicular to the long axis of the transducer. To calibrate for the third rotation, the calibration rig was altered to that shown in Figure 5.1.2. In this the rotation stage was mounted vertically so that one rod of the transducer passed through the centre of it. The calibration procedure was then repeated to give the final set of data.

The micrometers were marked in steps of 0.01 mm which, for the rotation stage, was equivalent to 0.012^{o} of rotation. The

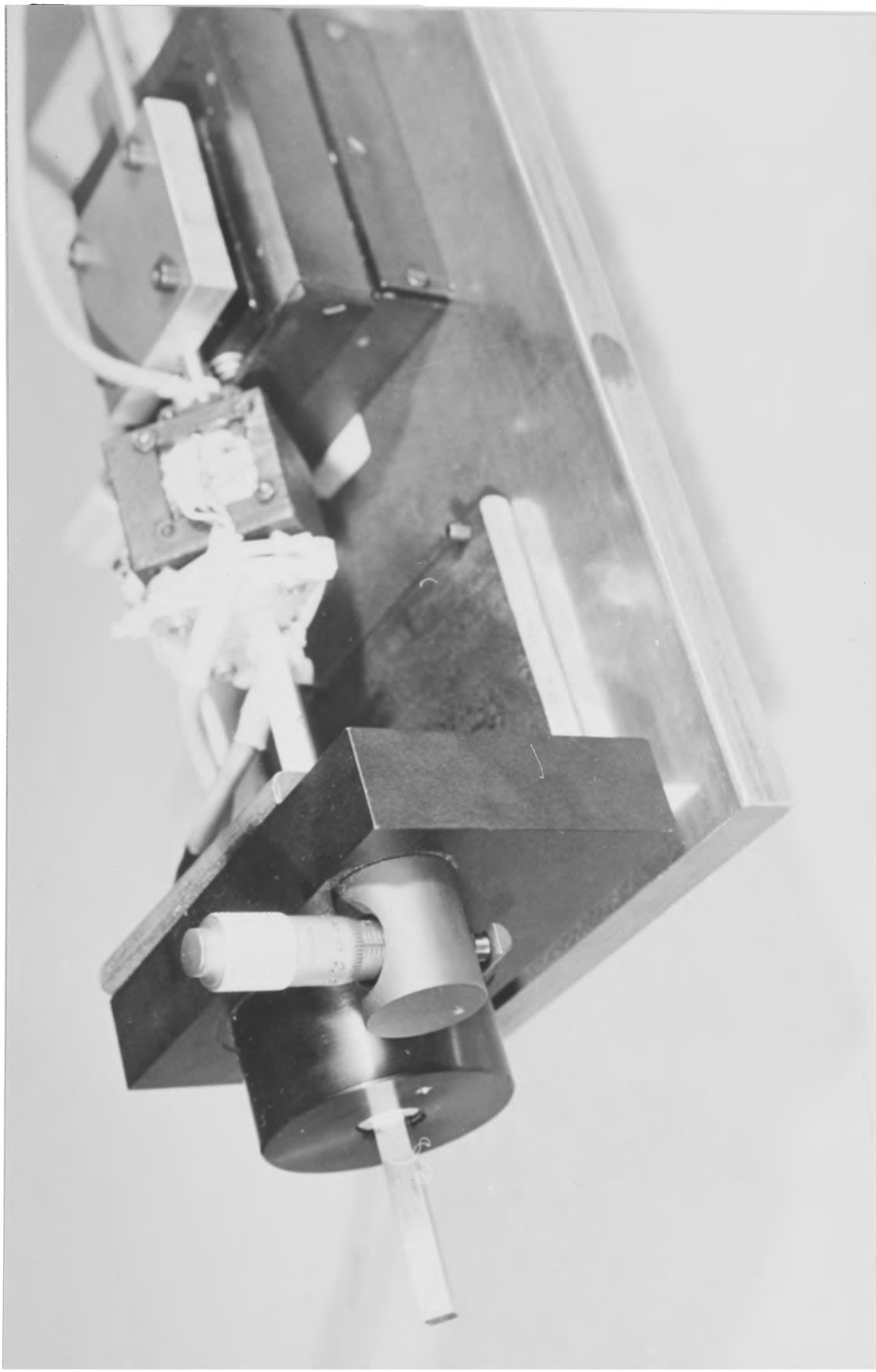

Fig. 5.1.2 Angular Displacement Calibration System

detector displacement corresponding to one bit in the A/D converter was 0.015 mm at the centre of the detector and 0.007 mm at the edges of the detector. Thus, using the 10 bit A/D converter the greatest possible resolution was 0.03mm. The results of the calibration are shown in Figures 5.1.3 to 5.1.8 and show that the errors between the calculated displacements and the actual displacements were less than 0.06mm or 0.12° at the extremes of the range of measurement.

In the drift test the zero position of the detectors was noted and the calibration data input program was used to take in ten samples of data at stated time intervals. For the first 45 minutes the apparent movement was less than that corresponding to one bit of the A/D converter. After this time the apparent movement of the transducer exceeded one bit. The drift measured at after this time was presumably due to the NiCad rechargable batteries running low. However, for patient testing, 45 minutes was more than sufficient - the tests for one patient did not take more than ten or fifteen minutes - and the batteries could be replaced after two or three patients had been tested in one session. If this transducer were required for longer use a mains powered 5V power supply, with appropriate patient insolation, could be used instead of the 5V dc converter and PP3 battery used in the present design.

The manufacturers of the lateral effect photodetectors claim an ability to measure to an accuracy of 0.0001 ins (0.0025 mm). The noise at the output of the Isolation Amplifiers was 2 mV p-p which was less than 1 bit of the A/D converter, which corresponded to 5 mV, so that using a 12 bit A/D converter would give a potential twofold increase in resolution. The quantization noise could as be reduced to 0.004 mm for each detector output.

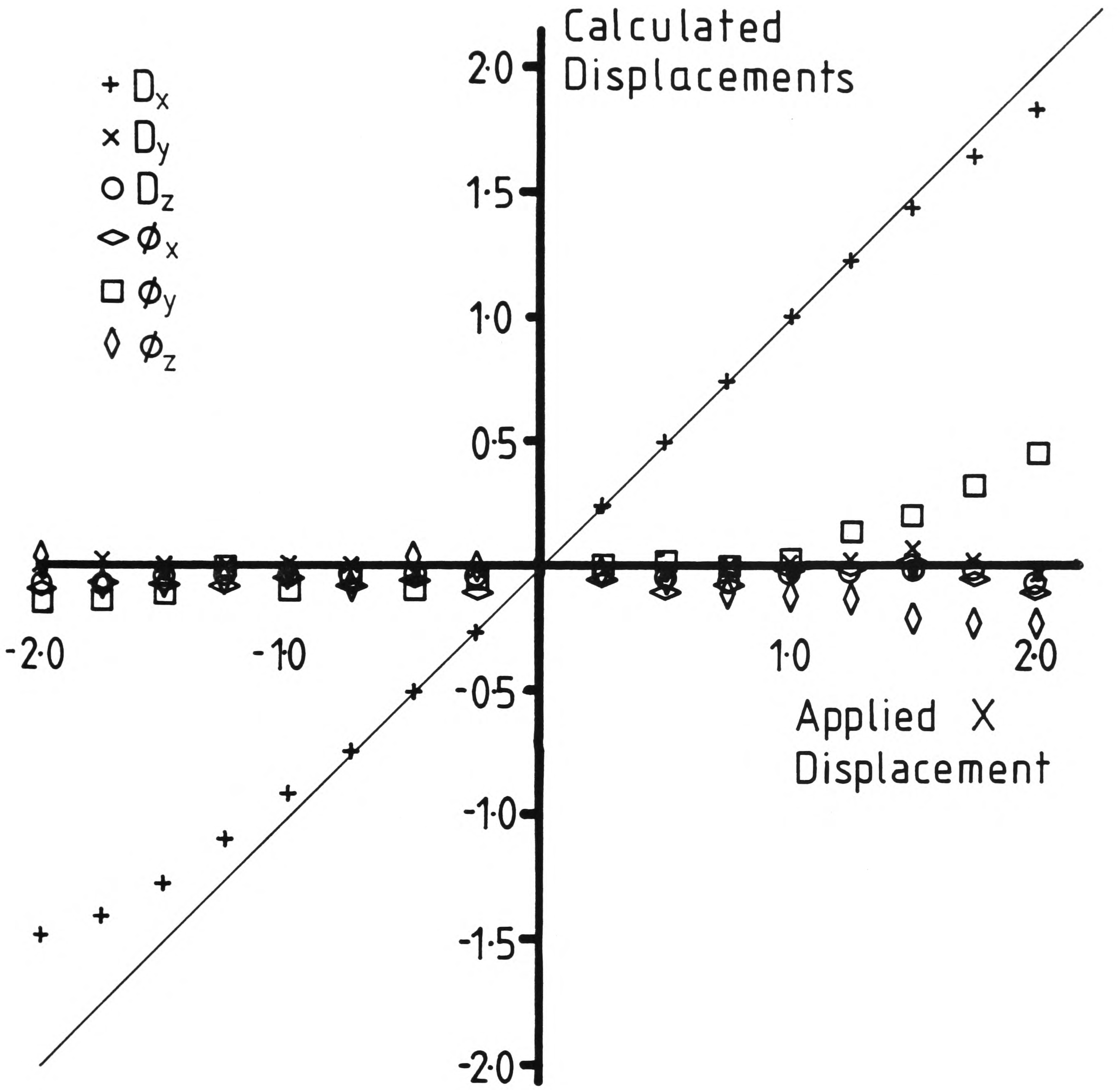

Calculated
Displacements
+ D_x
× D_y
○ D_z
ϕ_x
□ ϕ_y
◊ ϕ_z
2·0
1·5
1·0
0·5
-0·5
-1·0
-1·5
-2·0
-2·0
-1·0
1·0
2·0
Applied X
Displacement

Fig 5.1.3

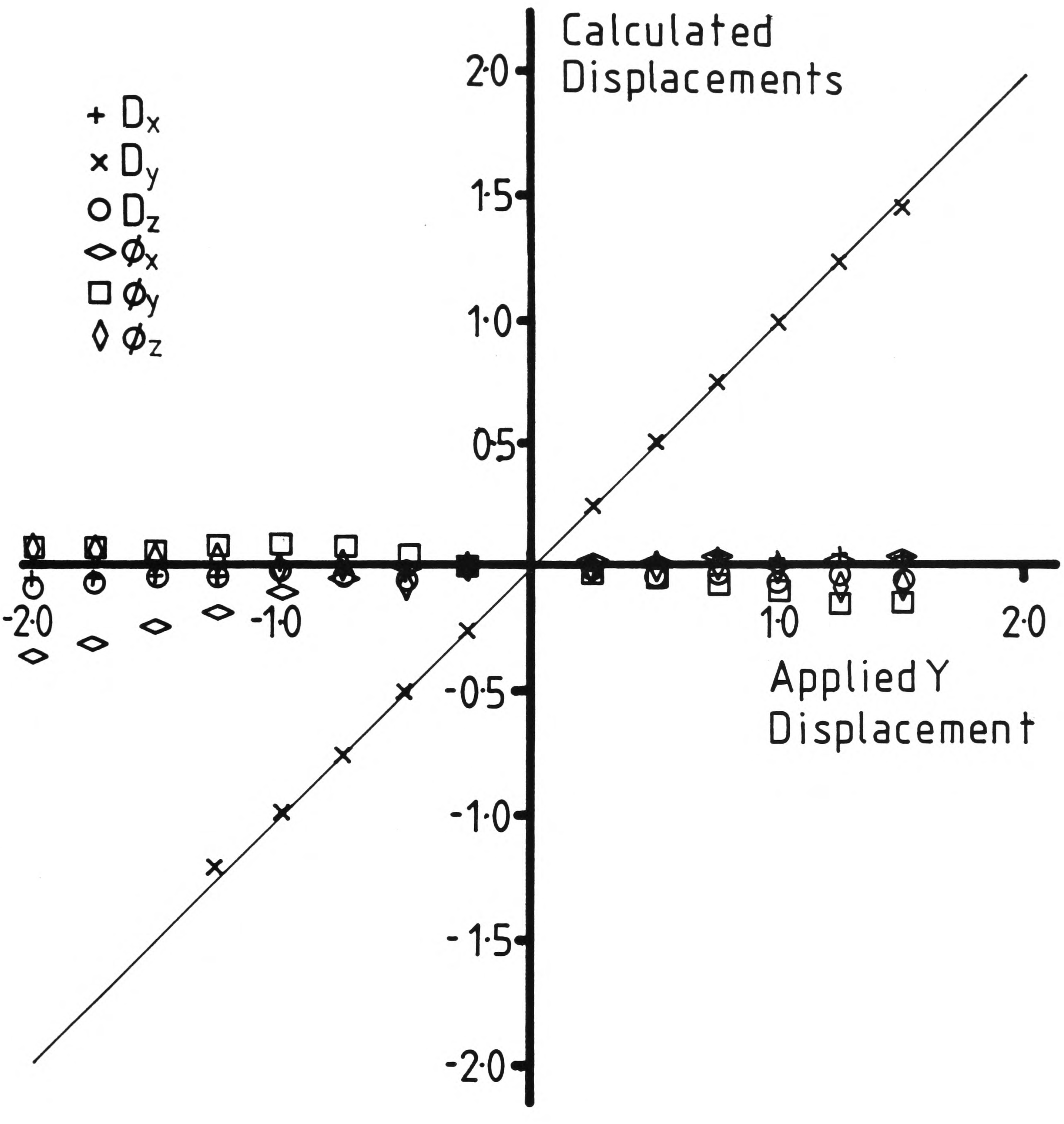
Calculated
Displacements
2·0
1·5
1·0
0·5
-0·5
-1·0
-1·5
-2·0
-2·0
-1·0
1·0
2·0
Applied Y
Displacement
+ D_x
× D_y
O D_z
◇ ϕ_x
□ ϕ_y
◊ ϕ_z

Fig 5.1.4

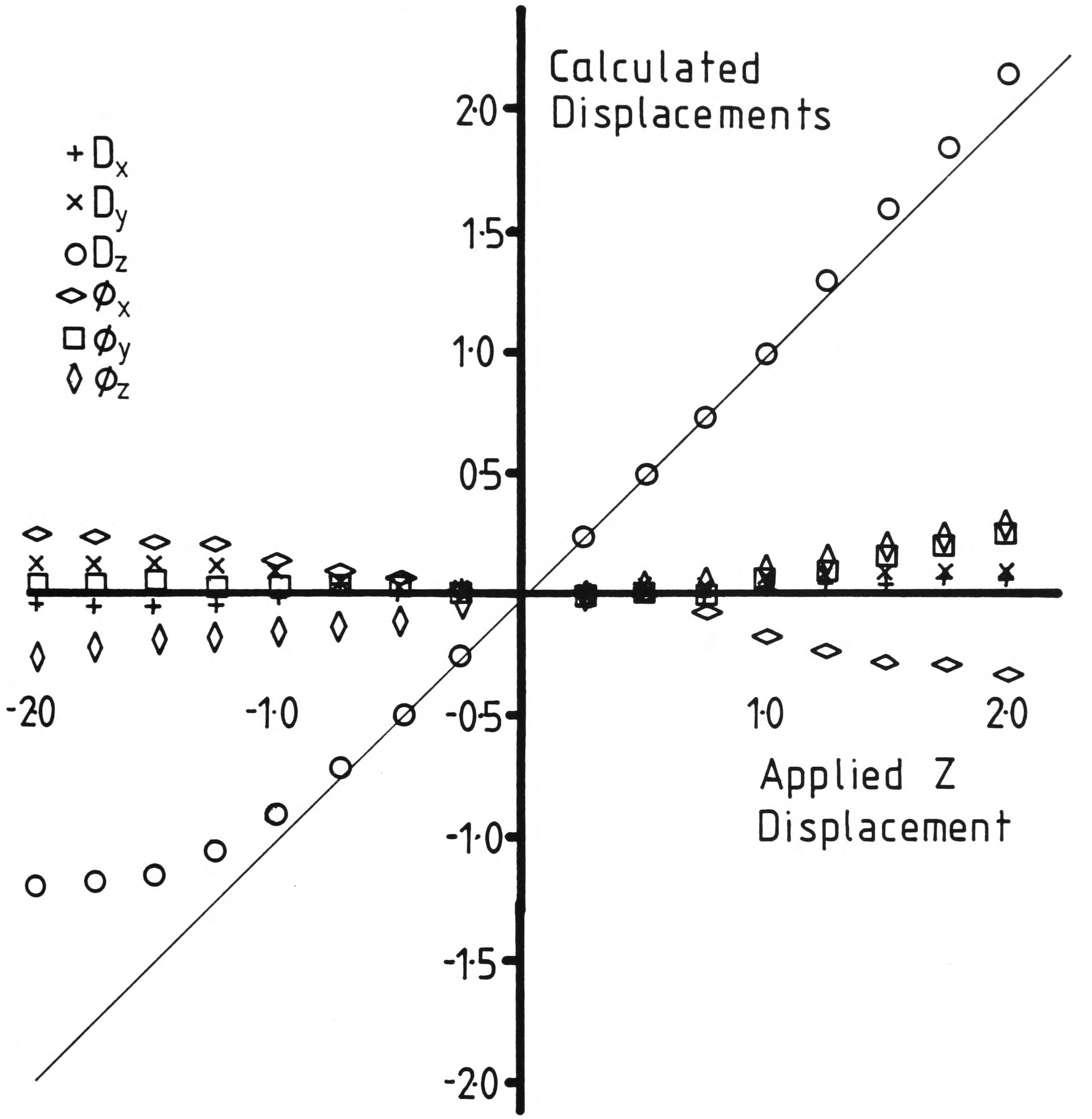
Calculated
Displacements
2·0
1·5
1·0
0·5
-0·5
-1·0
-1·5
-2·0
+ D_x
× D_y
○ D_z
ϕ_x
ϕ_y
ϕ_z
-2·0
-1·0
1·0
2·0
Applied Z
Displacement

Fig 5.1.5

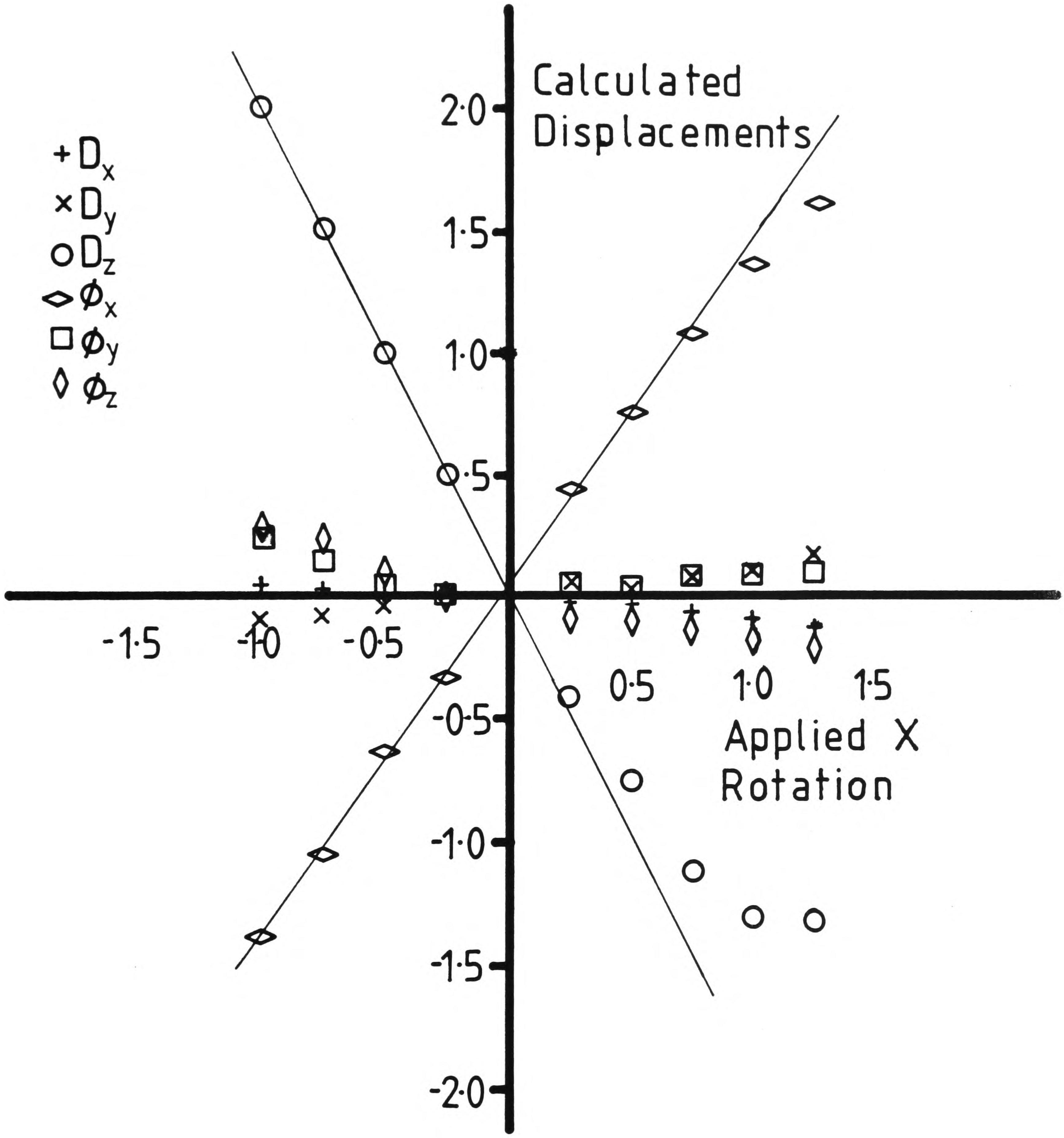
Calculated
Displacements
Applied X
Rotation
2·0
1·5
1·0
0·5
-0·5
-1·0
-1·5
-2·0
-1·5
-1·0
-0·5
0·5
1·0
1·5
D_x
D_y
D_z
ϕ_x
ϕ_y
ϕ_z

Fig 5.1.6

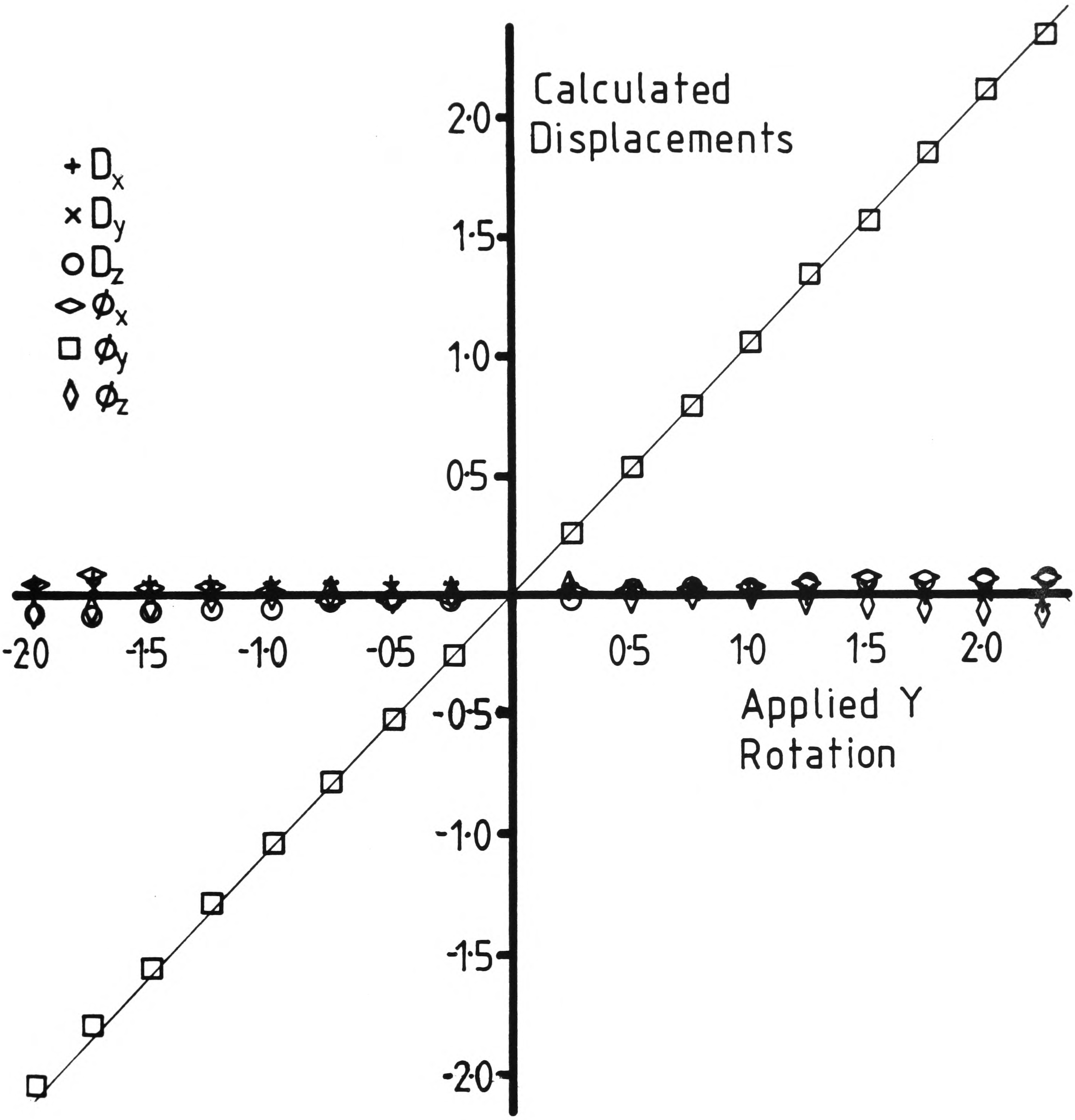
Calculated
Displacements
Applied Y
Rotation
D_x
D_y
D_z
ϕ_x
ϕ_y
ϕ_z
2·0
1·5
1·0
0·5
-0·5
-1·0
-1·5
-2·0
-2·0
-1·5
-1·0
-0·5
0·5
1·0
1·5
2·0

Fig 5.1.7

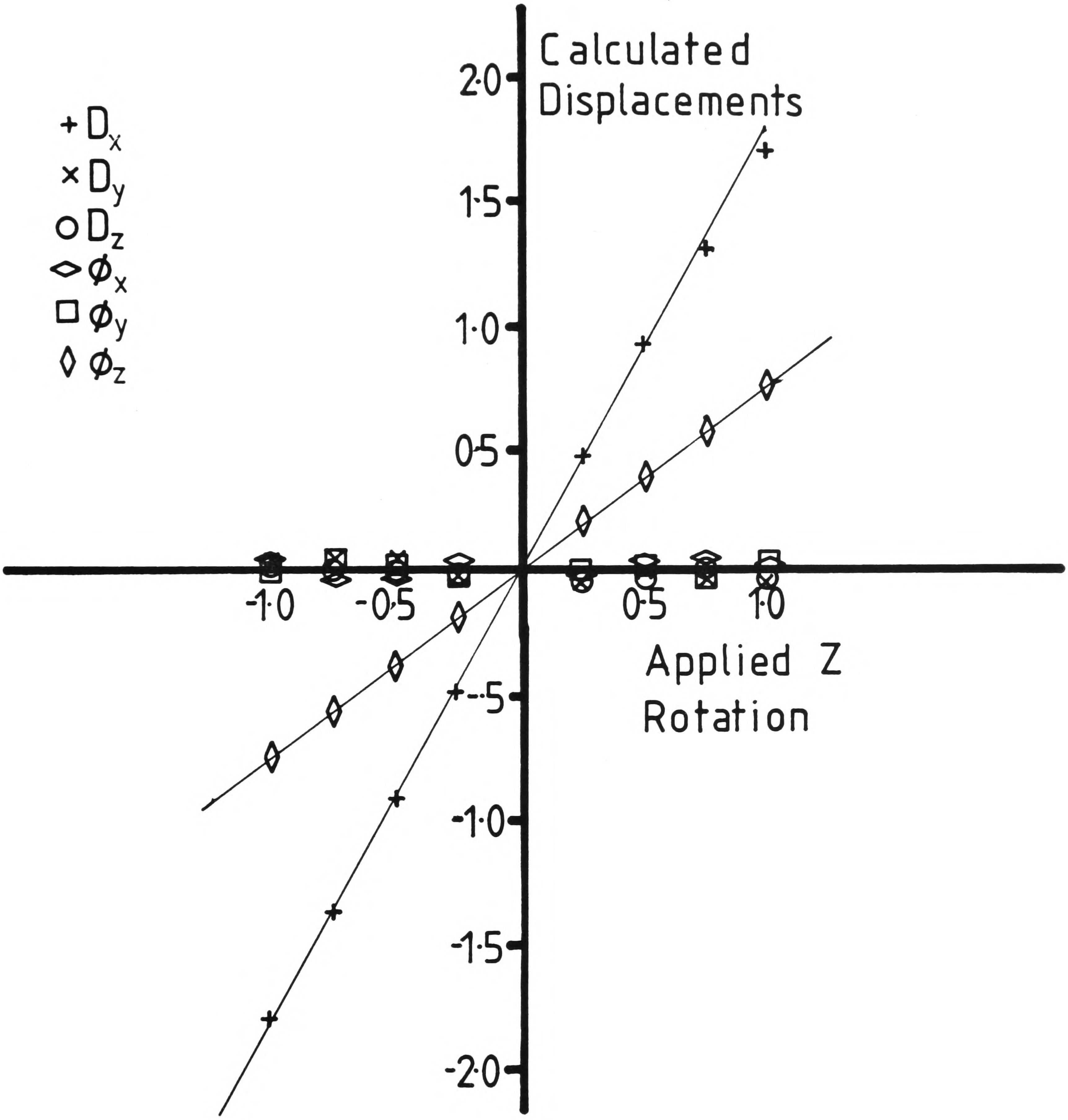
Calculated Displacements
+ D_x
× D_y
○ D_z
ϕ_x
□ ϕ_y
◊ ϕ_z
2·0
1·5
1·0
0·5
-·5
-1·0
-1·5
-2·0
-1·0
-0·5
0·5
1·0
Applied Z Rotation

Fig 5.1.8

It is claimed that this transducer is capable of measuring displacement over a ± 2 mm range with an accuracy of 0.06 mm in three mutually perpendicular directions, and of measuring rotations up to 3° with an accuracy of 0.2° about the same three axes. The drift of the signal is below one significant bit for a sufficiently long time to allow two or three patients to be tested before there is any appreciable effect.

5.2 Calibration of the Transducer for Fracture Movement

In conjunction with the work described in Churches et al (198 a,b,c) the accuracy of the transducer for fracture site movements was tested. The bone was represented by two lengths of square aluminium tube as shown in Figure 5.2.1 with a fixator attached in the normal manner, with both the strain gauge transducer and the displacement transducer applied to the fixator. Different stiffness springs, ranging approximately from 10 Nmm^{-1} to 2000 Nmm^{-1}, were placed between the 'bone' ends to simulate fractures of different stiffnesses. The system was loaded up in a model 1122 Instron materials testing machine under uniaxial compression along the centre of the aluminium tubing. The force-related electrical output of the load cell was monitored and the displacement of the crosshead was measured using a linear voltage-displacement transducer (LVDT). The 12 outputs of the fracture displacement transudcer, the two bending channels of the strain gauge transducer, the force signal and the LVDT signal were all sampled by the 16 channel A/D converter of a PDP 11/34 computer via the Isolation Amplifier. The program, LINCA2, designed to run under the RSX operating system, and similar to LCALIB described in the previous section, was used to obtain the displacements of the transducer. The algorithms obtained in section 4.2(i) were used to calculate the fracture site movements. The fixator dimensions were stored in a file called LFID**.DAT using the program LFIXAT, and accessed when required. The maximum load was approximately 400 N, and the output of the force transducer was amplified by a constant factor. However, as stiffer 'fracture' springs were used the maximum displacement of the cross-head decreased from a maximum of 5 mm to a

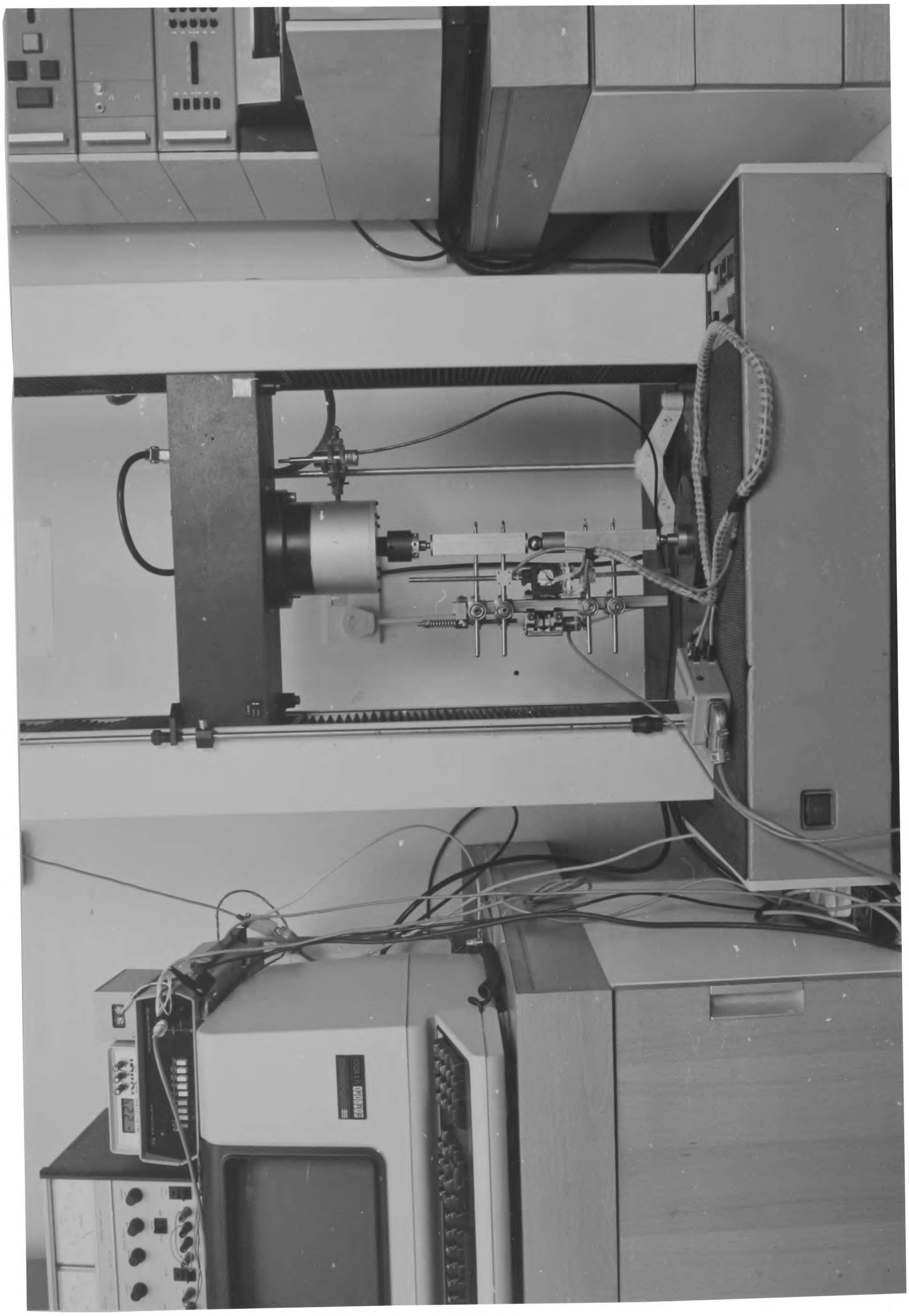

Fig. 5.2.1 System for Calibration of Entire Transducer

minimum of approximately 0.1 mm. To accommodate this variation three different gains were applied to the LVDT signal at the isolation amplifier giving maximum measurable displacements on the three ranges of approximately 5.0 mm, 2.4 mm and 1.0 mm. The LVDT signal, after amplification, was calibrated by taking in data after moving the cross head to various positions, which were measured to an accuracy of 0.01 mm. One pair of preamplifiers for the A/D converter was used to amplify the output signals from the strain gauge transducer, as normally occurs when this transducer is used in patient studies.

5.3 Effect of loose pins

In various clinical studies of external fixation the rate of pin loosening and infection have been estimated from 10% to 100%. The definitions of loosening have varied from slight rock in the pin to could be pulled out by hand without unscrewing, and those for infection from reddening of the skin to pus discharge. Infection of the pin tract will lead to loosening of the pin due to lysis of the bone, and it has been claimed that loosening of the pin will lead to infection as bacteria enter the pin tract.

Thus it is necessary in any study on external fixation, to consider the effects of pin loosening on the mechanical stiffness of the fixator, and in this study on the results from the strain gauge transducer and from the displacement transducer. The first two are also discussed in Churches et al (1985 a and b). The experimental work was done using the equipment discussed in Section 5.2, with the bone modelled by square aluminium tubing with a fixator mounted on it. The Schanz screws were tapped into the far "cortex" but a slot was cut in the near "cortex", and an aluminium wedge was made to fit the slot. Thus, when the wedge was removed the pin was loose in the near "cortex" and anchored in the far, so the pin could angulate but not telescope. When the wedge was in position the pin was tight in both cortices. Thus, the removal of the wedge changed the pin from a double encastre beam to a beam with one end encastre, the clamp end, and the other simply supported, and the effective length was increased by the thickness of the "bone". Load was applied to the fixator system by an Instron 1122 via steel balls in end plates on the "bone" ends, for axial loading. For bending, a four point bending rig was used to apply bending loads to the "bones", and for torsion a torsion rig developed for the Instron was used.

Pin lengths of 27.5, 45, 55 and 70mm between the "bone" and the clamps were used, and the inter pin distances in each segment were 25, 33 and 45mm. For axial loading, the stiffness was proportional to -2.0 power of the pin length for all pins tight, falling to -1.3 power for two pins loose in the same segment. The inter pin distance had no appreciable effect. When one pin was loose the axial stiffness dropped by about 20% and with two pins loose in the same segment it dropped by about 60%.

For bending in the plane of the pins, the length of the pins had no appreciable effect on the fixator stiffness, but the stiffness was approximately proportional to the inter pin spacing. The effect of loose pins is small, apparently less than the experimental error of about 7%.

For bending in the plane perpendicular to the pins, both pin length and pin separation affected the stiffness. The stiffness versus pin length graph is to the power of -1.5 for an inter pin distance of 45mm, but this power falls to -1.0 for an inter pin distance of 25mm, the absolute stiffness was also increased by increasing the inter pin distance. One loose pin decreased the stiffness but with the inter pin distance at 25mm or with two loose pins it was difficult to obtain reliable data.

In torsion the inter pin distance had little effect and increasing the pin length from 27.5 to 70mm decreased the stiffness from approximation 1.6Nm deg^{-1} to approximation 1.3Nm deg^{-1}. Loosening one pin decreased the stiffness by 12% when the pin length was 27.5mm but only by 6% when the pin length was 70mm.

The other effect on one loose pin in a bone segment is that due to its decreased stiffness the load on the other pin in the segment is increased. For example, in axial loading as one pin loosens the stiffness is decreased by 23%, but the pin loads, instead of being equal are varied so that the loose pin takes 20% of the load and the tight pin 80%. This excess load on the tight pin could easily lead to its loosening and with two pins loose in one segment the axial stiffness is decreased by 57%.

This work all assumed that there is a gap at the fracture site, once the fracture starts to heal and stiffness or even if initially there is contact between the bone ends, then there are two stiffnesses in parallel. One, the bone-fixator system and the other the fracture. Thus, as the fracture stiffness increases, the load taken by the fixator decreases, and this is the principle of the strain gauge transducer. When loads are applied to the limb some of these are applied to the fixator, and these produce bending movements in the support bar. These are then mechanically amplified by the offset of the strain gauges from the support bar, and lead to strains in the strain gauges. If the stiffness of the fixator is reduced by one of the pins loosening then for constant fracture stiffness the load in the fixator is reduced, and so is the strain gauge reading. However, when the fracture stiffness increases, the load in the support bar is decreased, so the effect of a pin loosening is the same as the fracture stiffening, as far as the strain gauge amplifier is concerned. If it is known that one pin is loose then using the graphs in Churches et al (1985a) the actual fixator stiffness may be used in eqns. 4.6.3 to 4.6.5.

If the displacement transducer is used then the result is dependent upon which pin is loose. If the transducer is not connected to the loose pin then there is no effect. If the transducer is applied to a loose pin then the results are erronous. In the calculations of the pin bending it was assumed that the pin was a double encastre beam with flexibilities at both ends but with a loose pin it becomes simply supported with flexibilities at the bone end and encastre with flexibilities at the clamped end. It would be possible to calculate a second set of equations for this condition similar to those in Section 4.2(i). However, there are two other possible types of loose pines. In one type there is a small amount of slack at the pin-bone interface so that upon applying a bending moment there is initially little resistance to angulation and then contact is made between solid bone and the pin. In this case initially it is a on end encastre one end simply supported system and then at some point the system becomes an angled encastre beam. In the worst case of pin loosening a sufficiently large amount of bone has been destroyed so that not only could the pin be moved appreciably by a small bending moment, but also by tension or compression along the length of the pin. This case would be very difficult to model. Thus, no calculations were made for loose pins, and the pins were always assumed to be tight.

5.4 The Effect of Errors in the Fixator Dimensions

The transformation matrix from the transducer movements to the fracture movements depends on the geometry of the fixator, the stiffness of the pin-bone interface and the pin-clamp connections. The stiffness of the pin-clamp connection is assumed to remain constant as it depends upon the tightening of the clamp grub screw. The stiffness of the pin-bone connection is also assumed to remain constant, and the effect of loose pins is discussed in section 5.3. Thus the last variable is the dimensions of the fixator.

To consider the effects of dimensions the results from a straight leg raise test were analysed with each of the dimensions in turn increased by 10%. The number of springs, which needed to be an integer, was increased from 6 to 7. The modified values are shown in Table 5.4.1 and the results in Table 5.4.2, with statistically significant differences by paired t-test at the 5% and 1% levels shown.

As the test chosen was a straight leg raise, there are two sets of results; those for the relaxed leg being raised (1), and those for the patient holding the limb by muscle force (2). Thus D_{X1} is the change in D_X from the leg resting on the couch to the leg being raised passively, and D_{X2} is the change from resting on the couch to active raising of the leg.

Table 5.4.1

	Previous value	After modification
Support Bar to Bone	65.0	71.5
Support Bar to Transducer	17.0	18.7
Transducer to Upper Pin	90.0	99.0
Transducer to Lower Pin	53.0	58.3
Fracture to Upper Pin	82.0	90.2
Fracture to Lower Pin	63.0	69.3
Length of Exposed Pin Unthreaded	61.0	60.6
Upper Pin Angle	0	-
Lower Pin Angle	0	-
Number of Springs	6	7
Spring Stiffness	0.00121	0.00131
Bone Radius	9.0	9.9

First the distance between the support bar and the bone was increased by 10%, and the displacement in the Y direction, i.e. along the long axis of the bone, increased by 11%. Compared with the standard formula for the deflection of a double encastrè beam,

$$\delta = \frac{Fl^3}{12EI}$$

for a 10% increase in l the pin length, the deflection should increase by 33%. The difference is due to a combination of the altered ratio between the support bar and the bone, and between the support bar and the transducer, the additional flexibilities at the pin-bone and pin clamp interfaces and the decreased percentage of the pin that is

TABLE 5.4.2

Changed dimension	D_{X1}	D_{X2}	D_{Y1}	D_{Y2}	D_{Z1}	D_{Z2}	ϕ_{X1}	ϕ_{X2}	ϕ_{Y1}	ϕ_{Y2}	ϕ_{Z1}	ϕ_{Z2}
None	-0.012	0	0.028	-0.565	-0.005	0.199	-0.181	0.030	-0.293	2.205	0.021	-0.702
None	-0 013	0	0 029	-0.562	-0 006	0 199	0 181	0 025	-0 293	2 200	0 022	-0 698
None	-0.014	0	0.019	-0.568	-0.003	0.198	-0.176	0.035	-0.278	2.199	0.009	-0.707
None	-0.014	-0.001	0 013	-0 573	-0.001	0 198	-0 174	0.043	-0.277	2.199	0.001	-0 714
None	-0.013	0	0.022	-0.567	-0.004	0.199	-0.178	0.033	-0.285	2.201	0.013	-0.705
f leg L → R	-0.004*	-0.112**	0 018	-0.565	-0 003	0 199	-0 179	0 028	-0 282	2.207	0 025	-0.704
Support bar → bone 65 → 71.5	-0.014	0	0.025	-0.628**	-0.014	0.303**	-0.184	0.028	-0.328**	2.510**	0.015	-0.749**
Support bar → Trans 17 → 18.7	-0.014	0	0.023	-0.556*	0	0.163**	-0.182	0.042	-0.282	2.231**	0.015	-0.712
Transducer → Upper Pin 90 → 99	-0.014	-0.001	0.019	-0.570	-0.003	0.198	-0.174	0.038	-0.279	2.199	0.009	-0.710
Transducer → Lower Pin 53 → 58.3	-0.013	0	0.023	-0.568	-0.012	0.198	-0.164	0.036	-0.276	2.199	0.014	-0.707
Fracture → Upper Pin 82 → 90.2	-0.014	0	0.024	-0.566	0.002	0.199	-0.183	0.032	-0.280	2.196	0.016	-0.703
Fracture → Lower Pin 63 → 69.3	-0.014	-0.001	0.018	-0.573	-0.003	0.198	-0.169	0.042	-0.277	2.202	0.008	-0.713
Length of exposed pin 63 → 69.3	-0.014	0	0.019	-0.569	-0.002	0.198	-0.176	0.035	-0.276	2.202	0.009	-0.708
No of springs 6 → 7	-0.014	0	0.023	0.568	-0.002	0.199	-0.182	0.033	-0.279	2.200	0.016	-0.707
Spring Stiffness 0.00121 → 0.00131	-0.014	0	0.021	-0.569	-0.002	0.199	-0.179	0.034	-0.278	2.200	-0.012	-0.705
Bone Radius 9 → 9.9	-0.015	0	0.016	-0.578	0.001	0.164**	-0.175	0.035	-0.276	2.199	0.005	-0.706

* 5% significance levels
** 10% " "

threaded. The shear displacement, D_Z, perpendicular to the direction of the pins increased by 56%. This displacement would, like D_Y, be expected to increase by 33%, and consideration must be given to why D_Y only increased by 10% but D_Z by 56%. The behaviour of the ends of the pins is theoretically identical, the displacements at the fracture site includes a factor of the offset from the end of the pins to the fracture and thus the rotation about the length of the pin is included in D_Z but the displacement D_Y does not include the offset. The rotation of the bone ϕ_y for both the zero to position 1 and the zero to position 2 were increased by 15%. Rotations of a point on the member acted on by a force are proportional to 1^2 and theoretically the rotation should have increased by 21%. However, these theoretical considerations do not include any allowance for the flexibilities at the pin/clamp and pin/bone connections, so the actual increases would be expected to be less than those for a double encastrè beam.

Change in the support bar-transducer distance resulted in a decrease of D_{Y2} of 1.9%, significant only at the 5% level. The change in D_{Z2} was a decrease of 18% and the change in ϕ_{Y2} an increase of 1.4%, although this was significant at the 1% level. By similar arguments to those given previously, these would be expected to decrease by 30% if the system consisted of double encastrè beams.

The only other change which had a significant effect was altering the bone radius. Here it would be expected to change D_X and D_Z by producing a greater effect at the ends of the pin. There is no significant effect on D_X and D_{Z1} but the original values were so small that a large change would be necessary to be significant. The change in D_{Z2} was 17.6%.

Thus the dimension that has the greatest overall effect was the support bar to bone distance; due to the interposition of skin this is one of the most difficult to measure accurately, unlike the fracture to pin distances, X-rays are not of much help in estimating this value. In practice, errors of 10% in this measurement may result in errors in the estimation of fracture stiffness of up to 11% in the Y axis and 56% in the Z axis.

CHAPTER 6

PATIENT STUDIES

6.1 Use of the Transducer in Patient Studies

Once the transducer had been built it was used to study 7 patients. The patients studied were all from the Accident Service of the John Radcliffe Hospital in Headington Oxford, they were all treated by the same consultant orthopaedic surgeon. The decision as to whether any particular patient was treated with an "Oxford" external fracture fixator rather than internal fixation, Plaster of Paris or traction, was made by the surgical team. Once a patient had had an "Oxford" external fixator applied he or she was then referred to the Orthopaedic Engineering Centre for testing. Similar arrangements were made by one of the consultant orthopaedic surgeons at Horton General Hospital in Banbury. All fixator patients were tested with the strain gauge transducer, and given exercises to do by a physiotherapist attached to the Engineering Centre. From this group of patients, numbering 30 to 40 during this study, the seven patients were drawn. Only those patients between the ages of 17 and 60 years were considered, to exclude any effects caused by accelerated healing due to youth, or decelerated healing due to old age. Any particularly "worried" patients were excluded, as this study meant a further test on each visit to the Engineering Centre. The last eliminating factor was whether the patient's fixator was geometrically such that the displacement transducer could be fitted between the fixator support bar and the patient's leg. This final condition meant that all the patients were from Oxford rather than Banbury, as the Banbury patients all had a shorter distance between their fixator support bars and their legs. Six of the seven patients had been involved in motor accidents and one in a footballing accident, they are individually discussed in Section 6.3. No statistics will be performed as seven patients are too small a group for statistical analysis. In comparison Nicholls (1964) in his study had 705 patients whom he divided into 9 clinical groups depending on their type of injury before performing statistical analysis.

The patients were brought into the Nuffield Orthopaedic Centre fortnightly for fracture monitoring. The patient was seated on an examining couch with the injured leg resting on a pillow, and the transducer in its set-up jig was then attached to the fixator. Care was taken to fix the transducer to the same points on each pin every time. Since the initial clamps caused indentations of the pins, accurate repositioning was reasonably easy to achieve along the length of the pins, but not so straight forward along the long axis of the leg. The second set of clamps did not indent the pins so the position of the transducer had to be checked by measurement. The "set-up jig" was then removed taking care not to alter the position of the transducer. With the leg still resting on the pillow the zero position of the transducer was determined by taking in 50 samples of the light and dark currents in one second and then calculating the average of the positions of the spots of light on the detectors. An output file was produced which contained the patient's hospital number, and the positions of the spots of light.

The patient was then asked to perform certain activities, dependent upon what he was able and permitted to do. In a fully mobile patient the tests consisted of:

i) Straight Leg Raise

An assistant raised the leg just clear of the couch on which it had been resting and held it in that position for 1-2 sec. The patients was then asked to support the raised leg by means of his own muscles (mainly quadriceps) for 1-2 sec, before allowing it to drop onto the couch and relaxing the muscles. (Fig. 6.1.1).

Fig. 6.1.1 Patient Performing Straight Leg Raise Test

Fig. 6.1.1 Patient Performing Straight Leg Raise Test

ii) Longitudinal Tibia Force

Here the patient was seated with the foot of the injured leg resting on a "Kistler" forceplate. The lower leg was positioned by eye, perpendicular to the plate, and the heel was wedged so that the thigh was just clear of the chair. The assistant then applied to the knee a manual load within the limits of comfort for the patient.

iii) Weight Transference Test

In this test the patient stood with the foot of the injured leg just above the "Kistler" forceplate. He then gradually transferred his weight onto the injured leg, within the limits of comfort. During the test the patient was allowed to use crutches or walking sticks, if needed to assist balance or control the weight taken by the injured leg.

iv) Walking

The patient was simply asked to walk in the assessment area taking the maximum comfortable load through the leg and using a walking aid if this was their custom. The walk included one step on the "Kistler" forceplate.

All the data for these tests were collected using the program LPADIN.FOR which had a sampling time of up to ten seconds and stored it for further analysis. Additionally, the Patient's Hospital Number and the number of samples taken were also stored.

Fig. 6.1.2 Patient Performing Longitudinal Tibial Load Test

6.2 Data Analysis

6.2(i) Analysis of the Patient Studies

For the four tests there were three types of analysis performed. The original tests performed had no forceplate data taken, so there were only the 12 channels of displacement transducer for each set of data. The 'dark' current values were subtracted from the 'light' current values. The positions of the spots of light on the three photodetectors were then calculated using the linearizing algorithms discussed in section 3.2. Similar calculations were performed on the fifty sets of zero data and these were then averaged and stored. These zero values were subtracted from the positions from the data file. These differences were then used to calculate the displacements of the transducer from its zero position using the formulae in section 4.1. These transducer displacements were used to calculate the fracture site displacements using the formulae in section 4.2. This was performed for each set of data and there were up to 500 sets of data in each file of data. This data was then stored; the program performing this was LTRANS and is listed in Appendix A.

For later files the forces in three directions were measured from the Kistler forceplates and thus each set of data consisted of 12 integers representing the 'light' current values, 12 integers representing the 'dark' current values and 3 integers representing the forces in three directions from the forceplate. The photodiode outputs were treated in the same manner as the previous program. The values of the forceplate data were multiplied by the appropriate scaling factor to get from the values from the A/D converter integers to Newtons force. This program was LTRFOR and is also listed in Appendix A.

Thus the data stored was three translations and three rotations either with or without three sets of forceplate data. The output programs were able to do three types of analysis. For all cases the data was smoothed using the smoothing routines in section 6.2(ii), for the reasons explained therein. The first two start by plotting three translations and three rotations against time. These can be sectioned into either one or two sections, if one section is marked then the maximum and minimum values of each graph were printed out with the record number at which the maximum or minimum value had occurred. If two sections were marked then the mean and standard deviation for each section were printed out for each graph. Only these two types of analysis were applicable to data without forceplate data, and the program for this was LPLOT, listed in Appendix A. When forceplate data was available either one of the two previous analyses were used or there were nine graphs plotted on the first screen with the three forces time graphs and on these two sections were marked. One of these was the zero force section and the other the section where gradients were required. On the second screen, there were four graphs of displacements against force were plotted; vertical force (F_V) against displacement along the line of the bone (d_Y) and against the rotation about the line of the bone (ϕ_Y), and the vector sum of horizontal forces (F_H) against the vector sum of the displacements perpendicular to the axis of the bone (d_h), and against the vector sum of the rotations about the perpendiculars to the axes of the bone (ϕ_h).

The gradients and correlation coefficients were calculated using the last squares fit method.

6.2(ii) Data Smoothing

The data produced by the transducer needs to be smoothed. As the A/D converter was only a 10 bit converter quantization noise was appreciable, and after the equations were used to calculate the translations and rotations, the quantization noise was increased.

Various smoothing routines were tested. These were smoothing by least squares quadratic fits of orders 5, 7, 9 and 11; and smoothing by 3's and 5's as described by Hamming (1977). Smoothing by 3's and 5's is a combination of smoothing by 3's, which is averaging three points and then smoothing by 5's, averaging over five points.

The frequency of the quantization noise signal is not known, but is produced by sampling at 50 Hz. The frequency of the wanted signal is dependent upon the type of test being performed, but is much lower, below 5 to 10 Hz. Thus the type of filter required will cut-off all signals above 10 Hz and leave those below this unaffected.

The least squares quadratics are:-

5 point

$$y_n = \frac{1}{35}\left[-3x_{n-2} + 12x_{n-1} + 17x_n + 12x_{n+1} - 3x_{n-2}\right] \qquad (6.2.1)$$

7 point

$$y_n = \frac{1}{21}\left[-2x_{n-3} + 3x_{n-2} + 6x_{n-1} + 7x_n + 6x_{n+1} + 3x_{n+2} - 2x_{n+3}\right] \qquad (6.2.2)$$

9 point

$$y_n = \frac{1}{231}\left[-21x_{n-4} + 14x_{n-3} + 39x_{n-2} + 54x_{n-1} + 59x_n + 54x_{n+1} + 39x_{n+2} + 14x_{n+3} - 21x_{n+4}\right] \qquad (6.2.3)$$

11 point

$$y_n = \frac{1}{429}\Big[-36x_{n-5} + 9x_{n-4} + 44x_{n-3} + 69x_{n-2} + 84x_{n-1} + 89x_n$$

$$+ 84x_{n+1} + 69x_{n+2} + 44x_{n+3} + 9x_{n+4} - 36x_{n+5}\Big] \qquad (6.2.4)$$

and that for smoothing by 3's and 5's is:-

$$y_n = \frac{1}{15}\Big[x_{n-3} + 2x_{n-2} + 3x_{n-1} + 3x_n + 3x_{n+1} + 2x_{n+2} + x_n\Big] \qquad (6.2.5)$$

The noise amplification factor for these filters may be calculated by the sums of the squares of the coefficients of the filter (Hamming, 1977):

i.e. 5 point quadratic = 0.4857

7 point quadratic = 0.3333

9 point quadratic = 0.2554

11 point quadratic = 0.2075

3's and 5's smoothing = 0.1644

Thus smoothing by 3's and 5's gave the best noise amplification factor, and this type of smoothing was applied to the data.

6.3 Patient Histories

These tests were performed on seven patients, six of whom were followed for two or more sessions with the fixator support bar in place. Two of these were also tested without the fixator support, prior to going to the operating theatre for removal of the pins; the remaining patient (No. 6) was only tested without the fixator support bar.

Patient 1 F.H. was a 17 year old female student who was riding pillion on a motor cycle when it was hit by a car.

She sustained a fractured left tibia, a fracture to her left femur and laceration of the left knee. She also had fractures of the bases of the third and fourth metacarpels and the distal ulna. The tibial fracture (Fig 6.3.1) was in the middle third, with grade II displacement, grade II comminution, grade II bone loss, and a grade I skin wound. The tibial fracture was treated within 24 hours of the accident with a four pin Mark I rigid Oxford External Fixator, and traction was applied to the femoral fracture. Two weeks, two days, post-injury the femur was fixed with an A.O. plate. Four weeks, one day, post-injury iliac bone graft was applied to the tibial defect, via an anterior approach. The fixed clamps above the fracture were replaced by sliding clamps to convert the fixator to a Mark II sliding fixator (Fig 6.3.2). Pumping was applied daily for ½ hour a day for 5 days, with maximum pressure of 20 psi (140 kPa) for ½ hour per day at 0.5 Hz.

At 5 weeks 3 days, post-injury, strain gauge testing was commenced with straight leg raise tests alone but at 6 weeks 3 days, post-injury, all three tests were performed, and these continued at 9 weeks 3 days, 11 weeks 3 days, 12 weeks 3 days, 16 weeks 3 days, 17

Fig. 6.3.1 Patient F.H. Original Injury

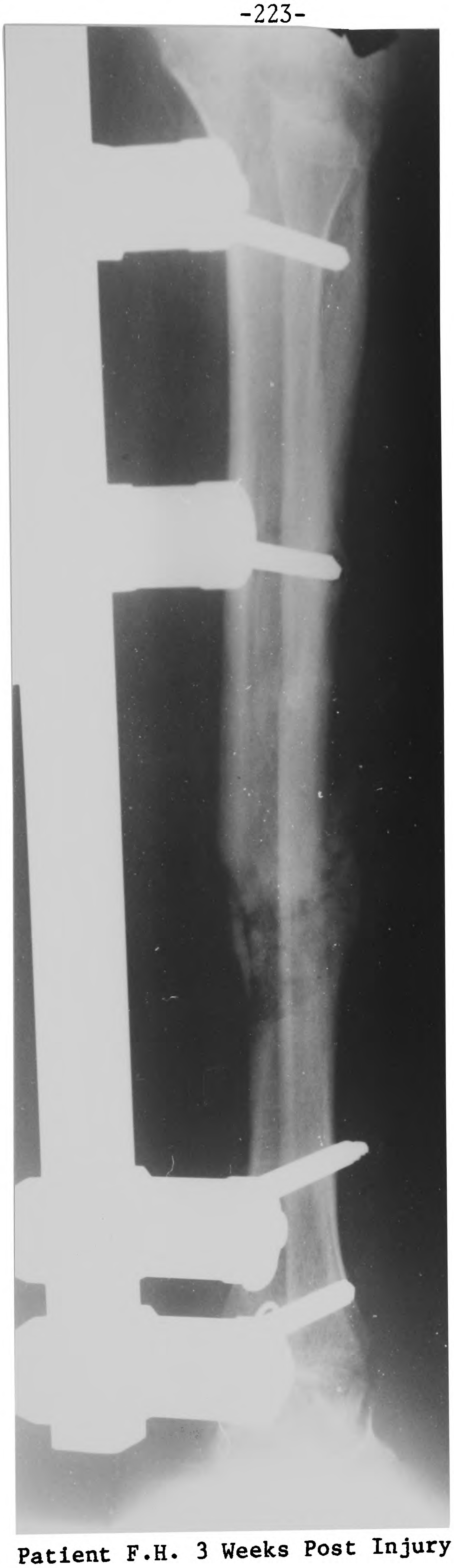

Fig. 6.3.2 Patient F.H. 3 Weeks Post Injury

weeks 3 days and finally at 18 weeks 3 days, post-injury (Fig 6.3.3). Displacement transducer tests were performed at 13 weeks 3 days, 17 weeks 3 days and 18 weeks 3 days post-injury. At 11 weeks 3 days post-injury there was definite pin tract infection of the second pin, and this was treated with Flucloxacillin and Ampicillin, and when she was seen one week later this was considered to be resolving satisfactorily. However, at 15 weeks 3 days the pin tract infection had reappeared, the antibiotic dose was doubled. It was decided at 18 week and 3 days post-injury to admit this patient and at 19 weeks and 1 day post-injury the fixator was removed. There was sound clinical union, and the patient was put in a Sarmiento cast. At 21 weeks and 3 days post-injury there was satisfactory clinical and radiological union. The Sarmiento cast was replaced by a plaster splint for a further month.

One year and 10 months post-injury the A.O. plate was removed from the left femur and 2 years and 4 months post-injury a derotation osteotomy was performed at the subtrochanteric level with 35° of external rotation applied.

Patient 2 J.H., a 48 year old nursing sister, was driving a car in the snow when it slid off the road and overturned catching her right foot in the pedals. Her injuries were a bruise to the left frontal region, small grazes to the dorsum of both hands, and a closed short oblique fracture of the right tibia and fibula at the junction of the middle and lower thirds (Fig 6.3.4). There was a large area of skin bruising and contusion around the posterior aspect of the right calf. She was initially treated with os calcis traction for approximately one week and then put in a long leg plaster, and discharged from hospital.

Fig. 6.3.3 Patient F.H. 18 Weeks Post Injury

Fig. 6.3.4 Patient J.H. Original Injury

She was readmitted later with a large haematoma in the distal aspect of the right calf with skin necrosis, which was excised under general anaesthetic. She was placed back on os calcis traction. Three weeks post-injury a Mark II fixator was applied (Fig 6.3.5). She had 5 days passive stimulation at 25 psi (172 kPa), 0.5 Hz for ½ hour per day. At 8 weeks 6 days post-injury, the second pin from the top was tight but a major discharge occured. The pin was removed and a new pin was inserted away from the previous pin site. She was tested at 11 weeks 1 day, 12 weeks 1 day, 13 weeks 1 day, 14 weeks 1 day and 17 weeks 5 days post-injury. At 17 weeks 6 days, the fibula was divided and a cortico-cancellous iliac bone graft was applied to the fracture, which was showing signs of union with a small mature bar of cortical bone laterally.

At 22 weeks and 1 day post-injury with discharge from the scar, a swab was taken showing the infection to be staphylococcus aureus, and she was given antibiotics. At 24 weeks 1 day, the fracture showed early callus formation, mainly laterally (Fig 6.3.6). Further tests were performed at 25 weeks 1 day, 29 weeks 1 day and finally at 30 weeks and 6 days post injury prior to the fixator being removed and a Sarmiento cast brace being applied. At 41 weeks 1 day she was out of plaster, and told to mobilize with caution, 6 weeks later she was permitted to return to work, and 13 months or 60 weeks 1 day post injury she was discharged, with a sound bony union, and the skin well healed over knee and ankle.

Patient 3 R.S., an 18 year old booksellers clerk was involved in a motorcycle accident. He sustained a fracture to the lower third of the left tibia, with no comminution, grade I displacement, and a skin wound (Fig 6.3.7). The other injuries were a fractured radius and ulna on the ipsilateral side. The next day a Mark I Oxford External

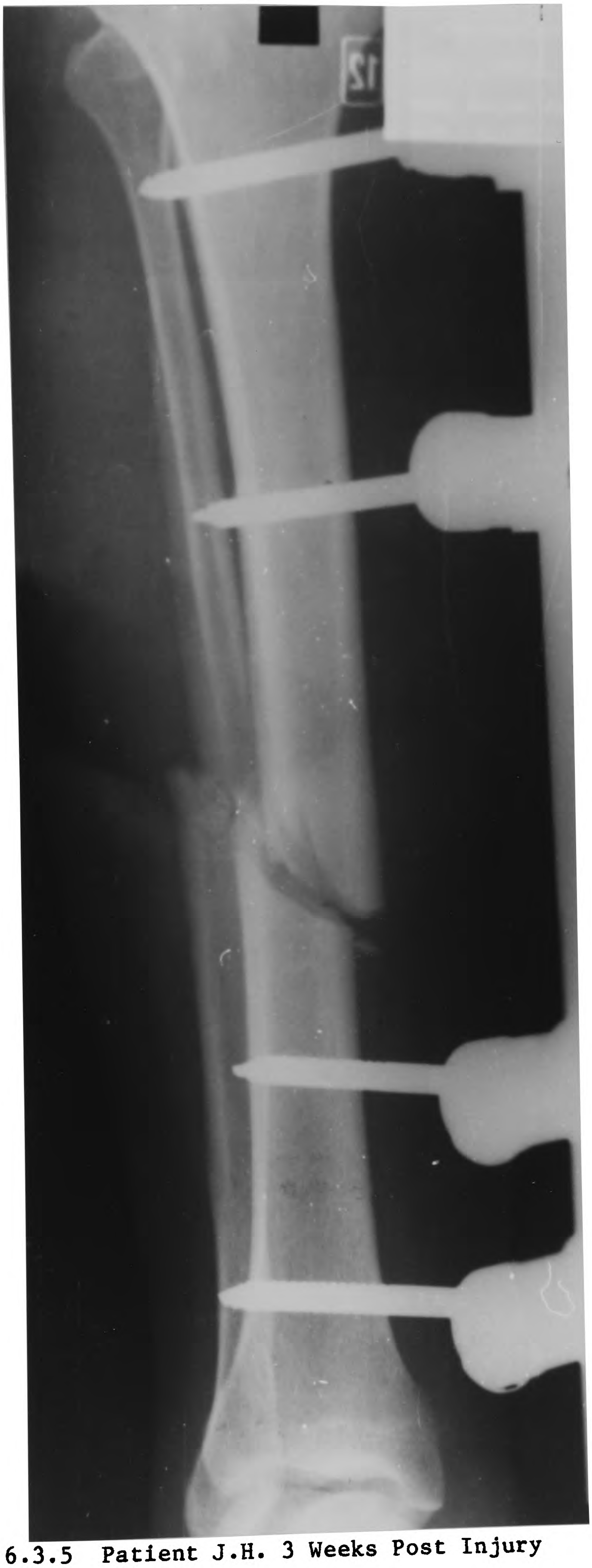

Fig. 6.3.5 Patient J.H. 3 Weeks Post Injury

Fig. 6.3.6 Patient J.H. 28 Weeks Post Injury

Fig. 6.3.6 Patient J.H. 28 Weeks Post Injury

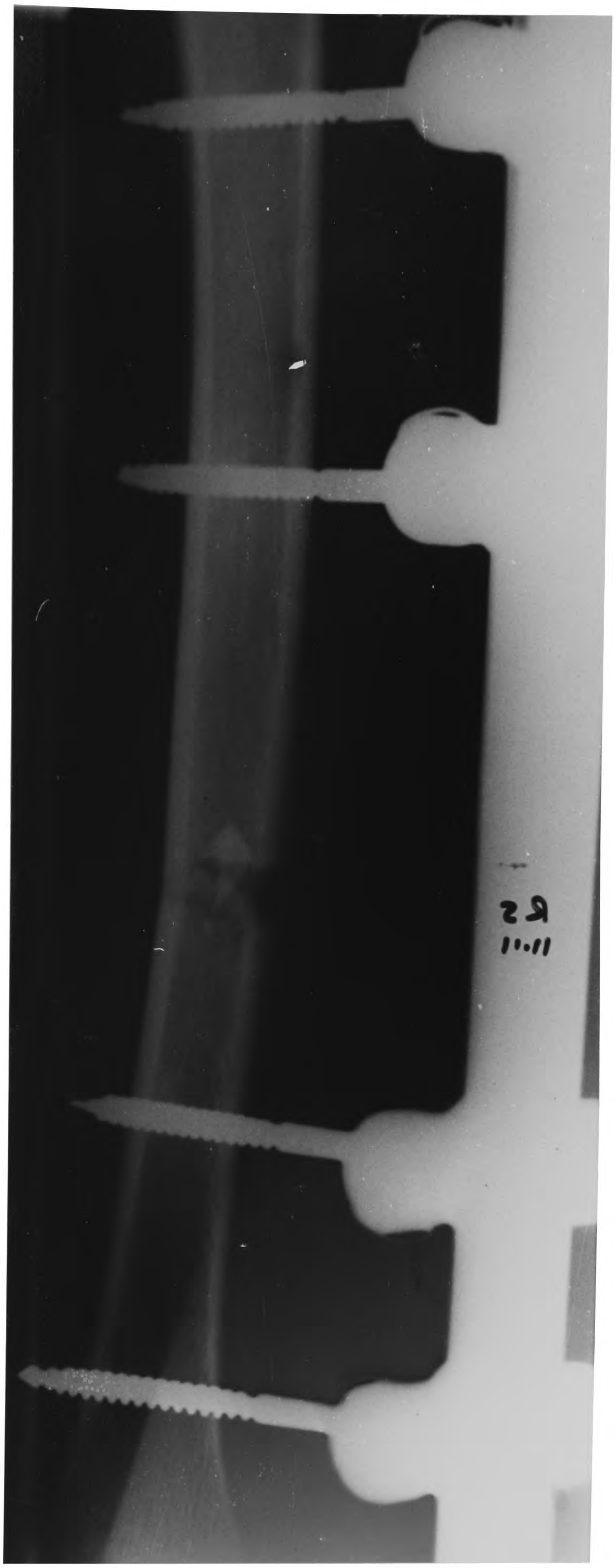

Fig. 6.3.7 Patient R.S. Original Injury

Fixator was applied, and a fasciotomy was performed for a compartmental syndrome . After discharge this patient was lost to follow up until 10 weeks 1 day post-injury, when he reappeared at the hospital. Apparently during the intervening time he had been sitting in a chair at home doing minimal walking with crutches and no weight bearing. He was started partial weight bearing and 12 weeks 6 days post-injury he had an iliac bone graft, and the Mark I fixator was converted to a Mark II fixator. He had eight days of passive stimulation, for half an hour a day with maximum air pressure of 40 psi (275 kPa) until he was discharged. He gradually increased his weight bearing.

This patient was tested weekly from 23 weeks 1 day to 27 weeks 1 day inclusive. X-rays taken 28 weeks 1 day post-injury 'showed early union' (Fig 6.3.8) and a further test was performed at 29 weeks 1 day. 32 weeks 6 days post-injury the fixator was removed after the patient had been tested without the support bar. The fracture was clinically sound, a Sarmiento patella tendon bearing case was applied for 3 weeks, when he was put into an 'Orthoplast' removable splint for 6 weeks. He later refractured with minimal trauma.

Patient 4 J.M., a 25 year old unemployed bricklayer was playing football when he received a kick on his right lower leg. This fractured his tibia and fibula, at the junction of the lower and mid-thirds, with grade II displacement and grade II comminution and no other injuries (Fig 6.3.9). The fracture was manipulated under anaesthetic and os calcis traction was applied. Two days later an acute anterior compartmental syndrome developed, and urgent release was required. Four days post-injury he had a skin graft. On X-ray, 13 days post-injury, there was poor fracture control, and 2 weeks 4 days

Fig. 6.3.8 Patient R.S. 28 Weeks Post Injury

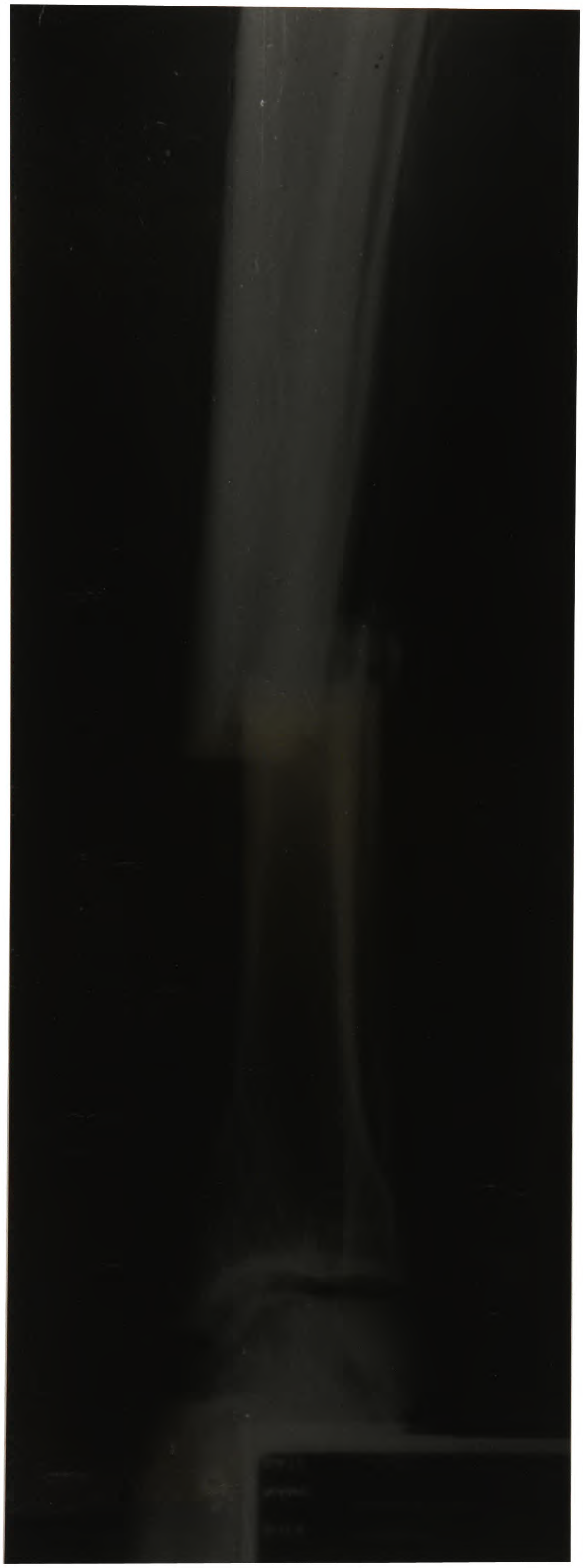

Fig. 6.3.9 Patient J.M. Original Injury

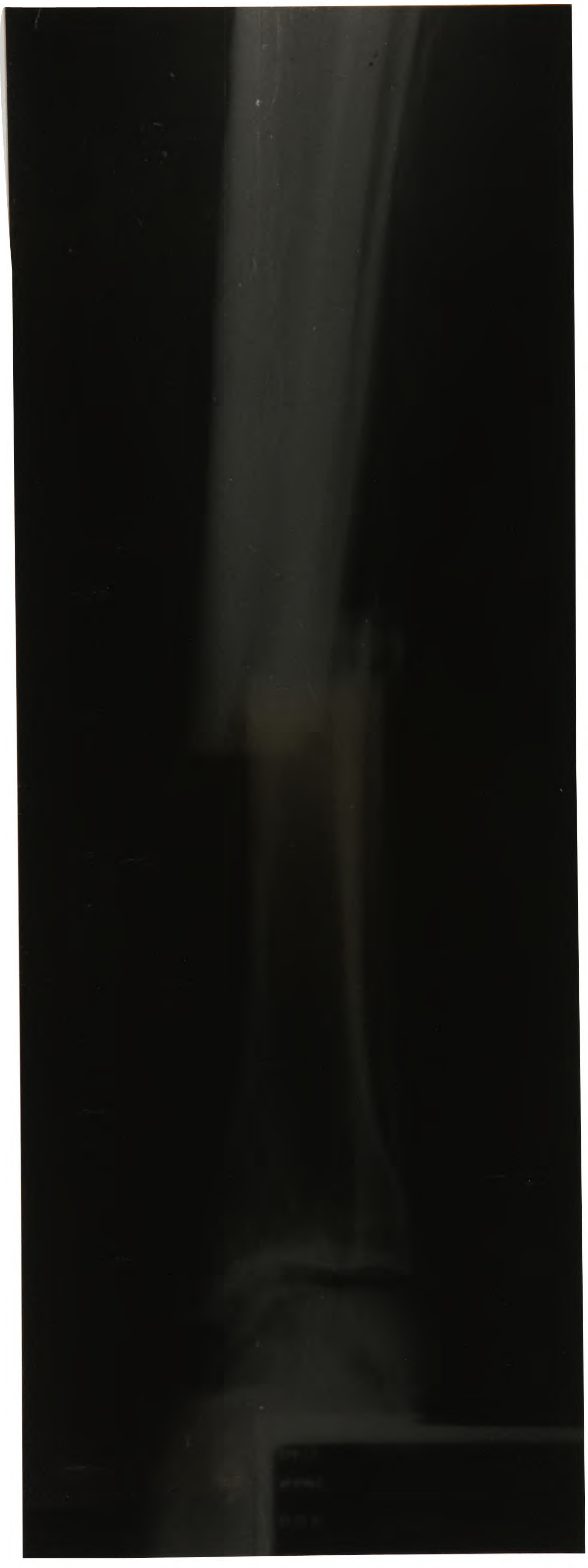

Fig. 6.3.9 Patient J.M. Original Injury

post-injury a 4 pin Mark II Oxford External Fixator was applied. He received passive stimulation for half an hour a day at a maximum pressure of 20 psi (140 kPa) for 2½ weeks. Four days post-fixation angulation was noted at the fracture site, on X-ray, and this was corrected 11 days later. Tests were performed at 6 weeks 3 days, 10 weeks 4 days and 12 weeks 4 days. At 3 months post-injury an iliac bone graft was performed. Further tests were performed at 16 weeks 4 days and 18 weeks 4 days. Figure 6.3.10 shows the fracture 8½ weeks and figure 6.3.11 at 26 weeks post injury. At 29 weeks 2 days post-injury the fixator was removed; tests were performed after the support bar was removed in the ward, before the patient was taken to the operating theatre, for removal of the pins and the application of a Sarmiento patella tendon bearing plaster. At operation all pins were tight with the exception of the lowest one, which had a 'slight rock' and could be screwed out by hand. The Sarmiento was worn for 2 months and then for a further month the patient wore a weight bearing gaiter. One year post-injury this patient underwent lengthening of flexor hallucis longus and fusion of the interphalangeal joint to correct the deformity which had occurred in the hallux.

<u>Patient 5 M.K.</u> This 26 year old motor mechanic was injured when a car crashed into the motorcycle he was riding, fracturing his left tibia and fibula, in the lower third, with grade II displacement and grade II comminution, a grade I puncture wound, but no other injuries (Fig 6.3.12). The fracture was manipulated under general anaesthetic and put in a plaster of paris cast, which was then wedged to improve the position. Four week post-injury the plaster was removed, because of skin necrosis, and poor fracture position. A four pin Mark II Oxford External Fixator was applied (Fig 6.3.13). Passive stimulation was applied for one week, half an hour a day at a maximum pressure of

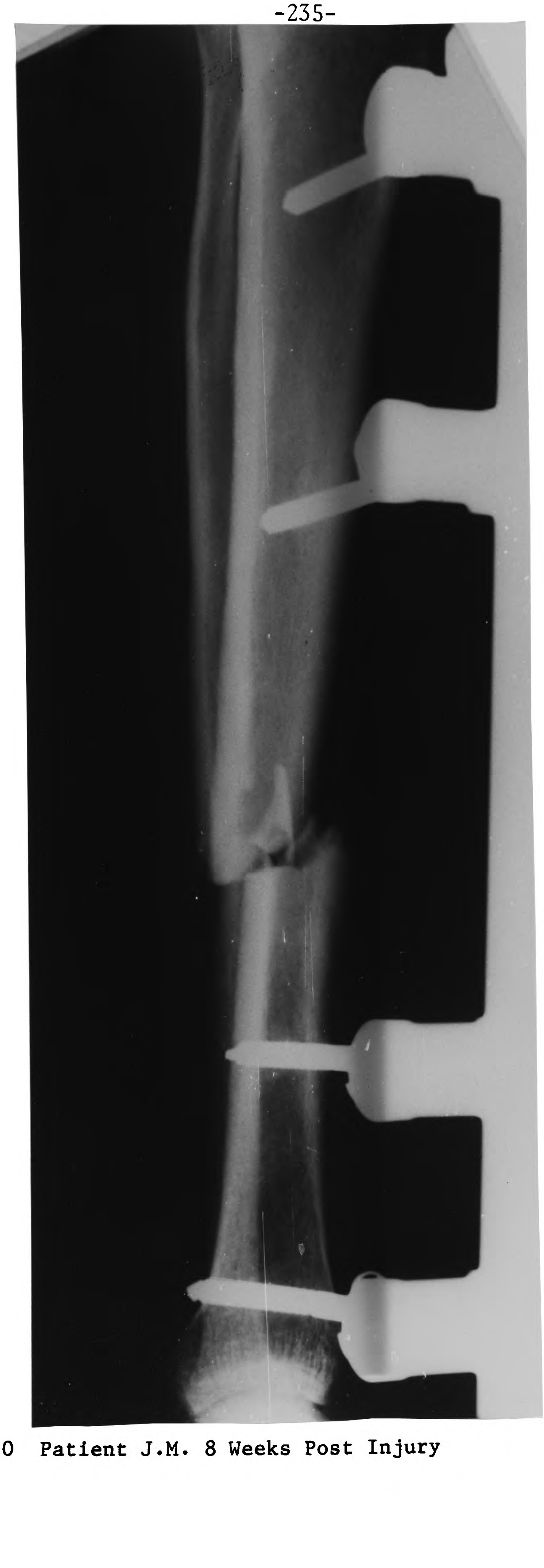

Fig 6.3.10 Patient J.M. 8 Weeks Post Injury

Fig 6.3.11 Patient J.M. 26 Weeks Post Injury

Fig 6.3.12 Patient M.K. Original Injury

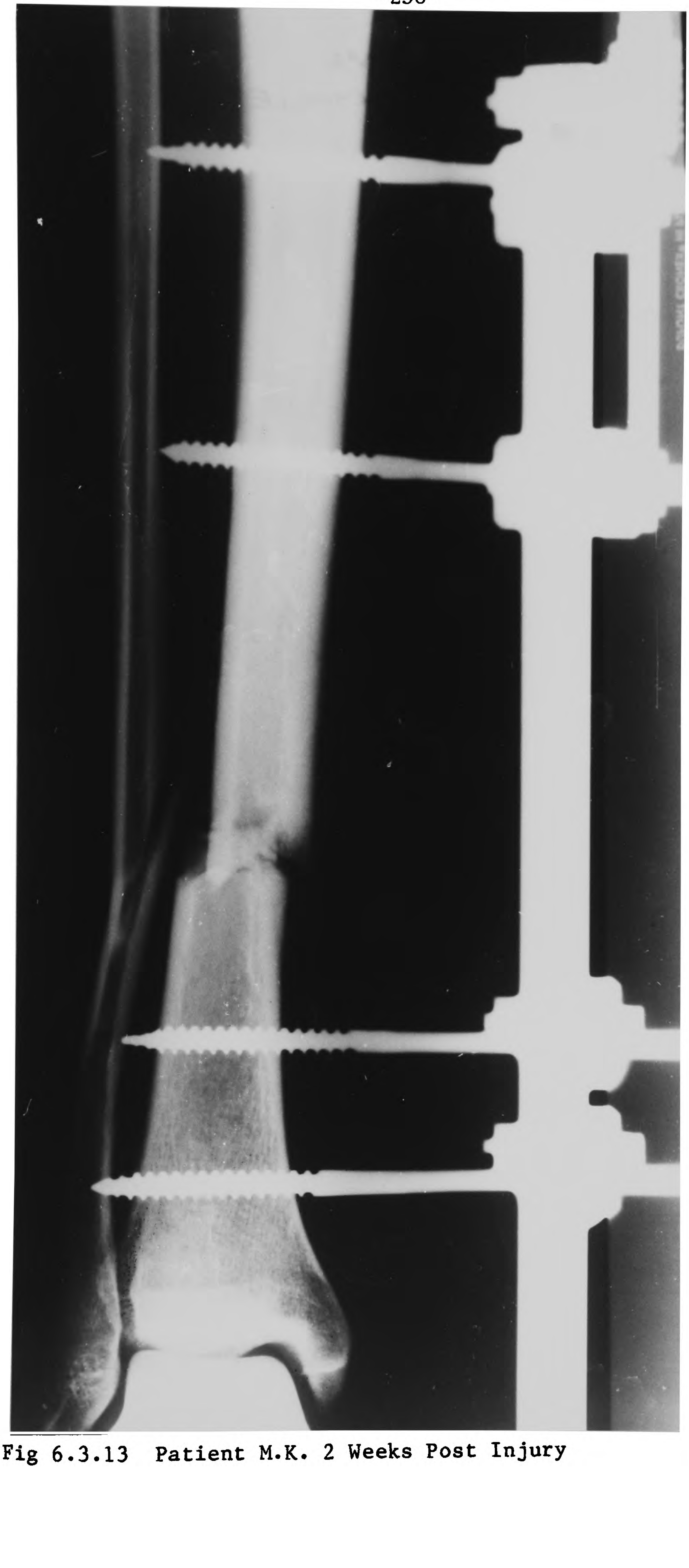

Fig 6.3.13 Patient M.K. 2 Weeks Post Injury

20 psi (140 kPa). Eight weeks post-injury the distraction of the fracture was reduced, no callus was visible on X-ray. Eleven weeks 1 day post-injury he was admitted to hospital for elevation of the limb and antibiotics for a pin site infection with staphylococcus aureus. At 12 weeks 2 days post-injury a test was done and 5 days later the fixator was removed. The lowest pin was loose, and all pin holes had low grade infection. No sound union was present but the bone ends were vascularised, and a Charnley-Juedae bone-grafting procedure was performed with bone from the left iliac crest. The lower fibula was divided, and a long leg plaster was applied. Twenty-seven weeks and one day post-injury the long leg plaster was replaced with a Sarmiento patella tendon bearing cast, but 3 weeks later a 1 cm diameter pressure sore developed below the knee (Fig 6.3.14). Thirty-five weeks and six days post-injury the patient was operated on for a pseudarthrosis of the tibia, with dead bone lying distally. This was excised down to bleeding bone, with cancellous bone graft from the iliac crest packed around the fracture. One inch (25.4 mm) of tibia was resected, and a Mark II Oxford External Fixator was applied medially. Two days later he developed a haematoma, and this was then drained. The patient then made satisfactory progress and X-rays showed increasing union (Fig. 6.3.15). Tests were performed at 37 weeks 1 day, 39 weeks 1 day, 40 weeks 1 day, 48 weeks 1 day and finally at 50 weeks 1 day. At 50 weeks 6 days post-injury the second fixator was removed. The distal two pins were loose, and removed by hand. A small amount of movement was present at the fracture site, and the patient was put into a Sarmiento plaster.

Three months later the fracture was still clinical mobile, and in varus. The patient was asked to come in for osteotomy of the fibula,

Fig 6.3.14 Patient M.K. 30 Weeks Post Injury

Fig 6.3.14 Patient M.K. 30 Weeks Post Injury

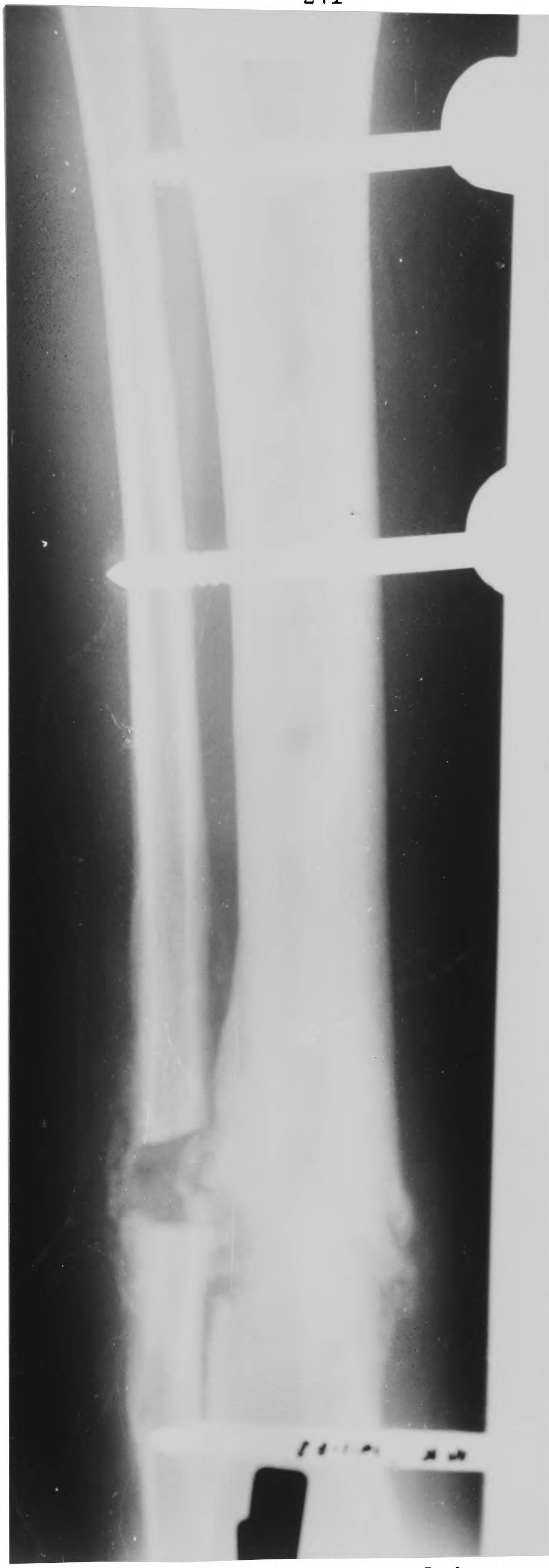

Fig 6.3.15 Patient M.K. 42 Weeks Post Injury

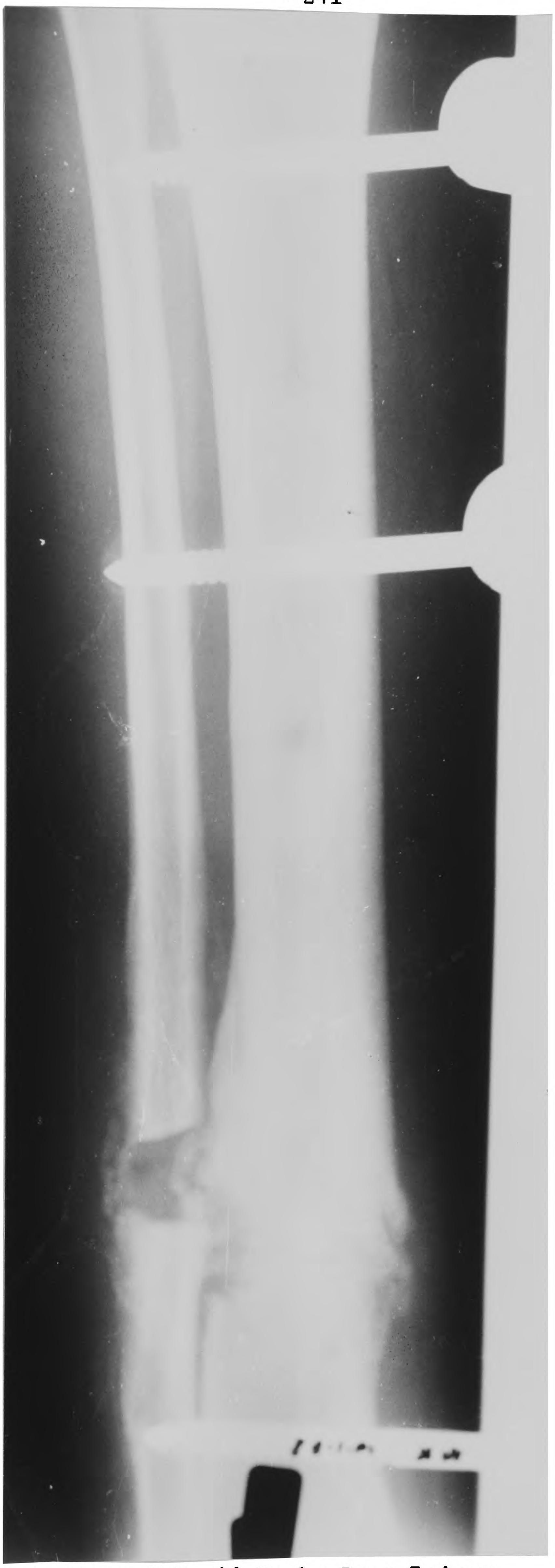

Fig 6.3.15 Patient M.K. 42 Weeks Post Injury

and bone grafting. Treatment is continuing.

Patient 6 D.H. This patient was only tested on the day of removal of his fixator. As a 17 year old he had a motorcycle accident sustaining a mid shaft fracture of his left tibia, which was treated with internal fixation. Eighteen months later he was due to have the plate removed but was knocked down by a car. He sustained a new fracture of his left tibia, at the distal end of the plate, at the junction of the mid and lower thirds, with a fracture of the fibula (Fig. 6.3.16). The tibial fracture was a complicated grade II displacement, grade II comminution, and a grade I + wound. He also dislocated his left knee and fractured his right femur. The femoral fracture was grade II displacement, grade I comminution with a grade II to III wound. Two weeks and three days post-injury a Mark I Oxford External Fixator was applied to the femoral fracture. The internal fixation plate was removed from the left tibia, and this fracture was found not to have healed; 4 weeks 2 days post-injury a five pin Mark II fixator was applied, with two pins above the unhealed mid shaft fracture, one pin between the two fractures and two pins below the new fracture (Figure 6.3.17). He received 2 months of passive stimulation to the femur for half an hour a day, at a maximum pressure of 26 psi (180 kPa) and to the tibia at 22 psi (150 kPa) for half an hour a day, for 6 weeks. At 14 weeks 6 days post-injury the femoral fixator was removed, and at 24 weeks 1 day the tibial fixator was removed and replaced by a Sarmiento patella tendon bearing cast.

Patient 7 J.W. This 20 year old girl was holidaying in Greece when she was knocked down by a car. She sustained multiple injuries to both legs and a skull fracture. The left femur was pinned with a Kuntscher nail and the right tibia had 2 lag screws across the fracture, and a double-sided external fixator. Upon her return to

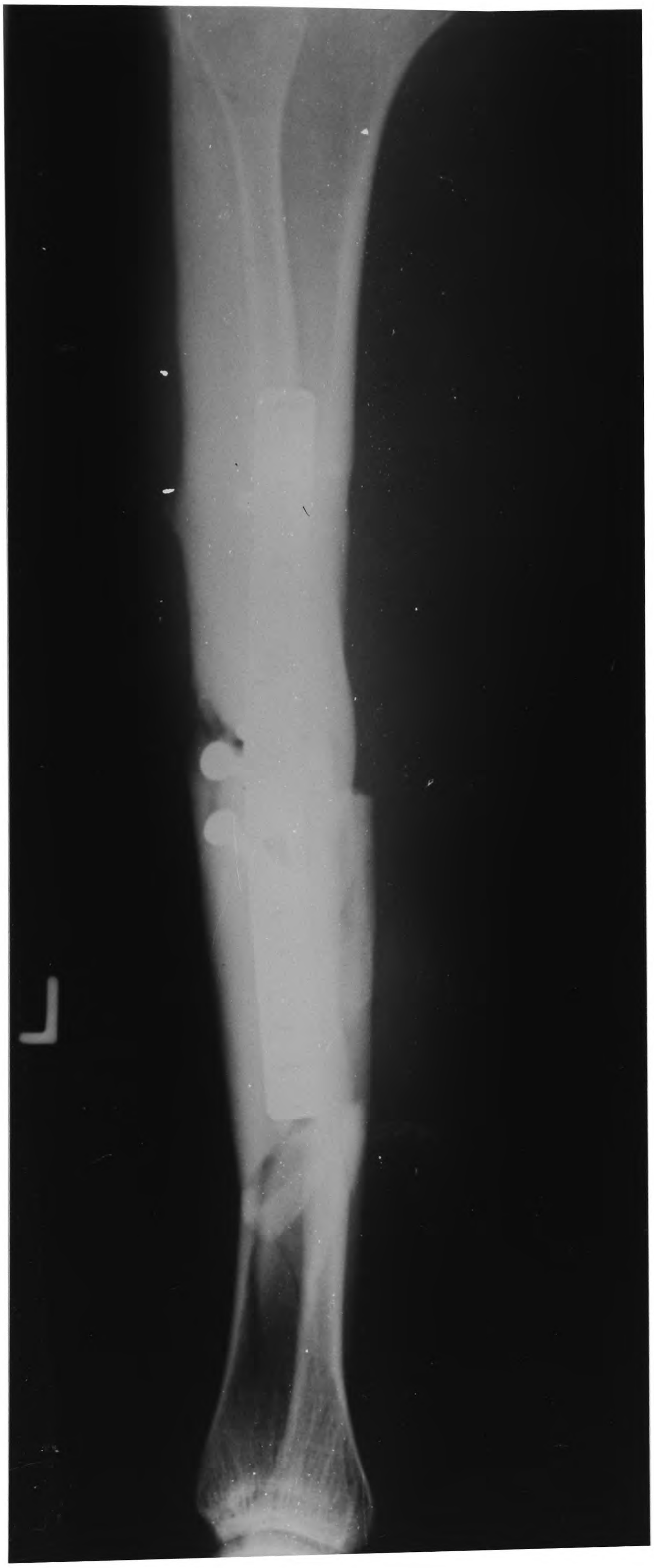

Fig 6.3.16 Patient D.H. Tibial Injury

Fig 6.3.17 Patient D.H. Fixator 2 Days Post Injury

Fig 6.3.17 Patient D.H. Fixator 2 Days Post Injury

England she went to her local hospital, who removed the external fixator, left in the screws and put her in a plaster cast (Fig. 6.3.18). Five months after her original accident she was referred to the Nuffield Orthopaedic Centre, where 21 weeks 6 days post-injury the two screws, which were holding the fracture distracted, were removed and a Mark II Oxford External Fixator was applied (Fig. 6.3.19). She received passive stimulation for 3 days. Tests were performed at 28 weeks 1 day and 34 weeks 1 day. At 34 weeks 6 days post-injury the fixator was removed, and she was put into a Sarmiento cast brace.

Fig 6.3.18 Patient J.W. 16 Weeks Post Injury

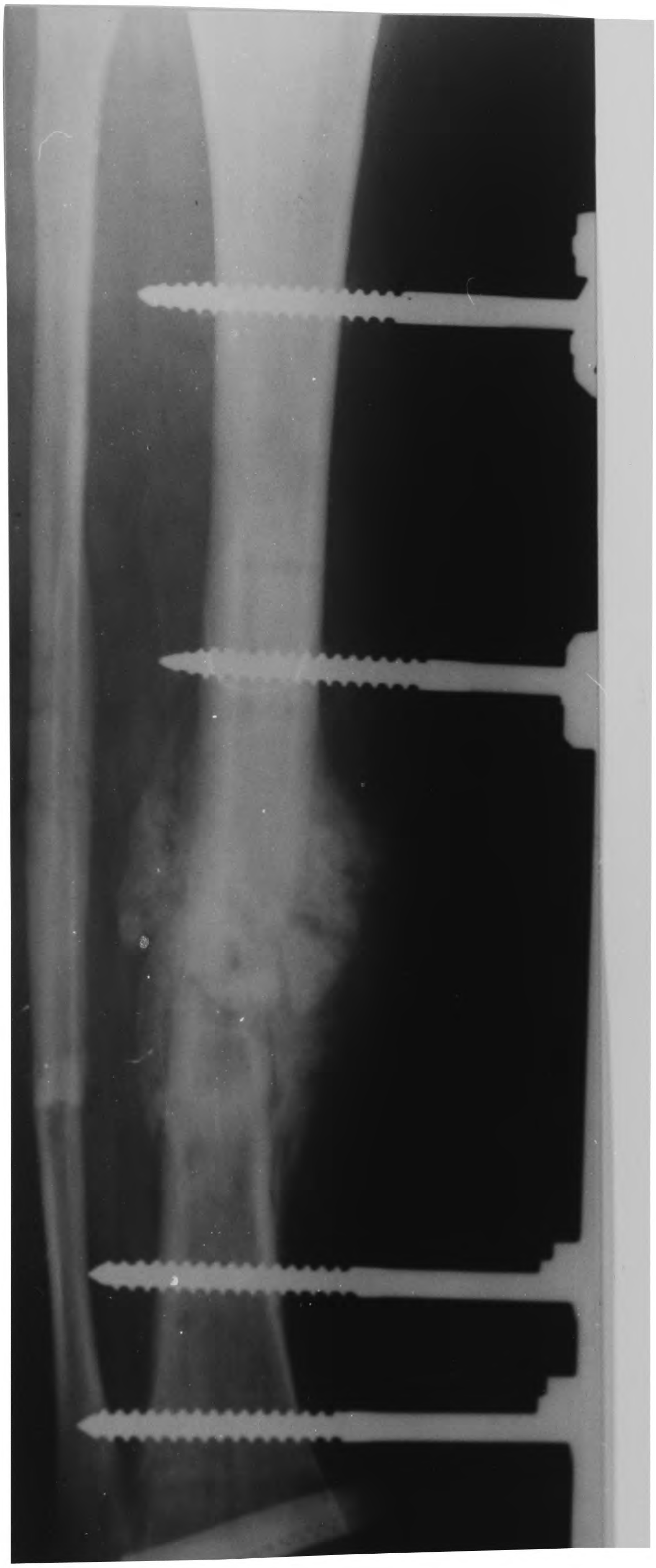

Fig 6.3.19 Patient J.W. 22 Weeks Post Injury

TABLE 6.3.1 Tibial Fracture

Patient	Type of Fracture	Position	Displacement Grade	Comminution Grade	Bone Loss Grade	Skin Wound Grade	Application of Mark I Fixator	Application of Mark II Fixator
1 F.H.	O	M	II	II	II	I	Day 1	4 weeks
2 J.H.	O	L/M	?	?	0	Bruise	-	3 weeks
3 R.S.	T	L	I	0	0	I	Day 2	13 weeks
4 J.M.	O	L/M	II	II	0	0	-	2½ weeks
5 M.K.	T	L	II	II	0	I	-	4 weeks
6 D.H.	O	L/M	II	II	0	I+	-	2½ weeks
7 J.W.	O	M	?	?	?	?	-	5 months

Fracture Type: T - Transverse
O - Oblique

Position: M - Mid-third
L/M - Junction of mid and lower third
L - Lower third

? Data not available from patient's records.

6.4 Results of Displacement Transducer Tests

For the straight leg raise test the three fracture site displacements D_x, D_y and D_z are shown in Figures 6.4.1, 6.4.2 and 6.4.3. D_x and D_z were vector summed to give the total shear movement at the fracture site, D_h, shown in Figure 6.4.4. The three angulations at the fracture site, $\emptyset_x$, $\emptyset_y$ and $\emptyset_z$ with $\emptyset_h$, maximum angulation are shown in Figures 6.4.5 to 6.4.8 respectively. The points marked 'No bar' are for those tests where the fixator support bar was removed.

For three patients (J.H., J.M. and M.K.) the ratio of force applied to the floor to the displacement at the fracture site ('quasi-stiffness') were obtained (Figs. 6.4.9 - 6.4.12). They are considerd separately for each test: LTF = Longitudinal Tibial Force, WT = Weight Transfer, and W = Walking. Four different stiffnesses have been found: the vertical floor force versus d_y the axial displacement, d_y, F_h the horizontal floor force versus d_h the vector sum of d_x and d_z, F_v the vertical force versus $\emptyset_v$ the rotation $\emptyset_y$ about the long axis of the bone, and F_n the horizontal force versus the $\emptyset_h$ the maximum angulation.

The maximum displacements and angulation for the longitudinal tibial force (LTF), weight transfer (WT) and walking (W) tests are shown in Figures 6.4.13 (D_x), 6.4.14 (D_y), 6.4.15 (D_z), 6.4.16 (D_h), 6.4.17 ($\emptyset_x$), 6.4.18 ($\emptyset_y$), 6.4.19 ($\emptyset_z$), 6.4.20 ($\emptyset_h$).

The ratios of D_y to D_h that is the compression/extension displacement to shear displacement is shown for straight leg raise in Figure 6.4.21 and for the remaining three tests in Figure 6.4.23 and the ratios $\emptyset_h$ to $\emptyset_y$ the angulational to torsional angulations are

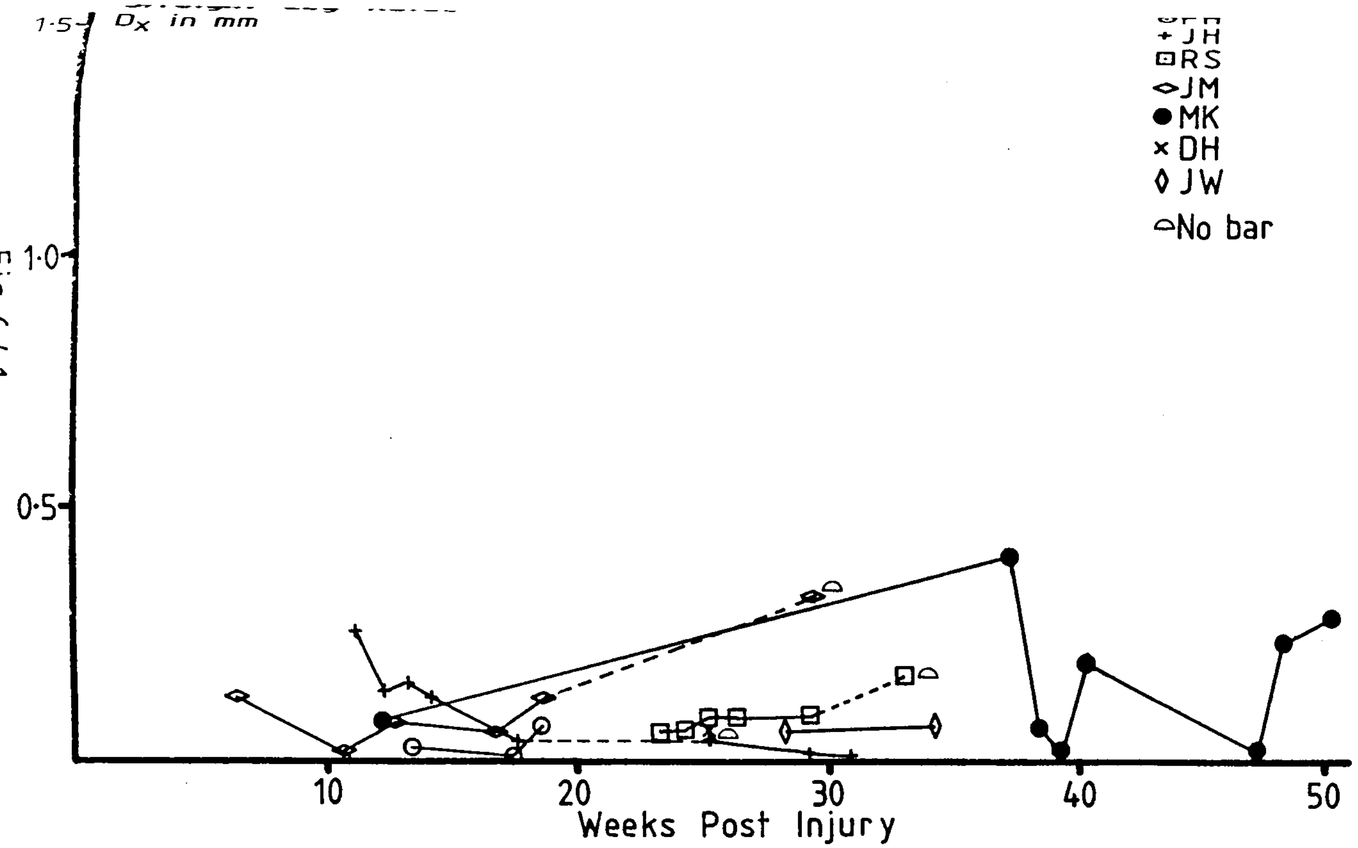

Fig 6.4.1

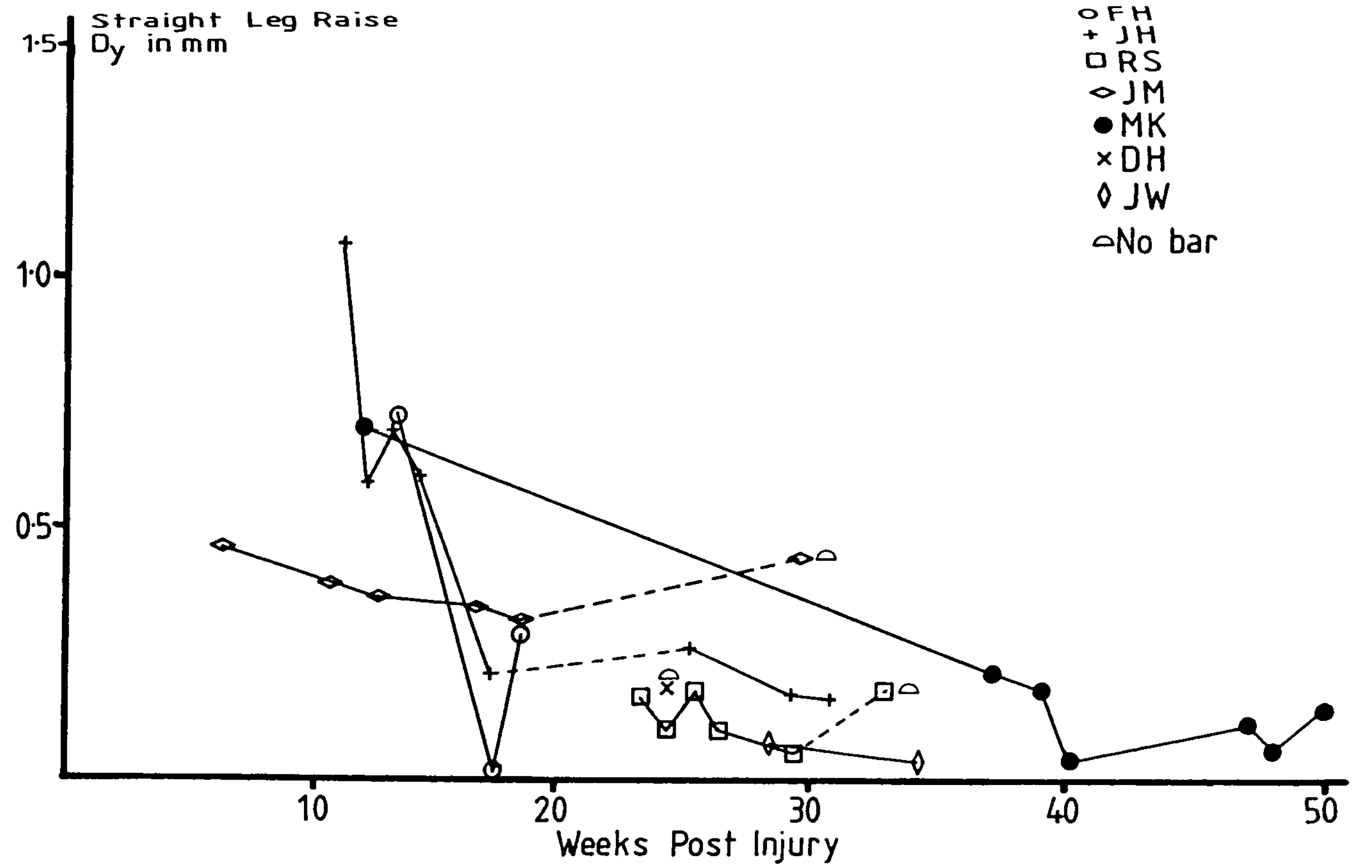

Fig 6.4.2

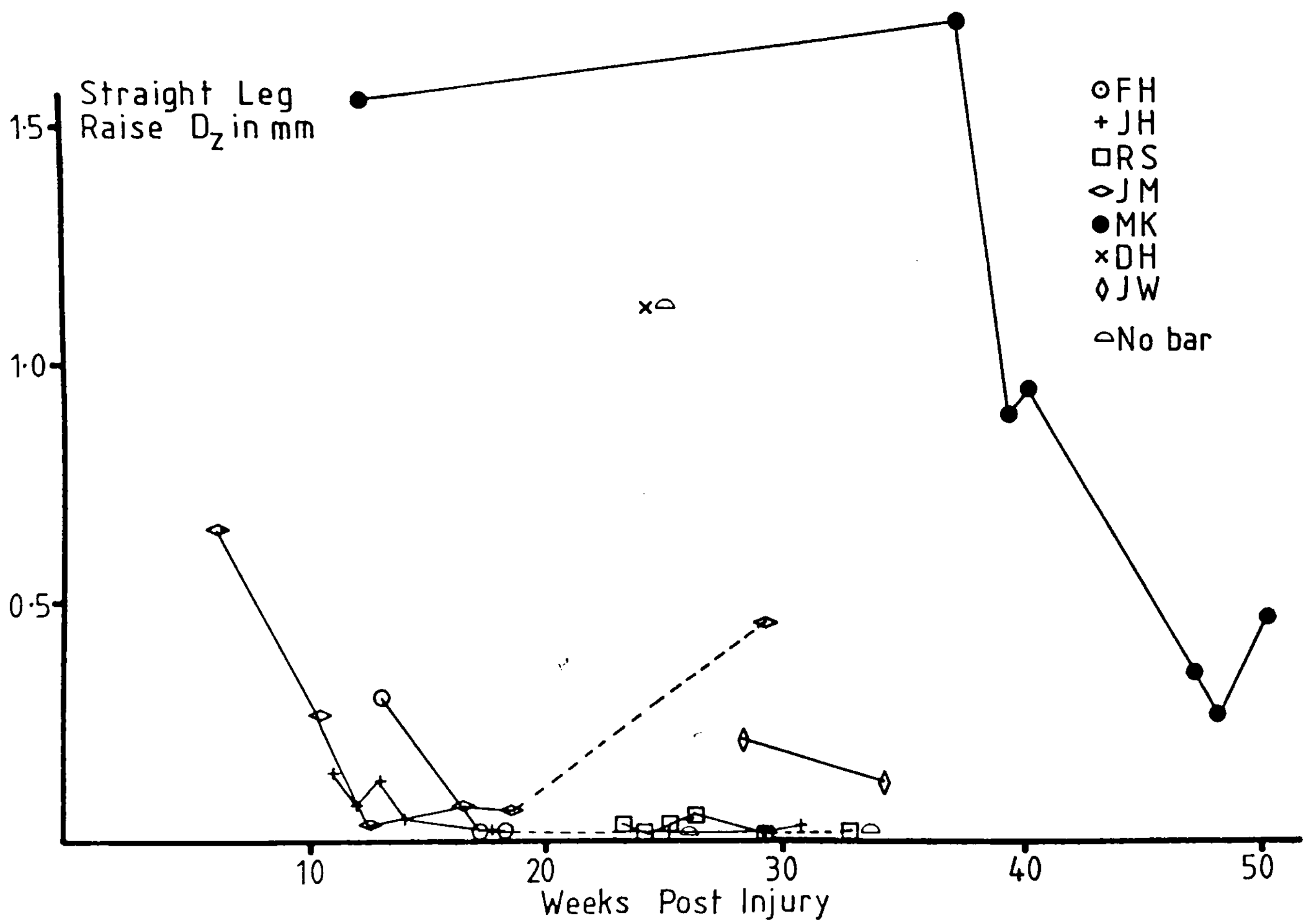

Fig 6.4.3

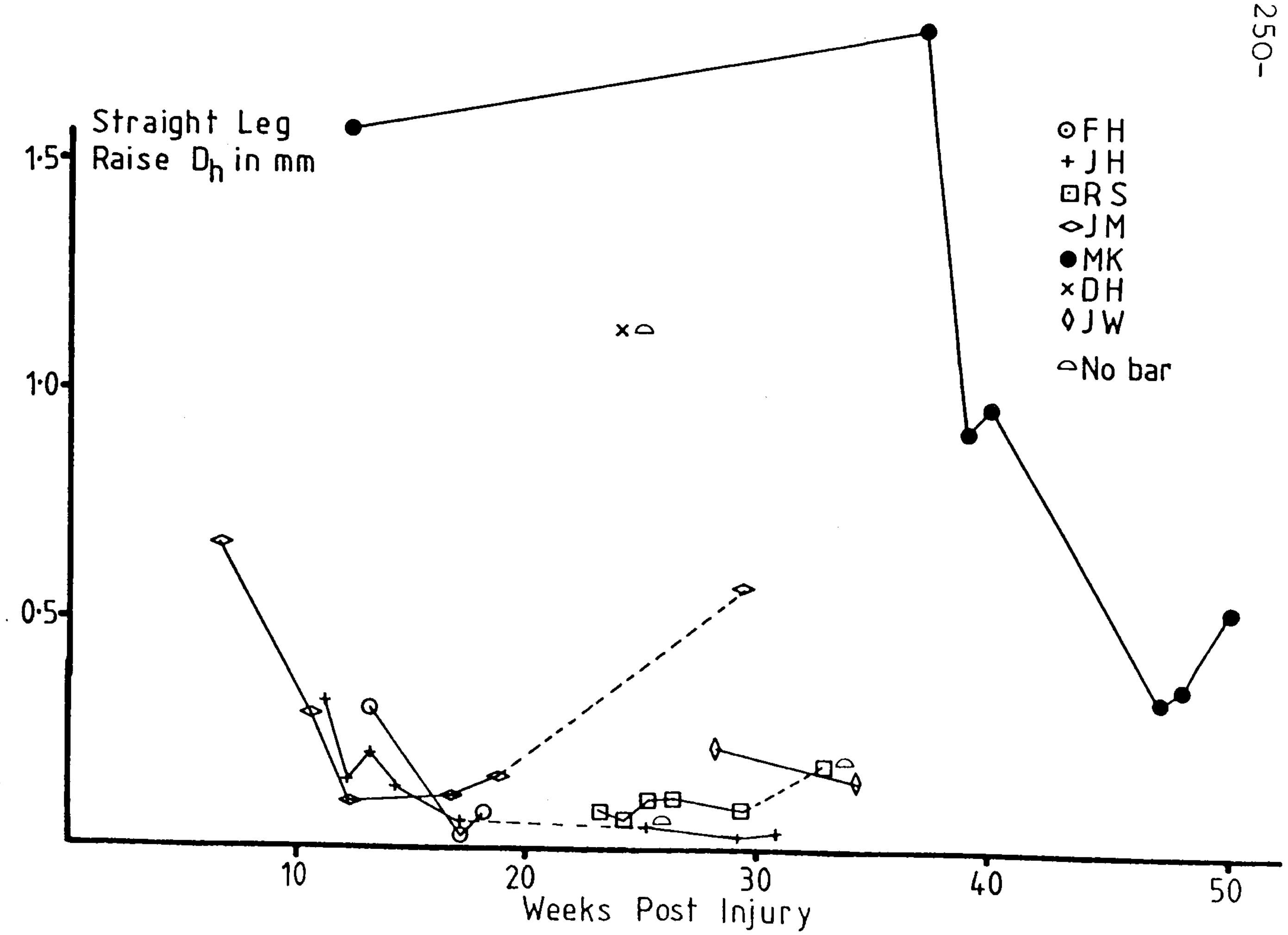

Fig 6.4.4

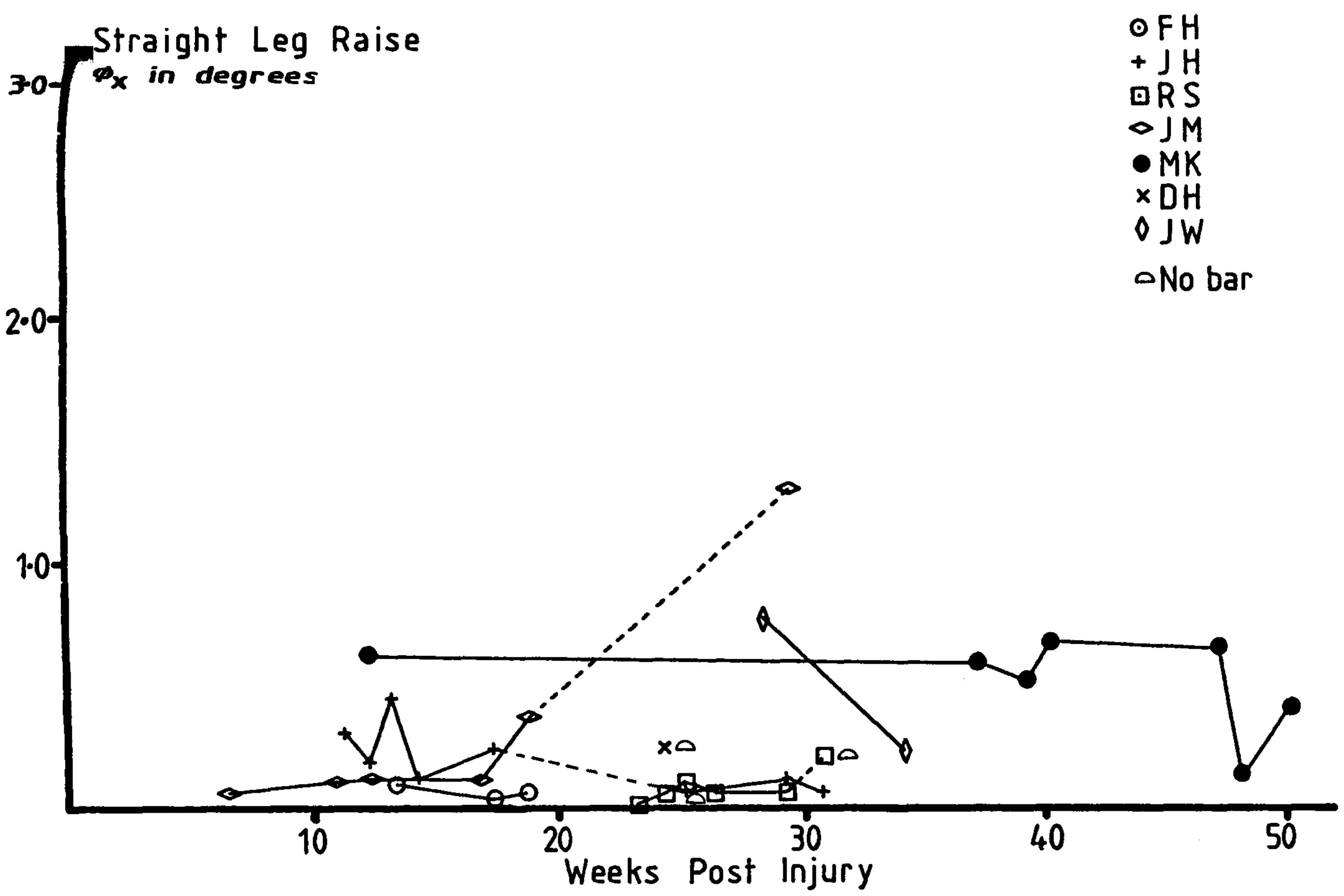

Fig 6.4.5

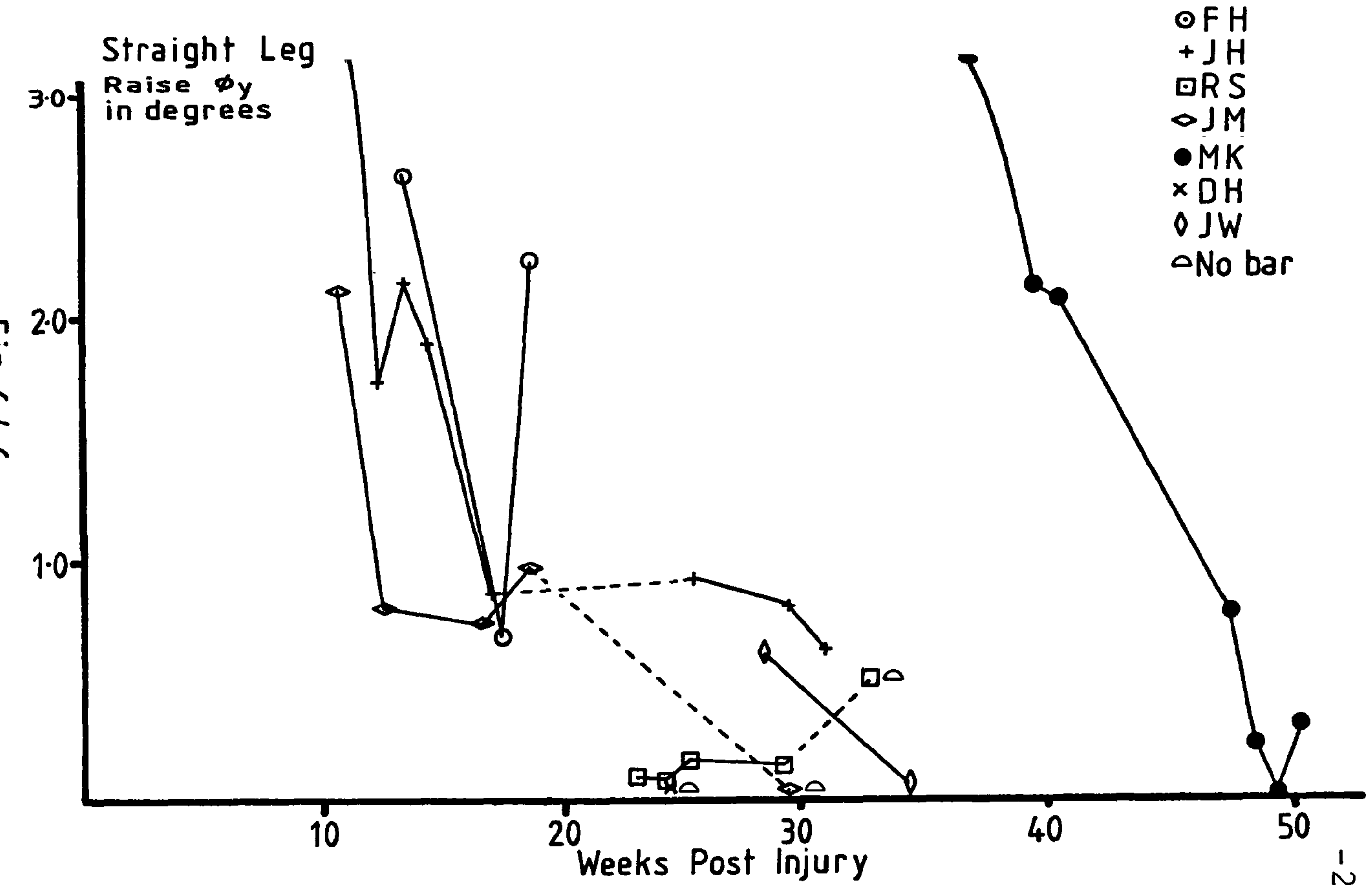

Fig 6.4.6

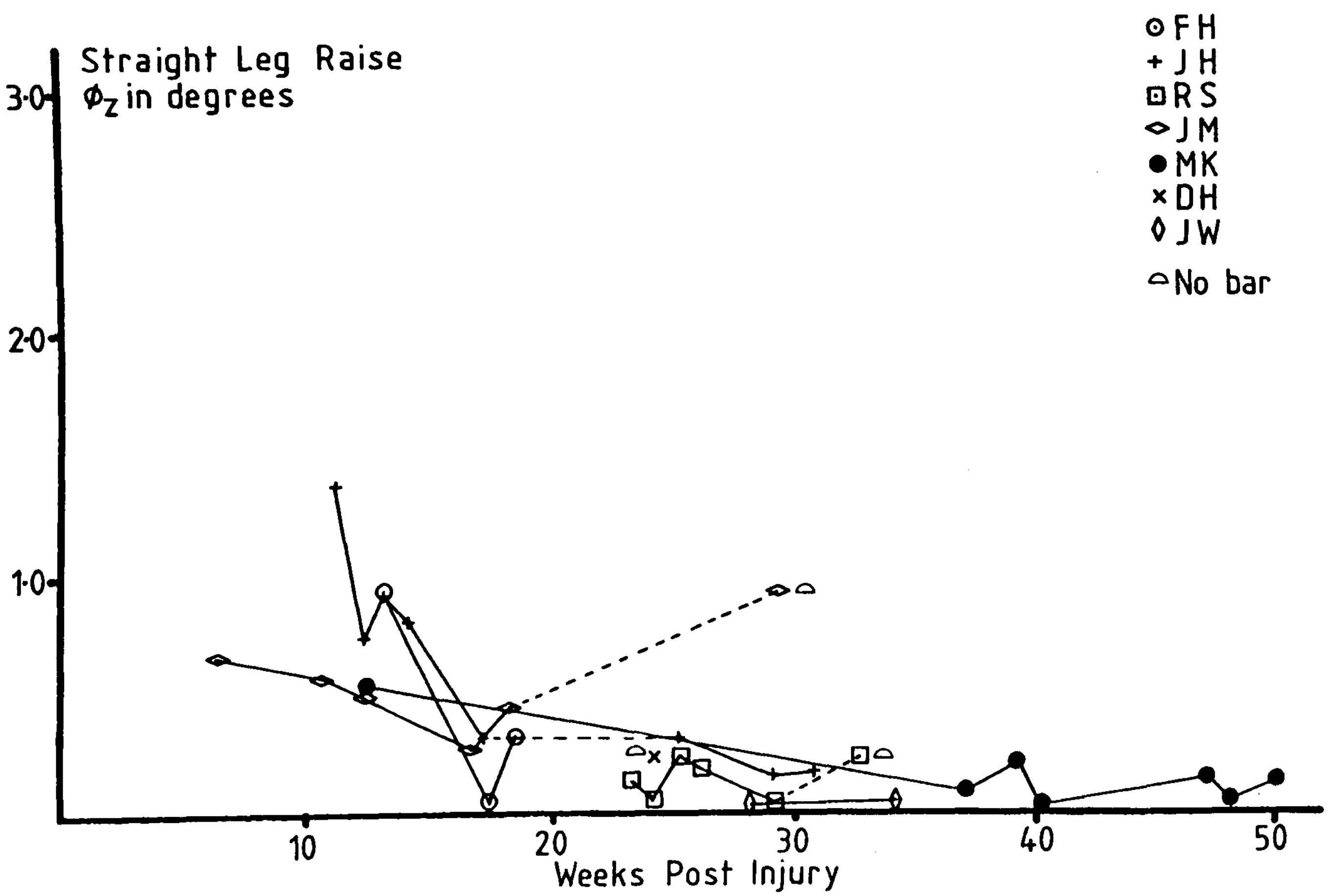

Fig 6.4.7

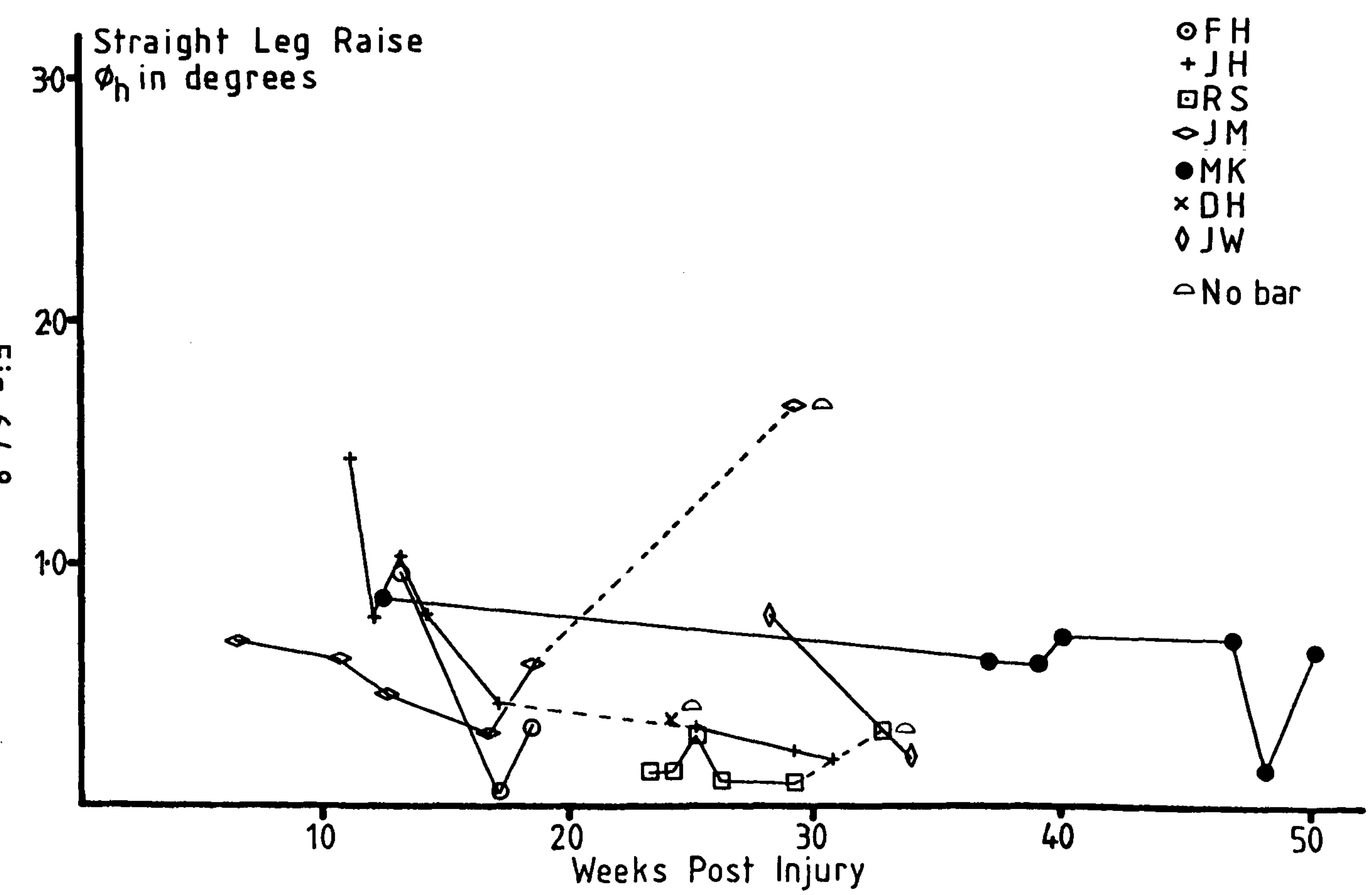

Fig 6.4.8

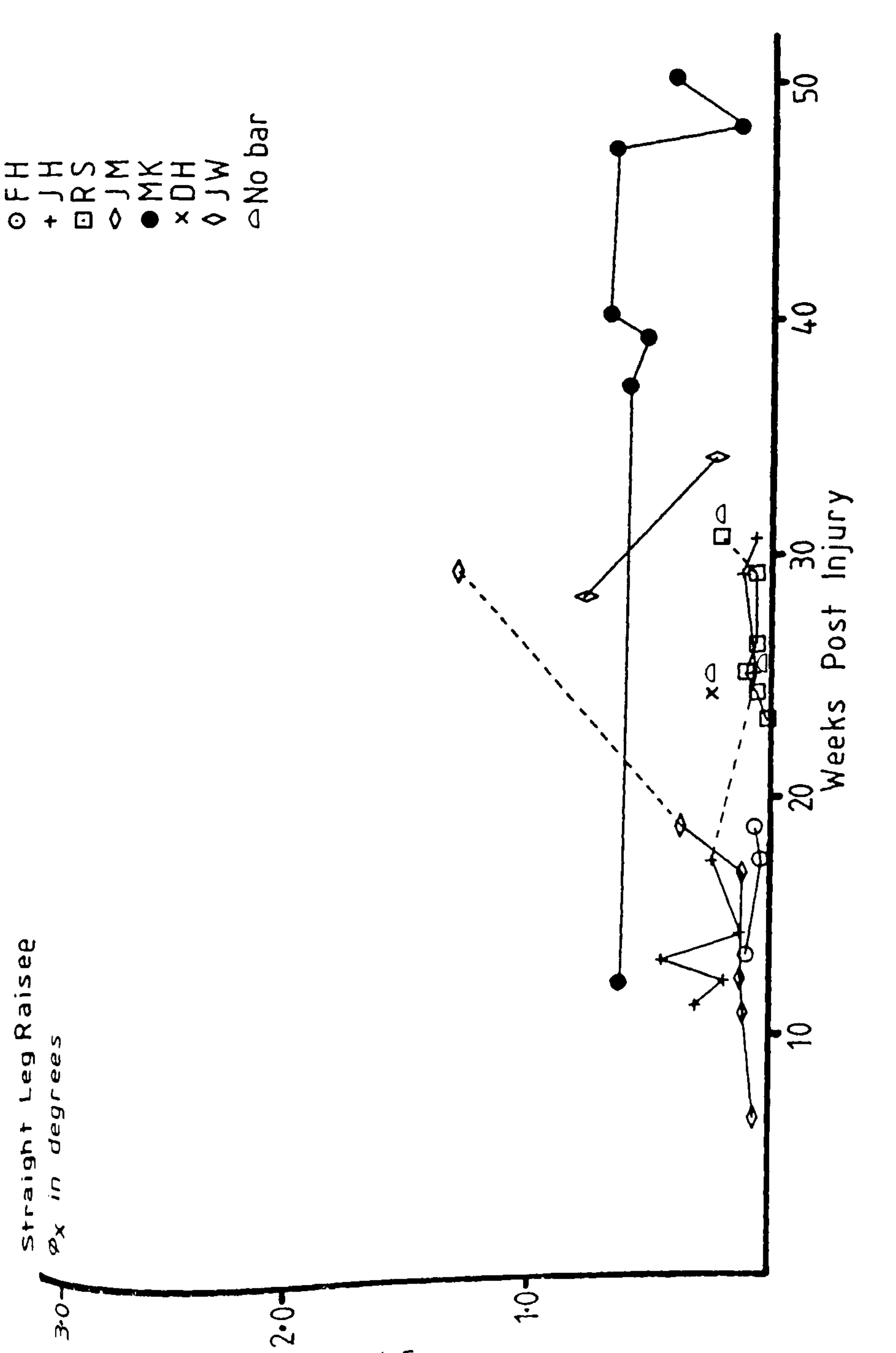

Fig 6.4.5

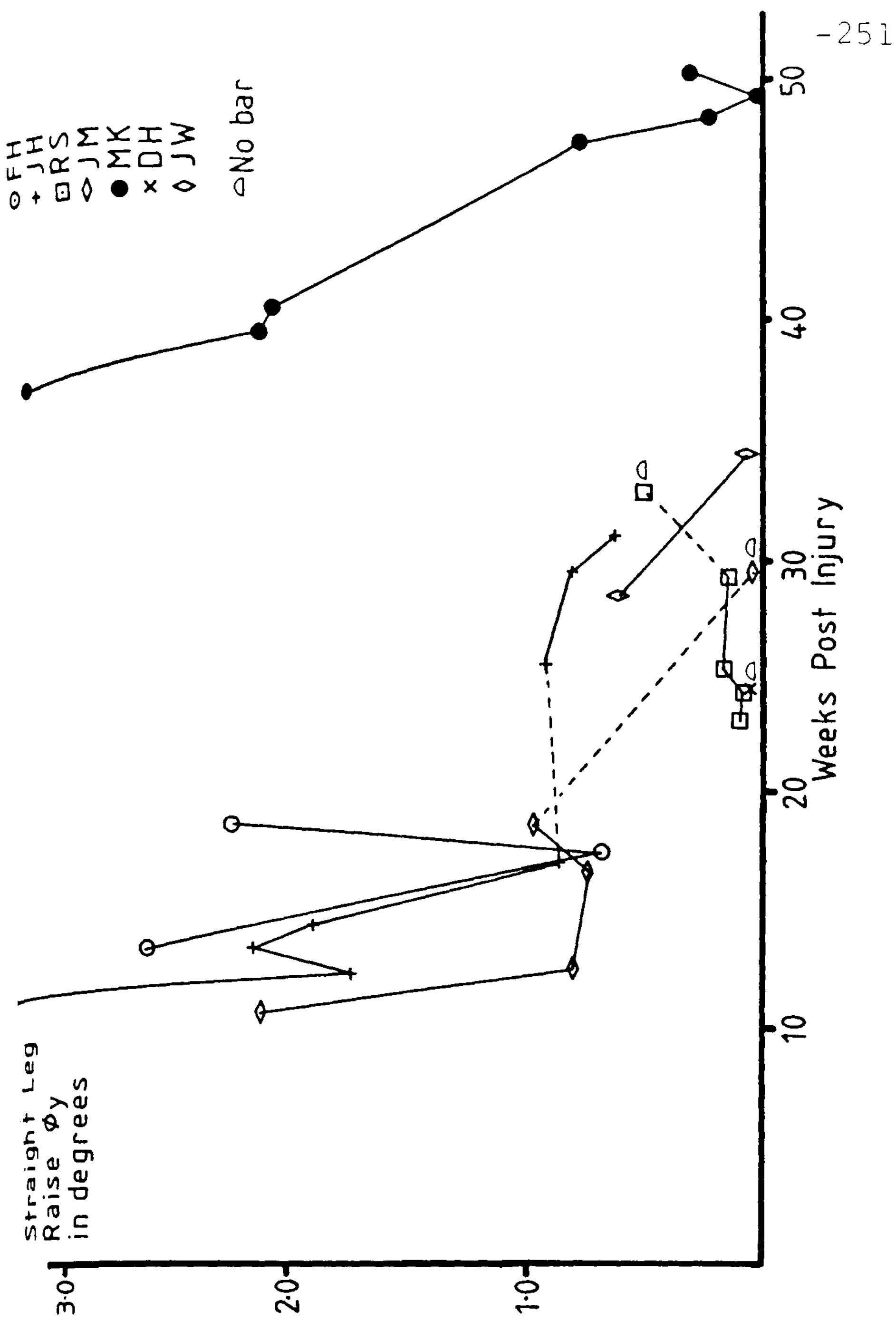

Fig 6.4.6

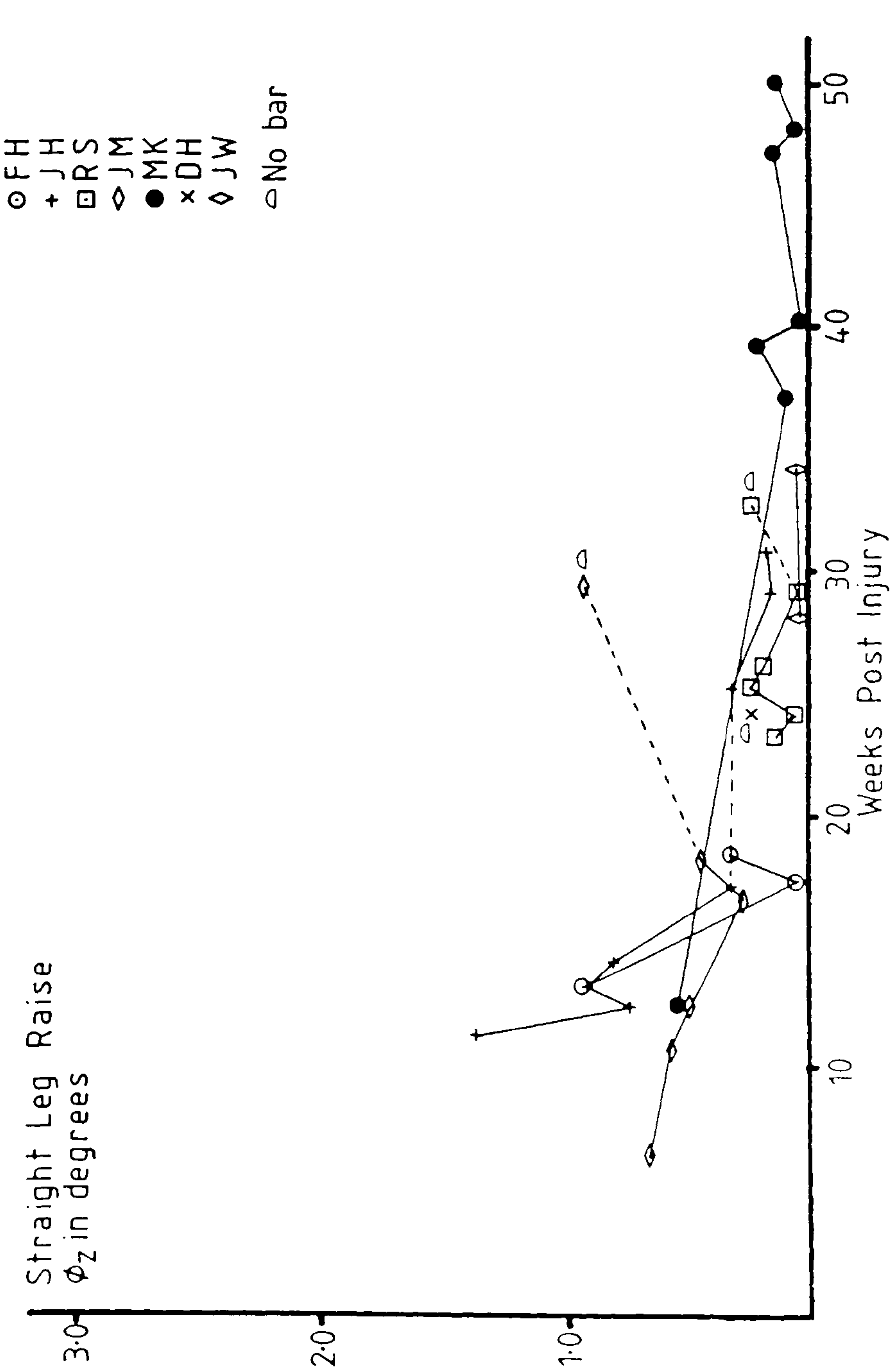

Fig 6.4.7

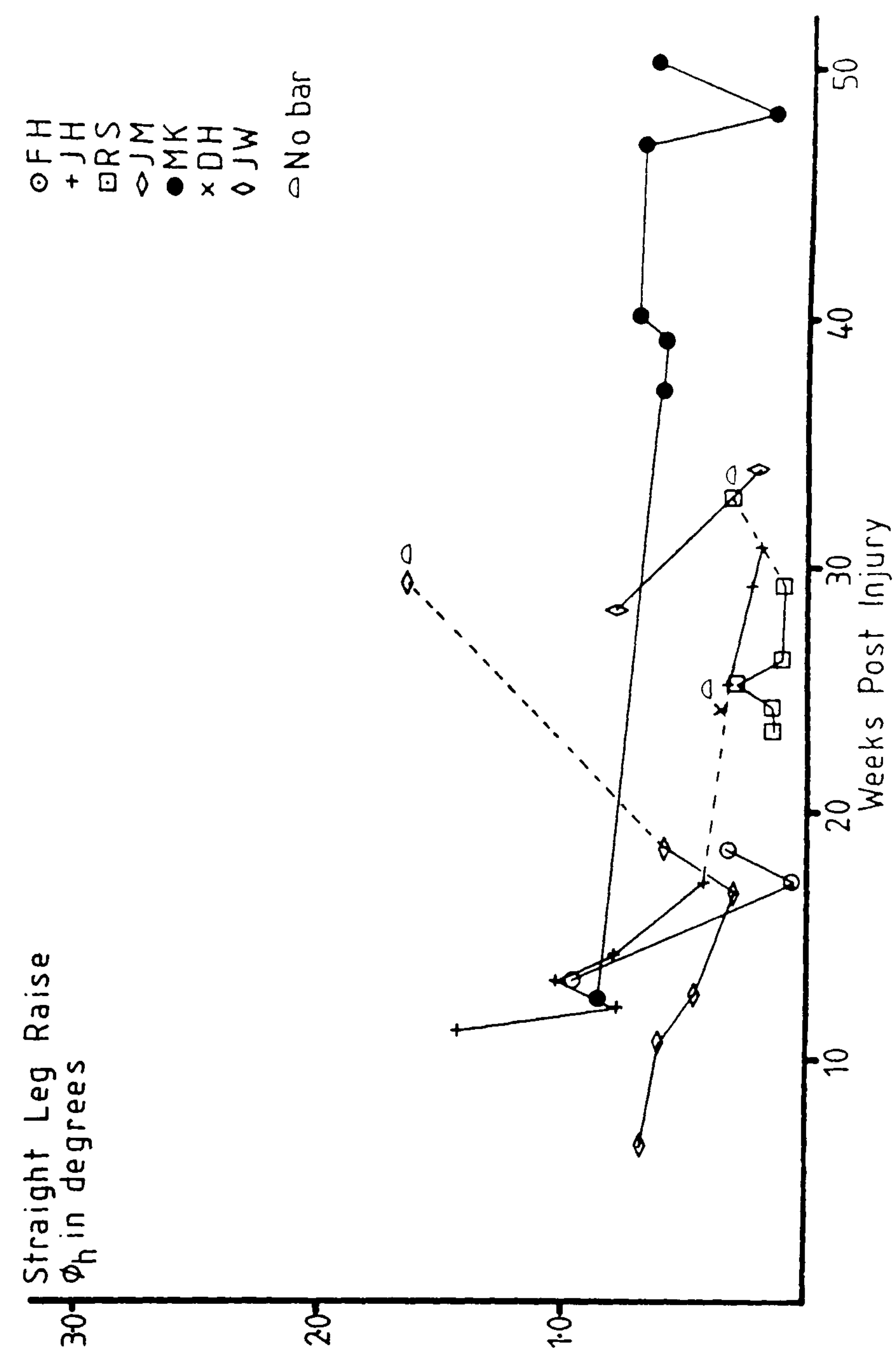

Fig 6.4.8

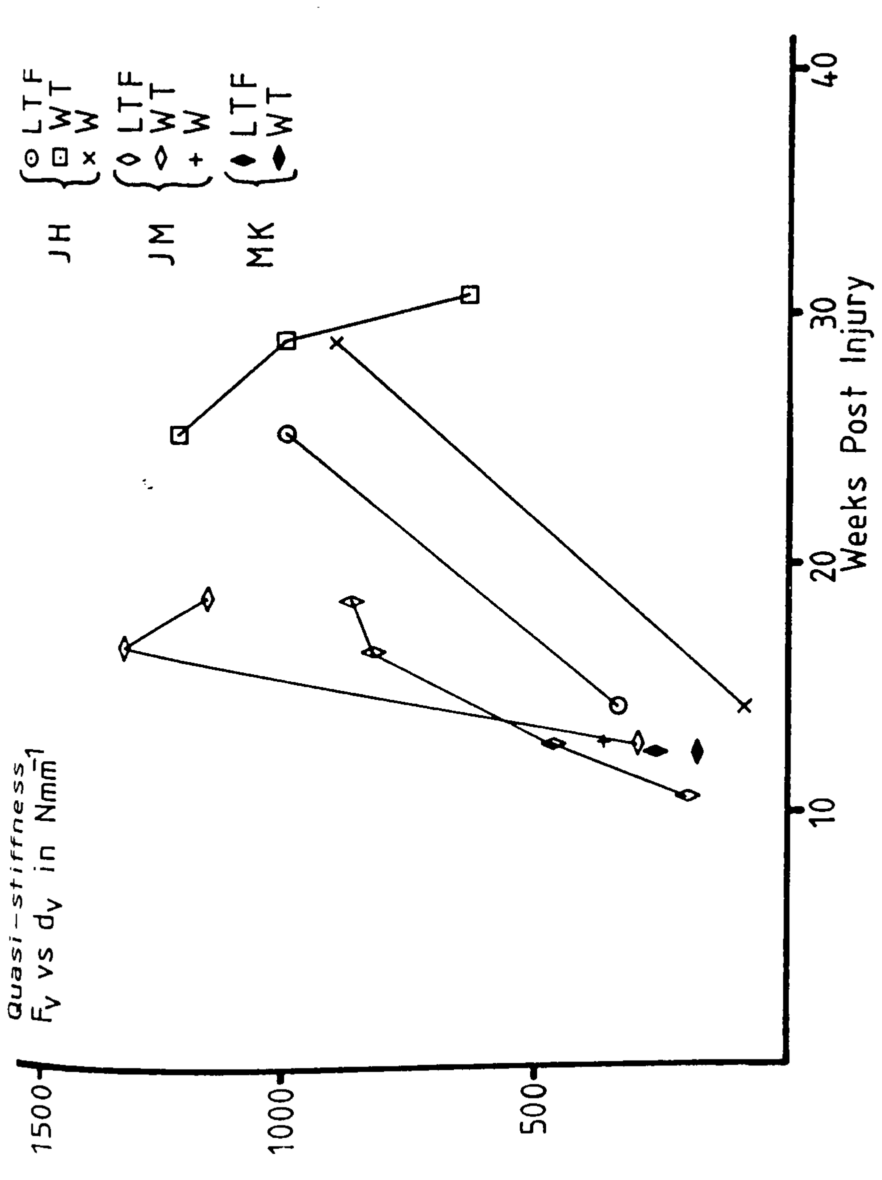

Fig 6.4.9

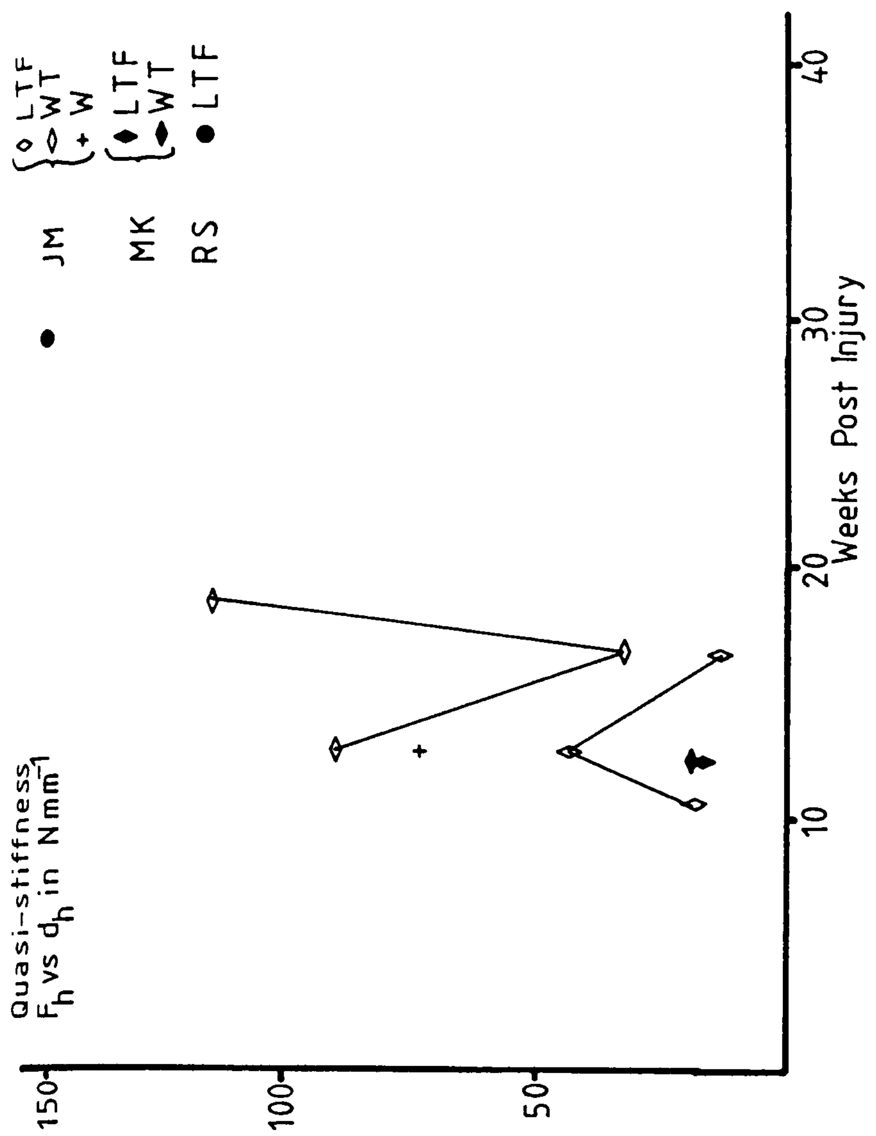

Fig 6.4.10

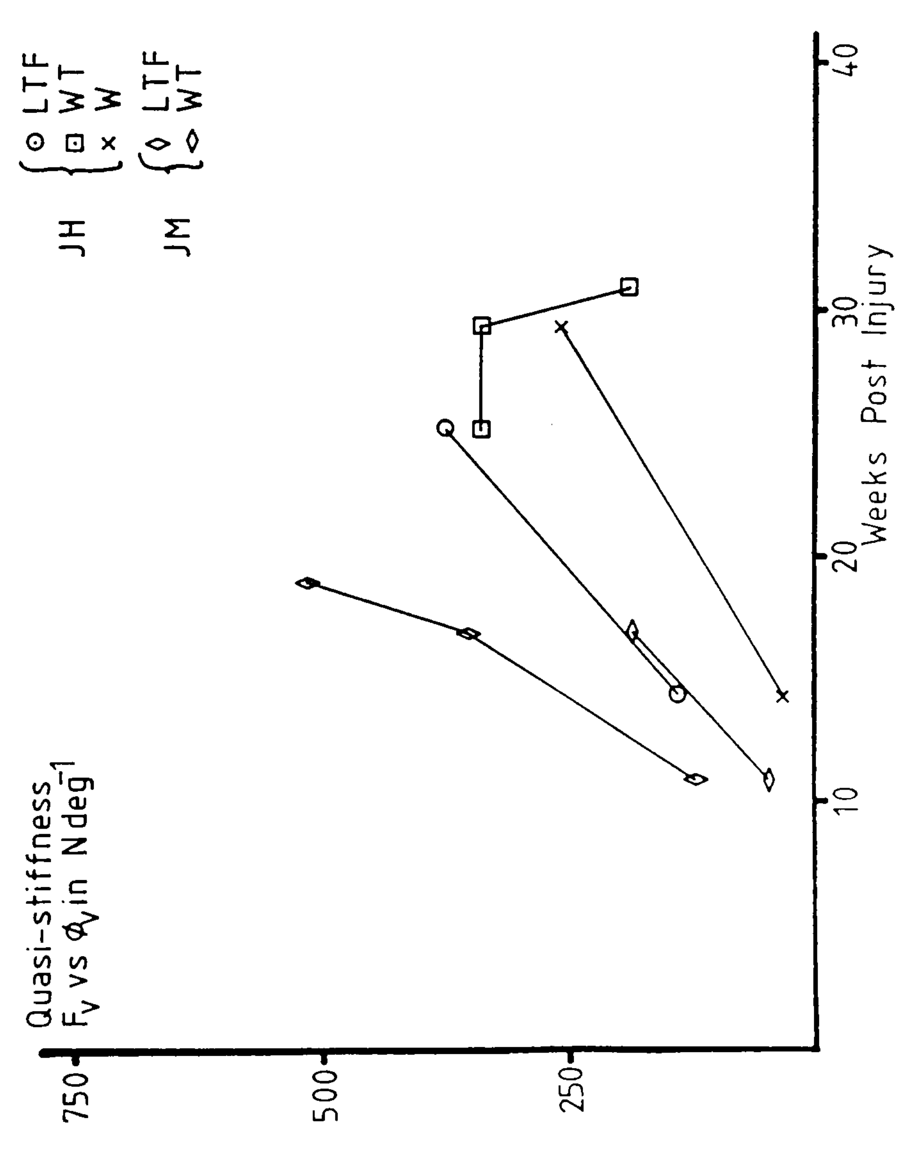

Fig 6.4.11

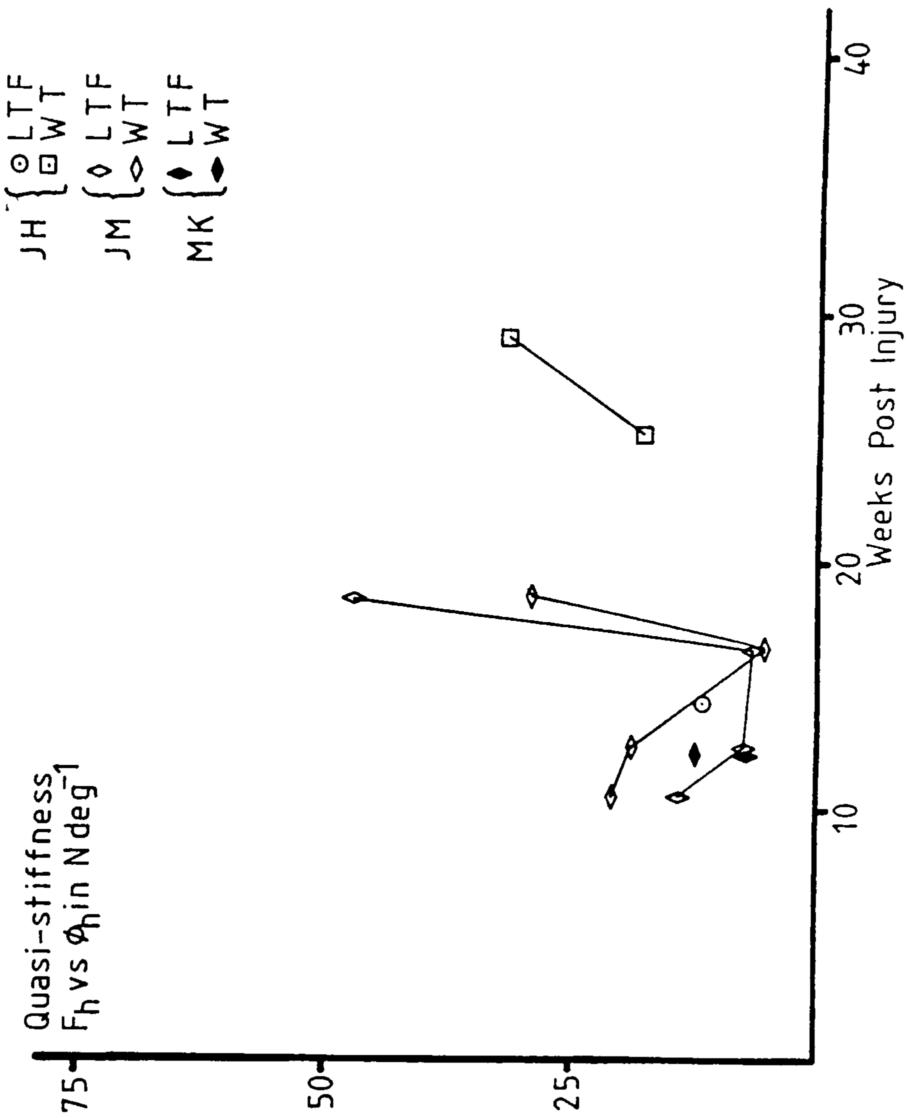

Fig 6.4.12

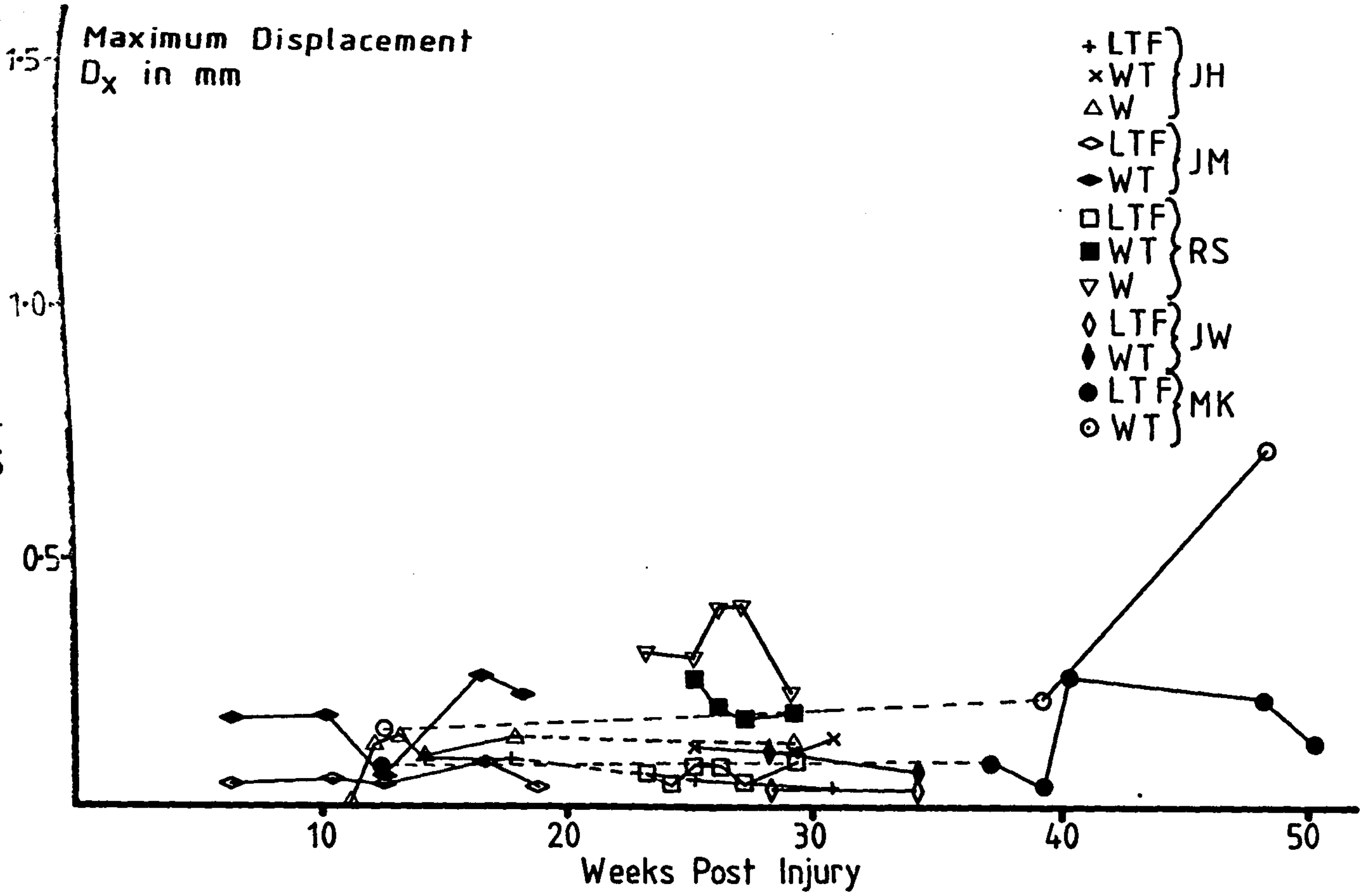

Fig 6.4.13

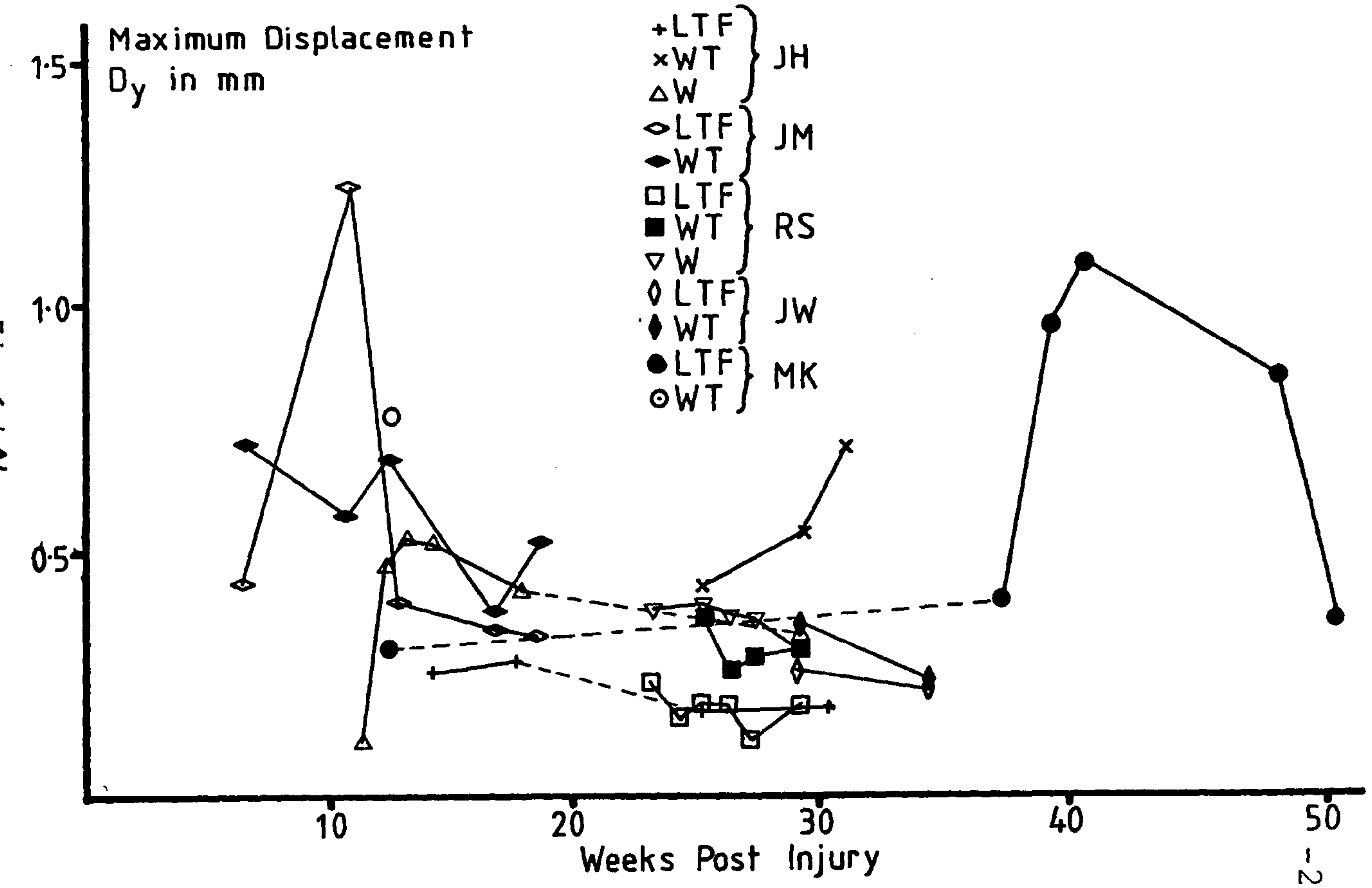

Fig 6.4.14

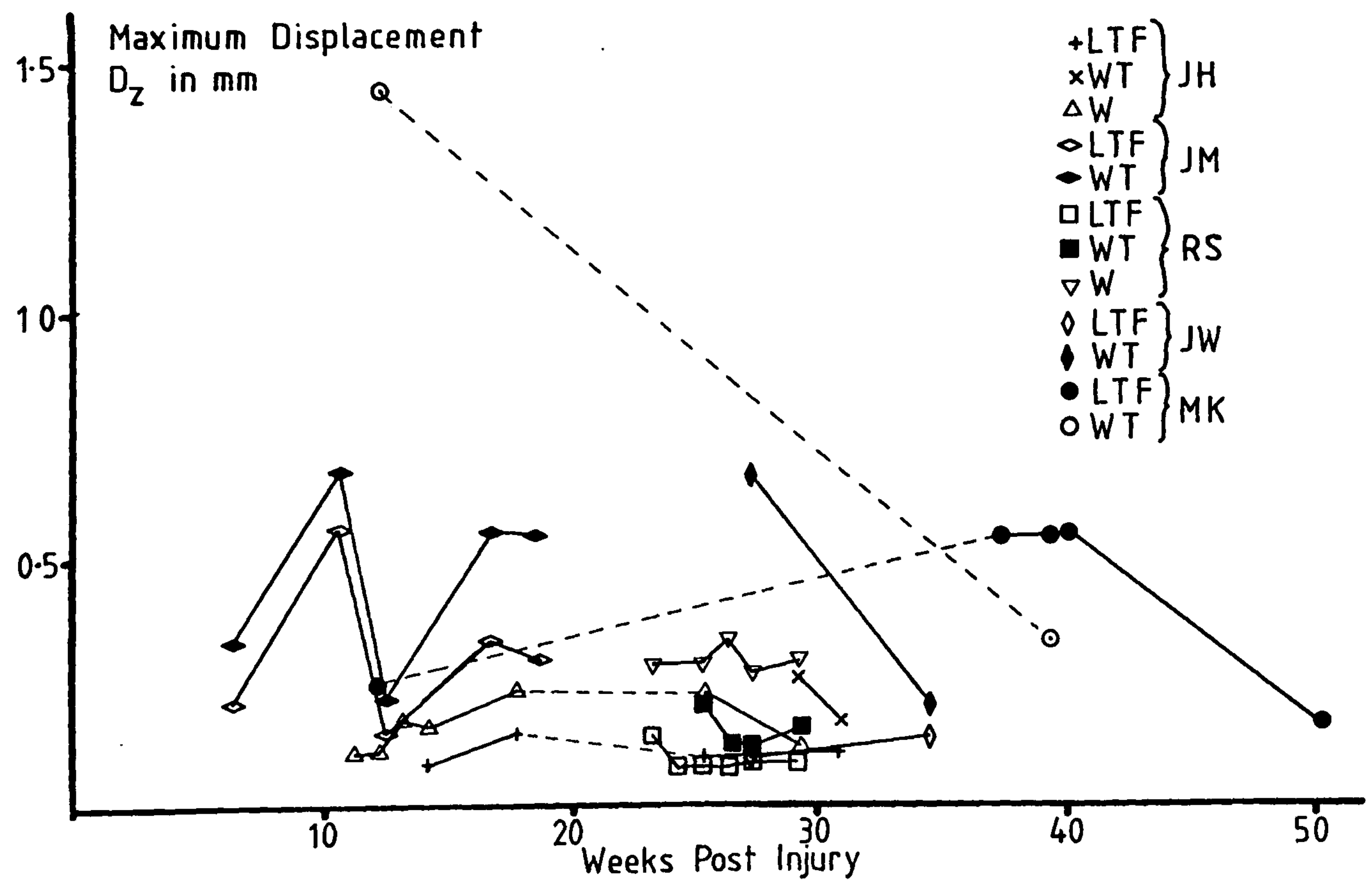

Fig 6.4.15

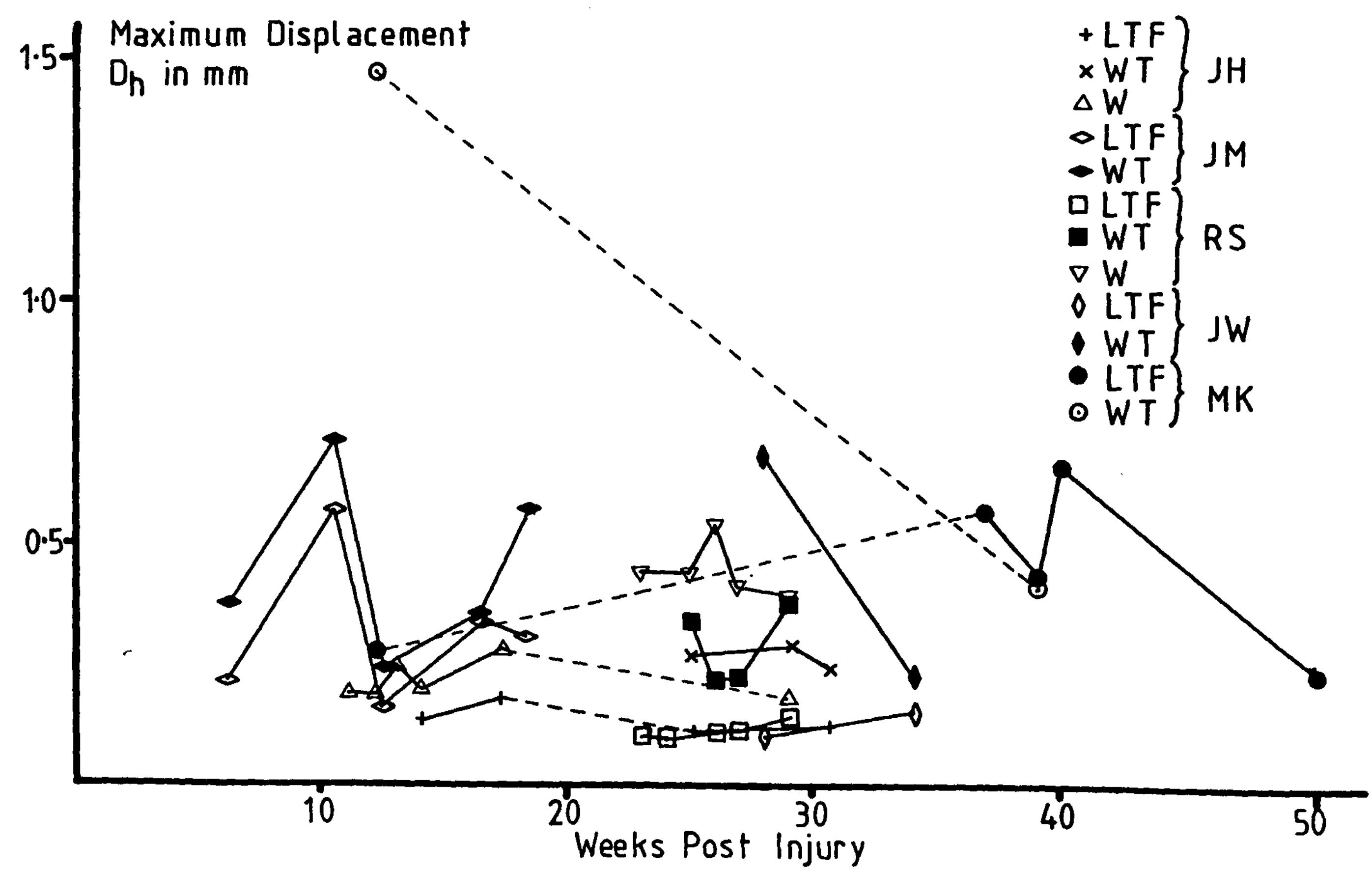

Fig 6.4.16

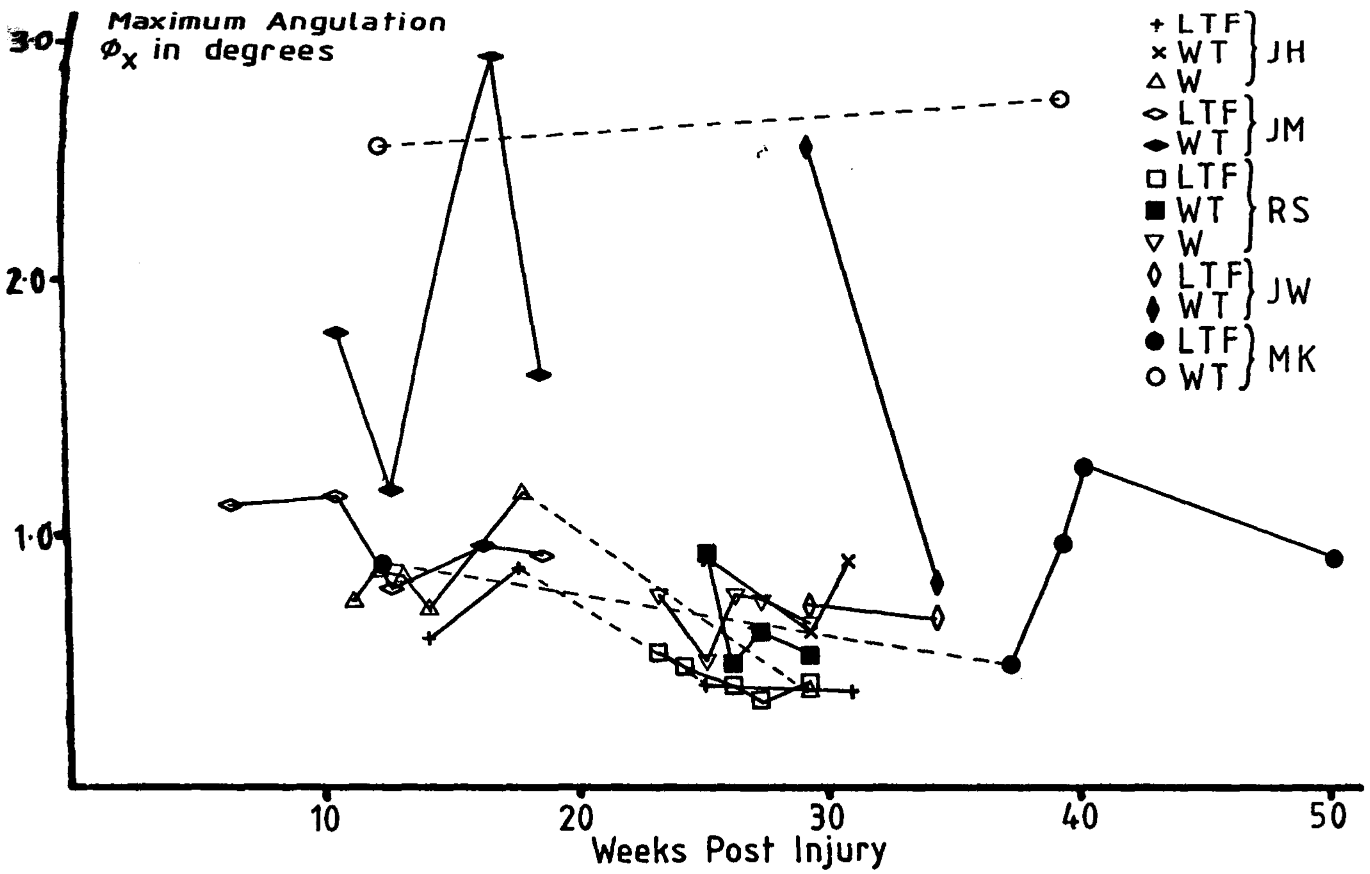

Fig 6.4.17

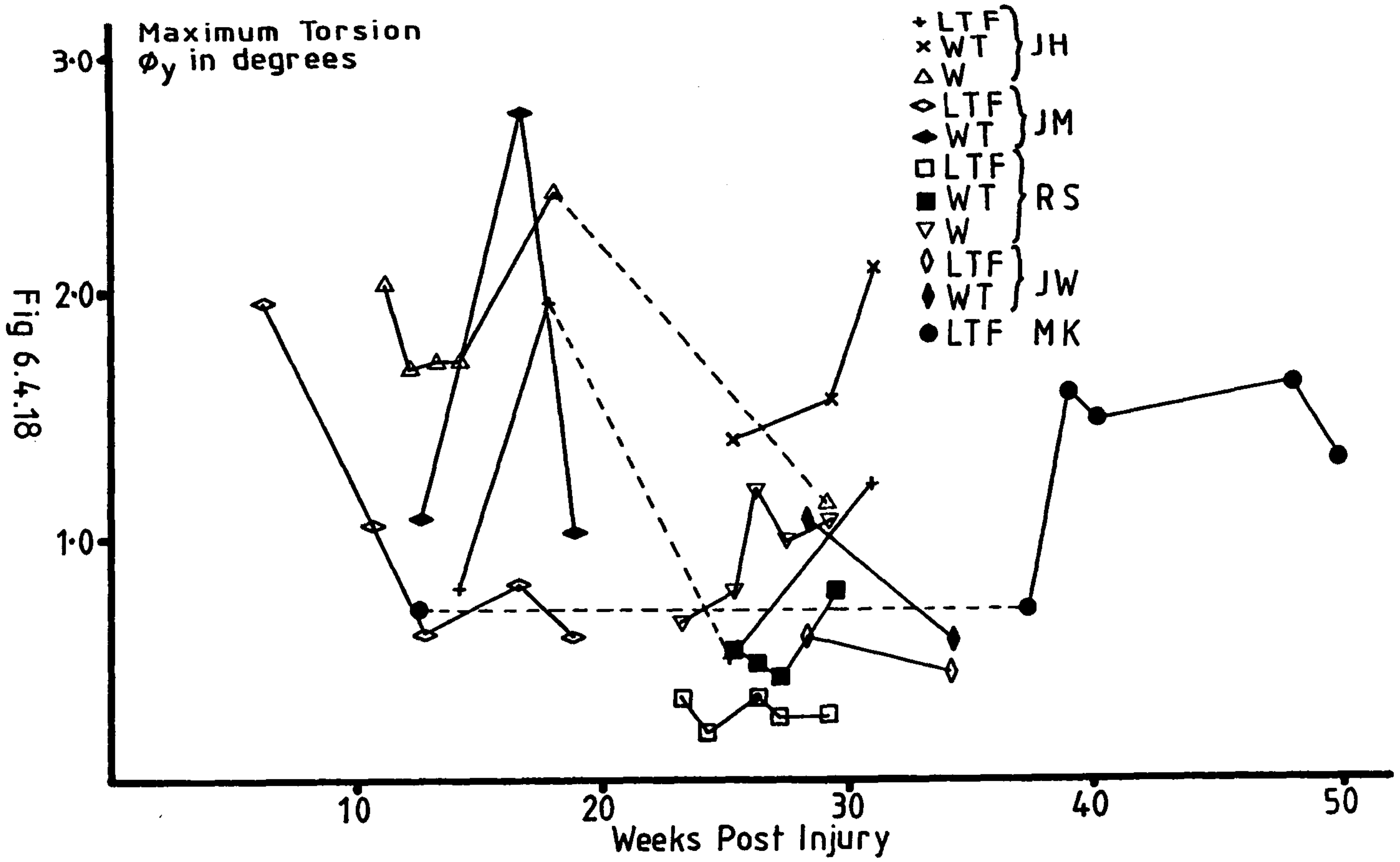

Fig 6.4.18

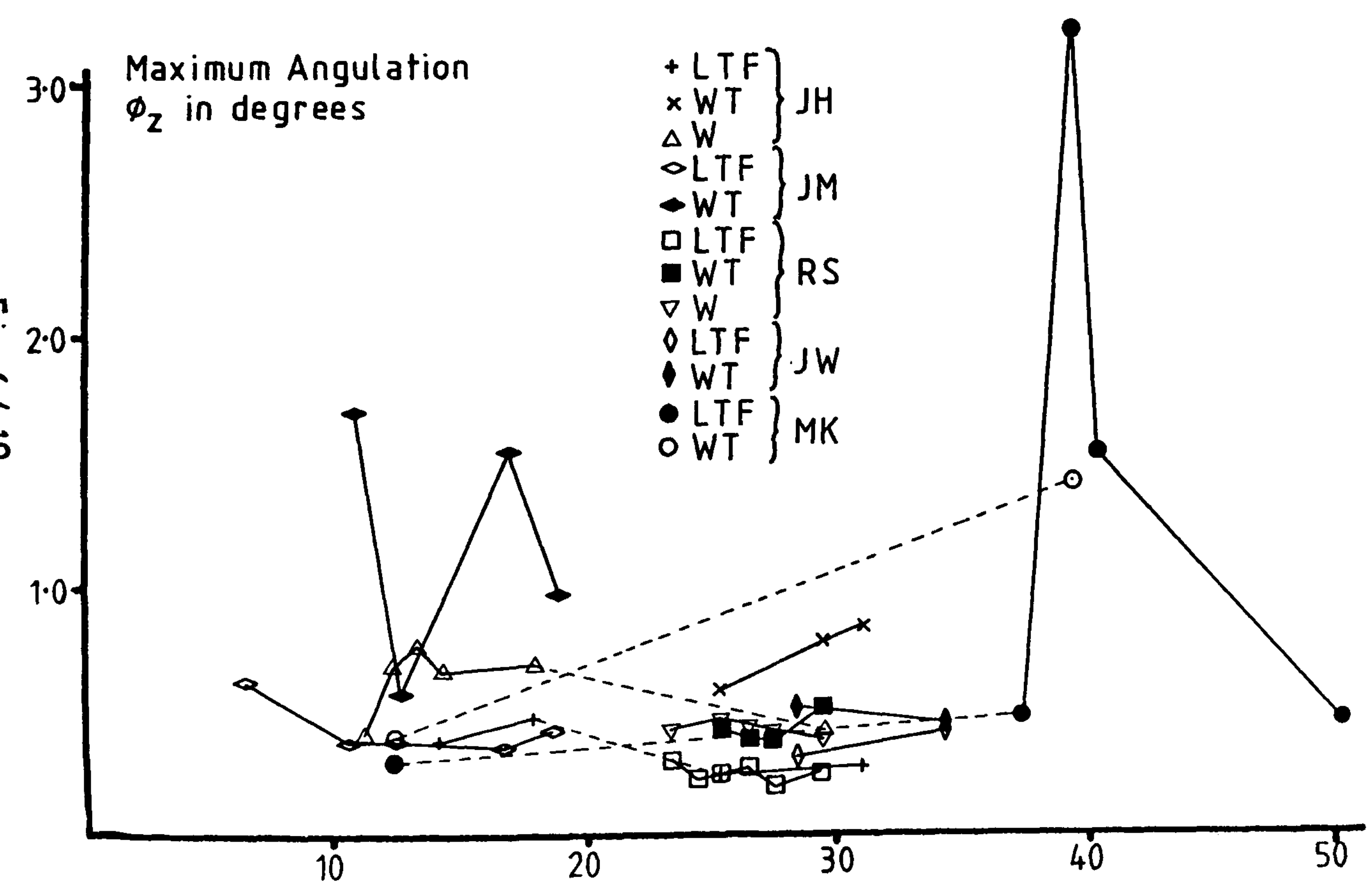

Fig 6.4.19

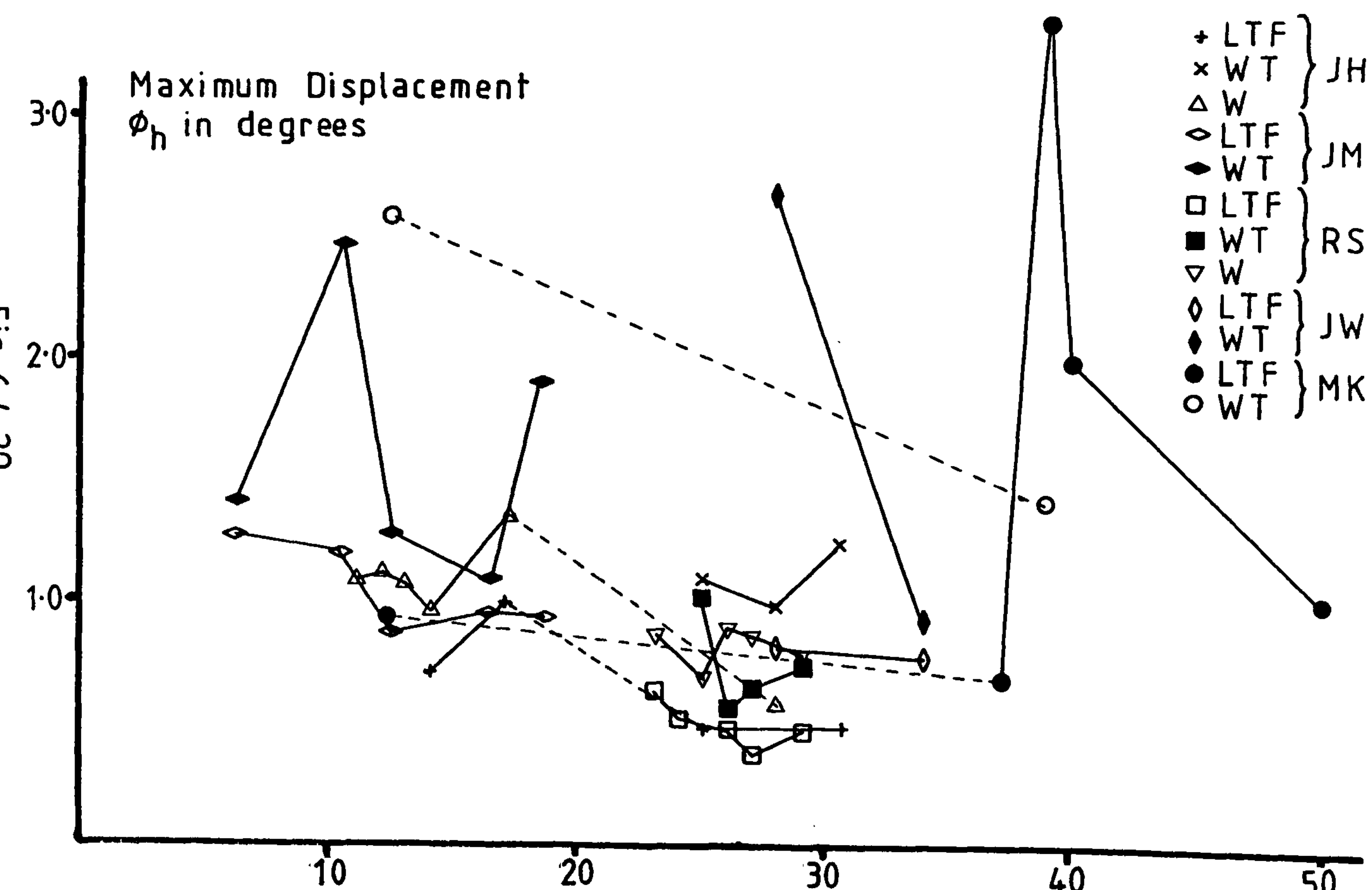

Fig 6.4.20

'wn for straight leg raise in Figure 6.4.22 and for the remaining 'ee tests in Figure 6.4.24.

The significance of these results, together with those from the 'ain gauge transducer, will be discussed in Chapter 7.

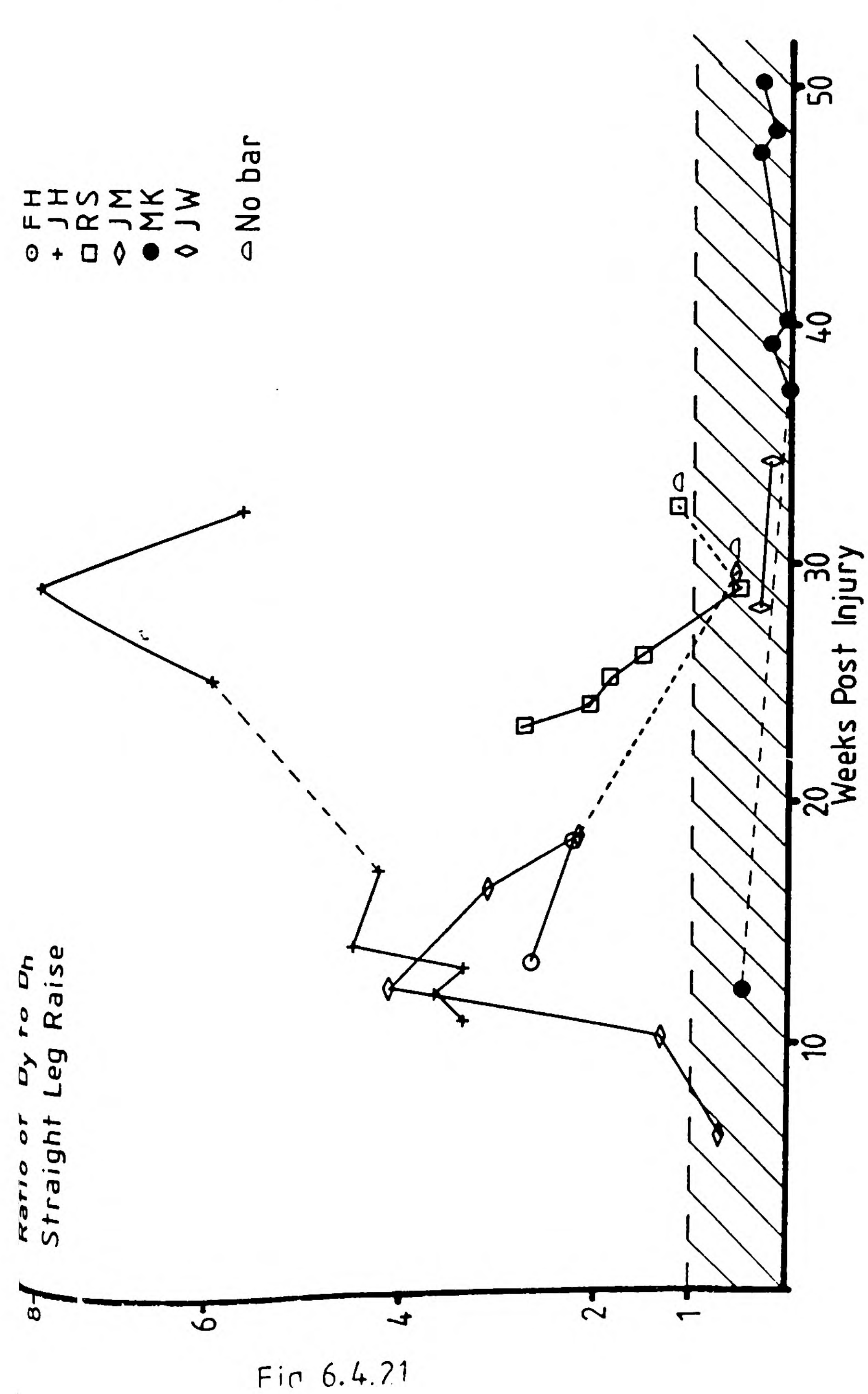

Fig 6.4.21

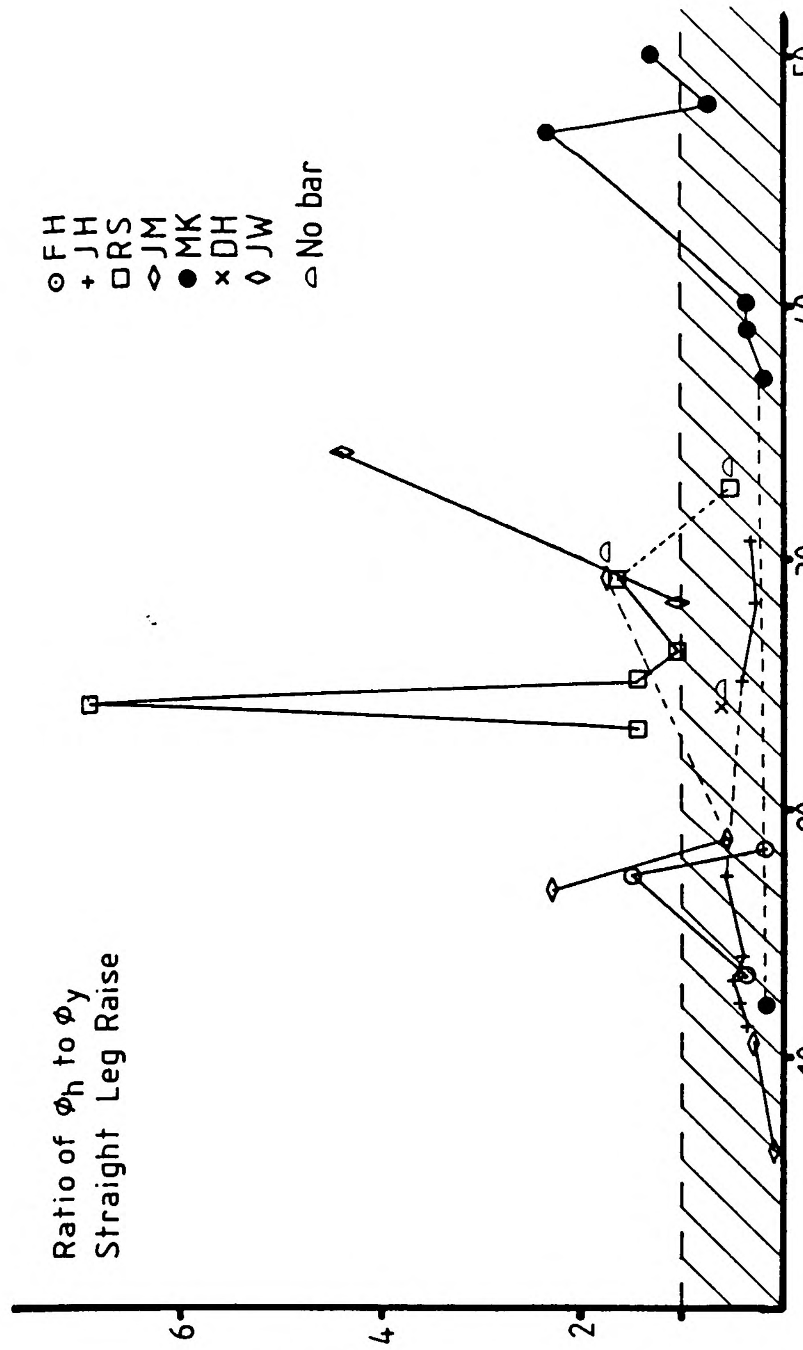

Fig 6.4.22

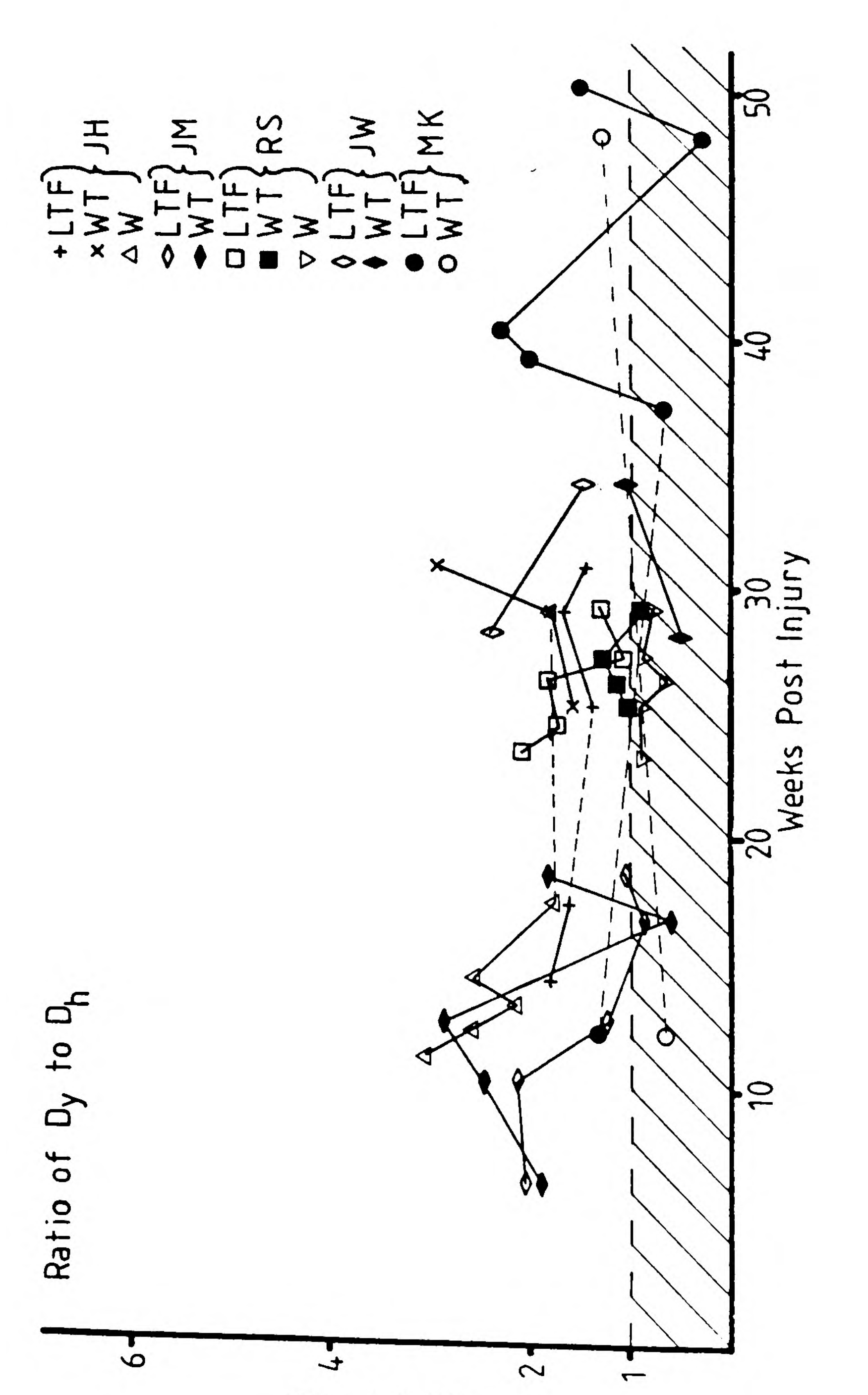

Fig 6.4.23

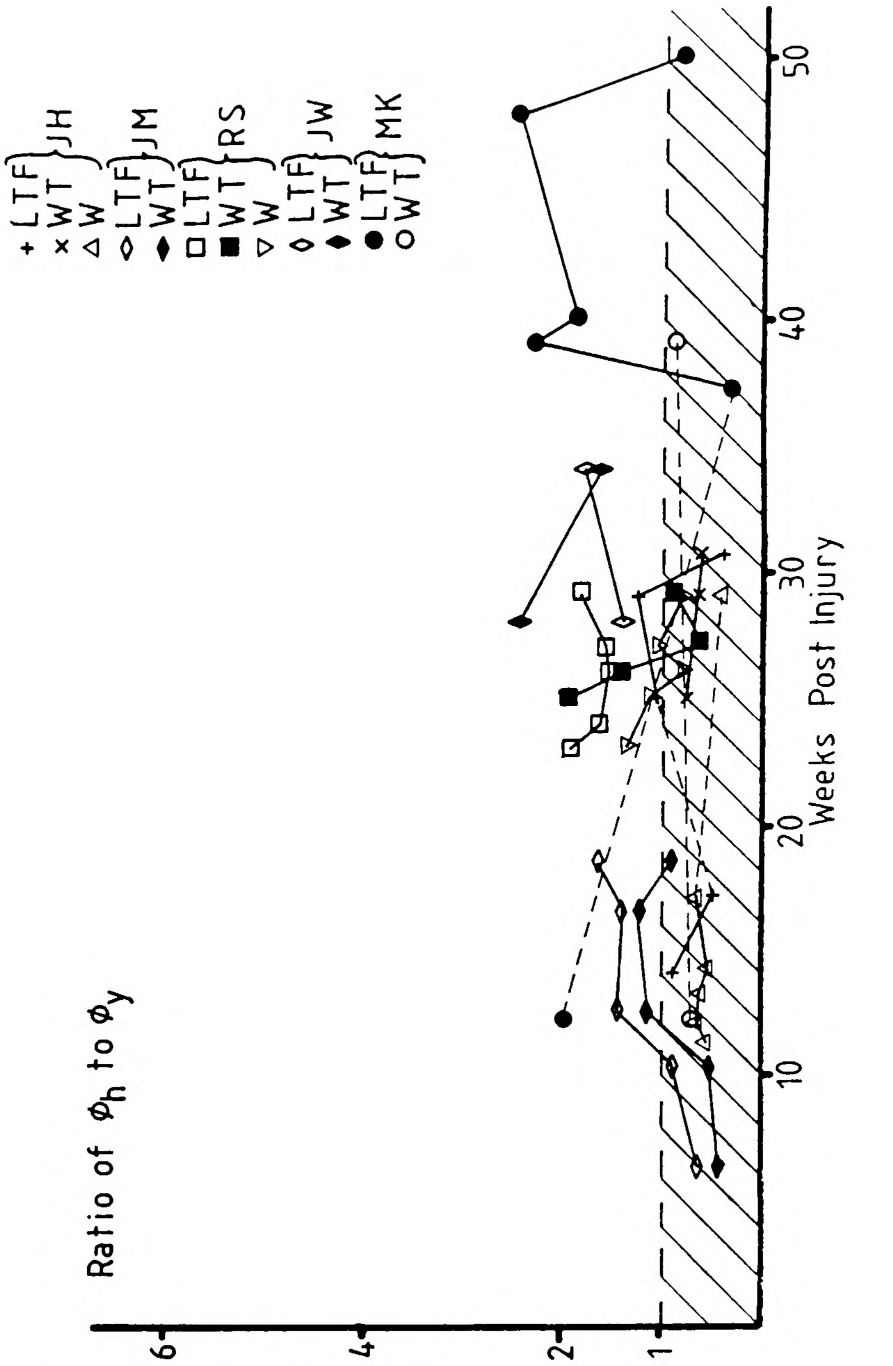

Fig 6.2.24

6.5 Results of Strain Gauge Transducer Tests

These are presented in Figures 6.5.1 to 6.5.9. Figure 6.5.1 shows the inverse strain reading in terms of weeks post-injury for comparison with the displacement transducer tests, the same tests are shown in Figure 6.5.2 but as weeks post-fixation.

Figures 6.5.2 and 6.5.3 show the stiffness index in $N\mu\varepsilon^{-1}$ for the longitudinal tibial force and weight transfer tests respectively. Figure 6.5.4 shows the maximum percentage body weight the patients were prepared to put on their fractured leg during the weight transfer tests.

Figures 6.5.5 and 6.5.6 are the fracture stiffnesses calculated using equation 4.5.7 and the estimated fixator stiffnesses based on the work of Churches et al (1985a,c) and tabulated in Table 6.5.1. These two graphs both assume that all pins were tightly fixed in the bone.

Figures 6.5.9 and 6.5.10 show the stiffness indices for the longitudinal tibial force and weight transfer tests normalized with respect to $(g^{*2} + 1^2)^{\frac{1}{2}}$ the distance between the centre of the bone and the centre of the support bar. These results will be discussed in the next chapter.

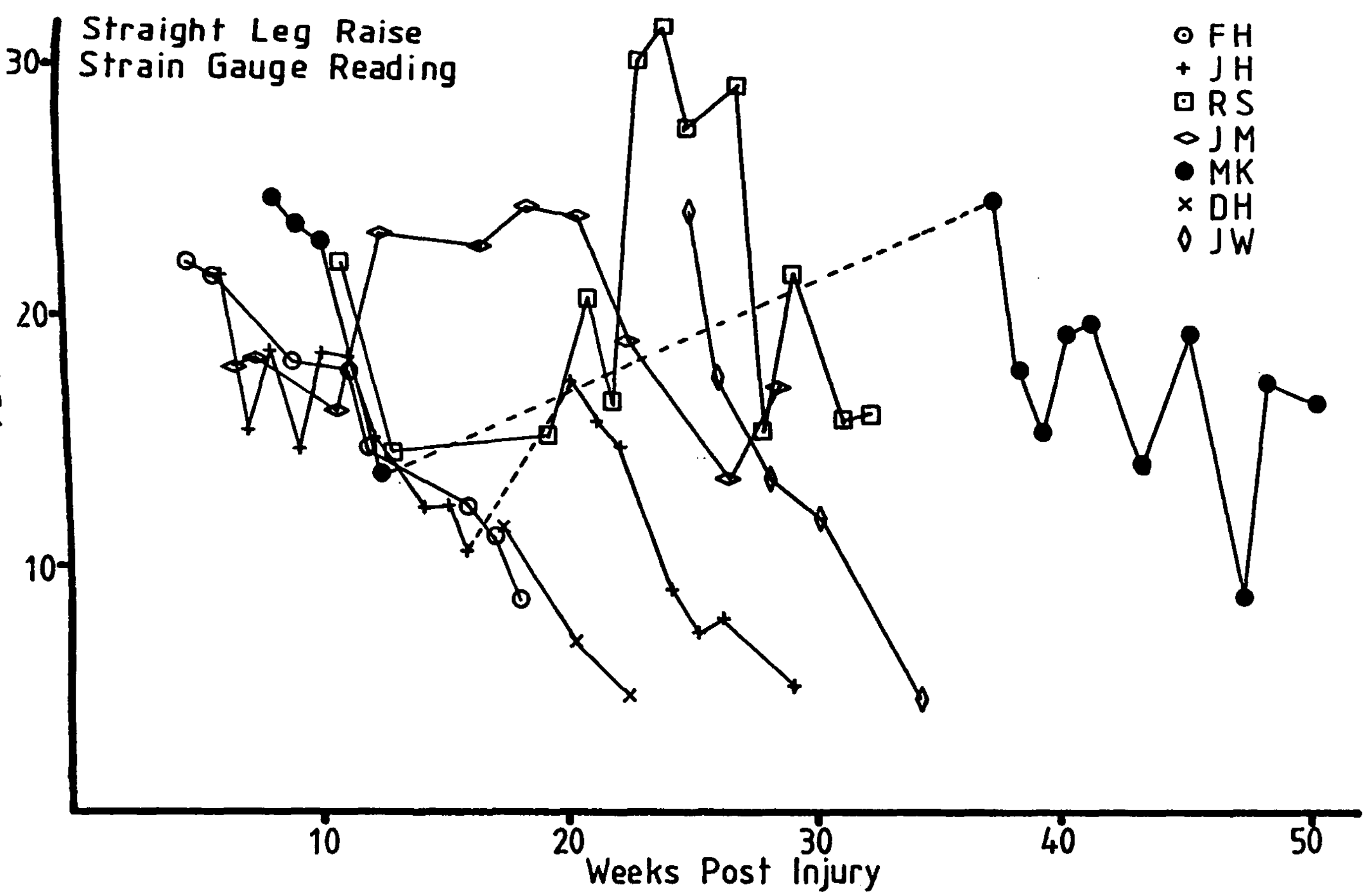

Fig 6.5.1

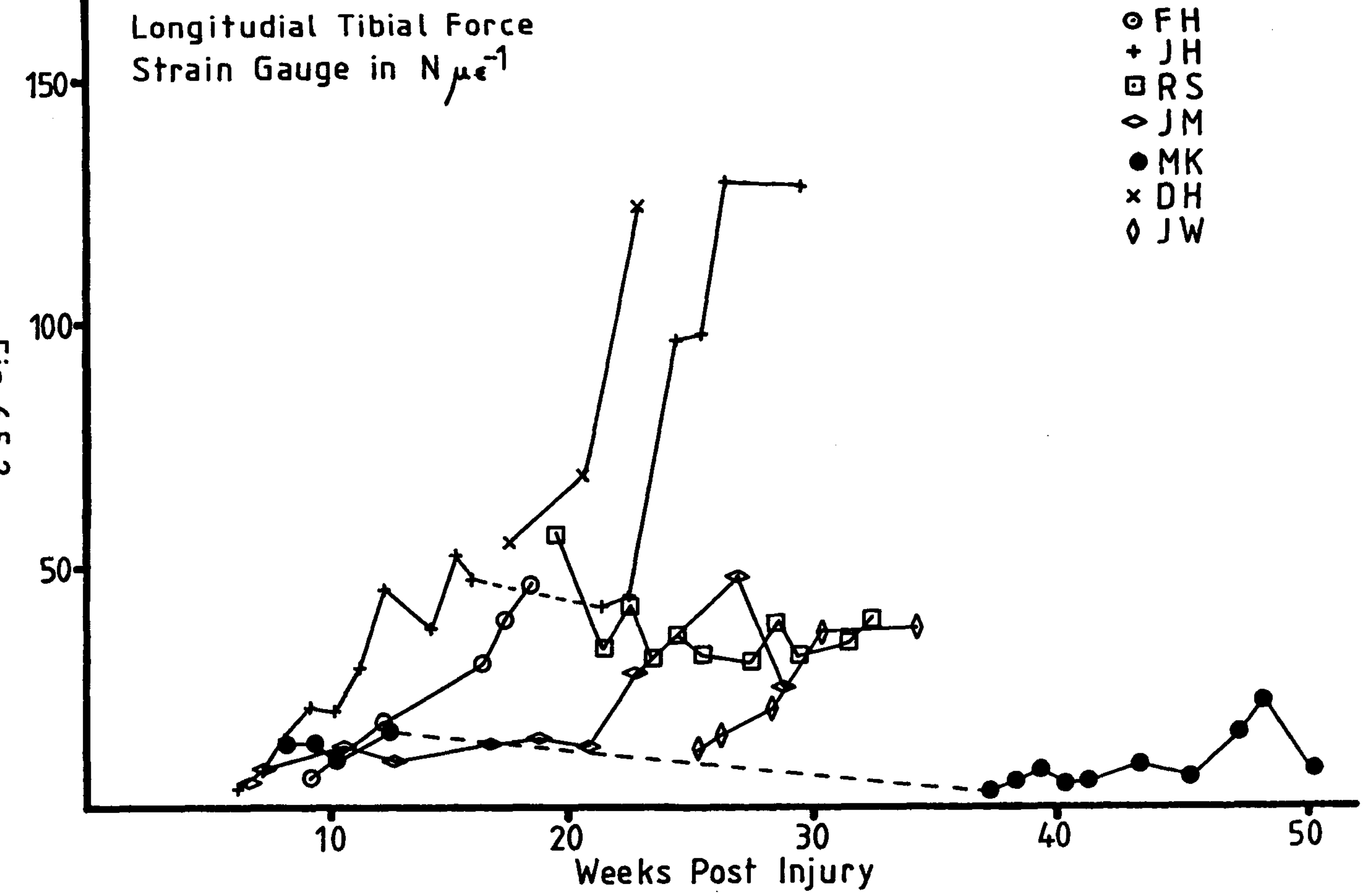

Fig 6.5.2

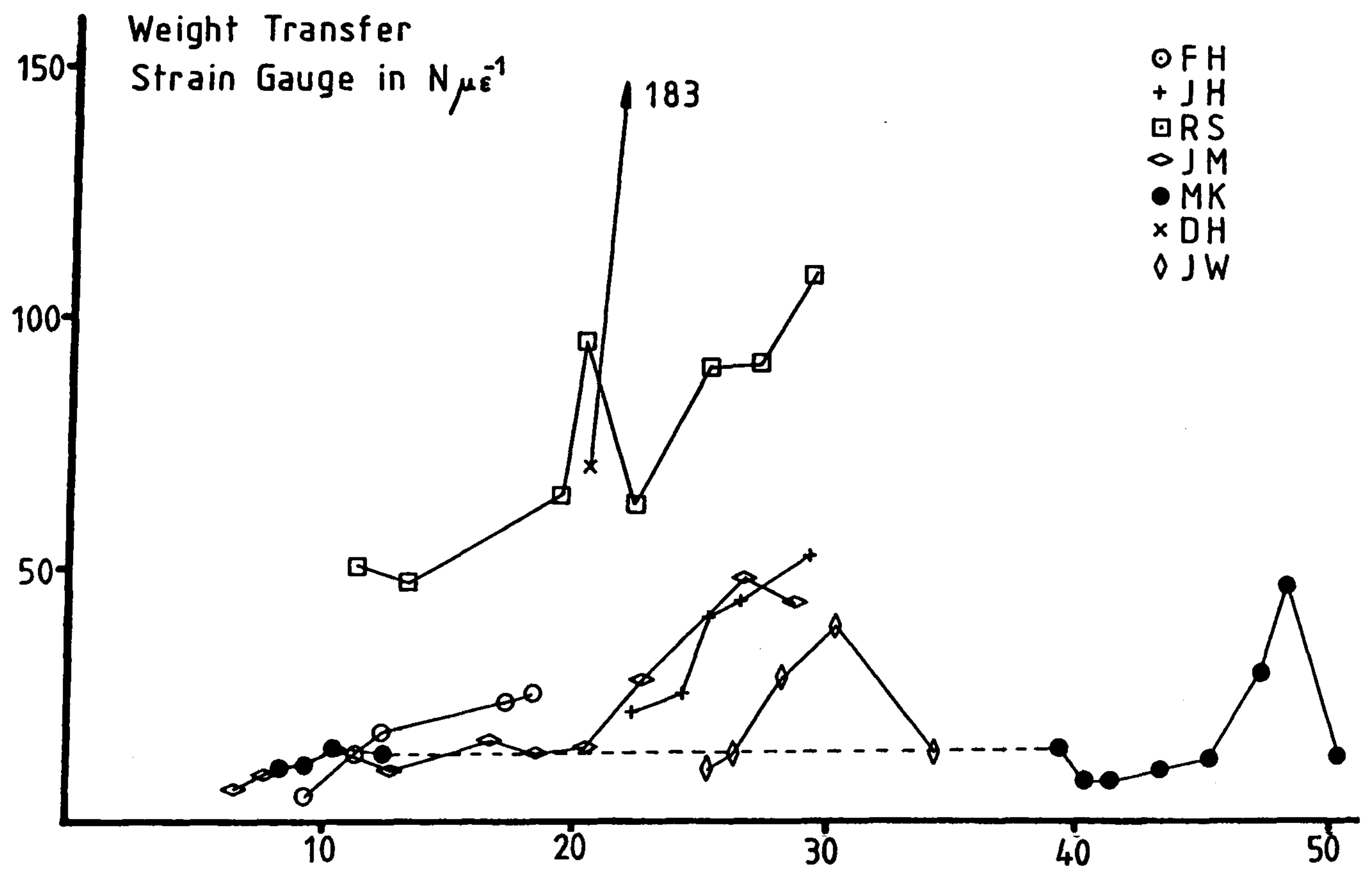

Fig 6.5.3

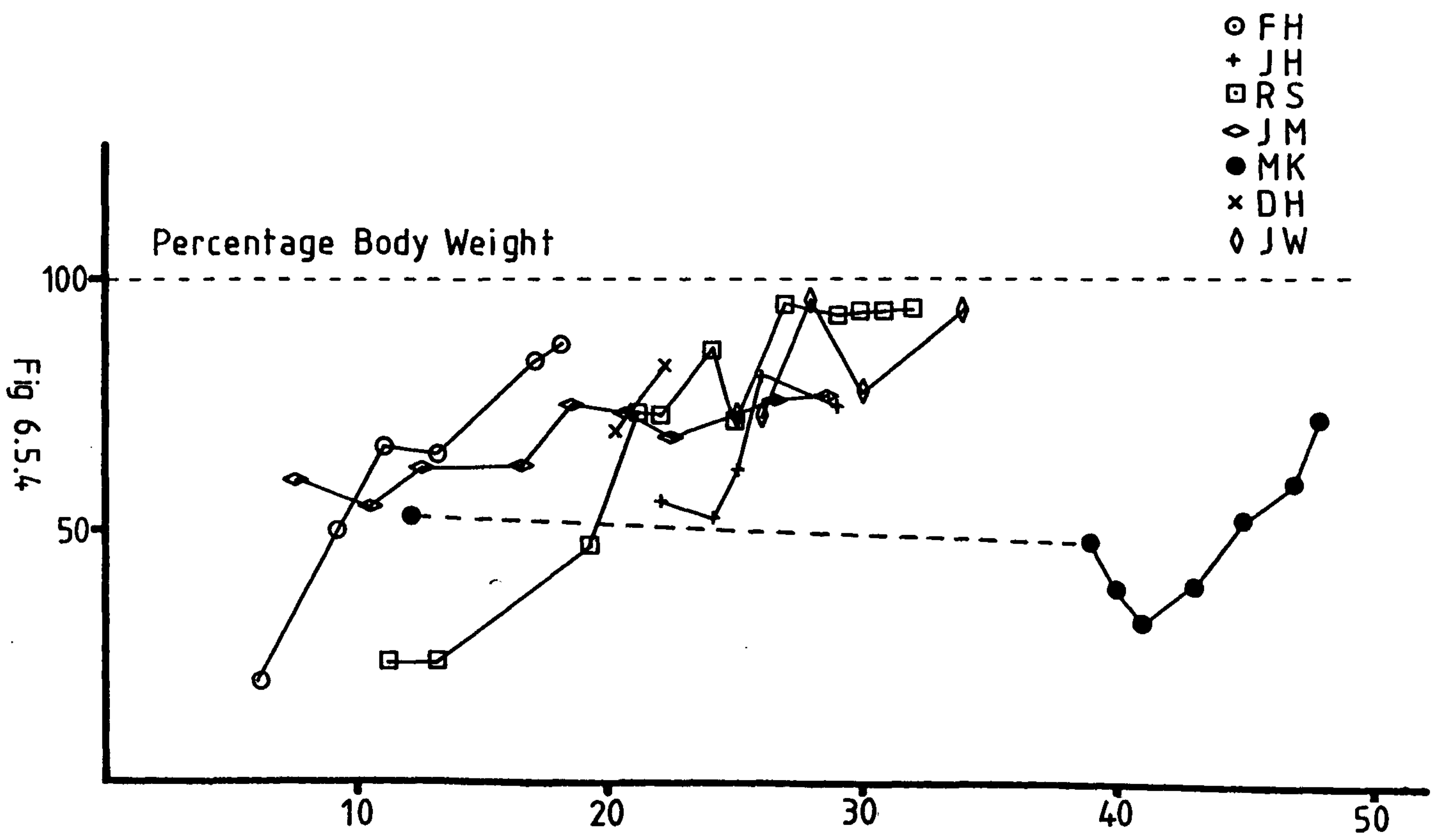

Fig 6.5.4

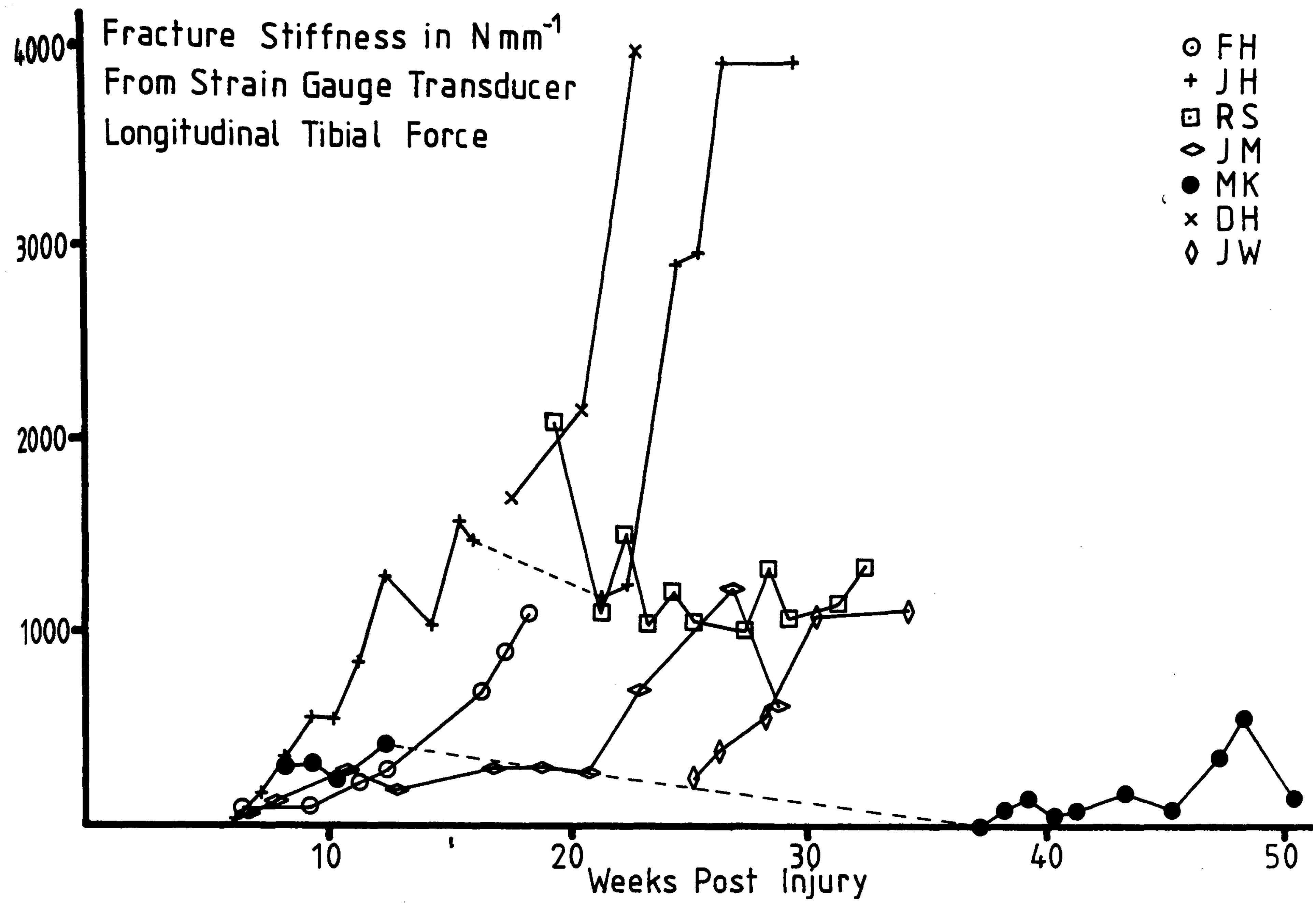
Fracture Stiffness in N mm^{-1}
From Strain Gauge Transducer
Longitudinal Tibial Force
FH
JH
RS
JM
MK
DH
JW
4000
3000
2000
1000
10
20
30
40
50
Weeks Post Injury

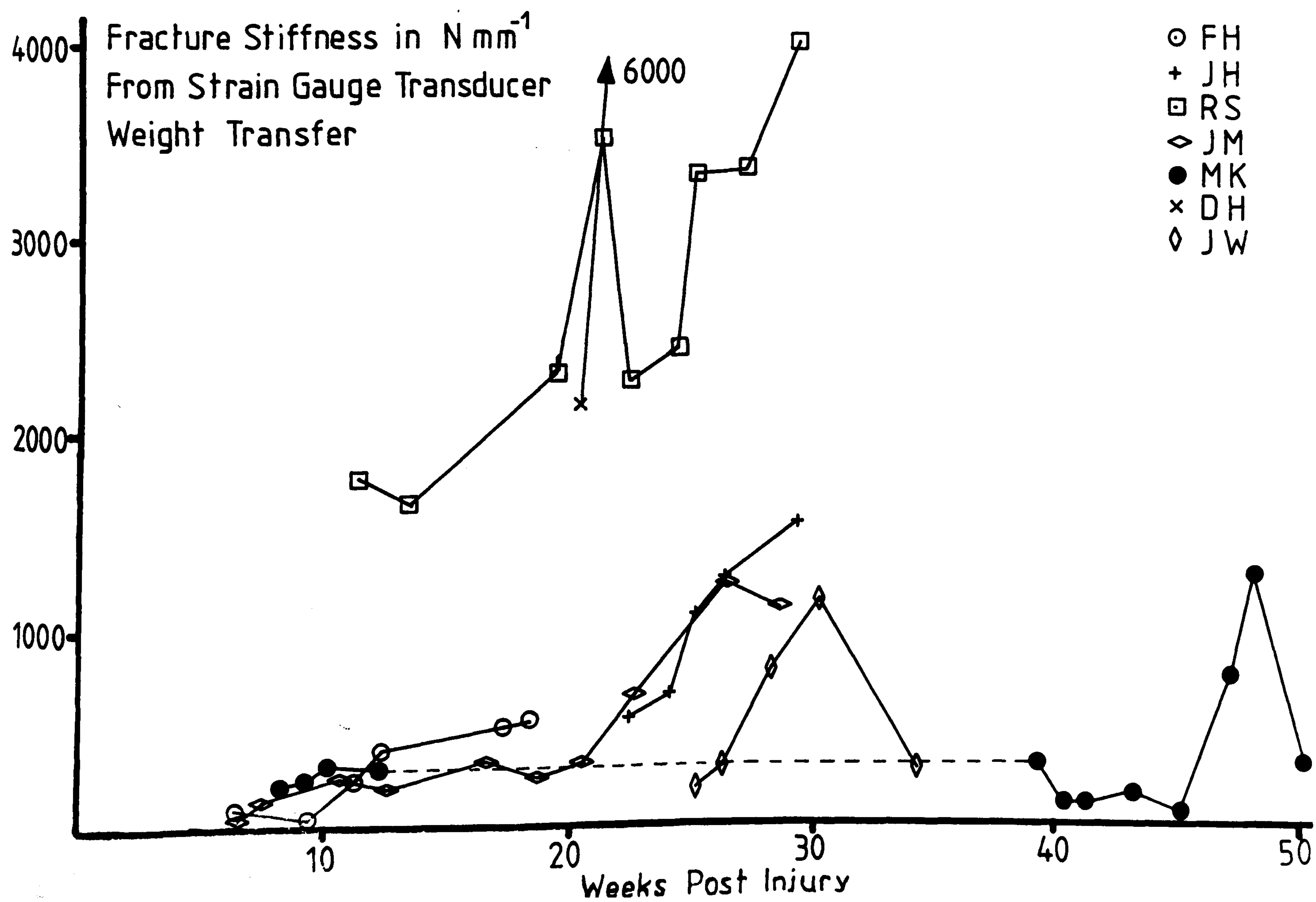
Fracture Stiffness in N mm^{-1}
From Strain Gauge Transducer
Weight Transfer
6000
FH
JH
RS
JM
MK
DH
JW
4000
3000
2000
1000
10
20
30
40
50
Weeks Post Injury

Table 6.5.1

Patient	l	b_1	b_2	k_1	k_2	k_3	k_4	k_5	k_6	M	l*	ø	W	d
1 - FH	65.0	67.0	33.0	81	60	37	1.89	14.4	1.23	6.11	0.0871	-	530	0.112
2 - JH I	50.0	65.0	40.0	117	89	52	2.65	14.8	1.32	7.24	0.0746	64	650	0.107
2 - JH II	50.0	35.0	40.0	117	89	52	2.01	12.7	1.32	7.24	0.0746	64	650	0.107
3 - RS	40.0	67.0	50.0	162	126	69	4.77	18.3	1.40	11.60	0.0666	60	845	0.140
4 - JM	60.0	70.0	55.0	90	67	40	3.19	19.1	1.26	7.87	0.0861	50	635	0.123
5 - MK I	50.0	65.0	28.0	117	89	52	2.23	12.5	1.32	7.89	0.0761	60	665	0.118
5 - MK II	55.0	68.0	25.0	102	77	45	1.98	11.1	1.29	7.89	0.0808	50	665	0.118
6 - DH	50.0	55.0	53.0 35.0	117	89	52	2.34	14.1	1.32	-	0.0775	-	550	-
7 - JW	45.0	67.0	27.0	136	105	60	2.47	12.1	1.36	7.03	0.0690	70	640	0.105

Table 6.5.1

l	Pin Length in mm
b_1	Upper Pin Seperation in mm
b_2	Lower Pin Seperation in mm
k_1	Axial Stiffness all pin tight in N mm^{-1}
k_2	Axial Stiffness one pin loose in N mm^{-1}
k_3	Axial Stiffness two pins loose in N mm^{-1}
k_4	Bending Stiffness about pin axis in Nm deg^{-1}
k_5	Bending Stiffness about normal to pin axis in Nm deg^{-1}
k_6	Torsional Stiffness in Nm deg^{-1}
M	Bending Moment at Fracture in Straight Leg Raise in Nm
l^*	Support Bar to Bone offset in m
ϕ	Angle of Fixator to Anterior Posterior Axis in deg
W	Patient Weight in N
d	Fracture to Foot Distance in m

CHAPTER 7

DISCUSSION OF RESULTS

7 DISCUSSION OF RESULTS

The results considered in this section are those presented in Section 6.4 (Results of the Displacement Transducer Tests) and Section 6.5 (Results of Strain Gauge Transducer Tests). Here they are compared with the clinical histories of these patients.

There are seven patients and, with knowledge of their clinical histories, they can be divided into three groups; those whose fractures progressed to good union at reasonable speed (F.H., J.H., J.W. and D.H.) (Group I), those whose fractures healed but more slowly (J.M. and R.S.) (Group II), and the one problem patient (M.K.) (Group III) whose fracture still had not healed at eighteen months post-injury. Due to the small number of patients no statistically significant results can be expected, but trends may be seen. It should be noted that this ratio of one delayed union out of seven patients is not typical of a larger study by Richardson (personal communication) where three non-unions/delayed unions occurred in 98 tibial fractures treated with Mark I and Mark II Oxford External Fixators. However, as far as this study is concerned, this one patient does provide an interesting comparison to the 'good' union cases.

Considering first the displacements during the straight leg raise test, Figures 6.4.1 to 6.4.4, for each of these graphs the accuracy is of the order of 0.1mm. Looking first at d_x, J.H. shows a decrease from 0.23mm, but the other patients vary, most of them within the experimental error. One patient, M.K., has variations larger than experimental error, his variations are not apparently related to anything in his clinical history. Both the patients who were tested with and without the fixator support bar, R.S. and J.M., show increases when the support bar was removed. This is to be expected, as the combined fracture-fixator stiffness will be reduced when the support bar is removed. Figure 6.4.2 shows the d_y displacement results. Here, in general, decreases in displacement are seen with time. J.M., R.S. and J.W. decrease only slightly, but J.H., F.H. and M.K. decrease to a greater extent. F.H. shows a large drop on her second test; this was at the time that she was having problems with a pin tract infection, and she may have not been relaxing properly during the first part of the test, thus giving an anomalously low result. Also the infection was of the second pin, one of the two pins to which the transducer was attached, and if the infection resulted in the pin becoming loose in the bone, then an extra flexibility would be inserted between the bone and the pin. This would result in less load being taken by that pin for a given fracture site displacement leading to less movement of the point of attachment of the displacement transducer, leading to a lower calculated displacement of the fracture site. M.K. shows a fall from the only test with his first fixator to those with his second although his second fixator had lower bending stiffnesses than the first.

D_z, the displacement perpendicular to the plane of the fixator, is shown in Figure 6.4.3. R.S. and J.M. show results that are constant with time within the experimental error. M.K. shows a fall from large initial values and F.H., J.H. and J.W. show gradual falls. For the two patients tested without their support bars, R.S. shows no increase whereas J.M. shows an increase from the previous tests. The two perpendicular shear displacements, d_x and d_z, are summed, by vector addition, to produce the maximum shear displacement d_h, shown in Figure 6.4.4. For most tests d_z was greater than d_x so d_z dominates. Thus, M.K. shows a fall from a high value; F.H., J.H. and J.M. show falls and R.S. and J.W. seem to be constant within experimental error. F.H. shows the same pattern as in Figure 6.4.2 of a fall from the first to the second test then a smaller rise to the third test.

Considering the four graphs of displacement of the fracture site during the straight leg raise test and how these can be related to the clinical history of the patients, D_x produces such small results that they are swamped by experimental error, with the exception of M.K. whose results wander. D_y shows gradual falls for the two Group II patients and one of the Group I patients; the other two Group I patients show sharper falls and M.K. (Group III) has variable results. D_z gives constant results or gradual falls for two Group I patients (J.H. and J.W.) and one Group II patient (R.S.) and sharp falls for one patient from each group. D_h is constant, or shows a small fall for one Group I (J.W.) and one Group II patient (R.S.) and large falls for the remaining patients. Thus the only significant result for d_x is the variation in the Group III patient. D_y divides the Group I and Group II patients but shows a tremendous fall for the Group III patient. D_z and d_h show falls or constant values for the Group I and II patients and a large fall for the Group III patient.

Progressing to the graphs of the angulations during the straight leg raise, shown in Figures 6.4.5 to 6.4.8, the estimated error on these graphs is 0.2 degrees. For ϕ_x, angulation about the line of the pins, all the results are constant within the experimental error, with the exception of J.W. who shows a sharp fall. Considering Figure 6.4.6, ϕ_y the angulation about the line of the pins, with the exception of R.S., the angulations in general reduce. F.H. again shows a much lower value for her second test than either of the other two tests. This is the only straight leg raise test where J.M. shows a fall from the test before the support bar was removed to that where it was removed, this does seem surprising. F.H. again shows a low value for the second test.

For ϕ_z, Figure 6.4.7, the Group III patients show either small falls or a constant level. Of the Group I patients, one, J.W., has two low results, but the other two show falls. M.K. the Group III patient has variable results. ϕ_h, the maximum angulation, is shown in Figure 6.4.8, the three Group I patients show falls, the two Group II patients remain fairly constant, with R.S. having a low reading. M.K. has a constant high reading, with the exception of one low result.

Considering the overall patterns for each patient obtained from the eight graphs of the straight leg raise tests, patient F.H., shows a fairly high initial result a very low second test and an intermediate result for the final test, and possible reasons for this have been discussed earlier. J.H. shows an early fall to the time she received a bone graft and her fixator stiffness was altered by moving one pin; from this her results remain at a low level. R.S. shows little movement but some variation of the order of the estimated experimental error. J.M. for some graphs shows a sharp initial fall and then fairly constant results, but for other graphs he shows a gradual fall. For all the graphs with the exception of ϕ_y he shows an increase in movement once the fixator support bar was removed. M.K. shows totally inconsistent results from graph to graph and within each graph. J.W. shows either falls or constant values, but with only two test occasions, it is impossible to estimate how the experimental error has affected her results. Thus, in general, the Group I patients had reducing displacements, the Group II had either constant but fairly low or more slowly reducing displacements, and the Group III patient had highly variable results.

There was no single graph which clinically the only useful one. D_y, d_z, d_h and ϕ_y were good with ϕ_z and ϕ_h being useful, d_x and ϕ_x did not, in general, give readings sufficiently greater than the experimental error to be any use. The most useful graphs were d_y and ϕ_y.

The results obtained by applying the same loads to the same fractures but measuring the strains produced by the loads applied to the fixator support bar are shown in Figure 6.5.1. In this graph the Group I patients all showed falls, and there are sufficient results for D.H. for him to be included in a discussion of these results. An odd result was produced by J.H. On the strain gauge transducer results she apparently had a reduction in fracture stiffness with the strain gauge transducer. If Table 6.5.1 is consulted it may be seen that the bending stiffnesses of her fixator were reduced at the time of bone grafting. If her fracture stiffness had remained constant then the decrease in the fixator stiffness would have resulted in a decrease in the strain gauge transducer reading, so the bone grafting operation must have decreased the stiffness of the healing fracture. This decrease in fracture stiffness is not apparent on the displacement transducer results because these were not resumed until 25 weeks post injury, and by then the strain gauge transducer readings had reduced to about 60% of the pre-grafting level.

The two Group II patients show even more variable results than were seen with the displacement transducer results. It is interesting to note from Table 6.5.1 that R.S. had the stiffest fixator of all these patients, up to 50% stiffer than any other patient but his fracture site bending moment was also approximately 50% greater than any other patient. This has resulted in lower displacements at the fracture site but fairly similar strain gauge transducer readings when compared with the other patients. It should be noted that this fracture may not have healed well, as the patient refracted, with minimal trauma, a few months after his fixator was removed.

The Group III patient, M.K., shows reducing strains with his first fixator but with his second fixator the results are oscillations possibly about a decreasing mean.

Thus the strain gauge readings transducer readings of the straight leg raise test are a reasonably effective method of assessing fracture leading. However, it did not show up the problems F.H. was having with infection.

During some of the longitudinal tibial force, weight transfer and walking tests measurements were made of the vertical and horizontal forces applied to the floor by the patients foot. These were used to calculate the quasi-stiffnesses shown in Figures 6.4.9 to 6.4.12. When the stiffnesses were calculated the correlation coefficient was also calculated and if this was low then the result was discounted. Considering Figure 6.4.9, F_v versus d_v, there are effectively only results for two patients J.H. and J.M. and these increase, except for J.H.'s three weight transfer results, which fall with time. A similar trend is shown in Figure 6.4.11, F_v versus ϕ_v. For Figures 6.4.10 and 6.4.12 there are insufficient data points to reach any conclusions.

The comparative strain gauge transducer results are shown in Figures 6.5.2 and 6.5.3 for the longitudinal tibial force and weight transfer tests respectively. In 6.5.2 the longitudinal tibial force results for the Group I patients all show rises. Although J.H. does show a fall in fracture stiffness after bone grafting as was seen in the strain gauge transducer results for the straight leg raise test. The Group II patients, one J.M. remains fairly constant for the first 21 weeks and then rises, about 8 weeks after bone grafting, and it may have taken 8 weeks to incorporate this bone graft. The other Group II patient R.S. has variable results although about a reasonably high mean. The Group III patient M.K. remains low throughout the time he was tested.

The weight transfer results produce much less definite results. R.S. produces gradually increasing results starting at a high level.

D.H. had high results for both his tests. The remaining patients had low results, gradually increasing later and then, in the cases of M.K. and J.W. falling for the final test. While this test was being performed the maximum load the patient was prepared to apply to the injured limb was measured as a percentage of the patients body weight. These results are shown in Figure 6.5.4, giving in general rises. R.S. achieves the highest consistent value of over 90% for five tests yet his fracture did not heal particularly well. In contrast, three of the Group I patients, F.H., J.H. and D.H., did not get above approximately 80%, the other Group I patient J.W. reached about 90% then dropped to 70% before reaching 90% for the final test. Thus neither the weight transfer test, or the percentage body weight are particularly good methods of assessing fracture healing.

From the results presented in Figures 6.5.2 and 6.5.3, the fractures stiffness were calculated using the equation 4.6.3 on page 185, and the results are shown in Figures 6.5.5 and 6.5.6. These are the same shape graphs as 6.5.2 and 6.5.3 but some patients results have moved relative to others; for example, R.S.'s results have risen relative to the others as his fixator was stiffer than the rest.

The other interesting result is for M.K. at 37 weeks post injury, he had had an inch of dead bone removed, and his calculated fracture stiffness was zero, as would be expected. If the longitudinal tibial force results are compared to those shown in Figure 6.4.9 there are 7 data points to compare with Figure 6.5.5. The displacement transducer result for M.K. from Figure 6.5.5 agrees fairly well with the strain gauge transducer result, those for J.M. start at approximately the same level but then the displacement transducer results become higher than the strain gauge transducer results. For J.H. the first displacement transducer result was low compared with the strain gauge result but the second was approximately the same comparing the weight transfer results, there are again 7 data points and one of these does not have an equivalent result from the strain gauge transducer. For M.K. the single result is comparable, for J.H. the initial displacement transducer result is similar, but then the displacement transducer results become higher than the strain gauge transducer results. For J.M. the single pair of results give comparable stiffnesses. It is difficult to come to any conclusion comparing the stiffnesses from the two transducer with only 13 pairs of points to compare, in two pairs of the results the displacement transducer gave low results, and in five high when compared with the strain gauge transducer results.

Returning to the displacement transducer results while the patients were performing the axial force tests the maximum values of all the displacements and angulations were measured. As can be seen from Figure 6.5.4 the load a patient is prepared to put onto an injured limb increases with time. There is presumably something controlling the amount of load the patient is applying to the limb and the fracture. It seems possible that the controlling factor is the displacement at the fracture site, as throughout the healing process the one event which must not occur is excess movement at the fracture causing damage to the maturing callus. Thus the maximum displacements were considered to be of possible interest. It was considered that there were various possible patterns that could be seen. One would be that the patients who did badly, Groups II and III, would permit higher displacements at their fracture sites, thus making it difficult for the callus to calcify. Another possibility would be decreasing displacements as according to Perren (1978) the fracture haemotoma has an extension at failure of 100%, the callus fails at 10%, and the bone at 1%.

Starting with Figure 6.4.13, d_x maximum, for all the displacements the estimated error is, as before, 0.1mm, and within this error all the graphs are constant and fairly similar in value. Progressing to Figure 6.4.14, d_y maximum, again no trend or bands can be seen although, in general, those tests where the patient applied the loads themselves the displacements were higher than in the longitudinal tibial force tests where the loads were applied by somebody else. This did mean that the assistant was not over stressing the fracture. For d_z, Figure 6.4.15, M.K. had a very high result for his only weight transfer test with his first fixator. J.M. seems to have fairly high values but R.S., the other Group II patient, had some of the lowest values. Similar trends are seen in Figure 6.4.16. In Figure 6.4.17, ϕ_x, M.K., J.M. and the first J.W. weight transfer tests gave large angulations, but R.S. remained small. In Figure 6.4.18, ϕ_y large angulations may be seen for most patients at some time. In Figure 6.4.19, ϕ_z the angulations are much smaller although M.K. and, to a lesser extent, J.M., occasionally produce some large angulations. When ϕ_x and ϕ_z are combined to produce ϕ_h, Figure 6.4.20, the results get even more confused. Thus, looking at the maximum displacements and angulations does not give an idea of the control mechanism of the loading which the patient permits to be applied to a fractured limb.

Another possibility is that it is not the movements that are important but the strains which are being applied to the fracture. It is difficult to assess the size of the fracture gap, partially because it requires an X-ray to be taken showing the plane of the fracture, partially because fractures have varying thicknesses if they are comminuted, and finally because they vary with time as after a bone has been broken, as bone sclerosis occurs in the bone ends, which are then resorbed. It has been suggested by various authors including Yamagishi and Yoshimura (1955) that shear movements lead to pseudoarthoses and that axial movements promote fracture healing.

Thus if the ratio of the axial movements to the shear movements are plotted then a comparison is obtained of the "advantageous" to the "disadvantageous" movements. In the graphs 6.4.21 to 6.4.24 the area beneath the 1:1 ratio line is marked as where there was greater "disadvantageous" than "advantageous" movement. For the displacements in the straight leg raise test, Figure 6.4.21, F.H. and J.H. remain out of the 1:1 region, J.M. starts in this region and then rises out and R.S. falls gradually into it. However, J.W. and M.K. remain constantly in this area. For the angulations shown in Figure 6.4.22, for the straight leg raise, only J.W. and R.S. remain out of the region below the 1:1 line. J.H. remains constantly below it and the other patients vary with time. For the patients the activities which they perform most regularly when not in a clinic are walking or standing about, as in the weight transfer test. Exercises like the straight leg raise and the longitudinal tibial force are not usual although they have proved to be useful for testing. In the axial loading tests two patients were tested walking; J.H. remained above the 1:1 line for displacements but below it for angulations where as R.S. was below this line for displacements, started just above it but fell below it for angulations. M.K. for all the tests varied in an apparently random manner. For the remainder of the patients no particular pattern could be seen. So the comparison of the axial displacement to shear movements produced no obvious method of discriminating between the three clinical groups.

Three methods of assessing fracture healing in seven particular patients have been considered. They are the displacement transducer, which was designed for this study, the strain gauge transducer and percentage body weight which could be used clinically with a set of standard "bathroom" type weighing scales instead of the "Kistler" force plates used in this study. With the displacement transducer, for the straight leg raise tests certain movements were useful guides to the healing of the fractures, these were d_y, d_z, d_h and ϕ_y. Insufficient results are available to discuss the uses of the stiffness from the axial loading tests. The results obtained on the maximum displacements during the axial loading tests did not lead to any conclusions on the effects of movements at the fracture site on the rate of fracture healing. For the strain gauge transducer tests, the straight leg raise and longitudinal tibial force tests gave good discrimination between the three clinical groups of patients. The weight transfer is not as useful and the walking test was not performed with the strain gauge transducer. The percentage body weight test does seem to have its uses although it is not as good as some of the other tests, however, it has major advantages over the other tests. It may be performed anywhere on patients using a piece of equipment that any hospital, however primitive, has. The other tests are only appropriate for patients with externally fixed fractures, although a strain gauge system of measurement may be used on internal fixation plates. The percentage body weight test may be applied to those fractures in Plaster of Paris, which is the majority of fractures. It also only takes a few minutes compared with 15-30 minutes for the other two tests. This test, purely subjective, but it may be that there is physiological or neurological control system of which we are not aware.

On the displacement transducer tests there were insufficient patients tested to be able to separate the experimental scatter from the patient scatter.

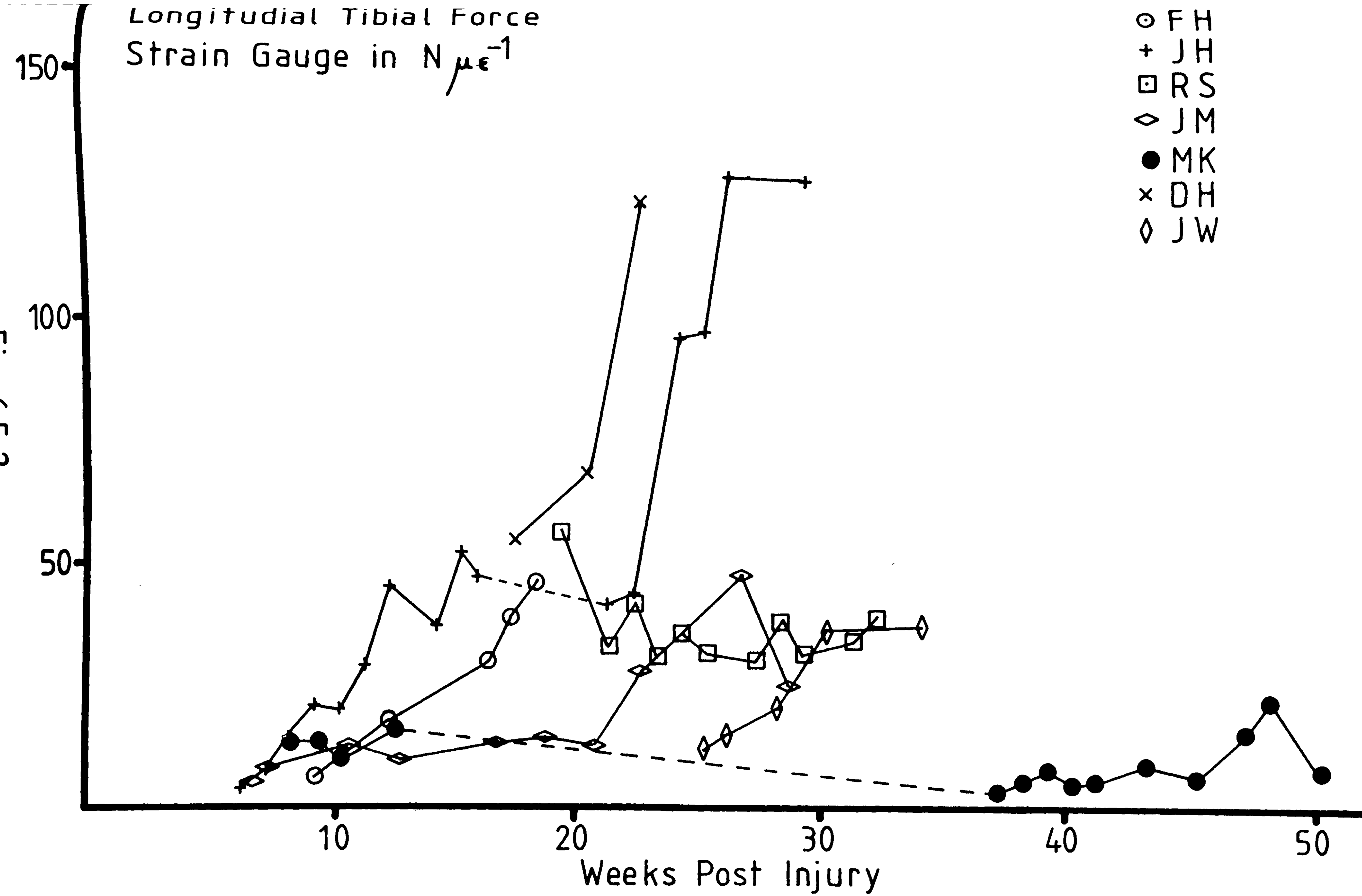
Longitudial Tibial Force
Strain Gauge in N $\mu\epsilon^{-1}$
FH
JH
RS
JM
MK
DH
JW
150
100
50
10
20
30
40
50
Weeks Post Injury

Fig 6.5.2

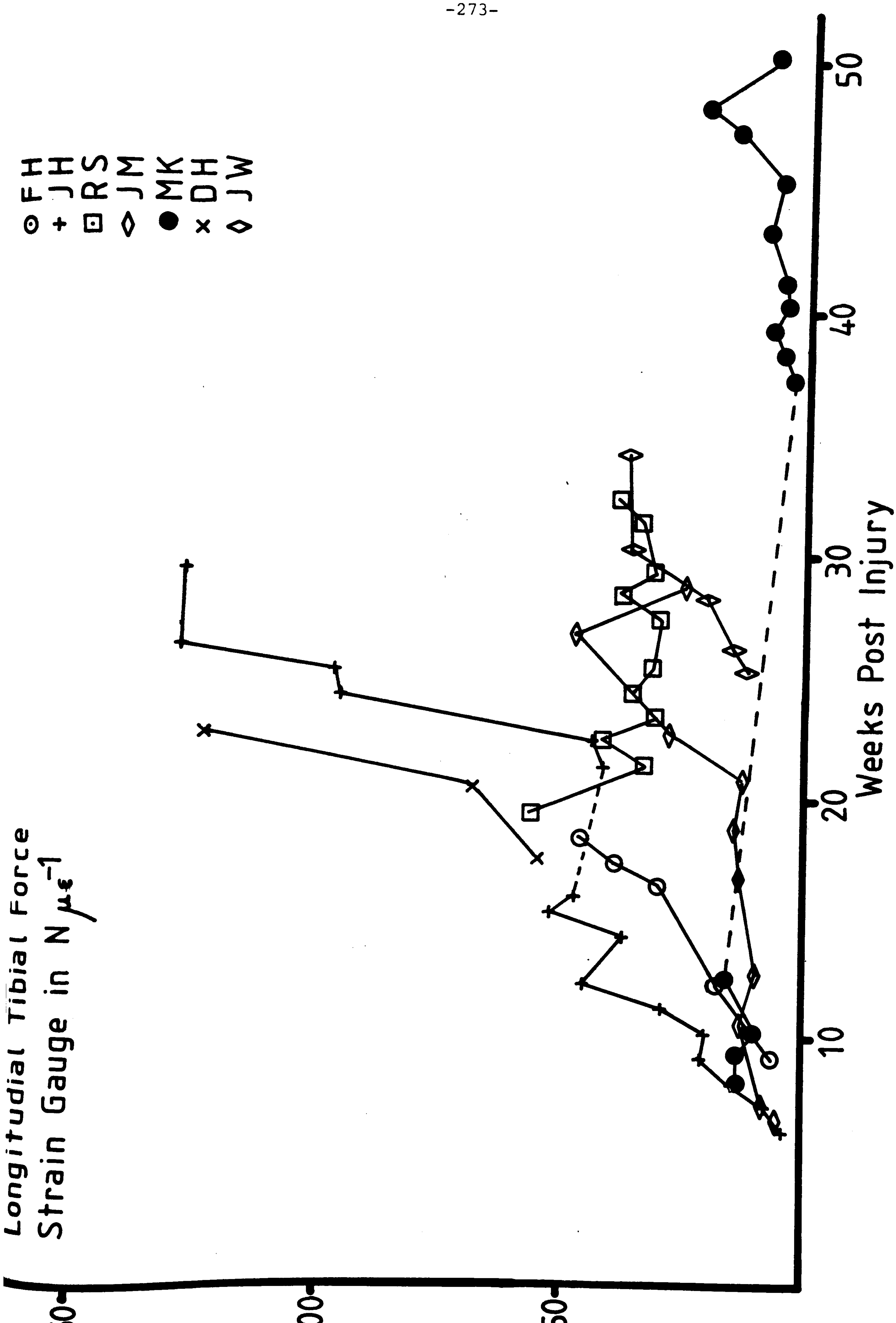

Longitudial Tibial Force
Strain Gauge in N με⁻¹
FH
JH
RS
JM
MK
DH
JW
150
100
50
10
20
30
40
50
Weeks Post Injury

Fig 6.5.2

CHAPTER 8

CONCLUSIONS AND RECOMMENDATIONS

8 CONCLUSIONS AND RECOMMENDATIONS

This transducer has uses; but in its present form these are limited. The major limitation is that the computer control and data processing system are merely functional rather than optimised. With the original clamps it took about five minutes to put the transducer on the patient's fixator, but with the redesigned clamps this was reduced to one or two minutes. The next problem was that the data collection program LPADIN had to run under a single user operating system RT11 so this had to be loaded into the DEC PDP 11/34 rather than the RSX11 multi-user system. This added several minutes onto the test procedure. The tests themselves take about ten minutes to perform, and then once the transducer was removed, this taking a couple of minutes, the patient was free to leave. Thus each set of tests took the patients about twenty minutes. Once the tests had been performed the data was transferred back to RSX11 multi-user operating system for analysis. It took about another ten minutes per patient to analyse the data. Thus, the total computer, and computer operator, time for a single set of patient tests was about half an hour. These tests could also only be performed within the Engineering Centre, as both "Kistler" force plates and a mini-computer were necessary.

Of the results obtained from the transducer, some were clinically useful, and others were not. The transducer was unable to elucidate the control system responsible for the limitations of the load applied to the fracture. In the axial loading tests, insufficient results were obtained for it to be possible to decide whether these were useful, but the longitudinal tibial force results for the strain gauge transducer were useful so may be that the similar results from the displacement transducer would be.

There are two possible methods of improving the data collection d analysis system. The choice depends on where the transducer is to used. The one requiring more hardware but a portable solution is use a micro-computer like an LSI 11 using the same programs along th a "control" program. In this solution the LSI could be mounted a box with the programs kept on a PROM chip and the data stored ther in some RAM or on floppy discs. Also a small printer could be ed to give hard copy of the results. If protability is not required ıen the DEC PDP 11/34 could be used, but there are various methods of creasing the time required for data acquisition and analysis. The ıta acquisition could, in fact, be done under RSX11 as there are thods of making this effectively single-user for the ten seconds quired to perform the data acquisition. For both systems the ease use of the transducer could be improved if a master control program as written, and the time for the analysis programs to run would be duced if the programs were written in machine code rather than)RTRAN. The master control program would require the patient's name r just their initials, and would then be able to look up the data of njury, the injured limb and the dimensions of the patient's fixator. he program would after a start signal have been received, take in ata for one test, then while waiting for the next signal to start ata collection it could start processing the previously collected ata. Then once data collection was finished, and while the ransducer was being taken off the patient's leg, the data could be nalysed, printed out, and possibly even after looking up previous esults for the patient, could draw the progress charts for the atient. To get this all to happen would require many hours of omputer programming time.

The improved electronics and clamping system introduced during he course of the project appear to be satisfactory. However, the transducer and LED heads could both be reduced in size. This would enable the system to be used on a greater percentage of the patients. The present transducer requires at least 40mm between the patients leg and the support bar and at least 80mm between the two pins to which the transducer is connected. A small reduction in size could be achieved by mounting the detectors in a thinner box, but the detector diameter is 25mm and the thickness of their mounting is 5mm giving a minimum box size of 30mm. However, the active area of the detectors is 10mm square and if this was mounted in a square container, rather than round the size of the detector mounting box could be reduced to less than 20mm which would be acceptably small. Square cases for the detector would also make it easier to mount the detectors square with the axes of the transducer. This smaller detector head would require the redesign of the LED head. It might be possible to reduce the size of the collimators, but this is limited by the size of the LED's, unless the miniature LED's used could be replaced with sub-miniature ones. The other solution to the problem would be to use one LED and then use fibre optics to produce the three thin perpendicular beams of light required.

This type of transducer could be used in other situations where multi-dimensional movement is occurring. It could also be simplified and used in one-dimensional situations. Starting with the simplest one-dimensional use, strain gauge type extensometers have a limit to the amount of extension they can measure before being damaged, and are thus not totally suitable for use on some polymers or for high speed testing. One-dimensional lateral effect photo detectors are commercially available, with length up to 75mm so these could be mounted in a suitable sliding case with a LED or other light source. If the mounting were designed to separate into two components then no damage would be done by over extending the extensometer. This would be particularly useful in high speed materials testing as it is often not possible to stop the cross-head before the end of travel of the extensometer has been reached. The sampling rate would need to be increased for this application, but the original electronics design had a sampling rate of 0.185 kHz, so an increased sampling rate could easily be implemented. The computer could be dispensed with as all it is doing to the detector outputs to calculate the displacements of the spots of light, is sampling and then adding, subtracting and dividing so if just the displacements of a spot of light are required then this could all be done with electronics, although it would need to be mains powered rather than battery powered.

The detectors used in this study had a 10mm square working area giving a possible measurement of ±3mm from the zero position. The manufacturers also make a detector with a 25mm square working area so ±10mm displacements could be achieved. One of the possible uses of the three-dimensional system would be in robotics, either in the measurement of the movement of a robot's arm relative to a fixed point or measuring the relative movement between two moving components of the robot while performing a task. This could either be used in the robot's control system as the measuring part of the feedback loop, or as a method of assessing the robot. The quantisation errors could be reduced but using a 12 bit A/D converter rather than the 8 bit one used.

To conclude, this transducer has enabled the movements at the patients' fractures to be measured throughout the healing period, something which has not been achieved before. Of the eight possible movements which could be measured at the fracture site, those of axial movement and torsion at the fracture site have proved to be the most useful at assessing the progress of fracture healing, although some of the others have added to the clinical information. This transducer also gave insight into some of the problems not illuminated by the strain gauge transducer which is in more routine clinical use. The transducer could easily be adapted for use in other fields of engineering.

CHAPTER 9

BIBLIOGRAPHY

ABENDSCHEIN W. and HYATT G.W. (1970)
Ultrasonics and Selected Physical Properties of Bone
Clinical Orthopaedics and Related Research Vol 69 pp 294-301

ACKERMAN J.J.H., GROVE T.H., WONG G.G., GADIAN D.G. and RADDA G.K. (1980)
Mapping of Metabolites in whole Animals by ^{31}PNuclear Magnetic Resonance using Surface Coils.
Nature Vol 283 pp 167-170

ADAMS J.C. (1978)
Outline of Fractures (7th. Edition)
Published by : Churchill Livingstone; Edinburgh, London and New York

ALLUM R.L. and MOWBRAY M.A.S. (1980)
A Retrospective Review of the Healing of Fractures of the Shaft of the Tibia with Special Reference to the Mechanism of Injury
Injury Vol 11 pp 304-308

ALMS M. (1961)
Fracture Mechanics
Journal of Bone and Joint Surgery Vol 43-B pp 162-166

ANDERSON R. (1934)
An Automatic Method of Treatment for Fractures of the Tibia and the Fibula
Surgery, Gynaecology and Obstetrics Vol 53 pp 639-646

ASCENZI A. and BELL G.H. (1972)
Bone as a Mechanical Engineering Problem.
The Biochemistry and Physiology of Bone Vol 1 Cpt 9
Edited by G.H.Bourne
Published by Academic Press

BANKS A.J. and DERVIN E. (1980)
The Salford Technique for the Treatment of Complicated Tibial Fractures.
Engineering in Medicine Vol 9 pp 84-86

BASSETT C.A.L. (1968)
Biologic Significance of Piezoelectricity
Calcified Tissue Research Vol 1 pp 252-272,

BASSETT C.A.L. (1972)
Biophysical Principles Affecting Bone Structure
The Biochemistry and Physiology of Bone Vol 3 Cpt 1
Edited by G.H.Bourne
Published by Academic Press

BEAUPRE G.S., HAYES W.C.,JOFE M.H. and WHITE A.A. (1983)
Monitoring Fracture Site Properties with External Fixation
Journal of Biomedical Engineering Vol 105 pp 120-126

BASSETT C.A.L., PILLA A.A. and PAWLUK R.J. (1977)
A Non-Operative Salvage of Surgically Resistant Pseudoarthroses and Non-Unions by Pulsing Electromagnetic Fields.
Clinical Orthopaedics and Related Research No 124 pp 128-143,

BEHIRI J.C. and BONFIELD W. (1980)
Crack Velocity dependance of Longitudinal Fracture in Bone
Journal of Materials Science Vol 15 pp 1841-1849

BEHIRI J.C. and BONFIELD W. (1984)
Fracture Mechanics of Bone-The Effects of Thickness and Crack Velocity on Longitudinal Fracture
Journal of Biomechanics Vol 17 pp 25-34

BEHRENS F., JOHNSON W.D. and KOCH T.W. (1982)
Bending Stiffness of Unilateral and Bilateral External Fixator Frames
Transactions of 28th. Annual Meeting of the Orthopaedic Research Society p 184

BELL G.H., EMSLIE-SMITH D. and PATTERSON C.R. (1976)
Textbook of Physiology and Biochemistry (9th. Edition)
Published by : Churchill-Livingstone; Edinburgh, London and New York

BICK E.M. (1948)
Source Book of Orthopaedics (2nd. Edition)
Published by : Williams, Baltimore.

BOLTZE W.H., CHIQUET C. and NIEDERER R.G. (1978)
Der Fixateur Externe (Rohrsystem) Stabilitatsprufung
A.O.Bulletin

BOLTZE W.H., FERNANDEZ D.L. and SCHATZKER J. (1976)
The External Fixator (Tubular System)
A.O.Bulletin

BONFIELD W. and GRYNPAS M.D. (1982)
Spiral Fracture of Cortical Bone
Journal of Biomechanics Vol 15 pp 555-559

BONFIELD W., GRYNPAS M.D. and YOUNG R.J. (1978)
Crack Velocity and the Fracture of Bone
Journal of Biomechanics Vol 11 pp 473-479

BOTTOMLEY P.A. and ANDREW E.R (1982)
Radiofrequency Magnetic Field Penetration, Phase Shift, and Power Dissipation i Biological Tissue: Implications for Nuclear Magnetic Resonance Imaging
Physics in Medicine and Biology Vol 23 pp 630-643

BOURGOIS R. and BURNY F. (1972)
Measurement of the Stiffness of Fracture Callus in Vivo, A Theoretical Study
Journal of Biomechanics Vol 5 pp 85-91

BOURNE G.H. (Ed) (1972)
The Biochemistry and Physiology of Bone.(4 volumes)
Published by Academic Press, New York and London.

BRADLEY G.W., McKENNA G.B., DUNN H.K., DANIELS A.U. and STATTON W.O. (1979)
Effects of Flexural Rigidity of Plates on Bone Healing
Journal of Bone and Joint Surgery Vol 61-A pp 866-872

BRIGGS B.T. and CHAO E.Y.S. (1982)
The Mechanical Performance of the Standard Hoffmann-Vidal External Fixation Apparatus
Journal of Bone and Joint Surgery Vol 64-A pp 566-573

BRITISH STANDARD 5724
Safety of Medical Electrical Equipment
Part 1: General Requirements (1979)
Published by British Standards Institute

BROOKER A.F., and EDWARDS C.C. (1979)
External Fixation - The Current State of the Art.
(Proceedings of the 6th International Conference on Hoffmann External Fixation)
Published by: The Williams and Wilkins Co., Baltimore.

BUCHOLZ R.W. and TENSER A. (1982)
Personnal Comminucation

BURNY F. and BOURGOIS R. (1972)
Etude Biomecanique du Fixateur Externe d'Hoffmann
Acta Orthopaedica Beligica Vol 38 pp 265-280

BURNY F., BOURGOIS R., DONKERWOLCKE M. and MOULART F. (1978)
Utilisation Clinique de Jauges de Constrainte- Situation actuelle et perspectives d'avenir.
Acta Orthopaedica Belgica Vol 44 pp 895-920

CHAMAY A. and TSCHANTZ P. (1972)
Mechanical Influences in Bone Remodelling. Experimental Research on Wolff's Law
Journal of Biomechanics Vol 5 pp 173-180

CAMPBELL D.and KEMPSON G.E. (1981)
Which External Fixation Device?
Injury Vol 12 pp 291-297

CHAO E.Y.S., BRIGGS B.T. and McCOY M.T. (1979)
Theoretical and Experimental Analyses of the Hoffmann-Vidal External Fixation System.
External Fixation - The Current State of the Art Cpt. 23
Edited by A.F.Brooker and C.C.Edwards
Published by Williams and Wilkins Co.

CHAO E.Y.S., KASMAN R.A. and AN K.N. (1982)
Rigidity and Stress Analysis of External Fracture Fixation Devices- A Theoretical Approach
Journal of Biomechanics Vol 15 pp 971-983

CONNOLLY J.F., HAHN H. and DAVY D. (1978)
Fracture Healing in Weight-Bearing and Non-Weight-Bearing Bones.
Journal of Trauma Vol 18 pp 766-770

CONNORS W.P. (1971)
Lateral Effect Photodetector Operating in the Fully Reverse Biassed Mode
Institute of Electrical and Electronic Engineers
Transactions on Electronic Devices Vol ED-18 pp 591-596

CHURCHES A.E, TANNER K.E., and HARRIS J.D. (1986a)
The Oxford External Fracture Fixator: Fixator Stiffnesses and the Effects of Bone Pin Loosening
Accepted by Engineering in Medicine

CHURCHES A.E., TANNER K.E., EVANS M. and GWILLIM J. (1986b)
The Oxford External Fracture Fixator: Fracture Healing Assessment in External Fixation.
Accepted by Engineering in Medicine

CHURCHES A.E., TANNER K.E., HARRIS J.D. and EVANS M (1986c)
An Engineering Evaluation of the Oxford External Fracture Fixator with Sliding Clamps: Fixator Stiffness and Fracture Healing Assessment
Accepted by Engineering in Medicine

DANIS R. (1949)
Theorie et Practique de l'Osteosynthese
Published by : Masson, Paris

DE BASTANI G., ALDEGHERI R. and RENZI BRIVO L. (1984)
The treatment of Fractures with A Dynamic Fixator
Journal of Bone and Joint Surgery Vol 66-B 538-545

DE CHAULIAC G. (1300-1368)
Wounds and Fractures.
Translated and Published by : W.A.Brennan, Chicago (1923)

DOEMLAND H.H. (1982)
Assessment of Fracture Healing of Long Bones using the Spectral Content of the Impulse Response
Transactions of the 28th meeting of the Orthopaedic Research Society p186

DOYLE F., BROWN J and LACHANCE C. (1970)
Relationship between Bone Mass and Muscle Weight
Lancet Vol 1 pp 391-393

DWYER W.St.J.P. (1973)
Preliminary Report upon a new Fixation Device for Fractures of a Long Bone.
Injury Vol 5 pp 141-144

EAGLESON W.M., DECKERT K.I., TOWNSEND E.E. and ARNOTT J.R. (1967)
The Effect of Heat on the Healing of Fractures: A Preliminary Experimental Report.
Canadian Medical Association Journal Vol 97 pp 274-280

EDGE A.J. and DENHAM R.A. (1977)
The Portsmouth Method of External Fixation of Complicated Tibial Fractures.
British Orthopaedic Association Meeting, September 1977

EGGARS G.W.N., SHINDLER T.O. and POMERAT G.M. (1949)
The Influence of the Contact-Compression Factor on Osteogenesis in Surgical Fractures.
Journal of Bone and Joint Surgery Vol 31-A pp 693-716

EPSTEIN S. (1937)
Art, History and the Crutch
Annals of Medical History Vol 9 p 304

EVANS F.G. (1973)
Mechanical Properties of Bone
Published by : Charles C.Thomas; Springfield, Illinois

EVANS M., KENWRIGHT J., GOODSHIP A.E., GWILLIM J. and HARRIS J.D. (1982)
The Influence of Induced Movement on Fracture Healing with External Fixation
Proceeding of the Conference on "Engineering in Orthopaedic Surgery and Rehabilation" Edinburgh September 1982

EVANS M., KENWRIGHT J. and TANNER K.E. (1979)
Analysis of a Single-Sided External Fracture Fixator.
Engineering in Medicine Vol 8 pp 133-137

FORSTER I.W. (1984)
Structural Aspects of Tendons and Ligaments
Natural and Living Biomaterials Chapter 8
Edited by G.W.Hastings and P.Ducheneyne
Published by CRC Press Florida U.S.A.

FREIDENBERG Z.B. and FRENCH G. (1952)
The Effect of Known Compression Forces on Fracture Healing.
Surgery, Gynaecology and Obstetrics Vol 94 pp 743-748

FUKADA E. (1957)
On the Piezoelectric Effect of Bone
Journal of the Physiological Society of Japan Vol 12 p 1159

GOODSHIP A.E., LANYON L.E. and McFIE H. (1979)
Functional Adaption of Bone to Increased Stress- An Experimental Study
Journal of Bone and Joint Surgery Vol 61-A pp 539-546

GUI L., GUALTIERI I. and GODOLI N. (1980)
A New Device (G3-IOR) for External Fixation
Italian Journal of Trauma Vol 6(3) pp 321-328

HAM A.W. and HARRIS W.R. (1972)
Repair and Transplantation of Bone
The Biochemistry and Physiology of Bone Vol 3 Cpt 10
Edited by G.H.Bourne
Published by Academic Press

HAMMER R., EDHOLM P. and LINDHOLM B (1984)
Stability of Union after Tibial Shaft Fracture- Analysis by a non-invasive Technique.
Journal of Bone and Joint Surgery Vol 66-B pp 529-534

HAMMING R.W.(1977)
Digital Filters pp 32-37, 115-117
Published by Prentice-Hall New Jersey U.S.A.

HAMSTRA H.R. Jr and WENDLAND P. (1972)
Noise and Frequency Response of Silicon Photodiode Operational Amplifier Combination
Applied Optics Vol 11 pp 1539-1547

HASSLER C.R., RYBICKI E.F., CUMMINGS K.D. and CLARK L.C. (1980)
Quantification of Bone Stresses during Remodelling.
Journal of Biomechanics Vol 13 pp 185-190

HASSLER C.R., RYBICKI E.F., SIMONEN E.A. and WEISS E.B. (1974)
Measurement of the Healing at an Osteotomy in a Rabbit Calvarium: The Influence of Applied Compressive Stress on Collagen Synethesis and Calcification
Journal of Biomechanics Vol 7 pp 545-550

HAVERS C. (1691)
Osteologia Nova
Published in London

HAYNES H.H. (1939)
Treating Fractures by the Skeletal Fixation of the Individual Bone
Southern Medical Journal Vol 32 pp 720-724

HEALTH TECHNICAL MEMORANDRUM No 8 (1969)
Safety code for electro-mechanical Apparatus
Published by Her Majesty's Stationary Office

HENRY A.N., FREEMAN M.A.R. and SWANSON S.A.V. (1968)
Studies on the Mechanical Properties of Healing Experimental Fractures.
Proceedings of the Royal Society of Medicine Vol 61 pp 902-906

HEIRHOLZER G., KLEINING R., HORSTER G. and ZEMENDES P. (1978)
External Fixation - Classifications and Indications
Archives of Orthopaedic and Traumatic Surgery Vol 92 pp 175-182

HIPPOCRATES (c.420 B.C.)
Hippocratic Writings
Edited by : G.E.R.Lloyd
Published by : Pelican Classics, London, 1978

HIRSCH T.J. (1962)
Modulus of Elasticity of Concrete Affected by Elastic Modulus of Cement Paste Matrix and Aggregate
Journal of the American Concrete Institute Vol 59 pp 427-451

HOAGLUND F.T. and STATES J.D. (1967)
Factors influencing the Rate of Healing in Tibial Shaft Fractures
Surgery, Gynaecology and Obstetrics Vol 124 pp 71-76

HOFFMANN R. (1938)
Rotules a os pour la reduction dirigee non sanglante des fractures
Helventia Med. Acta Vol 5 p 844

HOROWITZ P. and HILL W. (1980)
The Art of Electronics
Published by Cambridge University Press, Cambridge

HUTZCHENREUTER P., PERREN S.M., STEINEMANN S., GERET V. and KLEBL M. (1969)
Some Effects of the Rigidity of Internal Fixation on the Healing Patterns of Osteotomies
Injury Vol 1 pp 77-81

ILISAROV L. (1976)
Results of Clinical Trials and Experiance Obtained from the Clinical Use of the set of Ilisarov Compression-Distraction Apparatus.
Medical Exports Moscow.

JANKOVICH J.P. (1972)
The Effects of Mechanical Vibration on Bone Developement in the Rat.
Journal of Biomechanics Vol 5 pp 241-250

JAWORSKI Z.F.G., LISKOVA-KIAR M. and UHTOFF H.K. (1980)
The Effects of Long-Term Immobolisation on the Pattern of Bone Loss in Older Dogs.
Journal of Bone and Joint Surgery Vol 62-B pp 104-110

JERNBERGER A. (1970)
Measurement of the Stability of Tibial Fractures.
Acta Orthopaedica Scandinavica Supplement 135

JOFE M.H., HAYNES W.C., BEAUPRE G.S., GERHART T.N. and WHITE A.A. (1982)
Biomechanical Monitoring of Healing with External Skeletal Fixation
Transactions of the 28th Annual Meeting of the Orthopaedic Society p185

JOHNSON R.J. and POPE M.H. (1977)
Tibial Shaft Fractures in Skiing
The American Journal of Sports Medicine Vol 5 pp 49-62

JOHNSTON R.M. (1980)
Advances in External Fixation
Published by Year Book Medical Publishers U.S.A.

JORGENSEN T.E. (1972(a))
Measurements of Stability of Crural Fractures Treated with Hoffmann Osteotaxis
1.Method and Measurement of Deflection on Autopsy Crura
Acta Orthopaedica Scandinavica Vol 43 pp 188-206

JORGENSEN T.E. (1972(b))
Measurements of Stability of Crural Fractures Treated with Hoffmann Osteotaxis
2.Measurements on Crural Fractures
Acta Orthopaedica Scandinavica Vol 43 pp 207-218

JORGENSEN T.E. (1972(c))
Measurements of Stability of Crural Fractures Treated with Hoffmann Osteotaxis
3.The Uncomplicated Terminal Phase of Healing of Crural Fractures.
Acta Orthopaedica Scandinavica Vol 43 pp 264-279

JORGENSEN T.E. (1972(d))
Measurements of Stability of Crural Fractures Treated with Hoffmann Osteotaxis
4.The Complicated Terminal Phase of Healing of Crural Fractures.
Acta Orthopaedica Scandinavica Vol 43 pp 280-291

KARAHARJU E.O. and AALTO K. (1983)
The Deformation of External Fixation Devices During Loading
International Orthopaedics Vol 7 pp 179-183

KARLSTROM G. and OLERUD S. (1974)
Fractures of the Tibial Shaft - A Critical Evaluation of Treatment Alternatives
Clinical Orthopaedics and Related Research Vol 105 pp 82-115

KARLSTROM G. and OLERUD S. (1975)
Percutaneous Pin Fixation of Open Tibial Fractures
Journal of Bone and Joint Surgery Vol 57-A pp 915-924

KELLY B.O. (1976)
Lateral-Effect Photodetectors
Laser Focus Vol 12 pp 38-40

KENWRIGHT J., HARRIS J.D. and EVANS M. (1979)
External Fracture Fixation - The Analysis and Design of a New System
Engineering in Medicine Vol 8 pp 134-142

KIRILLOV S.K., LAURENTIEV V.V. and FIRSOV N.N. (1978)
Study of the Mechanical Properties of the Bone Regenerate in the Process of its Formation.
Ortopaediia Travmatologiia Protezirovanie Vol 1 pp 34-39

KREYSIG E (1974)
Advanced Engineering Mathematics
Published by Wiley

KOCH J.C. (1917)
The Laws of Bone Architecture.
American Journal of Anatomy Vol 21 pp 177-298

LAMBOTTE A. (1907)
L'Intevention Operatoire dans les Fracteurs.
Published by: Lamartin; Brussels.

LAROS G.S. (1974)
Fracture Healing - Compression vs. Fixation.
Archives of Surgery Vol 108 pp 698-702

LETTIN A.W.F. (1965)
The Effects of Axial Compression on the Healing of Experimental Fractures of th
Rabbits Tibia.
Proceedings of the Royal Society of Medicine Vol 58 pp 882-886

LEVY D.D. (1974)
A Pulsed Electrical Stimulation Technique for Inducing Bone Growth.
Annals of the New York Academy of Science Vol 238 pp 478-490

LEWIS J.J. (1975)
A Dynamic Model of a Healing Fractured Long Bone
Journal of Biomechanics Vol 8 pp 17-25

LIPPERT F.G. (1973)
The Feasibility of Photogrammetrey as a Clinical Research Tool.
Journal of Biomechanics Vol 6 pp 459-473

LIPPERT F.G., and HIRSCH C. (1974)
The Three-Dimensional Measurement of Tibial Fracture Motion by Photogrammetry.
Clinical Orthopaedics and Related Research Vol 105 pp 130-143.

LONDON P.S.(1980)
Principles of Fracture Management
Scientific Foundations of Orthopaedics and Traumatology Chapter 49
Edited by R. Owen, J.W. Goodfellow and P.G. Bullough
Published by Heinemann Scientific Books London

LUCOVSKY G. (1960)
Photoeffects in Non-uniformly Irradiated p-n Junctions
Journal of Applied Physics Vol 31 pp 1088-1095

MACAULEY W.H.(1919)
Note on the Deflection of Beams
Messenger of Mathematics Vol 48 pp 129-130

McELHANEY J.H. (1966)
Dynamic Response of Bone and Muscle Tissue
Journal of Applied Physiology Vol 21 pp 1231-1236

McKIBBIN B. (1978)
The Biology of Fracture Healing in Long Bones.
Journal of Bone and Joint Surgery Vol 60-B pp 150-162

MALGAIGNE (1853)
Considerations cliniques sur les Fractures de la Notule et leur Traitment par les griffes.
Journal des Connaissances Medical Practiques Vol 16 pp 9-12

MEARS D.C. (1979)
History of External Fixation
Cpt 1. External Fixation, The Current State of the Art.
Edited by A.F.Brooker and C.C.Edwards
Published by Williams and Wilkins

MOORE A.R. and WEBSTER W.M. (1955)
The Effective Surface Recombination of a Germanium Surface with a Floating Barrier
Proceedings of the Institute of Radio Engineers Vol 43 pp 427-435

MOSTAFA A.G.S.A., EL ATTAR S., MILI F. and WRIGHT E.A. (1980)
The Effect of Enviromental Temperature on the Rate of Healing of Fractures in the Tail Vertebrae of Mice.
Journal of Bone and Joint Surgery Vol 62-B pp 102-103

NEWMAN R.J. (1983)
Nuclear Magnetic Resonance Studies of Abnormal Muscle
D.Phil. Thesis University of Oxford

NICOLL E.A. (1964)
Fractures of the Tibial Shaft - A survey of 705 Cases
Journal of Bone and Joint Surgery Vol 46-B pp 373-387

OLSON G. (1977)
Non-Contact Electro-optical Position Measurement
Electro-Optics/Laser '77 Conference and Exposition

O'REILLY R.J., COOK D.J., GAFFNEY R.D., ANGEL K.R. and PATERSON D.C. (1981)
Can Serial Scintigraphic Studies Detect Delayed Fracture Union in Man?
Clinical Orthopaedics and Related Research Vol 160 pp 227-232

OWEN R., GOODFELLOW J.W. and BULLOUGH P.G (1980)
Scientific Foundations of Orthopaedics of Orthopaedics and Traumatology
Published by Heinemann Medical Books, London

PAAVOLAINEN P., SLATIS P., KARAHARJU E. and HOLMSTROM T. (1978)
Studies on the Mechanical Strength of Bone. II Torsional Strength of Cortical Bone after Rigid Plate Fixation with and without compression.
Acta Orthopaedica Scandinavica Vol 49 pp 506-511

PANJABI M.M., WHITE A.A. and SOUTHWICK W.O. (1973)
Mechanical Properties of Bone as a Function of the Rate of Deformation
Journal of Bone and Joint Surgery Vol 55-A pp 322-330

PANJABI M.M., WHITE A.A. and SOUTHWICK W.O. (1977)
Temporal Changes in the Physical Properties of Healing Fractures in Rabbits.
Journal of Biomechanics Vol 10 pp 689-699

PARKHILL C (1897)
A New Apparatus for the Fixation of Bones after Resection and in Fractures with a Tendency to Displacement
Transactions of the American Surgical Association Vol 180 pp 3-6

PARKHILL C. (1898)
Further Observations regarding the use of the Bone Clamp in Ununited Fractures, Fractures with Malunion, and Recent Fractures with a Tendancy to Displacement
Annals of Surgery Vol 27 pp 553-570

PAUL OF AEGINA (625-690 A.D.)
Collected Works
Translated by : Fr. Adams
Published in London 1834 et seq.

PETERSON L.T. (1949)
External Skeletal Fixation
Bulletin of the United States Army Medical Department Vol 27 pp 553-570

PIEKARSKI K. (1973)
Analysis of Bone as a Composite Material.
International Journal of Engineering Science Vol 11 pp 557-565

PRITCHARD J.J. (1972(a))
General Histology of Bone.
The Biochemistry and Physiology of Bone Vol 1 Cpt 1
Edited by G.H.Bourne
Published by Academic Press

PRITCHARD J.J. (1972(b))
The Osteoblast
The Biochemistry and Physiology of Bone Vol 1 Cpt 2
Edited by G.H.Bourne
Published by Academic Press

POPE M.H. and OUTWATER J.O. (1972)
The Fracture Characturistics of Bone Subtance
Journal of Biomechanics Vol 5 pp 457-465

RALIS Z.A. (1980)
Influence of Paralysis and Interuterine Pressure on the Ossicification Growth and Quality of Developing Bone
Mechanical Factors and The Skeleton
Edited by I.A.F.Stokes
Published by John Libbey London

REZAIAN S.M. (1971)
The Effect of a New External Bone-Fixator on the Treatment of Fractures of Long Bones
Annals of the Royal College of Surgeons of England Vol 48 pp 336-343

RHINELANDER F.W. (1968)
The Normal Microcirculation of the Diaphysial Cortex and its Response to Fracture
Journal of Bone and Joint Surgery Vol 50A pp 784-800

ROMANO R.L., BURGESS E.M. and RUBENSTEIN C.P. (1976)
Percutaneous Electrical Stimulation for Clinical Tibial Fracture Repair.
Clinical Orthopaedics and Related Research Vol 114 pp 290-295

SAHA S. (1977)
Longditudinal Shear Properties of Human Compact Bone, and its Constitutents, an Associated Failure Mechanisms
Journal of Materials Science Vol 12 pp 1798-1806

SAHA S. and LAKES R.S. (1977)
The Effect of Soft Tissue on Wave Propagation and Vibration Tests for determining the "in vivo" Properties of Bone
Journal of Biomechanics Vol 10 pp 393-401

SALLEN R.P. and KAY E.L. (1955)
A Practical Method of Designing R-C Active Filters
Institute of Radio Engineers - Transactions on Circiut Theory Vol CT-2 pp 74-85

SARMIENTO A (1970)
A Functional Below-the-knee Brace for Tibial Fractures - A Report on its use in 135 cases
Journal of Bone and Joint Surgery Vol 52-A pp 295-311

SARMIENTO A., SCHAEFFER J.F., BECKERMAN L., LATTA L. and ENIS J.E. (1977)
Fracture Healing in Rat Femora as Affected by Functional Weight-Bearing.
Journal of Bone and Joint Surgery Vol 59-A pp 369-375

SCHATZKER J., SUMNER-SMITH G., CLARK R. and McBROOM R. (1978)
Strain Gauge Analysis of Bone Response to Internal Fixation
Clinical Orthopaedics and Related Research Vol 132 pp 244-251

SCHOTTKY W. (1930)
Ueber den Entstehungsort der Photoelektronen in Kupfer-Kupferoxydul Photozellen
Phys. Z. Vol 31 pp 913-925

SEDEL L., CHRISTEL P., DEWAS J., De CHARENTENAY F.X. and LERAY J. (1980)
Comparision of the Effect of Intermedullary Nailing or Plating on the Mechanica Properties of Fracture Callus
Journal of Biomedical Engineering Vol 2 pp 89-92

SIEGAL I.M., ANAST G.T. and FIELDS T. (1958)
The Determination of Fracture Healing by Measurement of Sound Velocity across the Fracture Site
Surgery, Gynaecology and Obstetrics Vol 107 pp 327-332

SMITH G.E. (1923)
Ancient Egyptians and the Origin of Civilization
Published by: Harpers and Brothers; London

SODERQUIST D. (1980)
Minimization of Noise in Operational Amplifier Applications
Precision Monolithics Inc. Applications Note AN-15

SONSTEGARD D.A. and MATTHEWS L.S. (1976)
Sonic Diagnosis of Bone Fracture Healing - A Primary Study.
Journal of Biomechanics Vol 9 pp 689-694

STADER O. (1937)
A Preliminary Announcement of a New Method of Treating Fractures
North American Veterinary Journal Vol 18 pp 37-38

STADER O. (1939)
Treating Fractures of Long Bones with the Reduction Splint
North American Veterinary Journal Vol 20 pp 55-59

STOKES I.A.F., KENWRIGHT J., HARRIS J.D., and MacLARNON C. (1978)
Measurement of Fracture Rigidity by Biplanar Radiographic Techniques
Oxford Orthopaedic Engineering Centre Annual Report No. 6

TANNER K.E. (1979)
An Investigation of a Method of Increasing the Stability of a Single Sided External Fracture Fixator
Final Year Project Department of Engineering Science, University of Oxford

TASSELL C. (1980)
Photodetectors in Noise Sensitive Environments
New Electronics January 1980

TODD J.D. (1974)
Structural Theory and Analysis
Published by Macmillians, London

TONINO A.J., DAVIDSON C.L., KLOPPER P.J. and LINCLAU L.A. (1976)
Protection of Stress in Bone and its Effects - Experiments with Stainless Steel and Plastic Plates in Dogs.
Journal of Bone and Joint Surgery Vol 58-B pp 107-113

VIDAL J., RABISCHONG P., BONNEL F. and ADREY J. (1970)
Etude Biomecanique du Fixateur Externe d'Hoffmann dans les Fractures de Jambe.
Society de Chirurgie de Montpellier Seance de 20 Janvin 1970
pp 43-52

WALLMARK J.T. (1957)
A New Semiconductor Photocell using the Lateral Photoeffect
Proceedings of the Institute of Radio Engineers Vol 45 pp 474-483

WASHBURN S.L. (1947)
Anatomical Record Vol 99 p 239

WATSON J. (1979)
The Electrical Stimulation of Bone Healing.
Proceedings of the Institute of Electrical and Electronic Engineers Vol 67 pp 1339-1352

WATT D.G. and WILLIAMS C.M.H. (1951)
American Journal of Orthodontics Vol 37 p 895

WEISS C., PUGH J., GRUBER J. and SWETT R. (1977)
The Application of Structure-Bourne Sound to the Structural Analysis of Bone an
Fracture Healing
Bulletin of the Hospital for Joint Diseases Vol 38 pp 26-28

WHITE A.A., PANJABI M.M. and SOUTHWICK W.O. (1977(a))
The Four Biomechanical Stages of Fracture Repair
Journal of Bone and Joint Surgery Vol 59-A pp 188-192

WHITE A.A., PANJABI M.M. and SOUTHWICK W.O. (1977(b))
Effects of Compression and Cyclical Loading on Fracture Healing - A Quantitive
Biomechanical Study
Journal of Biomechanics Vol 10 pp 233-239

WILLIAMS W.S. and BREGER L. (1975)
Piezoelectricity in Tendon and Bone.
Journal of Biomechanics Vol 8 pp 407-413

WOLFF J. (1892)
Das Gesetz der Transformation der Knochen
Published by : Hirschwald, Berlin

WOLTRING H.J. (1975)
Single and Dual-Axis Lateral Photodetectors of Rectangular Shape
Institute of Electrical and Electronic Engineers
Transactions on Electronic Devices Vol ED-22 pp 581-590

WOO S.L-Y., AKESON W.H., COUTTS R.D., RUTHERFORD L., DOTY D., JEMMOTT G.F.
and AMIEL D. (1976)
A Comparision of Cortical Bone Atrophy Secondary to Fixation Plates with Large
Differences in Bending Strengths.
Journal of Bone and Joint Surgery Vol 58-A pp 190-195

WOO S.L-Y., SIMON B.R., AKESON W.H. and McCARTY M.P. (1977)
An Interdisciplinary Approach to Evaluate the Effect of Internal Fixation Plate
on Long Bone Remodeling
Journal of Biomechanics Vol 10 pp 87-95

WYNN-JONES C.H. (1978)
A Simple External Fixation Method using Wire and Bone Cement.
Injury Vol 9 pp 329-330

YAMAGISHI M. and YOSHIMURA Y. (1955)
The Biomechanics of Fracture Healing
Journal of Bone and Joint Surgery Vol 37-A pp 1035-1068

the problem, one would be to continue to use the three collimated LED's and reduce the size of the collimators, but there is a limit to the reduction in size due to the size of the LED's. The other method of reducing the size of the LED head would be to use fibre optics to produce three perpendicular thin beams of light from one LED mounted in the support bar of the LED head.

This transducer has potential for use in other situations where the movement in three dimensions between two objects is required. Either the two heads could be mounted between the two objects, or the transducer could be mounted on the side of the two objects, and in this case the equations used for the system with the fixator bar removed are appropriate. The size detectors used enabled up to 3 mm of displacement from the zero position to be measured, but the manufacturers do make a 25 mm square detector, so up to 10 mm from zero position could be measured although if the displacement is only in one direction the zero position can be offset. If the displacement is required to be measured more accurately then the number of bits on the A/D converter should be increased and this would reduce the digitizing errors.

In conclusion this transducer is useful for patient testing as a research tool only, in its present form. However, it would be possible to improve it to enable it to be used for more routine testing, and the methods of doing this are considered. With the seven patients tested there was a range of clinical problems ranging from those whose fractures healed quickly to those which developed a slow union. From the few cases tested there seems to be a difference between those patients whose fractures healed quickly and those with slow unions, but due to the small patient sample statistical tests have not been applied to the results. Further tests are required to test whether there is really a difference between these two groups of patients, but with the few patients tested it seems possible that it may be possible to find which patients are going to have slow unions at an early stage as they have large shear displacements at the fracture site. It is also possible to measure the stiffness of the fracture and to use this to measure the end of healing, or at least when no more fixation is required.

CHAPTER 9

BIBLIOGRAPHY

ABENDSCHEIN W. and HYATT G.W. (1970)
Ultrasonics and Selected Physical Properties of Bone
Clinical Orthopaedics and Related Research Vol 69 pp 294-301

ACKERMAN J.J.H., GROVE T.H., WONG G.G., GADIAN D.G. and RADDA G.K. (1980)
Mapping of Metabolites in whole Animals by ^{31}PNuclear Magnetic Resonance using Surface Coils.
Nature Vol 283 pp 167-170

ADAMS J.C. (1978)
Outline of Fractures (7th. Edition)
Published by : Churchill Livingstone; Edinburgh, London and New York

ALLUM R.L. and MOWBRAY M.A.S. (1980)
A Retrospective Review of the Healing of Fractures of the Shaft of the Tibia with Special Reference to the Mechanism of Injury
Injury Vol 11 pp 304-308

ALMS M. (1961)
Fracture Mechanics
Journal of Bone and Joint Surgery Vol 43-B pp 162-166

ANDERSON R. (1934)
An Automatic Method of Treatment for Fractures of the Tibia and the Fibula
Surgery, Gynaecology and Obstetrics Vol 53 pp 639-646

ASCENZI A. and BELL G.H. (1972)
Bone as a Mechanical Engineering Problem.
The Biochemistry and Physiology of Bone Vol 1 Cpt 9
Edited by G.H.Bourne
Published by Academic Press

BANKS A.J. and DERVIN E. (1980)
The Salford Technique for the Treatment of Complicated Tibial Fractures.
Engineering in Medicine Vol 9 pp 84-86

BASSETT C.A.L. (1968)
Biologic Significance of Piezoelectricity
Calcified Tissue Research Vol 1 pp 252-272,

BASSETT C.A.L. (1972)
Biophysical Principles Affecting Bone Structure
The Biochemistry and Physiology of Bone Vol 3 Cpt 1
Edited by G.H.Bourne
Published by Academic Press

BEAUPRE G.S., HAYES W.C.,JOFE M.H. and WHITE A.A. (1983)
Monitoring Fracture Site Properties with External Fixation
Journal of Biomedical Engineering Vol 105 pp 120-126

BASSETT C.A.L., PILLA A.A. and PAWLUK R.J. (1977)
A Non-Operative Salvage of Surgically Resistant Pseudoarthroses and Non-Unions by Pulsing Electromagnetic Fields.
Clinical Orthopaedics and Related Research No 124 pp 128-143,

BEHIRI J.C. and BONFIELD W. (1980)
Crack Velocity dependance of Longitudinal Fracture in Bone
Journal of Materials Science Vol 15 pp 1841-1849

BEHIRI J.C. and BONFIELD W. (1984)
Fracture Mechanics of Bone-The Effects of Thickness and Crack Velocity on Longitudinal Fracture
Journal of Biomechanics Vol 17 pp 25-34

BEHRENS F., JOHNSON W.D. and KOCH T.W. (1982)
Bending Stiffness of Unilateral and Bilateral External Fixator Frames
Transactions of 28th. Annual Meeting of the Orthopaedic Research Society p 184

BELL G.H., EMSLIE-SMITH D. and PATTERSON C.R. (1976)
Textbook of Physiology and Biochemistry (9th. Edition)
Published by : Churchill-Livingstone; Edinburgh, London and New York

BICK E.M. (1948)
Source Book of Orthopaedics (2nd. Edition)
Published by : Williams, Baltimore.

BOLTZE W.H., CHIQUET C. and NIEDERER R.G. (1978)
Der Fixateur Externe (Rohrsystem) Stabilitatsprufung
A.O.Bulletin

BOLTZE W.H., FERNANDEZ D.L. and SCHATZKER J. (1976)
The External Fixator (Tubular System)
A.O.Bulletin

BONFIELD W. and GRYNPAS M.D. (1982)
Spiral Fracture of Cortical Bone
Journal of Biomechanics Vol 15 pp 555-559

BONFIELD W., GRYNPAS M.D. and YOUNG R.J. (1978)
Crack Velocity and the Fracture of Bone
Journal of Biomechanics Vol 11 pp 473-479

BOTTOMLEY P.A. and ANDREW E.R (1982)
Radiofrequency Magnetic Field Penetration, Phase Shift, and Power Dissipation in Biological Tissue: Implications for Nuclear Magnetic Resonance Imaging
Physics in Medicine and Biology Vol 23 pp 630-643

BOURGOIS R. and BURNY F. (1972)
Measurement of the Stiffness of Fracture Callus in Vivo, A Theoretical Study
Journal of Biomechanics Vol 5 pp 85-91

BOURNE G.H. (Ed) (1972)
The Biochemistry and Physiology of Bone.(4 volumes)
Published by Academic Press, New York and London.

BRADLEY G.W., McKENNA G.B., DUNN H.K., DANIELS A.U. and STATTON W.O. (1979)
Effects of Flexural Rigidity of Plates on Bone Healing
Journal of Bone and Joint Surgery Vol 61-A pp 866-872

BRIGGS B.T. and CHAO E.Y.S. (1982)
The Mechanical Performance of the Standard Hoffmann-Vidal External Fixation Apparatus
Journal of Bone and Joint Surgery Vol 64-A pp 566-573

BRITISH STANDARD 5724
Safety of Medical Electrical Equipment
Part 1: General Requirements (1979)
Published by British Standards Institute

BROOKER A.F., and EDWARDS C.C. (1979)
External Fixation - The Current State of the Art.
(Proceedings of the 6th International Conference on Hoffmann External Fixation
Published by: The Williams and Wilkins Co., Baltimore.

BUCHOLZ R.W. and TENSER A. (1982)
Personnal Comminucation

BURNY F. and BOURGOIS R. (1972)
Etude Biomecanique du Fixateur Externe d'Hoffmann
Acta Orthopaedica Beligica Vol 38 pp 265-280

BURNY F., BOURGOIS R., DONKERWOLCKE M. and MOULART F. (1978)
Utilisation Clinique de Jauges de Constrainte- Situation actuelle et perspectives d'avenir.
Acta Orthopaedica Belgica Vol 44 pp 895-920

CHAMAY A. and TSCHANTZ P. (1972)
Mechanical Influences in Bone Remodelling. Experimental Research on Wolff's Law
Journal of Biomechanics Vol 5 pp 173-180

CAMPBELL D.and KEMPSON G.E. (1981)
Which External Fixation Device?
Injury Vol 12 pp 291-297

CHAO E.Y.S., BRIGGS B.T. and McCOY M.T. (1979)
Theoretical and Experimental Analyses of the Hoffmann-Vidal External Fixation System.
External Fixation - The Current State of the Art Cpt. 23
Edited by A.F.Brooker and C.C.Edwards
Published by Williams and Wilkins Co.

CHAO E.Y.S., KASMAN R.A. and AN K.N. (1982)
Rigidity and Stress Analysis of External Fracture Fixation Devices- A Theoretical Approach
Journal of Biomechanics Vol 15 pp 971-983

CONNOLLY J.F., HAHN H. and DAVY D. (1978)
Fracture Healing in Weight-Bearing and Non-Weight-Bearing Bones.
Journal of Trauma Vol 18 pp 766-770

CONNORS W.P. (1971)
Lateral Effect Photodetector Operating in the Fully Reverse Biassed Mode
Institute of Electrical and Electronic Engineers
Transactions on Electronic Devices Vol ED-18 pp 591-596

CHURCHES A.E, TANNER K.E., and HARRIS J.D. (1986a)
The Oxford External Fracture Fixator: Fixator Stiffnesses and the Effects of Bone Pin Loosening
Accepted by Engineering in Medicine

CHURCHES A.E., TANNER K.E., EVANS M. and GWILLIM J. (1986b)
The Oxford External Fracture Fixator: Fracture Healing Assessment in External Fixation.
Accepted by Engineering in Medicine

CHURCHES A.E., TANNER K.E., HARRIS J.D. and EVANS M (1986c)
An Engineering Evaluation of the Oxford External Fracture Fixator with Sliding Clamps: Fixator Stiffness and Fracture Healing Assessment
Accepted by Engineering in Medicine

DANIS R. (1949)
Theorie et Practique de l'Osteosynthese
Published by : Masson, Paris

DE BASTANI G., ALDEGHERI R. and RENZI BRIVO L. (1984)
The treatment of Fractures with A Dynamic Fixator
Journal of Bone and Joint Surgery Vol 66-B 538-545

DE CHAULIAC G. (1300-1368)
Wounds and Fractures.
Translated and Published by : W.A.Brennan, Chicago (1923)

DOEMLAND H.H. (1982)
Assessment of Fracture Healing of Long Bones using the Spectral Content of the Impulse Response
Transactions of the 28th meeting of the Orthopaedic Research Society p186

DOYLE F., BROWN J and LACHANCE C. (1970)
Relationship between Bone Mass and Muscle Weight
Lancet Vol 1 pp 391-393

DWYER W.St.J.P. (1973)
Preliminary Report upon a new Fixation Device for Fractures of a Long Bone.
Injury Vol 5 pp 141-144

EAGLESON W.M., DECKERT K.I., TOWNSEND E.E. and ARNOTT J.R. (1967)
The Effect of Heat on the Healing of Fractures: A Preliminary Experimental Report.
Canadian Medical Association Journal Vol 97 pp 274-280

EDGE A.J. and DENHAM R.A. (1977)
The Portsmouth Method of External Fixation of Complicated Tibial Fractures.
British Orthopaedic Association Meeting, September 1977

EGGARS G.W.N., SHINDLER T.O. and POMERAT G.M. (1949)
The Influence of the Contact-Compression Factor on Osteogenesis in Surgical Fractures.
Journal of Bone and Joint Surgery Vol 31-A pp 693-716

EPSTEIN S. (1937)
Art, History and the Crutch
Annals of Medical History Vol 9 p 304

EVANS F.G. (1973)
Mechanical Properties of Bone
Published by : Charles C.Thomas; Springfield, Illinois

EVANS M., KENWRIGHT J., GOODSHIP A.E., GWILLIM J. and HARRIS J.D. (1982)
The Influence of Induced Movement on Fracture Healing with External Fixation
Proceeding of the Conference on "Engineering in Orthopaedic Surgery and Rehabilation" Edinburgh September 1982

EVANS M., KENWRIGHT J. and TANNER K.E. (1979)
Analysis of a Single-Sided External Fracture Fixator.
Engineering in Medicine Vol 8 pp 133-137

FORSTER I.W. (1984)
Structural Aspects of Tendons and Ligaments
Natural and Living Biomaterials Chapter 8
Edited by G.W.Hastings and P.Ducheneyne
Published by CRC Press Florida U.S.A.

FREIDENBERG Z.B. and FRENCH G. (1952)
The Effect of Known Compression Forces on Fracture Healing.
Surgery, Gynaecology and Obstetrics Vol 94 pp 743-748

FUKADA E. (1957)
On the Piezoelectric Effect of Bone
Journal of the Physiological Society of Japan Vol 12 p 1159

GOODSHIP A.E., LANYON L.E. and McFIE H. (1979)
Functional Adaption of Bone to Increased Stress- An Experimental Study
Journal of Bone and Joint Surgery Vol 61-A pp 539-546

GUI L., GUALTIERI I. and GODOLI N. (1980)
A New Device (G3-IOR) for External Fixation
Italian Journal of Trauma Vol 6(3) pp 321-328

HAM A.W. and HARRIS W.R. (1972)
Repair and Transplantation of Bone
The Biochemistry and Physiology of Bone Vol 3 Cpt 10
Edited by G.H.Bourne
Published by Academic Press

HAMMER R., EDHOLM P. and LINDHOLM B (1984)
Stability of Union after Tibial Shaft Fracture- Analysis by a non-invasive Technique.
Journal of Bone and Joint Surgery Vol 66-B pp 529-534

HAMMING R.W.(1977)
Digital Filters pp 32-37, 115-117
Published by Prentice-Hall New Jersey U.S.A.

HAMSTRA H.R. Jr and WENDLAND P. (1972)
Noise and Frequency Response of Silicon Photodiode Operational Amplifier Combination
Applied Optics Vol 11 pp 1539-1547

HASSLER C.R., RYBICKI E.F., CUMMINGS K.D. and CLARK L.C. (1980)
Quantification of Bone Stresses during Remodelling.
Journal of Biomechanics Vol 13 pp 185-190

HASSLER C.R., RYBICKI E.F., SIMONEN E.A. and WEISS E.B. (1974)
Measurement of the Healing at an Osteotomy in a Rabbit Calvarium: The Influence of Applied Compressive Stress on Collagen Synethesis and Calcification
Journal of Biomechanics Vol 7 pp 545-550

HAVERS C. (1691)
Osteologia Nova
Published in London

HAYNES H.H. (1939)
Treating Fractures by the Skeletal Fixation of the Individual Bone
Southern Medical Journal Vol 32 pp 720-724

HEALTH TECHNICAL MEMORANDRUM No 8 (1969)
Safety code for electro-mechanical Apparatus
Published by Her Majesty's Stationary Office

HENRY A.N., FREEMAN M.A.R. and SWANSON S.A.V. (1968)
Studies on the Mechanical Properties of Healing Experimental Fractures.
Proceedings of the Royal Society of Medicine Vol 61 pp 902-906

HEIRHOLZER G., KLEINING R., HORSTER G. and ZEMENDES P. (1978)
External Fixation - Classifications and Indications
Archives of Orthopaedic and Traumatic Surgery Vol 92 pp 175-182

HIPPOCRATES (c.420 B.C.)
Hippocratic Writings
Edited by : G.E.R.Lloyd
Published by : Pelican Classics, London, 1978

HIRSCH T.J. (1962)
Modulus of Elasticity of Concrete Affected by Elastic Modulus of Cement Paste Matrix and Aggregate
Journal of the American Concrete Institute Vol 59 pp 427-451

HOAGLUND F.T. and STATES J.D. (1967)
Factors influencing the Rate of Healing in Tibial Shaft Fractures
Surgery, Gynaecology and Obstetrics Vol 124 pp 71-76

HOFFMANN R. (1938)
Rotules a os pour la reduction dirigee non sanglante des fractures
Helventia Med. Acta Vol 5 p 844

HOROWITZ P. and HILL W. (1980)
The Art of Electronics
Published by Cambridge University Press, Cambridge

HUTZCHENREUTER P., PERREN S.M., STEINEMANN S., GERET V. and KLEBL M. (1969)
Some Effects of the Rigidity of Internal Fixation on the Healing Patterns of Osteotomies
Injury Vol 1 pp 77-81

ILISAROV L. (1976)
Results of Clinical Trials and Experiance Obtained from the Clinical Use of the set of Ilisarov Compression-Distraction Apparatus.
Medical Exports Moscow.

JANKOVICH J.P. (1972)
The Effects of Mechanical Vibration on Bone Developement in the Rat.
Journal of Biomechanics Vol 5 pp 241-250

JAWORSKI Z.F.G., LISKOVA-KIAR M. and UHTOFF H.K. (1980)
The Effects of Long-Term Immobolisation on the Pattern of Bone Loss in Older Dogs.
Journal of Bone and Joint Surgery Vol 62-B pp 104-110

JERNBERGER A. (1970)
Measurement of the Stability of Tibial Fractures.
Acta Orthopaedica Scandinavica Supplement 135

JOFE M.H., HAYNES W.C., BEAUPRE G.S., GERHART T.N. and WHITE A.A. (1982)
Biomechanical Monitoring of Healing with External Skeletal Fixation
Transactions of the 28th Annual Meeting of the Orthopaedic Society p185

JOHNSON R.J. and POPE M.H. (1977)
Tibial Shaft Fractures in Skiing
The American Journal of Sports Medicine Vol 5 pp 49-62

JOHNSTON R.M. (1980)
Advances in External Fixation
Published by Year Book Medical Publishers U.S.A.

JORGENSEN T.E. (1972(a))
Measurements of Stability of Crural Fractures Treated with Hoffmann Osteotaxis
1.Method and Measurement of Deflection on Autopsy Crura
Acta Orthopaedica Scandinavica Vol 43 pp 188-206

JORGENSEN T.E. (1972(b))
Measurements of Stability of Crural Fractures Treated with Hoffmann Osteotaxis
2.Measurements on Crural Fractures
Acta Orthopaedica Scandinavica Vol 43 pp 207-218

JORGENSEN T.E. (1972(c))
Measurements of Stability of Crural Fractures Treated with Hoffmann Osteotaxis
3.The Uncomplicated Terminal Phase of Healing of Crural Fractures.
Acta Orthopaedica Scandinavica Vol 43 pp 264-279

JORGENSEN T.E. (1972(d))
Measurements of Stability of Crural Fractures Treated with Hoffmann Osteotaxis
4.The Complicated Terminal Phase of Healing of Crural Fractures.
Acta Orthopaedica Scandinavica Vol 43 pp 280-291

KARAHARJU E.O. and AALTO K. (1983)
The Deformation of External Fixation Devices During Loading
International Orthopaedics Vol 7 pp 179-183

KARLSTROM G. and OLERUD S. (1974)
Fractures of the Tibial Shaft - A Critical Evaluation of Treatment Alternatives
Clinical Orthopaedics and Related Research Vol 105 pp 82-115

KARLSTROM G. and OLERUD S. (1975)
Percutaneous Pin Fixation of Open Tibial Fractures
Journal of Bone and Joint Surgery Vol 57-A pp 915-924

KELLY B.O. (1976)
Lateral-Effect Photodetectors
Laser Focus Vol 12 pp 38-40

KENWRIGHT J., HARRIS J.D. and EVANS M. (1979)
External Fracture Fixation - The Analysis and Design of a New System
Engineering in Medicine Vol 8 pp 134-142

KIRILLOV S.K., LAURENTIEV V.V. and FIRSOV N.N. (1978)
Study of the Mechanical Properties of the Bone Regenerate in the Process of its Formation.
Ortopaediia Travmatologiia Protezirovanie Vol 1 pp 34-39

KREYSIG E (1974)
Advanced Engineering Mathematics
Published by Wiley

KOCH J.C. (1917)
The Laws of Bone Architecture.
American Journal of Anatomy Vol 21 pp 177-298

LAMBOTTE A. (1907)
L'Intevention Operatoire dans les Fracteurs.
Published by: Lamartin; Brussels.

LAROS G.S. (1974)
Fracture Healing - Compression vs. Fixation.
Archives of Surgery Vol 108 pp 698-702

LETTIN A.W.F. (1965)
The Effects of Axial Compression on the Healing of Experimental Fractures of the Rabbits Tibia.
Proceedings of the Royal Society of Medicine Vol 58 pp 882-886

LEVY D.D. (1974)
A Pulsed Electrical Stimulation Technique for Inducing Bone Growth.
Annals of the New York Academy of Science Vol 238 pp 478-490

LEWIS J.J. (1975)
A Dynamic Model of a Healing Fractured Long Bone
Journal of Biomechanics Vol 8 pp 17-25

LIPPERT F.G. (1973)
The Feasibility of Photogrammetrey as a Clinical Research Tool.
Journal of Biomechanics Vol 6 pp 459-473

LIPPERT F.G., and HIRSCH C. (1974)
The Three-Dimensional Measurement of Tibial Fracture Motion by Photogrammetry.
Clinical Orthopaedics and Related Research Vol 105 pp 130-143.

LONDON P.S.(1980)
Principles of Fracture Management
Scientific Foundations of Orthopaedics and Traumatology Chapter 49
Edited by R. Owen, J.W. Goodfellow and P.G. Bullough
Published by Heinemann Scientific Books London

LUCOVSKY G. (1960)
Photoeffects in Non-uniformly Irradiated p-n Junctions
Journal of Applied Physics Vol 31 pp 1088-1095

MACAULEY W.H.(1919)
Note on the Deflection of Beams
Messenger of Mathematics Vol 48 pp 129-130

McELHANEY J.H. (1966)
Dynamic Response of Bone and Muscle Tissue
Journal of Applied Physiology Vol 21 pp 1231-1236

McKIBBIN B. (1978)
The Biology of Fracture Healing in Long Bones.
Journal of Bone and Joint Surgery Vol 60-B pp 150-162

MALGAIGNE (1853)
Considerations cliniques sur les Fractures de la Notule et leur Traitment par les griffes.
Journal des Connaissances Medical Practiques Vol 16 pp 9-12

MEARS D.C. (1979)
History of External Fixation
Cpt 1. External Fixation, The Current State of the Art.
Edited by A.F.Brooker and C.C.Edwards
Published by Williams and Wilkins

MOORE A.R. and WEBSTER W.M. (1955)
The Effective Surface Recombination of a Germanium Surface with a Floating Barrier
Proceedings of the Institute of Radio Engineers Vol 43 pp 427-435

MOSTAFA A.G.S.A., EL ATTAR S., MILI F. and WRIGHT E.A. (1980)
The Effect of Enviromental Temperature on the Rate of Healing of Fractures in the Tail Vertebrae of Mice.
Journal of Bone and Joint Surgery Vol 62-B pp 102-103

NEWMAN R.J. (1983)
Nuclear Magnetic Resonance Studies of Abnormal Muscle
D.Phil. Thesis University of Oxford

NICOLL E.A. (1964)
Fractures of the Tibial Shaft - A survey of 705 Cases
Journal of Bone and Joint Surgery Vol 46-B pp 373-387

OLSON G. (1977)
Non-Contact Electro-optical Position Measurement
Electro-Optics/Laser '77 Conference and Exposition

O'REILLY R.J., COOK D.J., GAFFNEY R.D., ANGEL K.R. and PATERSON D.C. (1981)
Can Serial Scintigraphic Studies Detect Delayed Fracture Union in Man?
Clinical Orthopaedics and Related Research Vol 160 pp 227-232

OWEN R., GOODFELLOW J.W. and BULLOUGH P.G (1980)
Scientific Foundations of Orthopaedics of Orthopaedics and Traumatology
Published by Heinemann Medical Books, London

PAAVOLAINEN P., SLATIS P., KARAHARJU E. and HOLMSTROM T. (1978)
Studies on the Mechanical Strength of Bone. II Torsional Strength of Cortical Bone after Rigid Plate Fixation with and without compression.
Acta Orthopaedica Scandinavica Vol 49 pp 506-511

PANJABI M.M., WHITE A.A. and SOUTHWICK W.O. (1977)
Mechanical Properties of Bone as a Function of the Rate of Deformation
Journal of Bone and Joint Surgery Vol 55-A pp 322-330

PANJABI M.M., WHITE A.A. and SOUTHWICK W.O. (1977)
Temporal Changes in the Physical Properties of Healing Fractures in Rabbits.
Journal of Biomechanics Vol 10 pp 689-699

PARKHILL C (1897)
A New Apparatus for the Fixation of Bones after Resection and in Fractures with a Tendency to Displacement
Transactions of the American Surgical Association Vol 180 pp 3-6

PARKHILL C. (1898)
Further Observations regarding the use of the Bone Clamp in Ununited Fractures, Fractures with Malunion, and Recent Fractures with a Tendancy to Displacement
Annals of Surgery Vol 27 pp 553-570

PAUL OF AEGINA (625-690 A.D.)
Collected Works
Translated by : Fr. Adams
Published in London 1834 et seq.

PETERSON L.T. (1949)
External Skeletal Fixation
Bulletin of the United States Army Medical Department Vol 27 pp 553-570

PIEKARSKI K. (1973)
Analysis of Bone as a Composite Material.
International Journal of Engineering Science Vol 11 pp 557-565

PRITCHARD J.J. (1972(a))
General Histology of Bone.
The Biochemistry and Physiology of Bone Vol 1 Cpt 1
Edited by G.H.Bourne
Published by Academic Press

PRITCHARD J.J. (1972(b))
The Osteoblast
The Biochemistry and Physiology of Bone Vol 1 Cpt 2
Edited by G.H.Bourne
Published by Academic Press

POPE M.H. and OUTWATER J.O. (1972)
The Fracture Characturistics of Bone Subtance
Journal of Biomechanics Vol 5 pp 457-465

RALIS Z.A. (1980)
Influence of Paralysis and Interuterine Pressure on the Ossicification Growth and Quality of Developing Bone
Mechanical Factors and The Skeleton
Edited by I.A.F.Stokes
Published by John Libbey London

REZAIAN S.M. (1971)
The Effect of a New External Bone-Fixator on the Treatment of Fractures of Long Bones
Annals of the Royal College of Surgeons of England Vol 48 pp 336-343

RHINELANDER F.W. (1968)
The Normal Microcirculation of the Diaphysial Cortex and its Response to Fracture
Journal of Bone and Joint Surgery Vol 50A pp 784-800

ROMANO R.L., BURGESS E.M. and RUBENSTEIN C.P. (1976)
Percutaneous Electrical Stimulation for Clinical Tibial Fracture Repair.
Clinical Orthopaedics and Related Research Vol 114 pp 290-295

SAHA S. (1977)
Longditudinal Shear Properties of Human Compact Bone, and its Constitutents, and Associated Failure Mechanisms
Journal of Materials Science Vol 12 pp 1798-1806

SAHA S. and LAKES R.S. (1977)
The Effect of Soft Tissue on Wave Propagation and Vibration Tests for determining the "in vivo" Properties of Bone
Journal of Biomechanics Vol 10 pp 393-401

SALLEN R.P. and KAY E.L. (1955)
A Practical Method of Designing R-C Active Filters
Institute of Radio Engineers - Transactions on Circiut Theory Vol CT-2 pp 74-85

SARMIENTO A (1970)
A Functional Below-the-knee Brace for Tibial Fractures - A Report on its use in 135 cases
Journal of Bone and Joint Surgery Vol 52-A pp 295-311

SARMIENTO A., SCHAEFFER J.F., BECKERMAN L., LATTA L. and ENIS J.E. (1977)
Fracture Healing in Rat Femora as Affected by Functional Weight-Bearing.
Journal of Bone and Joint Surgery Vol 59-A pp 369-375

SCHATZKER J., SUMNER-SMITH G., CLARK R. and McBROOM R. (1978)
Strain Gauge Analysis of Bone Response to Internal Fixation
Clinical Orthopaedics and Related Research Vol 132 pp 244-251

SCHOTTKY W. (1930)
Ueber den Entstehungsort der Photoelektronen in Kupfer-Kupferoxydul Photozellen
Phys. Z. Vol 31 pp 913-925

SEDEL L., CHRISTEL P., DEWAS J., De CHARENTENAY F.X. and LERAY J. (1980)
Comparision of the Effect of Intermedullary Nailing or Plating on the Mechanical Properties of Fracture Callus
Journal of Biomedical Engineering Vol 2 pp 89-92

SIEGAL I.M., ANAST G.T. and FIELDS T. (1958)
The Determination of Fracture Healing by Measurement of Sound Velocity across the Fracture Site
Surgery, Gynaecology and Obstetrics Vol 107 pp 327-332

SMITH G.E. (1923)
Ancient Egyptians and the Origin of Civilization
Published by: Harpers and Brothers; London

SODERQUIST D. (1980)
Minimization of Noise in Operational Amplifier Applications
Precision Monolithics Inc. Applications Note AN-15

SONSTEGARD D.A. and MATTHEWS L.S. (1976)
Sonic Diagnosis of Bone Fracture Healing - A Primary Study.
Journal of Biomechanics Vol 9 pp 689-694

STADER O. (1937)
A Preliminary Announcement of a New Method of Treating Fractures
North American Veterinary Journal Vol 18 pp 37-38

STADER O. (1939)
Treating Fractures of Long Bones with the Reduction Splint
North American Veterinary Journal Vol 20 pp 55-59

STOKES I.A.F., KENWRIGHT J., HARRIS J.D., and MacLARNON C. (1978)
Measurement of Fracture Rigidity by Biplanar Radiographic Techniques
Oxford Orthopaedic Engineering Centre Annual Report No. 6

TANNER K.E. (1979)
An Investigation of a Method of Increasing the Stability of a Single Sided External Fracture Fixator
Final Year Project Department of Engineering Science, University of Oxford

TASSELL C. (1980)
Photodetectors in Noise Sensitive Environments
New Electronics January 1980

TODD J.D. (1974)
Structural Theory and Analysis
Published by Macmillians, London

TONINO A.J., DAVIDSON C.L., KLOPPER P.J. and LINCLAU L.A. (1976)
Protection of Stress in Bone and its Effects - Experiments with Stainless Steel and Plastic Plates in Dogs.
Journal of Bone and Joint Surgery Vol 58-B pp 107-113

VIDAL J., RABISCHONG P., BONNEL F. and ADREY J. (1970)
Etude Biomecanique du Fixateur Externe d'Hoffmann dans les Fractures de Jambe.
Society de Chirurgie de Montpellier Seance de 20 Janvin 1970
pp 43-52

WALLMARK J.T. (1957)
A New Semiconductor Photocell using the Lateral Photoeffect
Proceedings of the Institute of Radio Engineers Vol 45 pp 474-483

WASHBURN S.L. (1947)
Anatomical Record Vol 99 p 239

WATSON J. (1979)
The Electrical Stimulation of Bone Healing.
Proceedings of the Institute of Electrical and Electronic Engineers Vol 67 pp 1339-1352

WATT D.G. and WILLIAMS C.M.H. (1951)
American Journal of Orthodontics Vol 37 p 895

WEISS C., PUGH J., GRUBER J. and SWETT R. (1977)
The Application of Structure-Bourne Sound to the Structural Analysis of Bone an
Fracture Healing
Bulletin of the Hospital for Joint Diseases Vol 38 pp 26-28

WHITE A.A., PANJABI M.M. and SOUTHWICK W.O. (1977(a))
The Four Biomechanical Stages of Fracture Repair
Journal of Bone and Joint Surgery Vol 59-A pp 188-192

WHITE A.A., PANJABI M.M. and SOUTHWICK W.O. (1977(b))
Effects of Compression and Cyclical Loading on Fracture Healing - A Quantitive
Biomechanical Study
Journal of Biomechanics Vol 10 pp 233-239

WILLIAMS W.S. and BREGER L. (1975)
Piezoelectricity in Tendon and Bone.
Journal of Biomechanics Vol 8 pp 407-413

WOLFF J. (1892)
Das Gesetz der Transformation der Knochen
Published by : Hirschwald, Berlin

WOLTRING H.J. (1975)
Single and Dual-Axis Lateral Photodetectors of Rectangular Shape
Institute of Electrical and Electronic Engineers
Transactions on Electronic Devices Vol ED-22 pp 581-590

WOO S.L-Y., AKESON W.H., COUTTS R.D., RUTHERFORD L., DOTY D., JEMMOTT G.F.
and AMIEL D. (1976)
A Comparision of Cortical Bone Atrophy Secondary to Fixation Plates with Large
Differences in Bending Strengths.
Journal of Bone and Joint Surgery Vol 58-A pp 190-195

WOO S.L-Y., SIMON B.R., AKESON W.H. and McCARTY M.P. (1977)
An Interdisciplinary Approach to Evaluate the Effect of Internal Fixation Plates
on Long Bone Remodeling
Journal of Biomechanics Vol 10 pp 87-95

WYNN-JONES C.H. (1978)
A Simple External Fixation Method using Wire and Bone Cement.
Injury Vol 9 pp 329-330

YAMAGISHI M. and YOSHIMURA Y. (1955)
The Biomechanics of Fracture Healing
Journal of Bone and Joint Surgery Vol 37-A pp 1035-1068

APPENDICES

APPENDIX A

COMPUTER PROGRAMS

These have been microfisched by a DEC VAX computer using the username Newson. The microfische envelope has been affixed to the inside of the back cover of this thesis.

APPENDIX B

GLOSSARY

As this thesis is multidisciplinary, a glossary has been included to assist people from one discipline to understand the language of the other.

A.O. Arbeitsgemeinschaft fur Osteosynthesefragen, also known as

A.S.I.F. or the Association for the Study of Internal Fixation

Anisotropic Having different mechanical properties in different directions

Anterior Towards the front of the body

BiFET Integrated circuit combining bipolar and Field Effect transistors

Callus New bone formed at a fracture in the process of healing

Cancellous Bone Spongy bone found in the joints underneath a thin layer of more solid bone

CMOS Complementary Metal Oxide Semiconductor, these operate with supply voltages between +5V and +15V.

Comminuted Fracture Fracture having more than one fracture line, giving various fragments

Composite A material consisting of macroscopic particles or fibres of one material imbedded in another, e.g. Glass Fibre, consisting of fibres of glass in resin

Compound Fracture A fracture with direct connection to an open wound

Contralateral Opposite side to that under consideration

Cortex or **Cortical Bone** The outside bone forming the solid part of the cylinder of long bones

Creep Increasing deformation with time in a material under constant load

Distal Further away from the centre of the body, e.g. the hand is distal to the elbow

Elastic Deformation Deformation of a body when a load is applied such that when the load is removed the deformation is recovered

Femur Thigh bone

Fibula The thinner bone of the lower leg

Finite Element Analysis A method of dividing the structure under examination into small segments that can be analysed. Normally done by a computer

FORTRAN FORmula TRANslation, a high level computer language designed for mathematical applications, the computer compiles the program before running it.

Haematoma Blood clot

Hardware The pieces that make up a computer, e.g. chips boards etc..

Haversian Canal See osteone

Invasive A technique, or test which requires entry to the body

Ipselateral Same side as that under consideration

Lacuna A hole in bone containing an osteocyte

Lamellar Bone Bone laid down in layers; immature bone prior to being remodelled by Haversian systems

Lateral Away from the midline of the body e.g. the little toe is lateral to the great toe

Machine Code A computer language consisting of coded instructions immediately comprehensible to the computer

Medial Towards the midline of the body, opposite of lateral

Medullary Canal Centre canal of the long bones, filled with bone marrow

Medullary Nail or **Medullary Rod** A long rod placed in the medullary canal of a bone to immobilise a fracture

Non-Invasive Not invasive

Osteoblast A bone laying down cell

Osteoclast A bone absorbing cell

Osteocyte A cell derived from an osteoblast, and enclosed in a lacunae in the bone matrix

Osteone or **Haversian Canal** Consists of a central canal containing nerve fibres and blood vessels surrounded by concentric lamellae of bone, 0.2 to 0.5mm in diameter

Osteotomy An operation where a bone is cut, for example to straighten a bone or to create an artifical fracture

Pascal (Pa) S.I. measure of pressure it is equivalent to $N\ m^{-2}$

Periosteum The fiberous sheath surrounding bone containing blood vessels and nerves

Photogrammetry A method of measurement involving photographing an object from two directions and then reconstructing the object from the photographs

Piezoelectricity A phenomenon where electrical charge is produced by deformation of a material

Plastic Deformation Deformation that occurs when a body is loaded beyond its elastic limit, and on unloading not all the deformation is recovered

Poisson's Ratio (ν) Under uniaxial loading a material does not just deform in the direction of loading but also perpendicular to it. The ratio of these strains is known as Poisson's Ratio

Posterior The back of the body, or towards the back of the body

Proximal Nearer the trunk, opposite of distal

Scalar A quantity having magnitude but no given direction

Shear Modulus or **Modulus of Rigidity (G)** Ratio of shear stress to shear strain, can be related in an isotropic material to the Young's modulus and Poisson's Ratio: $E=2(1+\nu)G$

Singularity Function These functions written in the form $[x-a]^n$ obey the following set of rules; for n 0 $[x-a]^n$ is zero for x a or infinity for x a, and for n 0 $[x-a]^n = 0$ for x a and $=(x-a)^n$ for x a. They integrate and differentiate according to the normal laws of integration

i.e. $[x-a]dx = \frac{[x-a]^{n+1}}{n+1}$

Software The programs which control a computer

Strain (ϵ) The ratio of the change in length to the original length, or for shear strain the ratio of the change in a right angle to the original right angle. For normal engineering material it is usually measured either as percentage strain or as microstrain, 10^{-6} strain

Stress (σ) The force per unit area upon which the force is acting

Tibia Shin bone, the major bone of the lower leg

Vector A quantity having magnitude, direction and sense.

Young's Modulus or **Modulus of Elasticity (E)** The ratio of linear stress to linear strain

APPENDIX C

ABBREVIATIONS

A/D	Analog to Digital conversion
A.O. or	Arbeitsgemeinschaft fur Osteosythsesfragen
A.S.I.F.	Association for the Study of Internal Fixation
BiFET	Bipolar Field Effect Transistor
CMOS	Complementary Metal Oxide Semiconductor
D/A	Digital to Analog Conversion
DEC	Digital Equipment Corporation
EFF	External Fracture Fixation
LDVT	Linear Displacement Voltage Transducer
LED	Light Emmiting Diode
LSB	Least Significant Bit
LSI	Large Scale Integration
NAND	Not AND logic
NOR	Not OR logic
Op Amp	Operational Amplifier
PIN	P-type, Intrinsic, N-type photodiode
RAM	Ramdom Access Memory
TTL	Transistor - Transistor Logic

APPENDIX D

PAPERS

Published

Churches A.E., Tanner K.E., Evans M. and Gwillim J. (1985)
The Oxford External Fixator: Fracture Healing Assessment with External Fixation
Accepted for publication by Engineering in Medicine

Churches A.E., Tanner K.E. and Harris J.D. (1985)
The Oxford External Fixator: Fracture Stiffness and the Effect of Bone Pin Loosening
Accepted for publication by Engineering in Medicine

Churches A.E., Tanner K.E., Harris J.D. and Evans M. (1985)
An Engineering Evaluation of the Oxford External Fixator with Sliding Clamps: Fixator Stiffnes and Fracture Healing Assessment
Accepted for publication by Engineering in Medicine

Harris J.D., Kenwright J., Evans M., Tanner K.E. and Gwillim J. (1984)
Control of Movement and Fracture Stiffness Monitoring with External Fixation
Orthopaedics Vol 7(3) pp 485-490

Tanner K.E. (1985)

In Vivo Measurement of Fracture Movement
Chapter 6 in "Biomechanical Measurement in Orthopaedic Practice"
Edited by M.W. Whittle and J.D. Harris
In Press, Published by Oxford University Press

Presented at Meetings

Tanner K.E. (1983)
In Vivo Measurement of Fracture Movement
Meeting on "Biomechanical Measurement in Orthopaedic Practice", Oxford Orthopaedic Engineering Centre, Oxford, 14-15 March 1983

Tanner K.E. (1983)
The Causes of Fracture through Normal Bone
Injury Research Group Meeting, St. Catherine's College, Oxford, 28-29 March 1983

Tanner K.E. (1983)
Fracture Movement in External Fixation
10th International Conference on Hoffmann External Fixation, Brussels, Belgium, 22-24 September 1983